Cranfield University

School of Engineering
Department of Process and Systems Engineering

SAND TRANSPORT IN MULTIPHASE PIPELINES

Wei Yan

PhD Thesis

September, 2010

Cranfield University

School of Engineering

Ph.D. THESIS

Academic Year 2007-2010

Wei Yan

Sand Transport in Multiphase Pipelines

Supervisor: Prof. Hoi Yeung

This thesis is submitted in partial fulfilment of the requirements for the degree of Doctor of Philosophy

ABSTRACT

Over the life of an oil and gas reservoir, it is likely to encounter sand production. In offshore production fields, as there are lack of processing facilities nearby, gas, liquid and sand are often transported together in long distance pipelines. The existence of sand could accumulate in the pipelines under inappropriate operation condition and eventually will lead to a blockage. Thus, to design such systems requires knowledge on how sand is transported, when and where it will accumulate.

This thesis summarizes the experimental work undertaken using the 2 inch, 3 inch and 4 inch multiphase facilities. Generally, the main objectives of the experiments were to i) observe and enhance the understanding of sand transport characteristics in water and air-water flows; ii) investigate sand concentration effect and pipe diameter effect on sand minimum transport condition (MTC); iii) investigate the effect of pipeline orientation (0, +5, +10 and +20 degrees) and viscosity effect (Carboxy Methyl Cellulose (CMC) solution with viscosity of 7, 20cP; Oil with viscosity of 105, 250 and 340cP) on sand MTC; iv) validate the equivalent pressure drop concept for predicting sand MTC in sand-air-water flow and v) extend current MTC prediction model for sand-water flow to account for different sand concentrations .

Similar sand behaviour was observed in horizontal sand-water flow in all pipe sizes tested. At minimum transport velocity, sand particles were observed transporting in form of sand streaks. For horizontal sand-air-water flow, sand transport characteristics and MTC were strongly dependent on the air-water flow regime. Sand was found to be transported more efficiently within slug or roll wave body, where turbulence is generated intensively.

Parametric studies were conducted to investigate the factors affecting sand MTC in water and air-water flows in pipeline. It was found that the MTC will increase as sand concentration and pipe diameter increase. Pipeline orientation was found having little effect on sand behaviours and MTC in upwardly inclined water flow. However, in upwardly inclined air-water flow, although sand particles were observed sometime

moving backward with the liquid film, the superficial gas and liquid velocities required to transport sand were less than those in the horizontal pipeline due to the fact that slug flow regime was found more prevailing in inclined pipeline. In addition, the liquid viscosity effect on sand MTC in single phase liquid flow was investigated due to the increase of concerns relating to solids transport in high viscosity crudes. It appeared that, in turbulent flow, sand MTC increased slightly as the fluid viscosity increased. However, when the bulk flow became laminar, the MTC decreased as the fluid viscosity increased.

After visually obtained the sand MTC in air-water flow, the measured pressure gradients were compared between MTC condition for sand-water flow for different sand concentrations, the results indicate that the equivalent pressure gradients concept is a valid approach to extend the sand MTC prediction from water flow to air-water flow conditions for the purpose of pipeline design.

Two concentration correction correlations (dual range and single range) were proposed. The modified model could account for a wider range of sand concentration (from 0.000005 to 0.3 volume fraction) in water flow. The predicted MTC velocities showed good agreement with the experimental results.

ACKNOWLEDGEMENT

During my research, many people were of great help to me. This research project could not have been completed without them. I wish to express my special thanks and sincere gratitude to my supervisor Prof. Hoi Yeung and previous Research Assistant Dr. Salem Allababidi in Process and System Engineering Group for their continuing support and valuable comments and suggestions in every stage of my PhD research. The help of technical staff in DMG Group in Cranfield University for their devotion while working on the construction and maintenance of the experimental rigs is also greatly appreciated.

I also acknowledge the financial support and encouragement from Exploration & Production Technology Group (EPTG) in BP from Sunbury, UK. Thanks to the insightful perspectives provided by Mr. Phil Sugarman, Mr. Paul Fairhurst and Mr. Tim Lockett from BP during this research.

I would like to express my gratefulness and gratitude to my friends for their unconditional support, encouragement and tolerance over the life of this PhD. Without them, this would have been much harder.

Without the loving moral and material support of my wife, Limin Huang, and her understanding and patience during the entire period of PhD research, this thesis would not have seen the light of the day. My gratitude also goes to my parents for their self-giving support and continuous encouragement.

Finally, but no means least, my love to my sweet little girl, this thesis witnessed her new born with great happiness.

LIST OF PUBLICATION

1. S.Al-lababidi, W.Yan, H. Yeung, P Sugarman and C.P. Fairhurst, "Sand Transport Characteristics in Water and Two-Phase Air/Water Flows in Pipelines", *Conference of Multiphase Technology, BHRA*, Banff, Canada, June, 2008

2. W.Yan, S.Al-lababidi, H. Yeung, "Sand Transportation in Multi-Phase Pipelines", *Multi-strand Conference, Cranfield University*, Cranfield, UK, 2008

3. S.Al-lababidi, W.Yan, H. Yeung, "Solid Transport and Deposition Characteristics in Multiphase Flow in Pipelines", *Journal Energy Resources Technology* (Submitted to ASME)

LIST OF REPORT

1. W.Yan, S.Al-lababidi, H. Yeung, *"Sand Transportation in Multiphase Pipelines"*, BP Project Report (submitted to EPTG, BP Exploration, Sunbury, UK), Report Number 09/HY/540, 2009

Cranfield UNIVERSITY

Table of Contents

LIST OF FIGURES

LIST OF TABLES

NOMENCLATURE

a,b,c	constants	
d_p	particle diameter	microns
d_w	weighted mean particle diameter	m
f	Fanning friction factor	-
f_{TP}	two phase friction factor	-
f_{NS}	no-slip two phase friction factor	-
g	gravitational acceleration	$m \cdot s^{-2}$
k^*	universal constant in mixing theory	
l	mixing length	m
m,n	constants	-
m_g	gas mass flowrate	$kg \cdot s^{-1}$
m_l	liquid mass flowrate	$kg \cdot s^{-1}$
q_s	volumetric flow rate per bed width	$m^3 \cdot s^{-1}$
s	particle density/ liquid density	-
t	time	s
u	mean steam velocity	$m \cdot s^{-1}$
u^+	dimensionless velocity	
u_o^*	friction velocity at minimum transport condition for infinite dilution	$m \cdot s^{-1}$
u_c^*	friction velocity at minimum transport condition	$m \cdot s^{-1}$
u_t	terminal settling velocity	$m \cdot s^{-1}$
v'	eddy fluctuation velocity	$m \cdot s^{-1}$
x	fraction of eddies having velocity greater than the settling velocity of particles	-
x_g	vapour quality	-
y	actual distance from the wall	m
y^+	dimensionless distance from the wall	-
A_L	cross sectional area occupied by the liquid phase	m^2
A_p	projected particle area in direction of motion	m^2
C	Hazen-Williams pipe roughness factor	-
C_D	drag coefficient	-
C_L	lift coefficient	-
C_{ov}	percentage coefficient of variation	-
C_v	sand volume fraction, v/v	-
D	pipe diameter	m
D_{EQ}	hydraulic equivalent diameter	m
F_B	Buoyancy force acting on solid	Pa
F_d	correction factor for particle diameter	-
F_D	drag force acting on solid	Pa
F_L	lift force acting on solid	Pa
F_G	gravity force acting on solid	Pa
F_{Durand}	Durand coefficient	-
$Fr_{modified}$	modified Froude number	-
Fr_m	mixture Froude number	-

L1,L2,L3,L4	parameter using in Beggs and Brill correlation	-
K	coefficients	-
$\left\|\frac{\Delta P}{\Delta x}\right\|_{Friction}$	friction pressure gradients	$Pa \cdot s^{-1}$
$\left\|\frac{\Delta P}{\Delta x}\right\|_{LO}, \left\|\frac{\Delta P}{\Delta x}\right\|_{GO}$	friction pressure gradients for single phase liquid/gas only	$Pa \cdot s^{-1}$
Q_L, Q_G	volumetric flowrate for liquid/ gas	$m^3 \cdot s^{-1}$
U_b	fluid drag velocity at the sand bed	-
Re_p	particle Reynolds number	-
R_{xy}	cross correlation function	-
S	Wicks' dimensionless group	-
$S^{'}$	transport rate in grain volume per second per metre of sand bed width	-
S_L	wetted perimeter by liquid	m
V_m	mixture velocity of gas and liquid	$m \cdot s^{-1}$
V_c	critical transport velocity	$m \cdot s^{-1}$
V_{slip}	particle slip velocity	$m \cdot s^{-1}$
V_{MTC}	liquid velocity at minimum transport condition	$m \cdot s^{-1}$
V_p	Volume of particle	m^3
V_{SL}	superficial liquid velocity	$m \cdot s^{-1}$
V_{SG}	superficial gas velocity	$m \cdot s^{-1}$
α	coefficient	-
β	pipe inclination	degrees
γ	ratio of particle slip velocity to critical velocity	-
δ	laminar sublayer thickness	microns
ε	pipe roughness	m
ε_L	no-slip liquid holdup	-
ε_{L0}	liquid holdup in horizontal air-water flow	-
$\varepsilon_{L\beta}$	liquid holdup in inclined air-water flow (with inclination β)	-
μ_l	liquid dynamic viscosity	Pa·s
ν_l	liquid kinematic viscosity	$m^2 \cdot s^{-1}$
ρ_g	gas density	$kg \cdot m^{-3}$
ρ_l	liquid density	$kg \cdot m^{-3}$
ρ_p	particle density	$kg \cdot m^{-3}$
ρ_m	mixture density	$kg \cdot m^{-3}$
σ	standard deviation of particle sizes	m
σ_l	liquid surface tension	dyne
τ_0	wall shear stress	Pa
τ	shear stress	Pa
ϕ	Function in Wicks' correlation	-
φ_s	dimensionless sand transport rate	-
Φ_L^2, Φ_G^2	Lockhart & Martinelli two-phase multiplier	-
Ψ	Wicks' dimensionless group	-
Ψ_L	dimensionless liquid flowrate	-
Ω	function of C_V	-

ABBREVIATION

ACPD	actual pressure drop
CMC	Carboxy Methyl Cellulose
GVF	gas void fraction
MTC	minimum transport condition
PE	percentage Error

1 Introduction

The prediction of sand transport in multiphase pipelines is a topic of increasing industrial interest. Many reservoirs are prone to sand production. Oil and gas production rate can reduce due to sand accumulation. Removal of large sand quantities is difficult and time consuming. The removal of sand may be relatively simple using pigging, provided that only small amounts are deposited. Pigging can often result in a stuck pig if not carried out early and frequently enough.

If sand production is expected at the early life of a field, it will be prevented by installing the downhole sand exclusion systems such as gravel packs and screens. However, in many cases, sand will be produced at some later date. There are three options for the operator under this condition: (1) equip the wells with downhole sand exclusion system from the beginning, (2) complete the downhole sand exclusion system at a later date when sand production starts, (3) manage sand production by designing facilities with capability of handling sand without a downhole sand exclusion system. The last option, sand production management, is preferred by many commercial applications which can reduce the risk of loss of production or causing the plugging and mechanical damage. In order to keep the optimal production rates while maintaining acceptable equipment integrity and safety levels, the system design requires knowledge of how the sand is transported, when and where it will accumulate.

There are three key elements for the effective sand production management strategy: sand erosion, sand minimum transport condition (MTC) and sand monitoring. Sand erosion predictions are used to establish the maximum production rate without affecting the mechanical integrity of the system. Identifying sand minimum transport condition accurately is important for flowlines which are not designed for frequent pigging. Quantitative sand monitoring is necessary for verifying the effectiveness of sand erosion and MTC prediction.

1.1 Sand Erosion

Erosion is defined as the removal of material from a solid surface by repeated application of mechanical forces. These forces could be induced by solid particles, liquid droplet or cavitations. “Unlike erosion in sand-free systems, where erosion rates is only related to mixture density and flow velocity, erosion due the presence of sand is influenced by several factors including fluid characteristics (flow rate, composition, density and viscosity), sand characteristics (concentration, impact velocity, impact angle, numbers of particles hitting the surface, shape, hardness, size distribution and density) and material properties (hardness and microstructure)”—Salama (2000).

There are five models used in industry for the prediction of sand erosion in piping system, Salama and Venkatech (1983), Kvernvold (1998, DNV), Shirazi et al. (1995, Tulsa Unversity), Lockett et al. (1997, AEA) and Salama (2000). However, these models are limited to the application of simple pipe geometries such as pipe bends and tees. Salama and Venkatech’ model (1983) was a closed-form equation whose predictions were proved to be accurate for most gas system. The models developed by Kvernvold (1998, DNV) and Shirazi et al. (1995, Tulsa Unversity) attempted to incorporate the flow condition, which relied on empirical formulae and simplified physical model to account for particle tracking respectively. Salama (2000) proposed a model for erosion velocity limit which was as simple as equation API 14E (1981, 1991) with the consideration of sand particle shape, pipe diameter and sand flowrate. Though

not explicitly determined, erosion work establishes the upper velocity limits, assuming that sand is present in the flow. In comparison, much less work has been devoted to determining the lower velocity limits to prevent the accumulation of sand in the pipeline.

1.2 Sand Monitoring

Sand monitoring is essential to determine the effectiveness of sand control procedure and provide the input to predict the erosion rates and erosion velocity limit. Current sand monitoring techniques can be classified as intrusive and nonintrusive. The intrusive monitoring includes the probes penetrating into the actual fluid, while the non-intrusive sensor is mounted on the outside wall of the pipe. Salama (2000) reviewed the performance of several commercial sand detection devices using above techniques. For non-intrusive sensors like acoustic sand monitors (by Clampon, Simrad etc.), the acoustic transducer signal is generated in response to the noise generated by sand impact and is compared to that for the solid free flow. The excess signal is converted to sand rate using a calibration curve which is empirically derived. Intrusive sensors such as electrical resistance sand probes (by CorrOcean) monitor the electrical resistance change due to reduction in element thickness by erosion. Salama (2000) concluded that the commercial monitors had the potential of providing high accuracy for detection of quantitative sand production, along with the effects of flow conditions and pipe geometry. Accurate calibration of these sensors is the key as erosion rate depends not only on flow conditions but also on fluid properties.

1.3 Sand Minimum Transport Condition (MTC)

Sand transportation in multiphase flow is a very complex issue and dependent on a large number of parameters. Key parameters include sand concentration, fluid viscosities, multiphase (gas-liquid) flow regime and sand particle size. Sand transportation in water flow has been thoroughly studied in the past 50 years with reference to slurry and hydraulic conveyance. However, in slurry studies, the sand concentration tested is usually higher than 0.01 ($C_v > 0.01$v/v), which is much higher than what experienced in oil pipelines ($C_v \approx 0.00005$v/v). In addition, studies of sand transportation in viscous fluid, i.e. oil, are limited as most hydraulic conveyance work used water as the medium. Moreover, only a few investigations have been conducted on sand transport characteristics in two phase air-liquid flow. The understanding towards sand transport mechanism and minimum transport condition (MTC) under those conditions is vital for oil pipeline design to assure sand transportation during operation. At the present time, it is very difficult to quantify the effect of certain parameters when so little data is available.

The work of this thesis focused on sand transport behaviour in single (water or oil) and two phase (air-water, air-oil) flows in order to enrich the data bank for sand transportation in multiphase flows. The effects of fluid properties, sand concentration, pipe diameter and orientation were studied. The experimental sand minimum transport conditions (MTC) were obtained by visual observations. The pressure drops and slug characteristics at different MTC conditions in water and air-water flow were also measured to aid the development and analysis of design criteria for oil pipelines. A new set of correlations is proposed to embed a sand concentration correction into Thomas model (1962) and extended it for MTC prediction in both water and air-water flows.

1.4 Research Objectives

The main objectives of this thesis are to improve the understanding sand transport characteristics and the prediction of the minimum sand transport conditions (MTC) under single and multiphase flows and pipeline orientations.

To satisfy the above stated objectives, the following tasks were undertaken

- Conduct intensive literature review of sand transport in hydraulic and multiphase system and summarize prediction methods on transport condition.
- Experimentally study the sand transport characteristics in single-phase liquid flow and two-phase air-liquid flow regimes.
- Study the pipeline orientation effect (horizontal, vertical, +5, +10, +20 degree uphill pipelines) on MTC in water-sand and air-water-sand flows.
- Investigate the sand concentration and particle size effect on MTC in water-sand and air-water-sand flows.
- Investigate the fluid viscosity effect (using water, CMC solution and oil) on MTC in single-phase liquid flow and two-phase air-liquid flow.
- Perform analysis on measured pressure drops and slug characteristics under different MTC conditions in water and air-water flows.
- Evaluate other published sand minimum transport condition prediction models against experimental data and develop new correlations to account for sand concentration effect

1.5 Thesis Outline

The main objectives and outline research aspects of this project are presented in Chapter 1. Chapter 2 reviews previous research findings on solid transportation in single phase liquid flow and two phase air-liquid flow, with the discussion on the parameters which could affect solid transportation. The experimental setup is provided in Chapter 3. The sand transportation rigs (2 inch, 3 inch and 4 inch facilities) in PSE Lab in Cranfield University are detailed. The sand distribution used in this work and the test methodology are also presented in this Chapter. In Chapter 4 and Chapter 5, the sand transport characteristics observed in 2 inch and 4 inch pipeline are described under different flow conditions (water and air-water flows) and different pipe orientations. The liquid viscosity effect on sand transport characteristics are studied in the 4 inch and 3 inch facility by using CMC solution and oil respectively. The results are described in Chapter 6. Chapter 7 analyses the experimental results from this work and compares with findings from previous investigation available in the literature. Chapter 8 compares the pressure gradients and carrier fluid velocities at MTC condition in water and air-water flows, in order to explore some insights to provide guideline for pipeline design. A set of new correlations for the prediction of MTC to account for sand concentration effect is proposed in Chapter 9. Thomas lower models (1962), before or after concentration correction, are validated with experimental data. Chapter 10 gives the conclusion and recommendations for future work.

2 Literature Review of Solid Transportation in Hydraulic and Multiphase Pipeline

2.1 Sand-Liquid Flow in Pipeline

2.1.1 General Concepts for Single-Phase Liquid Flow

All single phase liquid flow can be characterized into one of two regimes. These two flow regimes are laminar and turbulent flows. The flow regime, whether laminar or turbulent, is important in the design and operation of any fluid system. The shear stress from fluid acting on the pipe wall determines the amount of energy required to maintain the desired flow, which depends upon the mode of flow.

Experimental evidence shows the type of fluid flow that occurs in straight circular pipes is dependent on Reynolds number, Re, which indicates the ratio between inertia force and viscous force.

$$Re=\rho uD/\mu \qquad [1]$$

where ρ is the fluid density, D is pipe diameter, u is mean fluid velocity and μ is the fluid viscosity. Laminar flow will occur when the Reynolds number is less than 2300, and the resistance to flow will be independent of the pipe wall roughness. Turbulent flow will occur when Reynolds number is beyond 4000. Between the laminar and turbulent flow conditions (Re 2300 to 4000) the flow condition is known as transition flow.

- **Laminar flow**

When a fluid flows through a pipe, the internal roughness of the pipe wall can create local eddy currents within the fluid adding a resistance to flow of the fluid. Viscous fluid will move more slowly and not support eddy currents, therefore the frictional resistance can hardly be affected by internal roughness of the pipe. This condition is known as laminar flow. In laminar flow, fluid particles move along straight, parallel paths in layers. Magnitudes of adjacent layers are not the same. Laminar flow is governed by the law relating shear stress to the rate of angular deformation, i.e. the product of viscosity of the fluid and velocity gradient given by:

$$\tau_{laminar} = \mu \frac{du}{dy} \qquad [2]$$

where τ is shear stress. The velocity distribution within a cross section of a pipe will follow a parabolic low for laminar flow (shown in Figure 1), and the maximum velocity will occur at the center of the pipe.

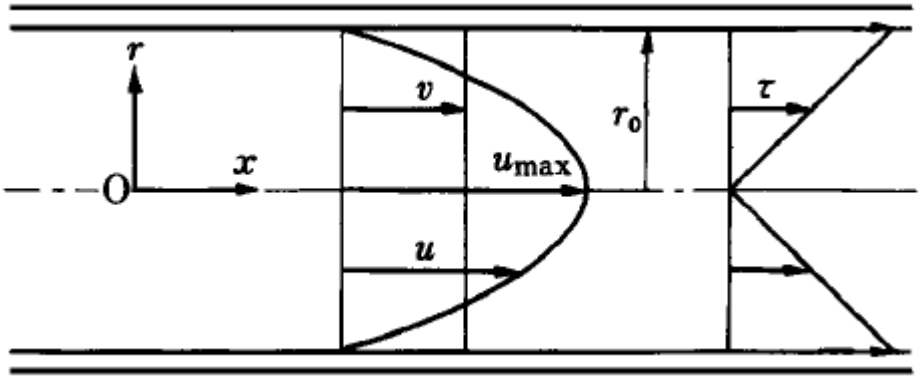

Figure 1: Laminar flow through a tube (Nakayama and Boucher, 2000)

- **Turbulent flow**

Turbulent flow is characterized by fluid particles moving in an apparently random fashion in all directions. It is virtually impossible to trace the motion of a particular fluid particle. Magnitudes and directions of velocity, pressure and shear force fluctuates in random order.

It is common to define turbulent velocity profiles through a near wall boundary layer. A typical velocity and shear stress distributions near a wall was illustrated in Figure 2. It can be described by a universal velocity profile which characterized by a viscous sublayer (i.e. laminar sublayer), a turbulent core, and a buffer zone in between.

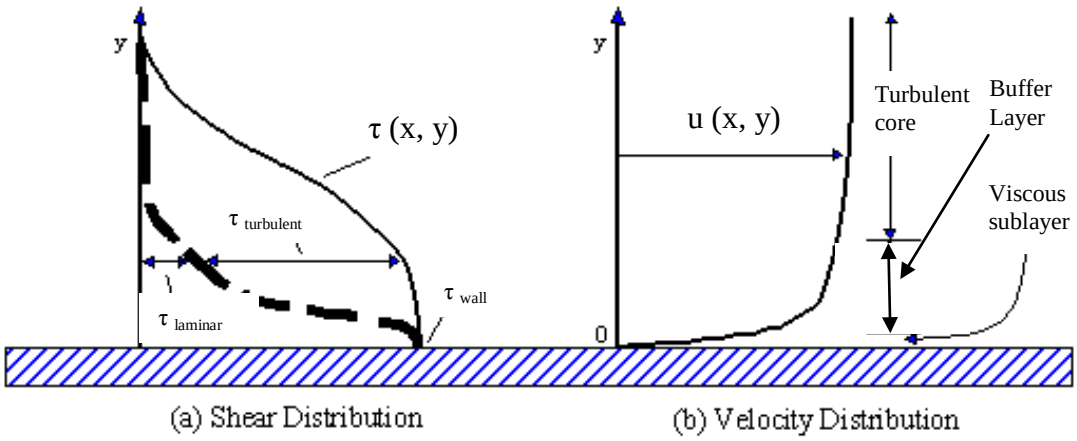

Figure 2: Typical velocity and shear stress distributions near a wall in turbulent flow (Kay and Nedderman, 1985)

The shear stress for turbulent flow was defined as:

$$\tau_{turbulent} = \rho_l l^2 \left(\frac{du}{dy}\right)^2 \qquad [3]$$

where l was defined as mixing length, which is proportional to the distance from the wall:

$$l = k^* y \qquad [4]$$

k^* is a universal constant having a value around 0.4.

In order to better interpret the velocity profile for turbulent flow, the dimensionless, time-averaged axial velocity, u^+, and dimensionless distance from the wall, y^+, are usually used (Figure 3):

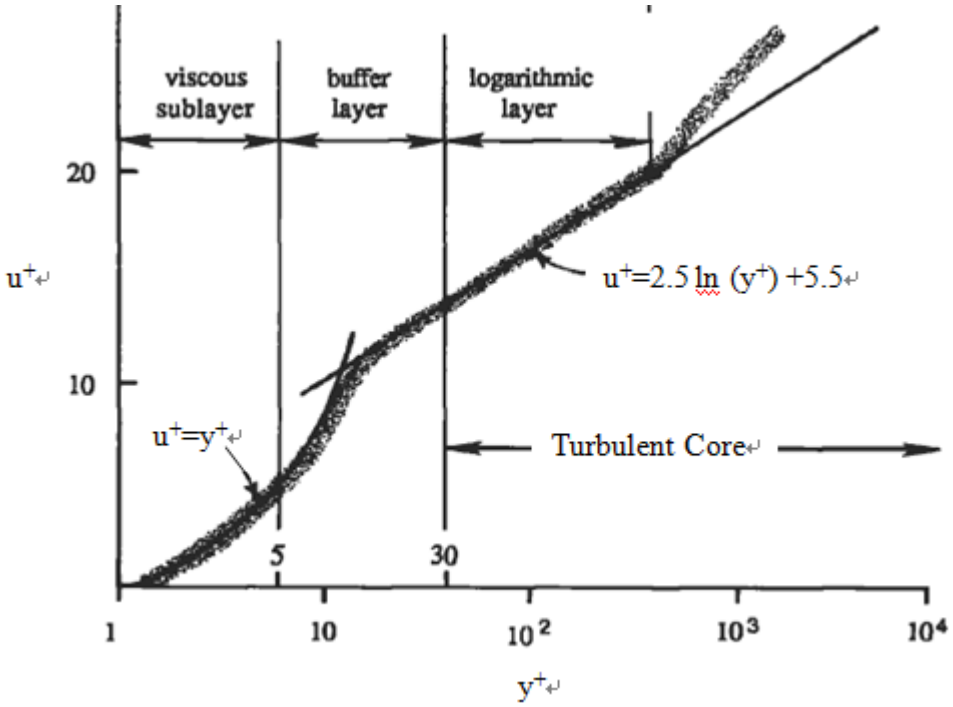

Figure 3: Interpretation of turbulent velocity profile using u^+ and y^+ (Coulson et al., 2010)

Viscous sublayer $$u^+ = y^+ \qquad [5]$$

Buffer layer $$u^+ = 5.0\ln(y^+) - 3.05 \qquad [6]$$

Turbulent core $$u^+ = 2.5\ln(y^+) + 5.5 \qquad [7]$$

u^+ is defined by:

$$u^+ = \frac{u}{u_0^*} \qquad [8]$$

where u is mean stream velocity and u_0^* is friction velocity, which is of the order of the

root mean square velocity fluctuation perpendicular to the wall in the turbulent core. u_0^* is defined by

$$u_0^* = \sqrt{\left(\frac{\tau_0}{\rho}\right)} \qquad [9]$$

where τ_0 is the wall shear stress.

And y^+ is defined by:

$$y^+ = \frac{u_0^* \rho y}{\mu} \qquad [10]$$

where y is actual distance from the pipe wall.

Within the viscous sublayer (i.e. laminar sublayer, $y^+ \leq 5$), where right next to the wall, viscous stress is dominating. In spite of the fluctuations, the Reynolds stresses (due to the random turbulent fluctuations in fluid momentum) are still small here because of the dominance of viscous effects. Also, because of the thinness of the viscous sublayer, the stress can be taken as uniform within the layer and equal to the wall shear stress. Therefore, the thickness of laminar sublayer could be represented as:

$$\delta = 62D\left(\frac{Du\rho}{\mu}\right)^{-7/8} \qquad [11]$$

The velocity profile is no longer linear when $y^+ > 5$. The velocity distribution become either non-linear ($5 < y^+ < 30$, buffer layer) or logarithmic ($y^+ > 30$, logarithmic layer). In these layers, neither the viscous stress nor the Reynolds stress is negligible.

Pressure drop in a straight horizontal pipe, which happens due to the frictional resistance, can be calculated by the following equation:

$$\frac{\Delta P}{\Delta x} = 2f\left(\frac{1}{D}\right)\rho u^2 \qquad [12]$$

where f is Fanning friction factor, Δx is unit length and ΔP is pressure loss over this length. When Re is less than 2300, f=16/Re. When Re is higher than 4000, f can be calculated by $f=0.079Re^{-0.25}$ for a smooth pipe.

2.1.2 Forces Acting on Particles in Liquid Flow

Solid particles within liquid flow experience forces acting from the surrounding flow. Especially, the force balance on the vertical axis can determine whether the particle will settle on the pipe bottom or not. There are four common forces, acting on a spherical particle on vertical axis (Figure 4, Green and Perry, 2007):

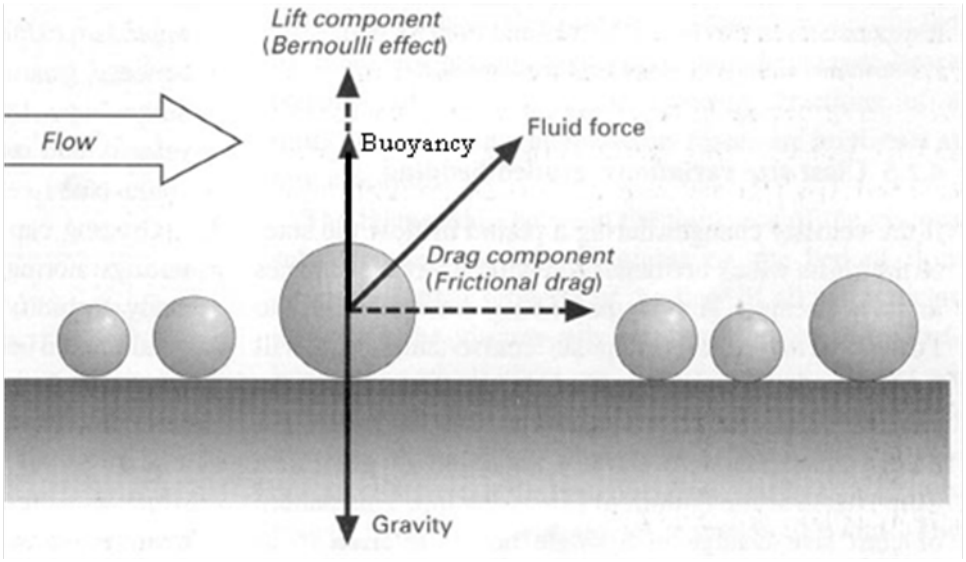

Figure 4: Forces acting a spherical particle within a flow

- Force due to gravity, F_G

$$F_G = \rho_p g V_p \quad [13]$$

where ρ_p is particle density, Vp is the volume of a single particle.

- Force due to buoyancy, F_B

$$F_B = \rho_l g V_p \quad [14]$$

where ρ_l is liquid density.

- Drag force, F_D, due to the viscous drag from fluid

$$F_D = \frac{1}{2}\rho_l C_D u^2 A_p \quad [15]$$

where C_D is the drag coefficient, and A_p is the projected particle area in direction of motion.

- Lift force, which is a result of pressure differences around the particle (Bernoulli effect)

$$F_L = \frac{1}{2}\rho_l C_L u^2 A_p \quad [16]$$

where C_L is the lift coefficient.

For different particles, their settling behaviour can be categorized into three flow regimes (settling laws) based on the Re_p, i.e. particle Reynolds number, which can be calculated by:

$$Re_p = \frac{d_p \rho_l u}{\mu_l} \quad [17]$$

where d_p is the particle diameter.

The classification of those three flow regimes are summarized in Table 1:

Table 1: Classification of solid settling flow regimes

Settling Law	Criteria	Terminal Settling Velocity ($m \cdot s^{-1}$)
Stoke's Law	$Re_p < 1$	$u_t = \frac{g d_p^{\,2} (\rho_p - \rho_l)}{18 \mu_l}$
Intermediate Law	$1 < Re_p < 1000$	$u_t = \left[\frac{2g}{27} \left(\frac{\rho_p - \rho_l}{\rho_l} \right) \right]^{5/7} \frac{\rho_l^{\,3/7} d_p^{\,8/7}}{\mu_l^{\,3/7}}$
Newton's Law	$Re_p > 1000$	$u_t = 1.73 \sqrt{d_p g \left(\frac{\rho_p - \rho_l}{\rho_l} \right)}$

Particles within concentrated suspensions bump into one another, slowing their settling. This is referred to as **hindered settling**. It occurs for solid concentrations ≥ 0.03 of volume faction (v/v). The velocity gradients around each particle are affected by the presence of nearby particles. So the normal drag correlations do not apply. Also, the particles in settling displace liquid, which flows upward and make the particle velocity relative to the fluid greater than the absolute settling velocity. If particles of a given size are falling through a suspension of much finer solids, the terminal velocity of the larger particles should be calculated using the density and viscosity of the fine suspension.

For a non-spherical particle, the drag acting on it also depends upon its shape and orientation with respect to the direction of motion.

2.1.3 Sand-Liquid Flow Regimes

Sand being transported in pipe lines (whether they be multiphase or single phase pipelines) can adopt a number of configurations or 'flow regimes'. The Multiphase Design Handbook (2005) depicts these flow regimes as following (Figure 5):

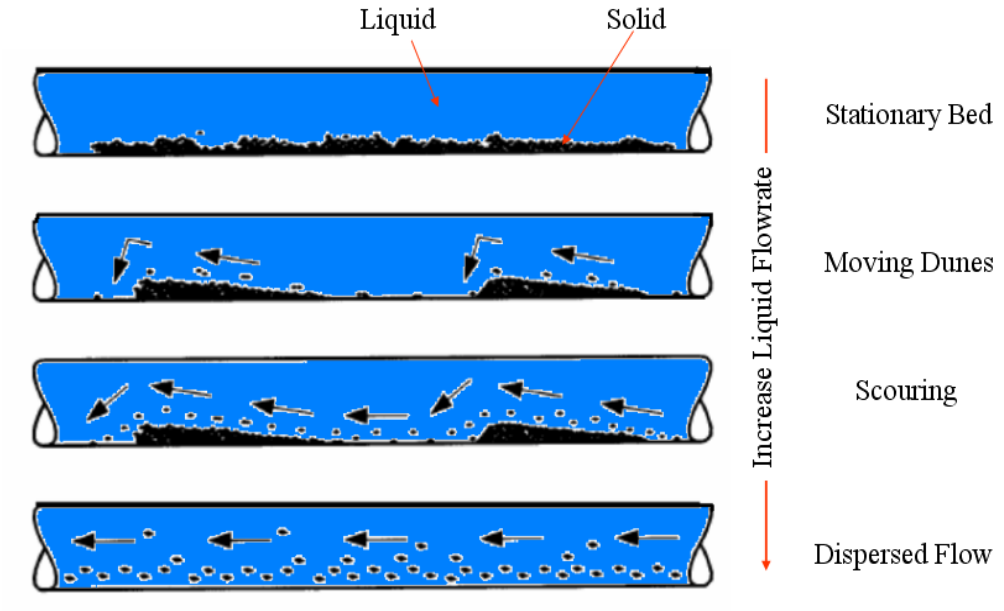

Figure 5: Liquid/sand flow regimes in horizontal pipelines

- **Stationary bed**

At very low liquid flowing velocities a stationary bed is formed with sand particles at the bottom and no grains move at all. With an increase in the velocity a stable bed height is reached where the particles at the top are transported further downstream to increase the length of the bed. The upper surface of the bed is flat at very low flowrates but becomes wavy as the flowrate increases. At higher liquid flowrates the height of the stationary bed decreases. An equilibrium bed is reached when the shear at the upper surface of the bed transports sand downstream at a rate equal to the sand inflow rate.

- **Moving dunes**

If the liquid flowrate is increased further the bed breaks up and the particles arrange themselves into moving dunes in which the grains on the upper surface of the dune are rolled along from back to front (downstream). The grains then fall into the sheltered region at the front of the dune. The dune passes over these particles until they are once again on the top surface. The motion of dunes is similar to sand dunes in the desert and to snow drifts. Smaller dunes move faster than larger ones and a given length of stationary deposit will break up into a number of dunes, each with a characteristic length and velocity.

- **Scouring**

As the flowrate is increased further the grains roll along the top of the dunes with sufficient momentum that they escape from the sheltered downstream region and are swept away as individual scouring grains. Dunes can still survive in this environment by replenishment from upstream particles.

- **Dispersed**

At high liquid flowrates the dunes are dispersed. The sand particles now move in the produced fluid in an erratic pattern. However, a strong concentration gradient is usually observed.

2.1.4 Definitions and Prediction of Sand Transport Velocities

From the early 1940's, many researchers conducted experimental investigations to observe the particles behaviour and to develop correlation to predict the deposit velocity in hydraulic slurry transport pipeline. As a result, a large number of correlations were developed for predicting the various "design" velocities for horizontal pipe flow. However, these correlations were developed based on different settling velocity definitions. And it is not always made clear as to which definition a particular correlation is used. From the literature review, the "design" velocities were classified into six main definitions which can be summarised as follows (Yan, 2009):

- **Sliding bed velocity**

This is the velocity at which the shearing forces in the liquid are just sufficient to move sand particles on the pipe surface. This velocity is an inefficient method of transporting slurry, but it may well be the mechanism by which coarse solids are conveyed over a relatively short distance at high concentrations.

- **Saltating velocity**

At this velocity, the solid particles are repeatedly picked up by the liquid and deposited further along the pipe. This mechanism is not used for long distance pipelines carrying fine particles, however for short pipelines carrying coarse particles it may be necessary to operate in this mode.

- **Suspending velocity**

The suspending velocity is the lowest velocity at which all particles are picked up and remain in suspension. Most of the developed correlations were based on this definition, and this velocity is widely used to for designing most slurry or hydrotransport pipelines.

- **Deposit velocity (or limiting deposit velocity)**

This is the velocity at which particles settle out as the flowrate is reduced. The particles may settle to form a static or sliding bed. It is of importance to mention that the suspending and deposit velocities are the same if there is no hysteresis present when the condition for solids pickup is approached by either increasing or decreasing the slurry flowrate in the pipe.

- **Critical velocity, V_c (or velocity corresponding to a minimum in the pressure gradient versus velocity curve)**

The determination of this velocity does not require observations of the flow regime but the minimum point is difficult to locate with precision because the curve is often shallow and not necessarily continuous. It is usually assumed that the critical velocity is higher than the suspending velocity so that its use leads to a safe design.

- **Homogenous flow velocity**

In theory, this is the velocity at which the particles become evenly distributed through the pipe. In practice, it is defined as the velocity at which the concentration profile across the pipe attains some arbitrary degree of uniformity. Using this velocity pipeline design can lead to a design that is too conservative.

In addition to the above definitions, the minimum transport condition proposed by Thomas (1962) is used by some of oil companies for designing transport pipeline. The Thomas' definition for minimum transport condition (MTC) is ***"the mean stream velocity required to prevent the accumulation of a layer of sliding particles at the bottom of horizontal pipe"***. Thomas (1964) also claimed his definition for MTC also could be related to the minimum value of pressure curve. Therefore, his definition is quite close to that for critical velocity.

In conventional slurry system practice, there were two approaches to predict the transport velocity. One of them was correlating the transport velocity directly to fluid and solid parameters ie. liquid and solid density, liquid viscosity, particle size etc.(Durand, 1953; Oroskar and Turian, 1980, Al-Mutahar, 2006, etc.). The other important approach was that, instead of correlating to transport velocity, it related those parameters to the ratio of particle terminal settling velocity to friction velocity: u_t/u_o^*, where $u_o^* = (\tau_0/\rho)^{1/2}$ (so called wall shear velocity). The u_t/u_o^* actually represents the ratio of settling tendency of particles to the turbulent fluctuation which providing a driving force to maintain particles in suspension. Chien (1956) concluded that the key factor affecting the distribution of suspended solid in a flowing stream was the ratio of terminal settling velocity to the friction velocity based on his experimental results. Liu (1956) also suggested that initial condition for particle movement was a function of u_t/u_o^*. This method was considered more useful by some researchers (Thomas, 1961, 1962 and 1964; King et al., 2000) since the friction velocity can be easily related to the pressure drop and flow rate, parameters that are important for system design.

2.1.5 Thomas (1961, 1962, and 1964) Correlation

Thomas (1961, 1962 and 1964) was concerned with flow regime between two extremes: flow with the fluid over a stationary bed and flow with solid particles uniformly distributed over a vertical cross section of the pipe. While decreasing the fluid velocity from homogeneous suspended flow, he identified solid/liquid flow regimes as follows:

- **Fully suspended flow**
  - all sand particles are suspending with the bulk of the fluid

- **Heterogeneous flow**
  - which lower limit is given by the minimum sand transport condition

- **Longitudinal waves**
  - ribbons and streaks of sediment, sometime unstable

- **Periodic disposition**
  - which behave as transverse waves or dunes, having the appearance of discrete clumps or islands of sediment particles. The waves creep along the bottom of pipe, and have a reproducible length, height and velocity.

The critical velocity of sand transportation was defined as "**minimum transport condition**" (MTC) – "*…the minimum velocity demarcating flows in which the sand*

form a bed at the bottom of the pipe from fully suspended flows", referring to the lower limit of heterogeneous flow.

He considered two major factors that affect the vertical distribution of suspended solids in flow stream. Firstly, the ratio of the terminal settling velocity to the friction velocity (u_t/u_0^*) and secondly, the thickness of laminar sublayer and buffer layer and turbulent core. A particle characteristics map was generated based on friction velocity, terminal velocity law regions, particle Reynolds number, laminar sublayer, buffer layer and turbulent core. The map coordinates are the ratio of terminal settling velocity to the friction velocity (u_t/u_0^*) and particle Reynolds number in terms of friction velocity. The u_t/u_0^* actually represents the ratio of settling tendency of particles to the turbulent fluctuation which providing a driving force to maintain particles in suspension, while the particle Reynolds number in terms of friction velocity indicates the fluctuations at the vicinity of the pipe wall. This map was divided into two major flow regimes to account for the minimum transport condition, as shown in Figure 6:

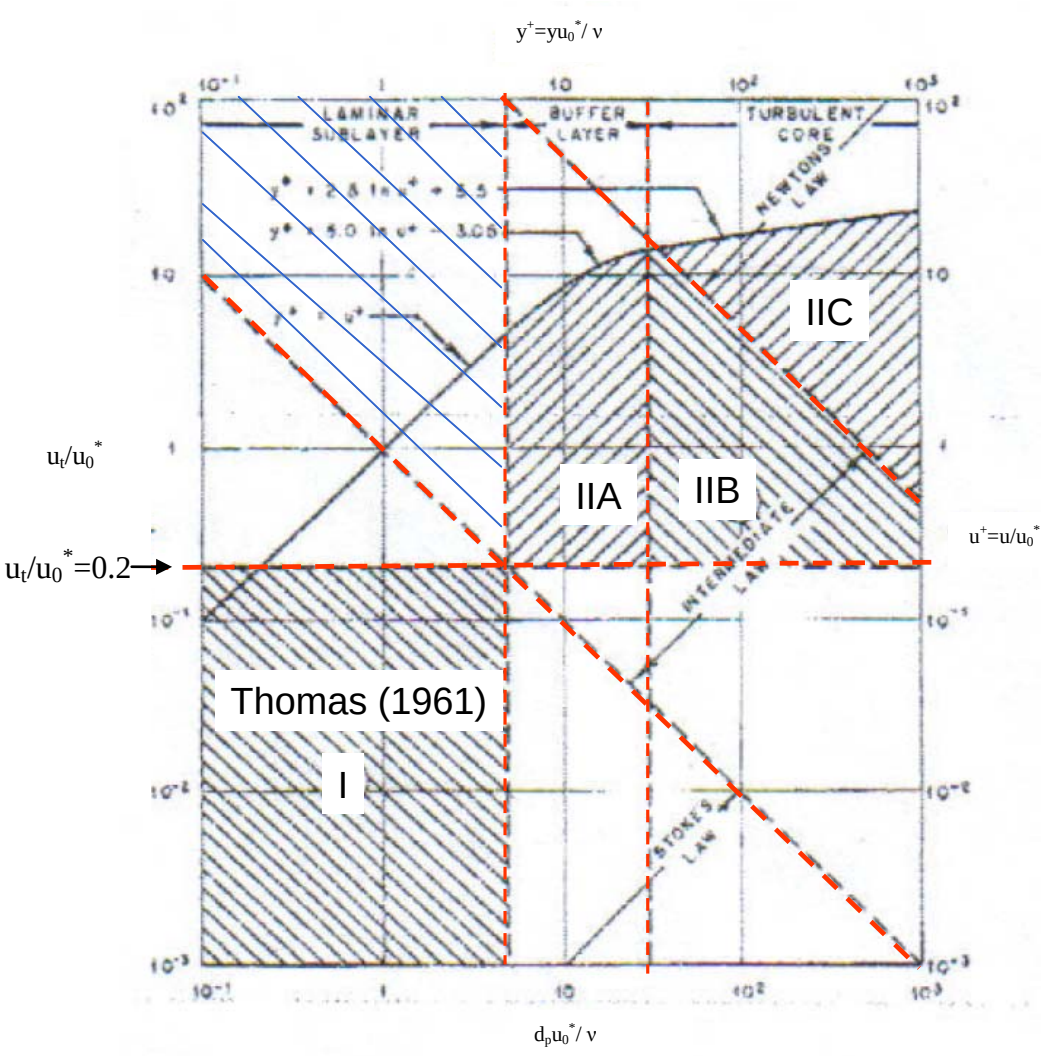

Figure 6: Particle flow regime classification for MTC (Thomas, 1962)

Flow regime I: Flow with particles predominantly in suspension and are smaller than the thickness of laminar sublayer, and which settle according to the Stokes' law. The relationship $u_t/u_0^*=0.2$ was applied as the transition between the particles being transported between heterogeneous suspension or forming a stationary bed, i.e. when $u_t/u_0^* < 0.2$, the particulate phase is transported in suspension and at $u_t/u_0^* > 0.2$, the particulate phase is transported predominantly in a layer along the bottom of the pipe. This flow regime was verified by observation for particle concentration ranged from 0.01 to 0.17 solid volume fractions (v/v) and with mean diameter ranged from 56 to 78 microns, Thomas (1961). Based on this flow regime I, Thomas developed correlation:

$$u_0^* = \left[100 u_t \left(\frac{\nu_l}{d_p} \right)^{2.71} \right]^{0.269} \qquad [18]$$

where u_0^* is friction velocity (ft/s) for infinite dilution; u_t is terminal settling velocity (ft/s); d_p is the particle diameter (ft); ν is kinematic viscosity (ft/s).

Flow regime II: Flow with particles transported predominantly in lower portion of pipe:

a) II A: Particles which are smaller than the thickness of buffer layer and greater than the laminar sublayer and which settle according to the intermediate law
b) II B: Particles which are larger than the thickness of the buffer layer and which settle according to the intermediate law.
c) II C: Particles which are larger than the thickness of buffer layer and which settle according to Newton's law.

For Flow regime II, Thomas (1962) developed a correlation based on dimensional analysis and previous correlations from others' work.

$$u_0^* = \left[0.204 u_t \left(\frac{\nu_l}{d_p} \right) \left(\frac{\nu_l}{D} \right)^{-0.6} \left(\frac{\rho_p - \rho_l}{\rho_l} \right)^{-0.23} \right]^{0.714} \qquad [19]$$

where ρ_l is density of liquid (lb/ft^3), ρ_p is density of solid (lb/ft^3), and D is the pipe diameter (ft).

Based on his data from experiments on 1 inch facility and others' data (> 0.0007 v/v for Thomas' tests and > 0.01 v/v for others' work), he found that the difference between the friction velocity at the MTC and that MTC under infinite dilution condition was proportional to the square root of the v/v for all the concentrated liquid-solid suspensions. He proposed the Equation [20] for concentration correction:

$$u_c^* = u_0^* \left[1 + 2.8 \left(\frac{u_t}{u_0^*} \right)^{0.33} \sqrt{C_v} \right] \qquad [20]$$

where C_v is solid volume fraction (v/v), and u_c^* is the friction velocity (ft/s) for a certain sand concentration.

He also claimed that the friction velocity increased by 10% as the v/v was increased from 0 to 0.317.

The use of Equations [18], [19] and [20] requires prediction of u_0^* or u_c^* as a function of flow velocity. One commonly used relationship is,

$$u_c^* = (f/2)^{0.5} \times V_{MTC} \quad [21]$$

where V_{MTC} is the solid minimum transport velocity, and f is the fanning friction factor. This is derived from the balance relationship between pressure drop and shear stress for a certain length of pipe.

2.1.6 Durand (1953) Correlation

Durand (1953) developed a correlation for critical velocity, defined as the velocity at which particles can be transported without forming a stationary bed with minimum head loss (economical transportation of slurry was the main objective behind developing the correlation). Durand conducted a series of tests with sand, coal and gravel covering particle sizes from 0.05 mm to 25 mm and pipe diameters from 0.0381 m (1.5 inch) to 0.7112 m (28 inches) with a maximum v/v of 0.15. He considered the effect of concentration, pipe diameter, particle size, solid density and liquid density in his correlation.

$$V_c = F_{Durand}\left[2gD(s-1)\right]^{1/2} \quad [22]$$

where V_c is critical velocity ($m \cdot s^{-1}$), F_{Durand} is Durand coefficient, and s is the ratio of solid density and liquid density.

2.1.7 Condolios and Chapus (1963) Correlation

Condolios and Chapus (1963) developed a critical velocity correlation for v/v less than 0.02.

$$V_c = 3.0 C_v^{0.148} \sqrt{gD} \quad [23]$$

2.1.8 Cairn (1960) Correlation

Cairns et al. (1960) derived a dimensionless empirical correlation which can be used to predict settling velocity (inferred as the velocity at which particles drop out from suspension).

$$\frac{V_c^2}{gD} = 9.8 C_v^{0.3} \left[\frac{DV_c\rho_l}{\mu_l}\right]^{0.3} \left[\frac{(\rho_p - \rho_l)}{\rho_l}\right]^{0.6} \quad [24]$$

2.1.9 Hughmark (1961) Correlation

Hughmark (1961) developed a dimensionless correlation to predict the mean velocity of flow at which all the particles are in suspension using the data from literature (Hughmark used data of Smith (1953), Newitt et al. (1955), Murphy et al. (1954)). It is reported that Smith's data is for the velocity at which particles started to settle. Despite of the little difference between the velocities at which particles start settling and the mean velocity of flow at which all the particles are in suspension, Hughmark used Smith's data in developing his correlation.

He correlated the experimental data with particle diameter, pipe size, liquid density, solid density, and solid concentration as variables and mean velocity of flow as the dependent variable. The dimensionless correlation presented by Hughmark is

$$\frac{V_c}{\sqrt{gD}} = f\left(C_v\left(\frac{\rho_p - \rho_l}{\rho_l}\right)F_d \right) \qquad [25]$$

where F_d : correction factor for particle diameter (F_d is 1 for 0.0145 inch < d_p < 0.08 inch) and f represents the function. The value of V_c could calculated from a graph of $\frac{V_c}{\sqrt{gD}}$ and $C_v\left(\frac{\rho_p - \rho_l}{\rho_l}\right)F_d$ by Hughmark (1961).

Hughmark made the following conclusions from the data collected

- The mean velocity of the flow at which all the particles are in suspension is independent of pipe diameter between 0.5 and 3 inches.
- The mean velocity of flow at which all the particles are in suspension is independent of particle size for particle sizes from 0.0145 to 0.08 inches.

2.1.10 Charles (1970) Correlation

Charles (1970) developed a correlation for the critical velocity defined as the velocity at which solid particles are deposited at the bottom of the pipe. Charles, following the fact that the minimum pressure gradient corresponds to the velocity at which particles begin to deposit, developed an equation to predict pressure gradients starting with Durand and Condolios' (1952) equation to correlate pressure gradients. By differentiating mixture pressure gradients with respect to the average velocity, he proposed the correlation to predict mean critical velocity V_c.

$$V_c = \frac{4.80 C_v^{1/3}\left(gD(s-1)\right)^{1/2}}{C_D^{1/4}\left(C_v(s-1)+1\right)^{1/3}} \qquad [26]$$

where s is ratio between particle and fluid density, and C_D was calculated by:

$$C_D = \frac{4gd_p(s-1)}{3u_t^2} \qquad [27]$$

2.1.11 Oroskar and Turian (1980) Correlation

Oroskar and Turian (1980) developed a correlation for critical velocity, V_c, defined as the minimum velocity demarcating flows in which the solids form a bed at the bottom of the pipe from fully suspended flows based on force balance and turbulence theory. With some assumptions, they developed Equation [27].

$$\frac{V_c}{\sqrt{gd_p(s-1)}} = \left\{ 5C_v(1-C_v)^{2n-1}\left(\frac{D}{d_p}\right)\left(\frac{D\rho_l\sqrt{gd_p(s-1)}}{\mu_l}\right)^{1/8}\frac{1}{x}\right\}^{8/15} \qquad [28]$$

where n is the exponent for hindered settling, and x is the fraction of eddies which having greater velocity than particle settling velocity.

Based on 357 data points collected from the literature, they modified their original equation as

$$\frac{V_c}{\sqrt{gd_p(s-1)}} = 1.85C_v^{0.1536}(1-C_v)^{0.3564}\left(\frac{d_p}{D}\right)^{-0.378}\left(\frac{D\rho_l\sqrt{gd_p(s-1)}}{\mu_l}\right)^{0.09}x^{0.30} \qquad [29]$$

$$x = \frac{2}{\sqrt{\pi}}\left\{\frac{2}{\sqrt{\pi}}\gamma e^{-4\gamma^2/\pi} + \int_{\gamma}^{\infty} e^{-4\gamma^2/\pi}d\gamma\right\} \qquad [30]$$

where $\gamma = \frac{u_{\text{hinder-settling}}}{V_c}$ (ratio of hindered settling velocity to critical velocity) and $u_{\text{hindered –settling}}=u_t\cdot(1\text{-}C_v)^n$. Based on the experimental data, Oroskar and Turian found x close to be unity (> 0.95).

2.1.12 Wani (1982) Correlation

Wani et al. (1982) developed a correlation for the critical velocity (defined as the mean flow velocity required to prevent the accumulation of a layer of stationary or sliding particles at the bottom of a horizontal pipe) in multi-size particle transport through pipes. Wani et al. collected a wide range of data from the literature and classified them into two groups based on their particle settling velocity with one group having particle settling velocities in the Stokes range and the other having particle settling velocities in the intermediate range, and then they developed equations to predict critical velocities in the Stokes range and intermediate range assuming that the Froude number of the particles is a function of the Reynolds number of the slurry at critical velocity, size distribution of solids, concentration of solids, and roughness of the pipe surface.

$$Fr_{\text{modified}} = \frac{V_C}{gd_w(s-1)} \qquad [31]$$

where

Fr_{modified} : modified Froude number

$$Fr_{modified} = 2.3\times10^{-4}\left(Re_p\right)^{0.27}\left(C_{OV}\right)^{0.973}(C)^{1.67}\left(C_V\right)^{0.307} \quad ; \text{ for } Re_p < 1$$

$$Fr_{modified} = 7.7\times10^{-6}\left(Re_p\right)^{0.0014}\left(C_{OV}\right)^{-1.25}(C)^{4.77}\left(C_V\right)^{0.272} \; ; \text{ for } 1<Re_p<1000$$

where Re_p : particle Reynolds number

C_{OV} : percent coefficient of variation

$$C_{OV} = \frac{100\sigma}{d_w}$$

σ : standard deviation particle sizes, m

d_w : weighted mean particle diameter, m

C : Hazen-Williams pipe roughness factor

2.1.13 Davies (1987) Correlation

Davies (1987) developed a theoretical equation based on simple turbulence theory for minimum mean flow velocity, V_m, defined as the velocity required to suspend particles in horizontal pipe flow, similar to the Durand correlation (1952). As a first step of his approach, Davies calculated the sedimentation force and the eddy fluctuation force. He considered that the sedimentation force was equal to the eddy fluctuation force when all the particles are suspended in the flow by eddies.

$$\frac{\pi}{6}d_p^3\Delta\rho g(1-C_v)^n = \rho_l\left(v'\right)^2\left(\pi d_p^2/4\right) \qquad [32]$$

From the above equation, the eddy fluctuation velocity necessary to suspend particles is derived

$$v' = 0.82\left(1-C_v\right)^{n/2}d_p^{1/2}\left[\Delta\rho g/\rho_l\right]^{1/2} \qquad [33]$$

The final attempt is to relate the eddy fluctuation velocity, v', to the critical flow velocity, V_c. Davies calculated v' as a function of eddy length and the power dissipated per unit mass of fluid, P_M, assuming that only the eddies which are of a particle size are active in suspending the particles as smaller eddies will not be able to lift the particles and larger eddies cannot be present close to the bottom of the pipe where some particles are suspended.

$$\left(v'\right)^3 = P_M d_p \qquad [34]$$

$$P_M = 2fV_c^3/D \qquad [35]$$

Davies considered the Fanning friction factor $f = \frac{0.079}{Re^{1/4}}$ and obtained

$$v' = \left(0.16\right)^{1/3}\nu_l^{1/12}V_c^{0.92}d_p^{1/3}D^{-0.42} \qquad [36]$$

Combining Equation 32-35 and introducing the turbulence correction factor $\left(\frac{1}{1+3.64C_v}\right)$ given by Davies, the final form of the equation for minimum mean flow velocity to suspend particles is obtained.

$$V_c = 1.08(1+3.64C_v)^{1.09}(1-C_v)^{0.55n}\nu_l - 0.09 d_p^{0.18}\left[\frac{2g(\rho_p - \rho_l)}{\rho_l}\right]^{0.54} D^{0.46} \qquad [37]$$

2.1.14 Kokpinar and Gogus (2001) Correlation

Kokpinar and Gogus (2001) proposed an empirical equation to predict critical velocity. They defined critical velocity as the velocity below which deposits will occur but above which no deposits in the pipeline will be encountered. As their first step, they assumed critical velocity as a function of solid density, ρ_p, particle diameter, d_p, fluid density, ρ_l, dynamic viscosity, μ_l, volumetric concentration of solid particles, C_v, pipe diameter, D, particle settling velocity in mixture flow, u_t, and gravitational acceleration, g. They used their data and the data from Graf et al. (1971), Durand (1952), Yotsukura (1961), Wicks (1971) and Sinclair (1962), and came up with the relation:

$$\frac{V_c}{\sqrt{gD}} = 0.055\left(\frac{d_p}{D}\right)^{-0.6} C_v^{0.27}(s-1)^{0.07}\left(\frac{\rho_l u_t d_p}{\mu_l}\right)^{0.30} \qquad [38]$$

2.1.15 Al-Mutahar (2006) Correlation

Al-Mutahar (2006) developed a mechanistic model for critical deposition velocity, defined as the minimum flow stream velocity needed for keeping sand particles in suspension in pipe flow to prevent sand deposition, based on a force balance and turbulent theory approach used by Davies (1987) and Oroskar and Turian (1980). Al-Mutahar developed his model in three steps. In the first step, the required turbulent velocity fluctuation necessary to keep the particles in suspension is calculated and then the turbulent velocity fluctuation generated by the flow is evaluated. Finally, with the assumption that the required and produced turbulent velocity fluctuations should be equal in order to keep the particles in suspension, he presented his final form of the critical deposition velocity, $V_{c,}$

$$V_c = 5.66\left[f(C_v)\sqrt{d_p g(s-1)}\right]^{8/7}\left(\frac{D\rho_l}{\mu_l}\right)^{1/7}\left(\frac{1}{\Omega}\right)^{8/7} \qquad [39]$$

where $\Omega = \frac{1}{1+3.64C_v}$, for higher concentrations (>1%) (as proposed by Davies), and

$\Omega = \frac{1}{0.5(1+3.64C_v)}$, for concentration around 1% and lower

2.2 Multiphase Sand-Gas-Liquid Flow in Pipeline

2.2.1 General Concept in Multiphase Flow

The multiphase flow is defined as the mixture of two or more distinct phases (such as oil, water, and gas) flowing through a closed conduit. The behaviour for multiphase flow is much more complex than that for single phase flow. The different phases tend to separate because of the density difference. Viscous resistance at the pipe wall are different for each phase as a result of their different densities and viscosities. In addition, different phases normally do not travel at the same velocities. The difference in the situ average velocities among different phases results in a very important phenomena, which is the "slip" of one phase relative to others (Sidsel et al., 2005).

For gas-liquid flow, the superficial velocity of the liquid, V_{SL}, and superficial velocity of gas, $V_{SG,}$ are defined as the volumetric liquid or gas flow rate (Q_L or Q_G) divided by the pipe cross sectional area, A.

$$V_{SL} = Q_L/A \qquad V_{SG} = Q_G/A \qquad [40]$$

The mixture velocity, V_m is given by the sum of superficial liquid and gas velocities:

$$V_m = V_{SL} + V_{SG} \qquad [41]$$

The "Holdup" of phase can be defined as the fraction of pipe volume occupied by a given phase. In practice, "liquid holdup" is usually defined as the in situ liquid volume fraction, while "void fraction" is used for the in-situ gas volume fraction.

The most distinguishing aspect of multiphase flow is variation in the physical distribution of the phases in the pipe flow, a characteristic known as flow pattern or flow regime. The flow regime depends on the relative magnitudes of the forces acting on the fluids. These forces such as buoyancy, turbulence, inertia and surface-tension forces, which vary significantly with flow rates, pipe diameter, pipe inclination and fluid properties.

There are some generally accepted descriptions for gas-liquid flow regimes. Concentrating on horizontal and near horizontal pipes, Hubbard (1966) suggested three basic flow regimes: segregated, intermittent and distributed flow. The gas/liquid flow regimes in horizontal pipes are depicted in Figure 7.

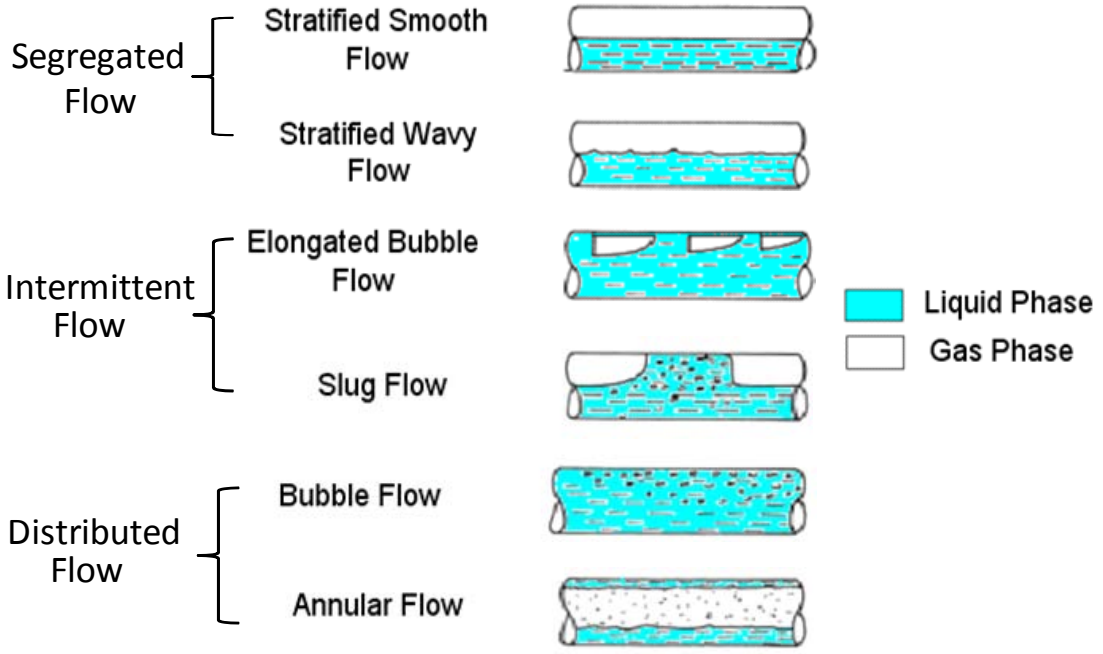

Figure 7: Liquid/gas flow regimes in horizontal pipelines (Hubbard, 1966)

- **Segregated Flow**

  - Smooth Stratified Flow:

    The plugs coalesce to produce a continuous gas flow along the top of the pipe with the smooth gas-liquid interface typical of stratified flow.

  - Wavy Stratified Flow:

    In real situations, the gas-liquid interface is rarely smooth, and ripples appear on the liquid surface. Wavy flow occurs as ripples, this is due to the gas flowing along the top of the pipe increasing in amplitude with increased gas flow rate.

- **Intermittent Flow**

  - Elongated Bubble Flow:

Collisions between the individual bubbles occur more frequently with increasing gas flow rate and they coalesce into elongated bubble (plugs). This is also called plug flow.

  - Slug Flow:

When the amplitude of the waves travelling along the liquid surface becomes sufficiently large enough for them to bridge the top of the pipe, the flow enters the slug

flow regime. The gas flows as intermittent slugs, with smaller bubbles entrained in the liquid.

- **Distributed Flow**

  - Bubble Flow:

In bubble flow, small gas bubbles flow along the top of the pipe.

  - Annular Flow:

This flow regime occurs when gas flow rate is large enough to support the liquid film around the pipe walls. Liquid is also transported as droplets distributed throughout the continuous gas stream flowing along the centre of the pipe. The liquid film is thicker along the bottom of the pipe because of the effect of gravity

2.2.2 Empirical Correlations for Pressure Drop in Air-Water Flow

The determination and prediction of pressure drop in multiphase flow are vital to the design of industrial transport systems and in chemical or petroleum process. Accurate prediction of pressure drop in multiphase pipeline is of great economic importance but has proved to be very difficult. In this section, several empirical correlations for pressure drop prediction are summarized.

The total pressure drop for given steady state two-phase flow is the sum of pressure drop due to kinetic energy (acceleration) effects, hydrostatic (elevation) effects and fluid friction effects:

$$\left|\frac{\Delta P}{\Delta x}\right|_{Total} = \left|\frac{\Delta P}{\Delta x}\right|_{Kinetic} + \left|\frac{\Delta P}{\Delta x}\right|_{Hydrostatic\ Head} + \left|\frac{\Delta P}{\Delta x}\right|_{Friction} \quad [42]$$

In steady, fully developed, isothermal flow of an incompressible fluid in a straight pipe of constant cross section, friction has to be overcome as does the static head, unless the pipe is horizontal. However there is no change of momentum and consequently the accelerative term is zero.

- Homogenous flow model

The simplest methods of two-phase flow prediction are the homogenous models. It is assumed that the two-phase flow can be treated as a hypothetical single-phase flow having some kind of average properties. An early example of a homogenous model was that by McAdams et al. (1942) which used values of the mixture density and viscosity to calculate the two-phase pressure gradient using single phase friction correlations.

- Separated flow model (flow-regime independent)

An alternative approach is the use of separated flow methods, where the flow of each phase is considered independently and then a procedure is applied to arrive at the result for the two phase mixture. The traditional method is to predict multiphase flow parameters by fitting correlations to large sets of experimental data. The relationships thus obtained are not easily extended to conditions which are physically very different from the original experimental systems. Therefore, correlations obtained in this way are regardless of the air-water flow regimes and have been used as closure for simplified phenomenological models.

In the separated flow models, the two-phase frictional pressure gradient is calculated from a reference single-phase frictional pressure gradient $|\Delta P/\Delta x|_{iO}$ with multiplying by the two-phase multiplier Φ_i^2, the value of which is determined from empirical correlations:

$$\left|\frac{\Delta P}{\Delta x}\right|_{Friction} = \Phi_i^2 \left|\frac{\Delta P}{\Delta x}\right|_{iO} \qquad [43]$$

where i is L or G (i.e. LO denotes liquid only and GO is gas only).

The most famous example of separated flow methods is undoubtedly the work by Lockhart & Martinelli (1949) who proposed a graphical correlation for the prediction of pressure drop and liquid holdup. The experimental work on which the correlation is based was done for horizontal flow of air-liquid mixtures at near-atmospheric pressures and with no change of phase. It is inadvisable to use the correlation for other conditions. For the conditions employed, the accelerative component of the pressure gradient was assumed to be negligible, while the static head component vanishes. They used 'only liquid' and 'only gas' reference flows and, having derived equations for the frictional pressure gradient in the two-phase flow in terms of shape factors and equivalent diameters of the portions of the pipe through which the phases are assumed to flow, argued that the two-phase multipliers Φ_L^2 and Φ_G^2 could be uniquely correlated against the ratio X^2 of the pressure gradients of the two reference flows.

The two-phase multiplier was also applied by other researchers (Friedel, 1979; Gronnerud, 1979; Müller and Heck, 1986). All empirical correlations for pressure drop prediction base on separated flow methods are listed in Table 2:

Table 2: Summary of empirical correlations for pressure drop prediction base on separated flow methods

Researcher	Correlation	Multiplier	Parameters
Lockhart & Martinelli (1949)	$\left\|\frac{\Delta P}{\Delta x}\right\|_{Friction} = \Phi_L^2 \left\|\frac{\Delta P}{\Delta x}\right\|_{LO}$	$\Phi_L^2 = 1 + \frac{C}{X} + \frac{1}{X^2}$ $Re_L > 4000$	$X = \left(\frac{1-x_g}{x_g}\right)^{0.9} + \left(\frac{\rho_g}{\rho_l}\right)^{0.5} + \left(\frac{\mu_g}{\mu_l}\right)^{0.1}$ $x_g = \frac{m_g}{m_g + m_l}$
Friedel (1979)	$\left\|\frac{\Delta P}{\Delta x}\right\|_{Friction} = \Phi_L^2 \left\|\frac{\Delta P}{\Delta x}\right\|_{LO}$	$\Phi_L^2 = E + \frac{3.24FH}{Fr_m^{0.045} We_m^{0.035}}$	$E = (1-x_g)^2 + x_g^{\,2} \frac{\rho_l f_g}{\rho_g f_l}$ $F = (1-x_g)^{0.224} + x_g^{\,0.78}$ $H = \left(\frac{\rho_l}{\rho_g}\right)^{0.91} \left(\frac{\mu_g}{\mu_l}\right)^{0.19} \left(1 - \frac{\mu_g}{\mu_l}\right)^{0.7}$ $We_m = \frac{(m_g + m_l)^2 D}{\sigma_l \rho_m}$
Gronnerud (1979)	$\left\|\frac{\Delta P}{\Delta x}\right\|_{Friction} = \Phi_G^2 \left\|\frac{\Delta P}{\Delta x}\right\|_{LO}$	$\Phi_G^2 = 1 + \left\|\frac{\Delta P}{\Delta x}\right\|_{Fr} \left(\frac{\rho_l}{\rho_g} \frac{\mu_l^{0.25}}{\mu_g} - 1\right)$	$\left\|\frac{\Delta P}{\Delta x}\right\|_{Fr} = f_{Fr}\left[x_g + 4\left(x_g^{\,1.8} - x_g^{\,10} f_{Fr}^{\,0.5}\right)\right]$ for $Fr_{LO} < 1$, $f_{Fr} = Fr_{LO}^{0.3} + 0.0055\left[\ln\left(\frac{1}{Fr_{LO}}\right)\right]^2$ for $Fr_{LO} \geq 1$, $f_{Fr} = 1$
Müller and Heck (1986)	$\left\|\frac{\Delta P}{\Delta x}\right\|_{Friction} = K(1-x_g)^{1/3} + \left\|\frac{\Delta P}{\Delta x}\right\|_{GO} x_g^{\,3}$	$K = \left\|\frac{\Delta P}{\Delta x}\right\|_{LO} + 2x_g\left(\left\|\frac{\Delta P}{\Delta x}\right\|_{GO} - \left\|\frac{\Delta P}{\Delta x}\right\|_{GO}\right)$	

where x_g is the vapour quality, σ_l is liquid surface tension, m_g and m_l are gas and liquid mass flowrate respectively. We_m is the mixture Weber Number, whereas Fr_m and ρ_m denotes the mixture Froude Number and density, which are defined as:

$$Fr_m = \frac{V_m^2}{gD} \quad [44]$$

$$\rho_m = \left(\frac{x_g}{\rho_g} + \frac{1 - x_g}{\rho_l} \right)^{-1} \quad [45]$$

The pressure gradient for a single-phase flow is given by:

$$\left| \frac{\Delta P}{\Delta x} \right|_{iO} = \frac{2 f_i \rho_i V_{Si}}{D} \quad [46]$$

where f is the Fanning friction factor and i denotes L and G to represent liquid and gas phase respectively.

- Models based on flow regime map (Beggs & Brill ,1973)

A limited number of pressure drop correlation incorporate a crude method of determining the flow pattern from the value of a parameter based on the phase velocities. The pressure drop correlation of Beggs & Brill (1973), used widely in the hydrocarbon industry, uses this method and is described in this section.

Beggs & Brill (1973) developed flow pattern-specific correlations to deal with both the friction pressure loss and the hydrostatic pressure difference. The appropriate flow regime for the particular combination of gas and liquid rates (Segregated, Intermittent or Distributed) is determined initially. The liquid holdup, and hence, the in-situ density of the gas-liquid mixture is then calculated according to the appropriate flow regime, to obtain the hydrostatic pressure difference. A two-phase friction factor is calculated based on the "input" gas-liquid ratio and the Fanning friction factor. From this the frictional pressure loss is calculated using "input" gas-liquid mixture properties.

The method for determination of air-water flow regime and the parameters required are listed in Table 3:

Table 3: Determination method of air-water flow regime using Beggs and Brill (1973) correlation

Determining flow regimes	Flow pattern	ε_{L0}	Parameters calculation
$\varepsilon_L<0.01 \& Fr_m < L1$ or $\varepsilon_L \geq 0.01 \& Fr_m < L2$	Segregated (Stratified/wavy)	$\frac{0.98\varepsilon_L^{0.4846}}{Fr_m^{0.0868}}$	$Fr_m = \frac{V_m^2}{gD}$ $\varepsilon_L = \frac{V_{SL}}{V_m}$ $L1=316\,\varepsilon_L^{0.302}$ $L2=0.0009252\,\varepsilon_L^{-2.4684}$ $L3=0.1\,\varepsilon_L^{-1.4516}$ $L4=0.5\,\varepsilon_L^{-6.738}$
$0.01<\varepsilon_L<0.4 \& L3<Fr_m \leq L1$ or $\varepsilon_L \geq 0.4 \& L3<Fr_m \leq L4$	Intermittent (plug/slug)	$\frac{0.845\varepsilon_L^{0.5351}}{Fr_m^{0.0173}}$	
$\varepsilon_L<0.4 \& Fr_m \geq L1$ or $\varepsilon_L \geq 0.4 \& Fr_m > L4$	Distributed	$\frac{1.065\varepsilon_L^{0.5824}}{Fr_m^{0.0609}}$	
$\varepsilon_L \geq 0.01 \& L2<Fr_m< L3$	Transition	$\left(\frac{L3-Fr_m}{L3-L2}\right)\frac{0.98\varepsilon_L^{0.4846}}{Fr_m^{0.0868}} - \left(\frac{Fr_m-L2}{L3-L2}\right)\frac{0.845\varepsilon_L^{0.5351}}{Fr_m^{0.0173}}$	

ε_L and ε_{L0} are the no-slip and actual liquid holdup in horizontal pipe. The liquid holdup at any pipe inclination, $\varepsilon_{L\beta}$ is then calculated:

$$\varepsilon_{L\beta} = \varepsilon_{L0}\left(1 + C\left(\sin 1.8\beta - \frac{\sin^3(1.8\beta)}{3}\right)\right) \qquad [47]$$

where β is the pipe inclination from the horizontal, in radians.

The two-phase density, ρ_{TP} (lb/ft^3), and the two-phase friction factor, f_{TP} is then calculated

$$\rho_{TP} = \rho_l \varepsilon_{L\beta} + \rho_g (1 - \varepsilon_{L\beta}) \quad [48]$$

$$\frac{f_{TP}}{f_{NS}} = \exp(S) \quad [49]$$

Here, f_{NS} is the no-slip friction factor and S is a liquid holdup parameter:

$$f_{NS} = \left(2\log_{10}\left(\frac{Re_{NS}}{4.5223\log_{10} Re_{NS} - 3.8215} \right) \right) \quad [50]$$

The "no slip" Reynolds number, Re_{NS}, is given by:

$$Re_{NS} = \frac{(\rho_g V_{SG} + \rho_l V_{SL})D}{\mu_l \varepsilon_L + \mu_g (1 - \varepsilon_L)} \quad [51]$$

The value of S is governed by the following conditions:

$$S = \ln(2.2y - 1.2) \qquad 1 < y < 1.2 \quad [52]$$

$$S = \frac{\ln(y)}{-0.0523 + 3.182\ln(y) - 0.8725[\ln(y)]^2 + 0.01853[\ln(y)]^4} \quad y \le 1 \text{ or } y \ge 1.2 \quad [53]$$

where y is calculated by

$$y = \frac{\varepsilon_L}{\varepsilon_{L\beta}^{\ 2}} \quad [54]$$

Finally, the friction pressure gradient (psi) is calculated:

$$\left| \frac{\Delta P}{\Delta x} \right|_{Friction} = \frac{2 f_{TP} V_m^{\ 2} \rho_{TP}}{144 g_c D} \quad [55]$$

where g_c is conversion factor =32.2lb$_m$·ft/(lb$_f$·s^2)

2.2.3 Sand-Gas-Liquid Flow Regimes

Since the sand particles are heavier than the carrying fluids they are usually transported along the bottom of the pipe when the concentration is low. For this reason the flow patterns observed in single phase sand/liquid flow are similar to those seen in stratified liquid/gas/sand flow since the liquid occupies the lower part of the pipe and the flowing velocity is steady. However this is not the case when the gas/liquid flow regime is plug or slug flow, as the depth of the film and the velocities vary.

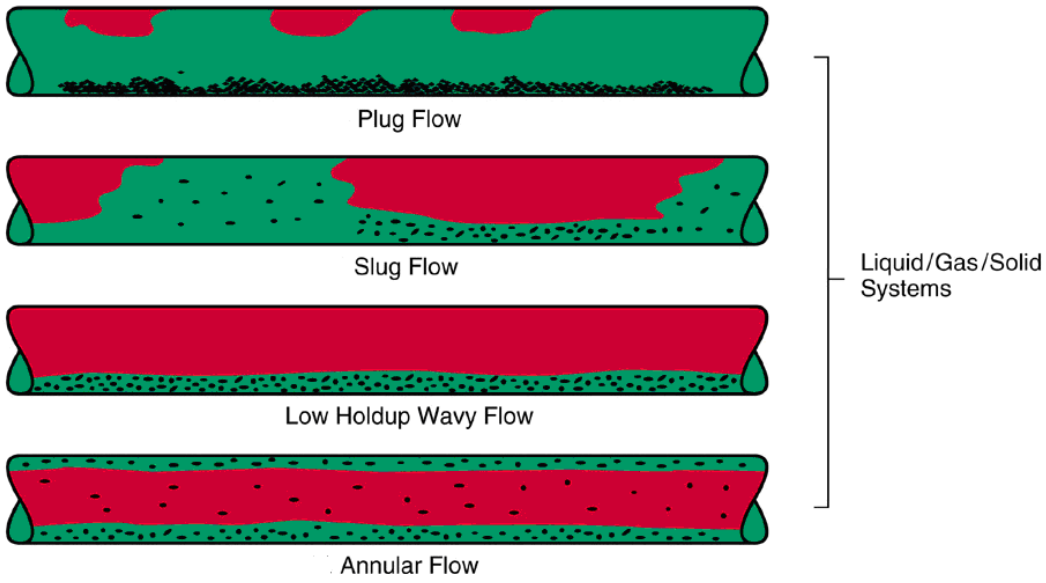

Figure 8: Sand/liquid/gas flow regimes in horizontal pipelines (Multiphase Design Handbook , 2005)

- **Plug flow**

In plug flow, the gas bubbles move along the top of the pipe and have little effect on the sand flow. As the amount of gas is increased the bubble depth increases and the fluctuating velocities affect the transport similar to that described in slug flow.

- **Slug flow**

In slug flow the transport of sand is complicated as the sand may settle during the passage of the film region and may be transported in the slug body. There can be a large diameter effect as the depth of the film varies and shields the bottom of the pipe from the turbulence of the slug. A bed can be formed if either the slug or film does not transport the sand. In cases where the sand is transported in the slug, only the motion is intermittent. The frequency between slugs may be a factor if bed compaction and stabilization by other products is a possibility.

- **Low holdup wavy flow**

In wet gas pipelines the liquid can be transported as a thin film along the bottom of the pipe, in which case the sand concentration in the film can be high, and in the extreme may appear as a wet sand bed. In this case little is known about the conditions required to remove the wet sand.

- **Annular flow**

In annular flow the sand may be transported in the liquid film and the gas core. Since the velocities are high in annular flow the usual concern is whether the erosion rate is excessive rather than if the sand will be transported or not.

2.2.4 King, Fairhurst and Hill (2000) Model

King et al. (2000) developed a model, namely "minimum transport pressure drop model", which is an extension on Thomas's solid/liquid equations (Thomas, 1962) for predicting minimum transport conditions in two phase air-water flow.

Thomas named a "lower model" that assumed the particle size, d_p, is smaller than the laminar sub-layer, δ, and an "upper model" that assumed the particle size is greater than the laminar sub-layer. The frictional velocities can be calculated using Thomas (1962) equations as follows:

Lower Model

$$u_0^* = \left[100 u_t \left(\frac{\nu_l}{d_p} \right)^{2.71} \right]^{0.269} \qquad [56]$$

Upper Model

$$u_0^* = \left[0.204 u_t \left(\frac{\nu_l}{d_p} \right) \left(\frac{\nu_l}{D} \right)^{-0.6} \left(\frac{\rho_p - \rho_l}{\rho_l} \right)^{-0.23} \right]^{0.714} \qquad [57]$$

From the fiction velocity, King et al. calculated the associated friction pressure drop at MTC in the fluid instead of the minimum transport velocity. The frictional pressure drop can be calculated based on the definition of the friction velocity as given by the equation:

$$\left| \frac{\Delta P}{\Delta x} \right|_{MTC} = \frac{4 \rho_l (u_0^*)^2}{g_c D} \qquad [58]$$

where the pressure is gives as (psi/ft)

If the actual pressure drop (ACPD) is greater than the pressure drop at the minimum transport condition (MTC), then the solids will be transported.

Using the ΔP_{King} as the pressure drop gradient at MTC for solid transport in single phase flow, a locus of points (triangle in the figures below) can be plotted on a two phase flow pattern map (e.g. Beggs and Brill flowmap), which indicates $\Delta P_{Beggs\&Brill} \cong \Delta P_{King}$. This series of points can be used as a design guide, where any liquid/air superficial velocity above the boundary should allow transport of the solids along the pipeline, as shown in Figure 9 and Figure 10:

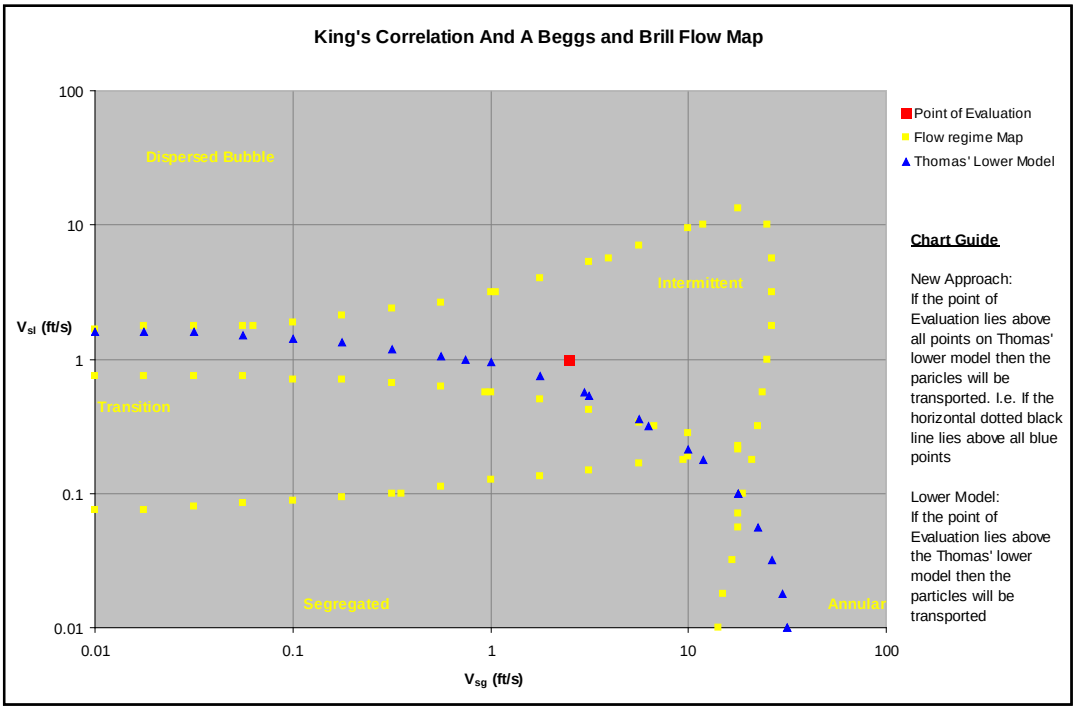

Figure 9: Evaluation point where sand particles transported

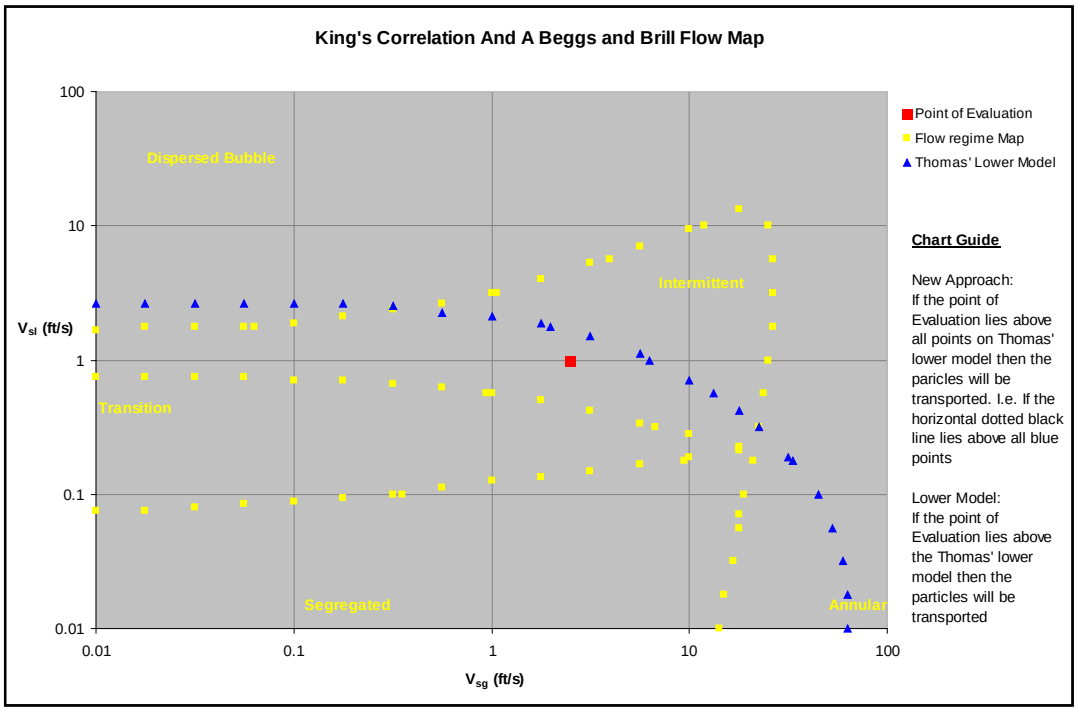

Figure 10: Evaluation point where sand particles not transported

2.2.5 Angelsen (1989) Model

Angelsen et al. (1989) conducted a set of experiments in 1 inch and 4 inch test loops with sand sizes of 30, 100, 200 and 500 microns. The range of flowrates were, water: 0 to 9 $m \cdot s^{-1}$, gas: 0 to 30 $m \cdot s^{-1}$ in 1 inch pipe and water 0 to 1 $m \cdot s^{-1}$, air: 0 to 30 $m \cdot s^{-1}$ in 4 inch pipe, to find whether or not a sand bed is formed for a given flow. They found that the stratified flow regime was the most critical flow regime with respect to the sand deposition. They also found sand also deposited for intermittent flow conditions, especially at low liquid and gas superficial velocities.

They also extended the Wicks' model (1971) by defining a characteristic liquid velocity and diameter for the liquid-particle system to account for the sand transport characteristics in air-water flow.

Wicks (1971) developed a correlation based on the experimental data to estimate the sand hold up assuming that a stationary sand particle at the bed surface is in contact with at least three other particles in a stable tripod type of support. The particle must be rolled out of this position before any net motion started. For this to happen, the moments of the forces about downstream contact point tending to cause downstream rotation must exceed the moments of forces opposing downstream rotation. After force balance analysis, Wicks proposed the criterion for onset of rotation:

$$F_B(1.44\sin\beta+\cos\beta) + F_L + 1.44F_D = F_G(1.44\sin\beta+\cos\beta) \qquad [59]$$

where β is pipe inclination angle. By analyzing the dependence of the forces in the flow, above criterion was expressed as:

$$S \times \Psi = 1 \quad [60]$$

$$S = \frac{1}{8}\left(C_D + 1.44 C_L\right)\phi^2 \quad [61]$$

$$\Psi = \frac{\rho_l^3 d_p V_c^4}{\left(\rho_p - \rho_l\right) g \mu_l^2} \quad [62]$$

where C_D and C_L are drag and lift coefficient respectively, and ϕ is a function of the Reynolds number and particle diameter to pipe diameter ratio (d_p/D). Therefore, Wicks proposed another dimensionless group for S

$$S = \frac{D_{EQ} V_c \rho_l}{\mu_l}\left(\frac{d_p}{D}\right)^{2/3} \quad [63]$$

when D_{EQ} is hydraulic equivalent diameter, calculated by

$$D_{EQ} = 4A_L/S_L \quad [64]$$

where A_L denotes the cross-sectional area occupied by liquid phase and S_L is the wetted perimeter by liquid.

By implementing experimental data in above equation Wicks plotted S versus Ψ in a Log-Log diagram and found the relation:

$$\Psi = 0.1S^3 \qquad S < 40 \quad [65]$$

$$\Psi = 100S^{3/2} \qquad S > 400 \quad [66]$$

Angelsen et al.(1989) considered stratified smooth or wavy flow and calculated the mean liquid velocity, u, and hydraulic equivalent diameter, D_{EQ}, and they used V_L as full pipe velocity and D_{EQ} as pipe diameter in Wicks model.

$$S = \frac{D_{EQ} u \rho_l}{\mu_l}\left(\frac{d_p}{D}\right)^{2/3} \quad [67]$$

where

$$u = \frac{V_{SL}}{\varepsilon_L} \quad [68]$$

He also stated that this model can be used for liquid-particle, gas-particle and three-phase flows simultaneously.

2.2.6 Oudeman (1993) Correlation

Oudeman (1993) conducted a series of experiments on sand transport in two-phase flow and came up with a correlation by defining two dimensionless parameters, sand transport rate and fluid flow rate. He started his experiments with a stationary bed and

moved on to different sand transport regimes by increasing the liquid or gas velocities. From observations, he classified the sand transport into three regimes (Figure 11): stationary bed (sand deposits at the bottom of the pipe and forms a stationary sand bed), moving bed (above certain critical velocity, the stationary bed starts moving as dunes and then as a continuous bed as velocity increases), and suspension (with increasing velocity the sand particles start suspending in the fluid and with further increase in the velocity all the particles are suspended in the flow).

Experiments were carried out in a 0.07 m internal diameter test section. Sand particle sizes of 150 microns to 300 microns and 690 microns with gas volume fractions of 0 to 0.2 and liquid velocities between 0.1 $m \cdot s^{-1}$ and 1.2 $m \cdot s^{-1}$ were used. The concentrations used for testing were not mentioned. To monitor the effect of viscosity, tests were conducted with water viscosified to 7 cP (carboxymethyl cellulose EHV was added to increase the viscosity of water).

From observations, he made the following conclusions:

1. The transition from moving bed to suspension takes place at higher superficial velocities than the transition velocity from stratified wavy flow to slug flow and concluded that gas-liquid flow regime has no direct influence on the sand transport mode.

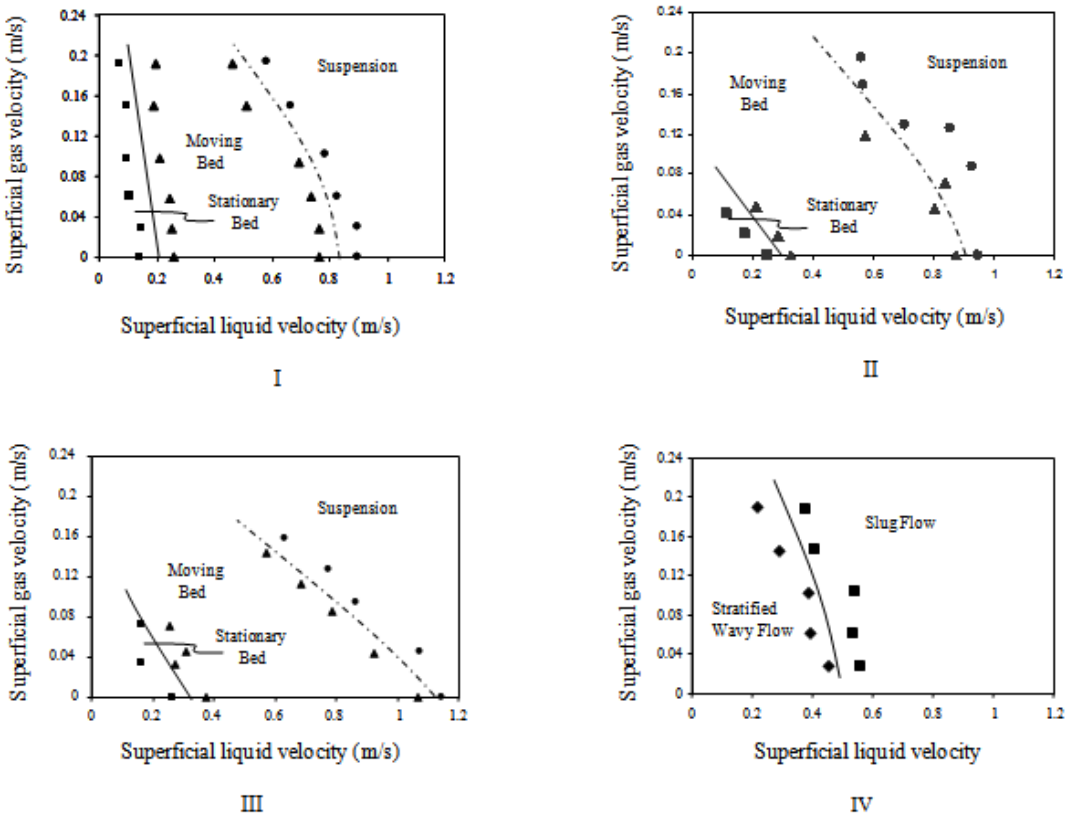

Figure 11: Experimental results from Oudeman (1993)

2. From Ⅱ and Ⅲ in Figure 11, Oudeman concluded that effect of liquid viscosity on

the sand transport is limited. For the viscosified water, the transition line between stationary bed and moving bed is more inclined compared to the transition line between stationary bed and moving bed for pure water. This means that for viscosified water the transition from stationary bed to moving bed occurs at lower superficial gas velocities with same superficial liquid velocity (less than 0.2 $m \cdot s^{-1}$) compared to that of pure water.

3. From Ⅱ and Ⅳ, it is clear that particle size had little influence on the transition from stationary bed to moving bed, but with larger sand particles the transition from moving bed to suspension occurs at higher superficial liquid velocities and decreases gradually with the increase in superficial gas velocities.

4. From Ⅲ and Ⅳ, one can observe that the gas fraction has a considerable influence on the transition from moving bed to suspension.

5. Oudeman also figured that the addition of surfactant to reduce the surface tension of the water has no influence on the sand transport regime boundaries.

A relationship between the dimensionless sand transport rate, φ_s, and the dimensionless liquid flowrate, Ψ_L, was established successfully:

$$\varphi_s = \frac{S'}{\sqrt{d_p{}^3 g\left(\frac{\rho_p}{\rho_l} - 1\right)}} \qquad [69]$$

$$\psi_L = \frac{U_b^2}{g d_p\left(\frac{\rho_p}{\rho_l} - 1\right)} \qquad [70]$$

where S' is transport rate in grain volume per second per metre of sand bed width, and U_b is fluid drag velocity at the sand bed, which can be derived for the mixture velocity, assuming a logarithmic velocity profile at the boundary layer. Oudeman followed the suggestion by Dallavlle (1948) who suggested that the dimensionless sand transport rate φ_s can be expressed as a function of the dimensioless liquid flowrate Ψ_L in the following equation:

$$\varphi_s = m\psi_L{}^n \qquad [71]$$

The values of (m) and (n) are experimentally derived constants, which will depend on the input gas fraction as listed in
Table **4**:

Table 4: Values of (m) and (n)

Gas Fraction %	m	n
0	220	3.6
10	75	2.8
20	67	2.5
Average of 10 and 20	70	2.7

2.2.7 Gillies (1997) Correlation

Gillies, McKibben and Shook (1997) extended the Meyer-Peter (1948) correlation, which models solids transport in single phase liquids, to apply to the transport of solids in multiphase systems. This model is very similar to the Oudeman's model as the equations used are comparable.

$$\varphi_s = \frac{q_s}{\left(\frac{\rho_p}{\rho_l}\right)\sqrt{d_p{}^3 g\left(\frac{\rho_p}{\rho_l}-1\right)}} \quad [72]$$

$$\psi_L = \frac{\rho_l g d_p\left(\frac{\rho_p}{\rho_l}-1\right)}{\tau_0} \quad [73]$$

$$\varphi_s = \left[\frac{4}{\psi_L} - 0.188\right]^{1.5} \quad [74]$$

where q_s is volumetric flow rate per bed width.

This model developed using experimental data of three-phase sand-air-liquid flow for the regime which a stationary deposit was present in horizontal pipelines with 2 inch diameter. The liquids employed in the experiments were water (density 998 $kg \cdot m^{-3}$, viscosity 1.0cP) and oil (density $872 kg \cdot m^{-3}$, viscosity 78cP) and liquid superficial velocity ranged from 0 $m \cdot s^{-1}$ to 1 $m \cdot s^{-1}$. The sand particle size ranged from 10 to 200

microns and GVF was between from 0 to 0.8. The axial pressure gradient and delivered concentrations were measured as functions of mean velocity and in-situ concentration.

They concluded that gas injection had a little influence on the ability of solid transportation at low liquid superficial velocity when the flow was laminar. However, if the flow was turbulent, the solids transport was enhanced. They also claimed that the Lockhart-Martinelli correlation provided reasonable estimates of the axial pressure gradient in the turbulent liquid flow regime at GVF below 0.5.

The disadvantages of Gillies' model are that it is only applicable to a small range of particle sizes and for moderate solids concentrations.

2.2.8 Salama (2000) Correlation

Salama (2000) developed a correlation for preventing sand bed deposition of a particle-laden flow, based on both Oroskar & Turian (1980) and Davies' (1987) model, which can be written in the following form:

$$V_m = K d_p{}^a \left(\frac{\mu_l}{\rho_l}\right)^b \left(\frac{\rho_p - \rho_l}{\rho_l}\right)^c D^d \qquad [75]$$

where a,b,c,d are the constants and K denotes the flow condition for air/liquid two phase flow.

A series of experiment were conducted on a 12m long 4 inch stainless steel flow loop covering the following parameters:

Sand particle size: 100, 280, 500 microns
Media: water, gas, oil, sand
Superficial liquid velocity: 0.03, 0.1, 0.2, 0.3, 0.4m·s^{-1}
Gas velocity: flow rate varied during test
Pressures: 4 and 8 bara
Temperature: ambient

By fitting the experimental data, Salama's model can be presented by:

$$V_m = \left[1.3\left(\frac{V_{SL}}{V_m}\right)^{0.53}\right] d_p{}^{0.17} \left(\frac{\mu_l}{\rho_l}\right)^{-0.09} \left(\frac{\rho_p - \rho_l}{\rho_l}\right)^{0.55} D^{0.47} \qquad [76]$$

where V_m is the mixture velocity to avoid sand settling (m·s^{-1}).

2.2.9 Stevenson (2000, 2001) Model

Most previous work in the related field of hydraulic conveying of solids has considered relatively high solids holdup, as it is uneconomical to transport solids (coal for instance) in a hydraulic pipeline at low holdup.

However, Stevenson et al. (2000, 2001) studied the behaviour of isolated grains in different flow regimes (intermittent and stratified flow) of multiphase flow, representing the low particle loading. Stevenson and Preston (1996) showed that sand holdup in a typical oil and gas flowline is likely to be <0.01v/v. Therefore, it is more pertinent to consider the behavior of isolated particles (that is, very low solids concentration) rather than moving beds of sand.

A series of experiments were conducted on transparent perspex pipe of 12 m in length and interchangeable internal diameters of 40 mm and 70 mm, which can be tilted up to 3^o to the horizontal. Liquids used were water and a solution of Rheovis CR2, an associative colloidal thickener (Allied Colloids Ltd.) with Newtonian rheology.

Pulses of approximately ten particles are introduced to the test pipe via a modified squeezable plastic wash bottle containing sand and water 3m downstream of the gas-liquid mixing section. The pulse of particles was seen to diffuse on entering the stream and little inter-particle interaction was observed as they progressed downstream. Particle velocity was measured by taking transit times of particles between starts and finish lines marked on the pipe. The observer would “spot” a particle, chosen at random, and follow it down the test section, timing the transit between start and finish lines by means of a stopwatch. This was repeated several times for each gas/liquid flow rate. Particle size ranged from 150 microns to 1000 microns.

The behaviour of small amount of sand particles was studied in intermittent flow and stratified flow also.

Stevenson et al. (2001) noticed similarities between the intermittent flow experiments and those conducted in hydraulic conveying and suggested that events at the slug nose may not be as significant as was previously thought by Stevenson and Preston (1996). Later on, they proposed an analogy between turbulent diffusions into the film and diffusion of turbulence in a slot jet, and developed a correlation based on the ratio between particle velocity and fluid superficial velocity by dimensional consideration. The threshold of critical velocity can be obtained by simple extrapolation. But they found that this extrapolation could not yield the accurate results for low concentration transport of sand due to enhanced turbulence at slug nose.

Therefore, in another paper, Stevenson and Thorpe (2003) performed a Lagrangian momentum and power balances across the slug nose in slug flow. The models were based on the long slug approximation; particle velocity was independent of slug length which is a notoriously difficult closure parameter to predict. The model considered the slug unit as part stratified flow and part hydraulic conveying.

They noted that despite the increased turbulence at the beginning of the slug, the particles did not necessarily move any easier. They suggested that particle transport in slug flow could be approximated by considering a hybrid model of particle transport in hydraulic conveying and in stratified flow. Other mechanistic models for particle transport in slug flow generally over-predict the experimental data of Stevenson. It is thought that as the data of Stevenson et al. (2000) was collected on a relatively short

pipe, it is unlikely that the slugs would have reached the stable state. This would make these models not applicable to industrial scale pipelines and so may not be of too much practical use.

2.2.10 Danielson (2007) Model

Danielson's (2007) experimental work aimed to study the critical condition of sand slurry flow under different fluid conditions:

- Gas phases: air, nitrogen, SF6
- Liquid phases: Exxsol D80, water
- Maximum pressure 8 bara
- Pipe diameter 0.069 m
- Loop length 215 m
- Maximum inclinations +1.35 to +4.0 degrees
- Superficial oil velocity 0.01-2 $m \cdot s^{-1}$
- Superficial water velocity 0.01-2 $m \cdot s^{-1}$
- Superficial gas velocity 0.1-8 $m \cdot s^{-1}$

Sand was injected into the flow as a dense slurry of sand in liquid (approximately 0.3 v/v) using a peristaltic pump. Water or Exxsol D80 were used for the liquid phases, and air was used as the gas phase. Sand used in the experiments had a median diameter of 280 and 550 microns.

Danielson also found that in the gas-liquid-solid experimental data the gas rate had no direct influence on the critical slip velocity between the sand and the carrier liquid. The liquid velocity can be a strong function of the pipe inclination angle in multiphase flow (particularly for wet gases), sand bed formation is also strongly correlated to pipe angle. This is a critical difference between liquid-solid (where pipe angle had negligible influence on sand bed formation) and gas-liquid-solid systems.

A model for critical solid-carrying velocity, $V_{C,}$ was developed by fitting to experimental data. The critical velocity in liquid-solid flow had no angle dependence over the range of angles investigated.

$$V_c = Kv^{-1/9} d_p^{1/9} (gD(s-1))^{5/9} \quad [77]$$

By assuming that the slip between the sand particle velocity, V_s, and carrier liquid velocity, V_{CL}, is maintained at V_C for all liquid rates,

$$V_{SLIP} = V_{CL} - V_S \quad [78]$$

$$V_C = V_{SLIP} \quad [79]$$

The model shows excellent fit to data, which indicated that when the carrier fluid velocity drops below this value, a sand bed begins to form. The bed height increases

until the cross-sectional area available to fluid flow is reduced enough to restore the fluid velocity over the bed back to the critical velocity, V_C.

The OLGA2000 code was used to determine the liquid velocity, V_{CL}, and an estimate of the sand hold-up by modeling sand as a pseudo-phase with a slip velocity equal to V_C. Good fit to data was obtained for both liquid-solid and gas-liquid-solid experiments using this approach.

2.3 Variables Affecting Solid Transportation

2.3.1 Sand Concentration

Hydraulic slurry transport had been investigated for nearly 50 years. The wide range of fluid and particle properties (particle size, fluid viscosity etc.) in different size of pipe has been studied. However, from the literature, the lower limit of solid concentration is 0.01v/v. In real oil pipelines, the sand C_v normally ranges from 0.00005 up to 0.0005v/v (50lb/1000bbl until 500lb/1000bbl), which has not been investigated by previous researchers, see Table 6.

Most of investigations in sand transport in multiphase system aimed to provide design criteria to avoid sand deposition in oil pipelines. However, very few models look at the effect of concentration of solids in the fluid. Instead, they focused on either the forces acting on an individual particle or with pre-set concentration (Table 5).

Table 5: Review of range of experimental variables for solid-air-water flow

Reference	Pipe (inch)	Particle Diameter (microns)	Particle Type	Cv
King et al. (2000)	1~4	255	Sand	0.00005 v/v
Angelsen et al. (1989)	1, 4	100, 200, 500	Sand	0.00003~0.0003 v/v
Oudeman (1993)	3	150, 300, 690	Sand	/
Gillies, McKibben and Shook (1997)	2	10~200	Sand	v/v of 0 ~0.30
Salama (2000)	1	150, 250	Sand	/
Stevenson et al. (2000, 2001)	1.5, 3	150, 1000	Sand	Isolated particle
Danielson (2007)	3	280, 550	Sand	0.0002v/v

Table 6: Review of range of experimental variables for solid-water flow

Reference	Pipe (inch)	Particle Diameter (microns)	Particle Type	Remarks
Ambrose (1953)	2 and 6	250	Quartz	Data From Craven (1953)
		580	Sand	
		1620	Sand	
Blatch (1906)	1	190	Sand	0.05 v/v
		584		
Craven (1953)	2 and 6	250	Quartz	
		580	Sand	
		1620	Sand	
Durand (1953)	1.5~28	200~2470	Sand and Gravel	v/v of 0.02~0.30
Durand and Condolios (1952)	1,4,5,6,10,13,23,27.5	up to nearly 102000	Coal, Ash, Sand and Gravel	v/v up to 0.15
Garde (1956)	12	200 and 600	Sand	
Howard (1962b)	2	10~400	Silt and Sand	
Howard (1939)	4	382	Sand	v/v of 0.27 ~0.29
		2520	Gravel	
Hughmark (1961)	0.5~28	66~1840	Boiled ash, Lime, Sand etc.	Data From Others
Newitt (1955)	1	203~5980	Perspex, Coal, Sand, Gravel	
Yufin (1949)	0.4~18	250~7360		0.3 v/v
Carins (1960)	0.75 ~ 2			v/v of 0.008 ~ 0.04
Yotsukura (1961)	4	231~1090	Bentonite Clay	
Sinclair (1962)		d85=0.6D~1500D		
Smith (1955)	2 and 3	203, 305, 1220	Sand	Mixed size
Spells (1955)	3~11.8	80~820	Lime, Boiler ash,Sand	Data from others, v/v of 0.28~0.36
Thomas (1962)	0.496~32	190~38000		v/v of 0.01 ~ 0.15
Weisman (1963)	0.5~24	12.5~2000	Sand, Steel, Glass etc.	v/v of 0.002~0.33
Worst (1952)	1	510~3200	Perspex, Coal, Sand, Gravel	Data from others
Zandi and Govators (1967)	1~24	100~12700		1452 points of data from others
Oroskar and Turian (1980)	v/v of 0.01~0.50, correlation derived from Turbulent Theory, others data also used,			
Wani (1982)	2~5	29.9~3875		Data from others, v/v of 0.05~0.12
Davis (1987)	Derived from Turbulent Theory, Other's data			
Kokpinar and Gogus (2001)	1~3	230~5340	Sand, Glass	Data from others, v/v of 0.01 ~ 0.30
Al-Mutahar (2006)	Correlation, derived from turbulent theory, Other's data			

2.3.2 Fluid Viscosity

Limited published work has been done to study the viscosity effect of the carrying fluid in slurry (Table 7).

From Table 7, the majority of these works were concentrated on low viscosity fluids. For sand transportation in multiphase system, the study of viscosity effect was also limited.

Fairhurst and Baker (1983) studied the viscosity effect by increasing the viscosity of the fluid to around 3 cP by adding glucose to the water. There was considerable scatter in the data and there appeared to be no effect of the increased viscosity compared to an air-water-sand system.

Oudeman (1993) also looked at a greater change in viscosity using a cellulose solution to increase the viscosity to 7 cP. He plotted the solid-fluid flow regime on traditional gas-liquid flow pattern map co-ordinates and the system was slightly less likely to form a stationary bed and was slightly more likely to form a suspension than the air-water system alone. Oudeman attributed the slight difference to the fact that the fluid is less likely to be able to erode the sand bed despite of the fact that it is more likely to be able to carry the particles.

Gillies et al. (1997) did research into using very viscous fluids. They used oil with a viscosity of 78 cP. The bulk flow in the pipe was in laminar regime throughout the experiments and the addition of gas (to make it a three-phase system) was found not to increase the ability of the fluid to transport the solids. The authors suggested that because of the high solids concentration in the region above the bed, the apparent viscosity there would be very high (more than ten times the liquid viscosity) and so the ability to transport solids would be very low. This was supported by their observation that very little sand was produced at the end of the test section. The threshold velocity for the transport of 100 microns sand was around 0.3 $m \cdot s^{-1}$, for 200 microns sand it was greater than 1 $m \cdot s^{-1}$. High pressure gradients (> 1.5 $KPa \cdot m^{-1}$) were required to transport the sand.

Gillies et al. (1994) was the only source of data for highly viscous fluids (up to 7500 cP). However this was for single-phase flow and not for a multiphase mixture. They noted that a stationary bed was never formed regardless of the velocity used. As soon as the pump was started, the sand was transported. This is a considerable deviation from the other studies performed with less viscous fluids for which bed formation played a significant role.

Table 7: Review of range of experimental variables for viscous fluids as a liquid carrier

Reference	Solid/Liquid	Solids C_v	Pipe Diameter (inch)	Particle mean diameter (microns)	Liquid density ($kg \cdot m^{-3}$)	Liquid viscosity $x10^{-3}$ ($kg \cdot m^{-1} \cdot s^{-1}$)
Shook et al. (1973)	sand/ethylene glycol	0.054	2	210	1096	5.79
Shook et al. (1973)	sand/ethylene glycol	0.053	2	210	1116.8	14
Shook et al. (1973)	sand/ethylene glycol	0.053	2	210	1116.8	14
Shook et al. (1973)	sand/ethylene glycol	0.0524	2	210	1132.6	38.1
Shook et al. (1973)	sand/ethylene glycol	0.0518	2	718	1121	21.4
Shook et al. (1973)	sand/CaCl2 brine	0.0542	2	210	1150	1.8
Shook et al. (1973)	sand/CaCl2 brine	0.0542	2	210	1250	2.91
Shook et al. (1973)	sand/CaCl2 brine	0.0542	2	210	1350	5.6
Shook et al. (1973)	iron/kerosene	0.05 to 0.2	1	495	779	1.238
Sinclair (1962)	sand/kerosene	0.2	1	833, 208	779	1.238
Smith (1973)	potash/brine	0.3-0.5	2	300 to 400	1140 to 1200	1.14 to 1.2
Wasp et al. (1970)	iron/kerosense	0.01 to 0.18	1	138	900	1.9 to 2.0
Gillies et al. (1997)	sand/oil	0.41-0.55	2	200, 100, 10	872	78

Because of the lack of experiments using very viscous fluids, few conclusions can be drawn. Gillies et al. (1994) recommend the extension of their work to include a viscosity of 1000 cP since it is likely that there is a threshold viscosity for which viscous re-suspension always occurs.

King et al. (2000) also studied the liquid viscosity effect on sand transport using CMC solution (300cP and 150cP) and oil (3cP) in a 6 inch dip pipeline. For these tests, 100 L of fluid was placed in the dip, and sand was placed 5 m downstream of the dip. The net forward transport condition was visually obtained as increasing the superficial gas velocity. They found that the threshold velocity for solids transport with a viscous liquid is significantly higher than for a light liquid.

2.3.3 Multiphase Flow Regime

The flow regime that prevails in a system with multiphase flow can have a large effect on the ability of the system to transport solids. For example, in plug flow, the bubbles of gas will flow along the top of the pipe and will have little effect on the solids flow. However, if the amount of gas is increased and slug flow develops then it is thought that the rate of solids transport could increase dramatically.

Danielson (2007) suggested that liquid velocity was the dominant part affecting the sand transport. Therefore, sand bed formation was strongly influenced by two-phase air-water flow regimes which change the liquid velocity. King et al. (2000) comments that at low superficial gas velocities his model works well but at higher velocities the transition to the upper model means predictions are less accurate. Gillies et al. (1997) found that air injection could increase solids transport rate if the liquid flow was turbulent. However, their tests that employed oil of 78 cP showed that when liquid flow was laminar, the sand transportation was not enhanced by the air injection. Oudeman (1993) observed that the transport of a moving bed is enhanced by the turbulence created by slug flow. Angelsen et al. (1989) agreed that higher gas flowrates leads to slugging which leads to more solids transport but did not try to quantify this.

However, Stevenson and Thorpe (2003), based on their experiments with non interacting particles, noted that despite the increased turbulence at the nose of the slug, particles did not necessarily move any easier. They suggested that particle transport in slug flow could be approximated by considering a hybrid model of particle transport in hydraulic conveying and in stratified flow.

Slug flow is, in particular, especially difficult to predict as the oil and water may be separated in the film region and the slug body, separated in the film and dispersed in the slug body, or dispersed everywhere. This is a function of the flowrates, geometry and, crucially, the physical properties of the fluids, including the surface chemistry of the fluids. This means that for any particular set of in-situ volume flowrates, the fluid in contact with the sand is not likely to be easily predictable. Another complication is added by the effect of phase inversion on the liquid viscosity which will in turn have an effect on the solids transport. All these factors are very difficult to quantify and very little research has been done in this area until very recently.

2.3.4 Pipeline Orientation

There had been quite a few investigations on pipeline orientation effect conducted based on slurry system. Shook and Roco (1991) commented that “the critical velocity increased slightly (of the order of 10%) for uphill flows at angles below about +15 degrees in slurry system” based on Roco and other researchers’ experiments, see Figure 12.

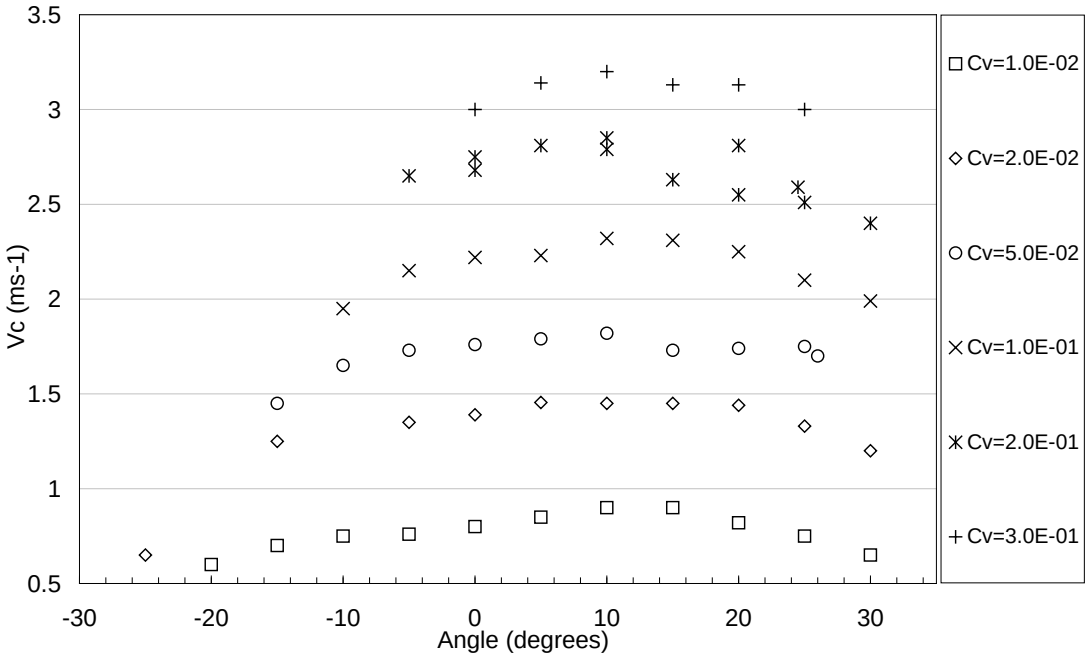

Figure 12: Effect of pipe inclination on sand transport velocity (Roco, 1977)

In addition, Angelsen et al. (1989) also claimed that inclination angle up to +15 degrees had less than 10% change on sand critical velocity in the solid-liquid cases. Rix and Wilkinson (1991), along with Danielson (2007) also gave the similar comments based on their experimental results.

However, only limited data was found for the inclination effect on sand transport in multiphase pipelines (Angelsen et al., 1989; Stevenson et al., 2001b; Stevenson and Thorpe, 2002; Rix and Wilkinson, 1991; Danielson, 2007). Angelsen et al. (1989) investigated the inclination effects (1 degree) on the velocity of sand removal from a bed only in stratified wavy flow. Stevenson et al. (2001b, 2002) investigated the behaviour of isolated sand grains (particle diameter 1100 microns) in intermittent flow in slightly inclined pipeline and stratified flow in slightly declined pipeline. Danielson (2007) also noticed that sand bed formation could be strongly correlated to the pipe angle due to the liquid velocity is a strong function of pipe angle without any further information.

For vertical pipes, Salama (2000) recommended a model developed by Chein (1993). Chein's model can be written as follows,

$$V_c = 1.2\left(\frac{\nu_l}{d_p}\right)\left[\sqrt{1+0.073\left(\frac{\Delta\rho}{\rho_l}\right)\left(\frac{d_p}{\nu_l}\right)^2}-1\right] \qquad [80]$$

2.3.5 Particle Diameter

Usually particles are assumed to be of uniform diameter rather than have a size distribution as is the case in practice. Generally in slurry system, the graph generated by Durand and Condolios (1952) was mostly common used.

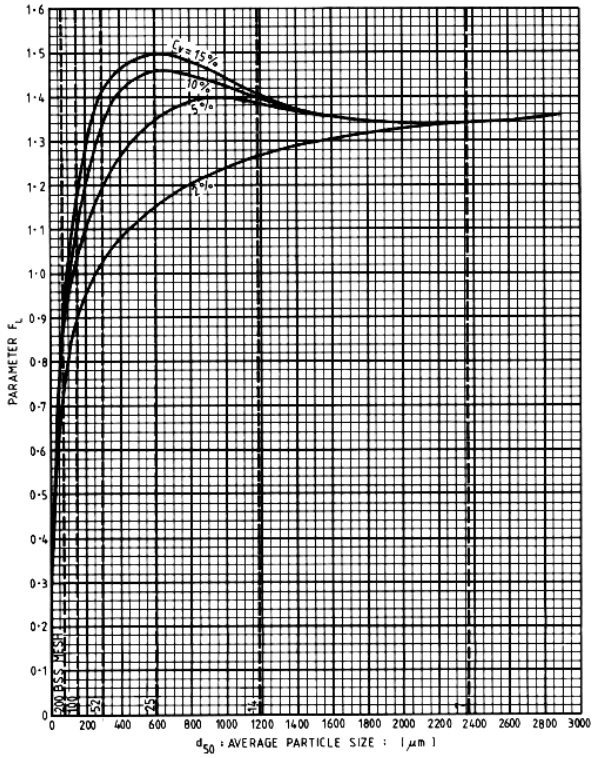

Figure 13: Varation of parameter F_L as a function of particle diameter
Durand and Condolios (1952)

From Figure 13, it was found that the critical velocity steeply increases with the increase of sand particle diameter until 600 microns. Further increasing the sand particle diameter, the critical velocity for 0.02 sand v/v was found gently increasing. However, the critical velocity for 0.05~0.15 sand v/v was found slightly decreased as increasing the sand particle diameter and then flattened.

For multiphase system, there is limited data regarding to the particle diameter effect on sand transport. Only data reported was from Angelsen et al. (1989). He studied the sand transport in stratified wavy flow for 100, 200 and 400 microns particle diameter in 4 inch pipe and found that more energy was required to achieve transporting bigger sand particle.

2.4 Summary

Sand transportation in water flow has been studied in past 50 years with reference to slurry and hydraulic conveyance. However, multiphase sand transport is a very complex issue and dependent on a large number of parameters. Key parameters include sand concentration, fluid viscosities, multiphase (air-liquid) flow regime and sand particle size.

Based on the literature reviewed above, it was found that the investigation into liquid viscosity effect and low sand concentration effect (v/v < 0.01) on sand transport is limited. The effect of fluid viscosity on the flow - especially the laminar-turbulent transition - is extremely significant in the ability of the particles to remain transporting. The behaviour of solids in very viscous fluids is not understood to any degree of sophistication. Transport in laminar flows (particularly with high viscosity fluids) and slug flows are poorly understood. Also, the data for sand transport in multiphase pipelines for different orientations was not sufficient.

Most of the available models generalise existing slurry models or solid-liquid correlations to multiphase systems. The range of applicability of the models is therefore limited and caution needs to be applied in their use outside the range. The data collected to date on multiphase transport of solids is often inconclusive and contradictory in places and would benefit from the collection of a consistent set of data. The modelling of the multiphase transport of sand is still at a very basic level with no model combining state-of-the-art gas-oil hydrodynamic analysis with slurry state-of-the-art models. Clearly more work is needed in this area.

3 Experiment Setup

The sand transportation experiments were conducted using the 2 inch, 3 inch and 4 inch multiphase flow loops in PASE lab in Cranfield University.

3.1 2 inch Test Facility

It was the intention at the beginning of the project to undertake preliminary tests using this 2 inch facility during the construction of the 4 in facility.

The 2 inch sand-air-water facility is designed and constructed using ABS plastic (Class E) pipe of 50 mm inner diameter (2 inch). The pipe length is 17m. A piece of flexible pipe is installed downstream of the test section to allow the test section to be tilted at 5 degrees as illustrated in Figure 14 and
Figure 15. The test section consists of a 1200mm observation section. A Druck pressure transducer (PMP 4110) is used to measure the differential pressure over a distance of 2170mm.

Water is stored in a water tank with a baffle inside for ensuring separation of sand-water mixture. The water is pumped to the flow loop using a centrifugal pump, which has a maximum capacity of 40 $m^3 \cdot hr^{-1}$ and a maximum discharge pressure of 5 barg. The water flow is metered using an electromagnetic flow meter, ABB K280/0 AS model, with a range of 0 - 20 $m^3 \cdot hr^{-1}$. Air is supplied from a screw compressor. This compressor has a maximum supply capacity of 400 $m^3 \cdot hr^{-1}$ free air delivery and a maximum discharge pressure of 10 barg. Air is metered by a pair of gas flowmeters (a 0.5-inch thermal mass flowmeter range 0 to 2 $m^3 \cdot hr^{-1}$ and a 1-inch vortex flowmeter range from 3 to 100 $m^3 \cdot hr^{-1}$). The superficial liquid and gas velocity are ranging from 0.07~0.55 $m \cdot s^{-1}$ and 0.02~15.5$m \cdot s^{-1}$ respectively to cover both slug and stratified wavy flow regimes.

The sand feeder unit consists of a cylindrical stirred tank with an axial flow impeller (Figure 15), and a LAFERT slurry centrifugal pump (0.5 $m^3 \cdot hr^{-1}$) with a plastic impeller for injecting water-sand mixture into the flow loop. After passing through the flow loop, the sand is dumped into the water tank. A data acquisition system is installed to monitor the water and air volumetric flowrates, line pressure, differential pressure and temperature. The data, which is stored as raw voltage information (0 - 10V) using the data acquisition system, NI USB-6210, is converted to engineering unit for the corresponding instrument using Labview version 7.

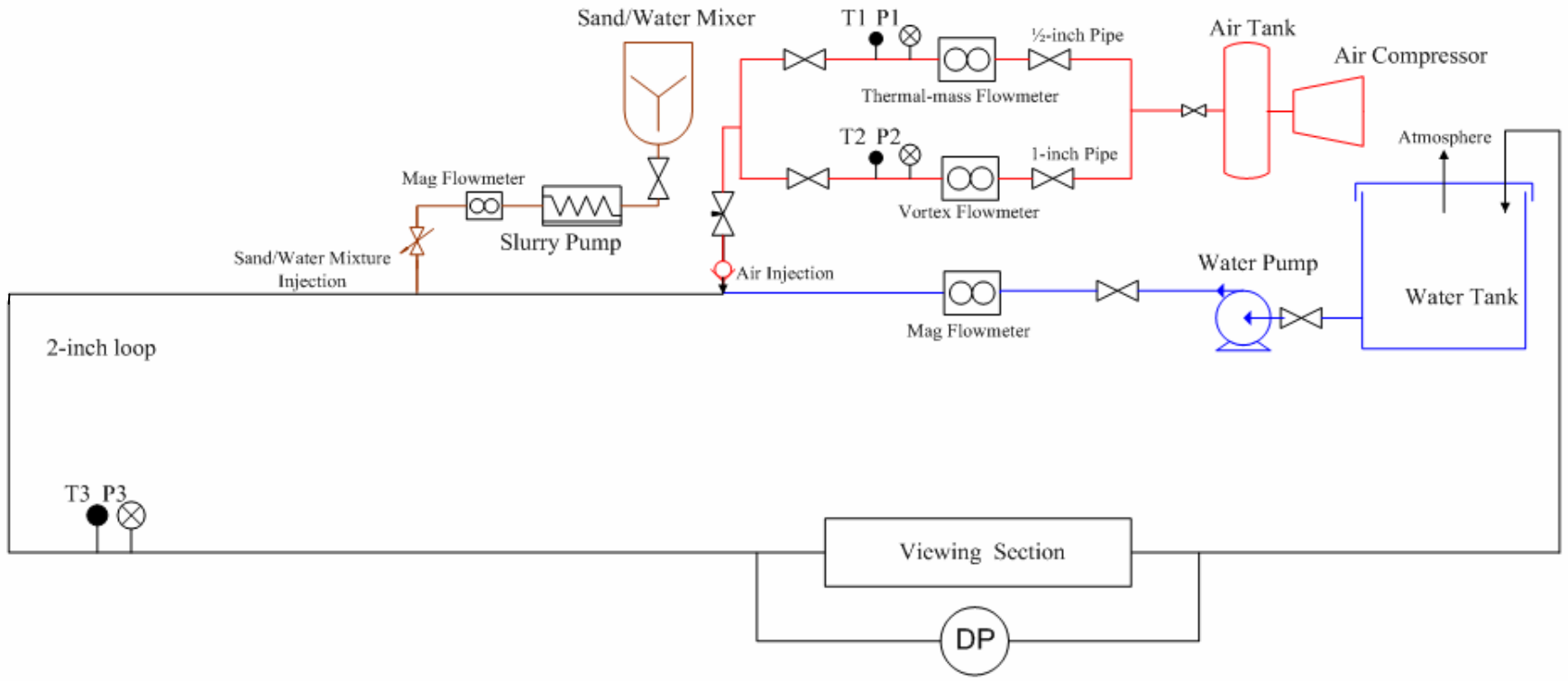

Figure 14: 2 inch sand transportation facility at Cranfield University

Figure 15: 2 inch test rig tilted at 5 degrees

3.2 3 inch Test Facility

Figure 16 and Figure 17 show the 3-inch sand-air-oil test facility. Oil is stored in a tank of 15.3m^3 capacity at the ground floor. The oil is pumped by a progressive cavity pump (PCP) through a 3-inch pipe. The oil progressive cavity pump has a maximum capacity of 90 $m^3 \cdot hr^{-1}$ and a maximum discharge pressure of 5 barg. Azolla 100 oil (hydraulic type oil) is used for the test programme. The inlet oil flow is metered by a Coriolis mass flowmeter (Endress+Hauser Promass 83I DN 80). The Coriolis flowmeter has three outputs i.e. mass flowrate, density and viscosity, the measurement accuracy for those parameters are 0.1%, 0.004 $kg \cdot m^{-3}$ and 0.5% reproducibility respectively. To investigate the oil viscosity effects on sand transport behaviour and mechanism, Azolla 100 oil is heated in the main oil tank to obtain the desired viscosities at those tests. The viscosities, temperature and density tested are 340cP at 16^oC and 884 $kg \cdot m^{-3}$, 200cP at 25^oC and 880 $kg \cdot m^{-3}$ and 105cP at 35^oC and 875 $kg \cdot m^{-3}$. The viscosity value given by the Coriolis meter is in agreement with the off line analysis using a viscometer. The oil velocities covered on this rig is from 0.07 $m \cdot s^{-1}$ up to 0.5$m \cdot s^{-1}$.

A sand-oil injection point is installed in the 7m long Perspex flowline. The sand feeder unit consists of a stirred vessel with an axial flow impeller and a 0.9 $kg \cdot m^{-3}$ slurry pump. For each experiment, a known amount of sand is mixed with the oil in the stirred vessel and injected at the appropriate rate to give the correct sand concentration in the 3 inch line.

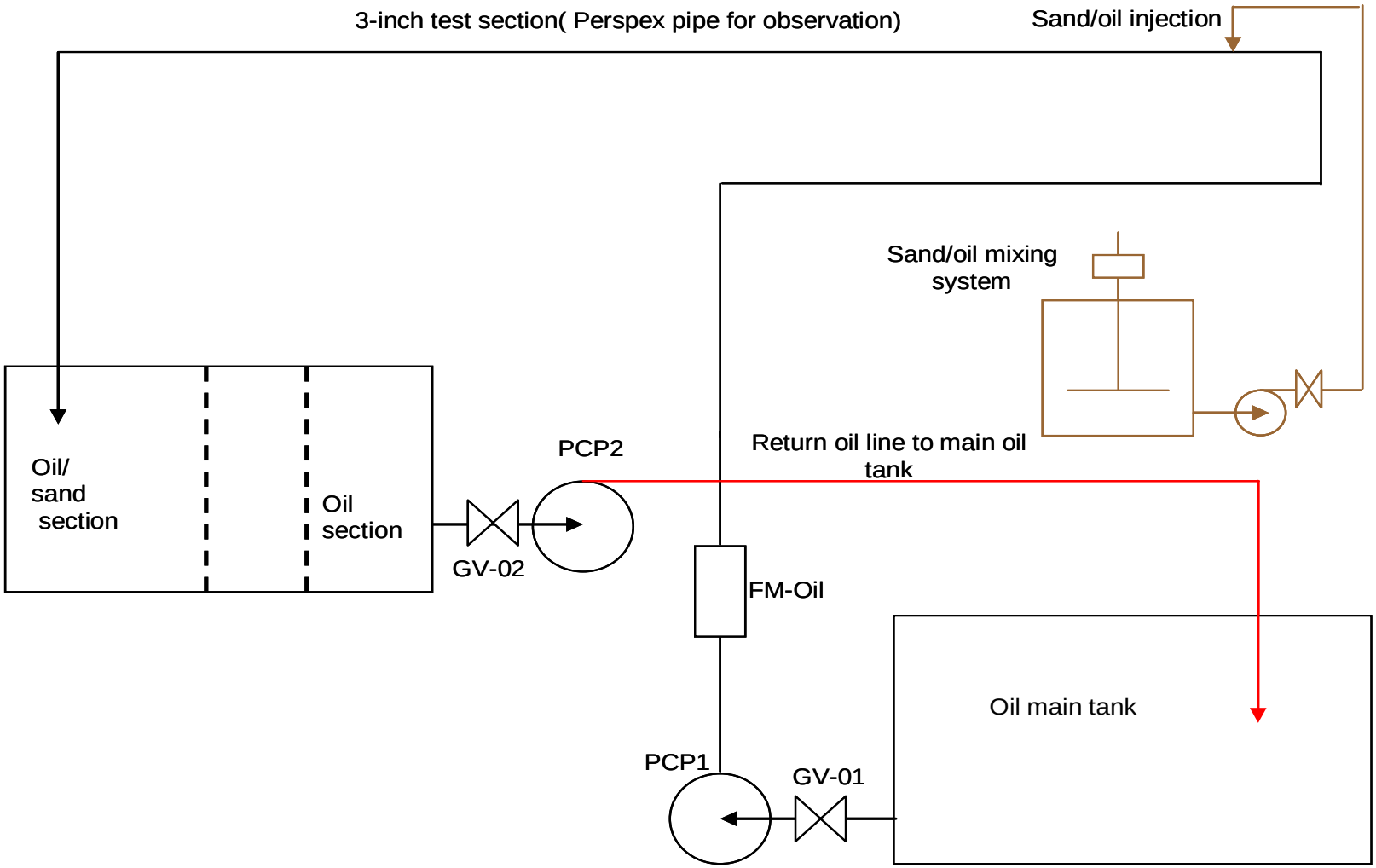

Figure 16: 3 inch sand transportation facility at Cranfield University

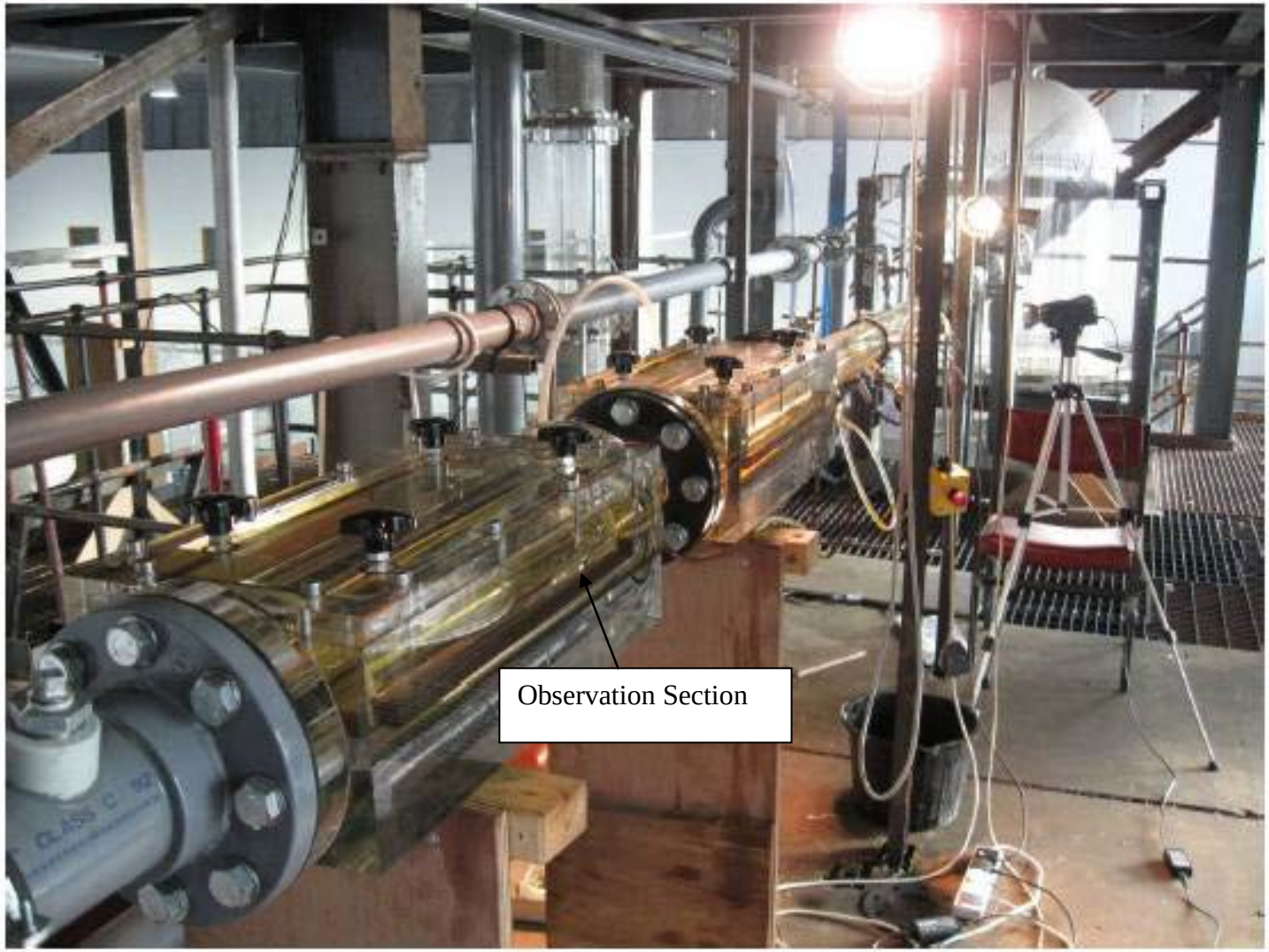

Figure 17: 3 inch sand transportation facility

3.3 4 inch Test Facility

The 4 inch multiphase test facility is designed to operate under different multiphase flows, with and without sand. For the experimental investigations conducted, air-water is used as the test fluid with and without sand. Figure 18 shows a schematic of the 4 inch test facility.

The test section is made of 4 inch (ID=0.1 m) stainless steel (SS316 L) pipes totalled 40 m in length. The 40m length is divided into a 20m outward flow pipeline, U shaped bend, and a 20m return flow pipeline. The test section pipeline is supported on a steel structure and different inclinations can be achieved using an A-frame and lifting chain blocks. Both the beginning and the end of the test section pipeline are fixed using a pivot to allow pipeline to be tilted at different angles including 5 up to 20 degrees as illustrated in Figure 19. The inclination is checked by a magnetic base 'protractor' (Starrett Exact, 492-005) at the beginning, middle and the end of the rig. Two 1.2 m long Perspex windows (viewing section) are installed in the outward and return legs to facilitate visual observations of the sand particles in the flow. A vertical section which made of PVC/Perspex is also attached on the horizontal pipeline.

Water is stored in a tank of 4.4 m^3 capacity and is pumped by a variable speed progressive cavity pump (PCP) to the test section through an approximately 8m long 3-inch (ID = 0.075 m) line. The water pump has a maximum capacity of 90 $m^3 \cdot hr^{-1}$ and a maximum discharge pressure of 5 barg. The water flow from the pump is also controlled by means of a by-pass line with the fluid from the pump outlet being recycled back to the water tank via a valve. The water flow to the test pipeline is metered using an electromagnetic meter, Endress+Hauser PROMAG 50W DN 80, with a range of 0 to 180 $m^3 \cdot hr^{-1}$. The electromagnetic flowmeter has a 4-20 mA HART output that can be connected to the data acquisition system. Air is supplied from a screw compressor. This compressor has a maximum supply capacity of 400 $m^3 \cdot hr^{-1}$ free air delivery and a maximum discharge pressure of 10 barg. Air is metered by a pair of gas flowmeters (a 0.5-inch thermal flowmeter for 0 to 2 $m^3 \cdot hr^{-1}$ and a 1-inch vortex flowmeter from 2 to 100 $m^3 \cdot hr^{-1}$). An air receiver before the test section stabilises the gas supply from the compressor. Air from the receiver passes through a bank of three filters (coarse, medium and fine) and then through a cooler where debris and condensates present in the air are stripped from the air before it flows into the flowmeters. The superficial liquid and gas velocity applied on this rig ranging from 0.15~0.55 $m \cdot s^{-1}$ and 0.02~4.0 $m \cdot s^{-1}$ respectively. Two MFT300 capacitance, sensor supplied by Siemens Milltronics Process Instruments B.V. in the Netherlands, are installed upstream of the flow loop. The MFT300 flow sensor is an assembly of flow-through electrodes with an attached electronics module, the driver. The driver circuit generates the measurement signal and compensates for parasitic capacitances in the sensor and cabling. The output signals are calibrated to relate the signals to various liquid holdups (0V correspond to air and 5V correspond to water).

A sand injection point is installed after the mixing point of water and air. The sand feeder unit consists of a cylindrical stirred vessel (800 mm in diameter and 500mm high), with a 365mm diameter axial flow impeller), and a variable speed progressive cavity pump (PCP) with a capacity of 0.3 $kg \cdot hr^{-1}$ and 5 barg maximum discharge pressure.

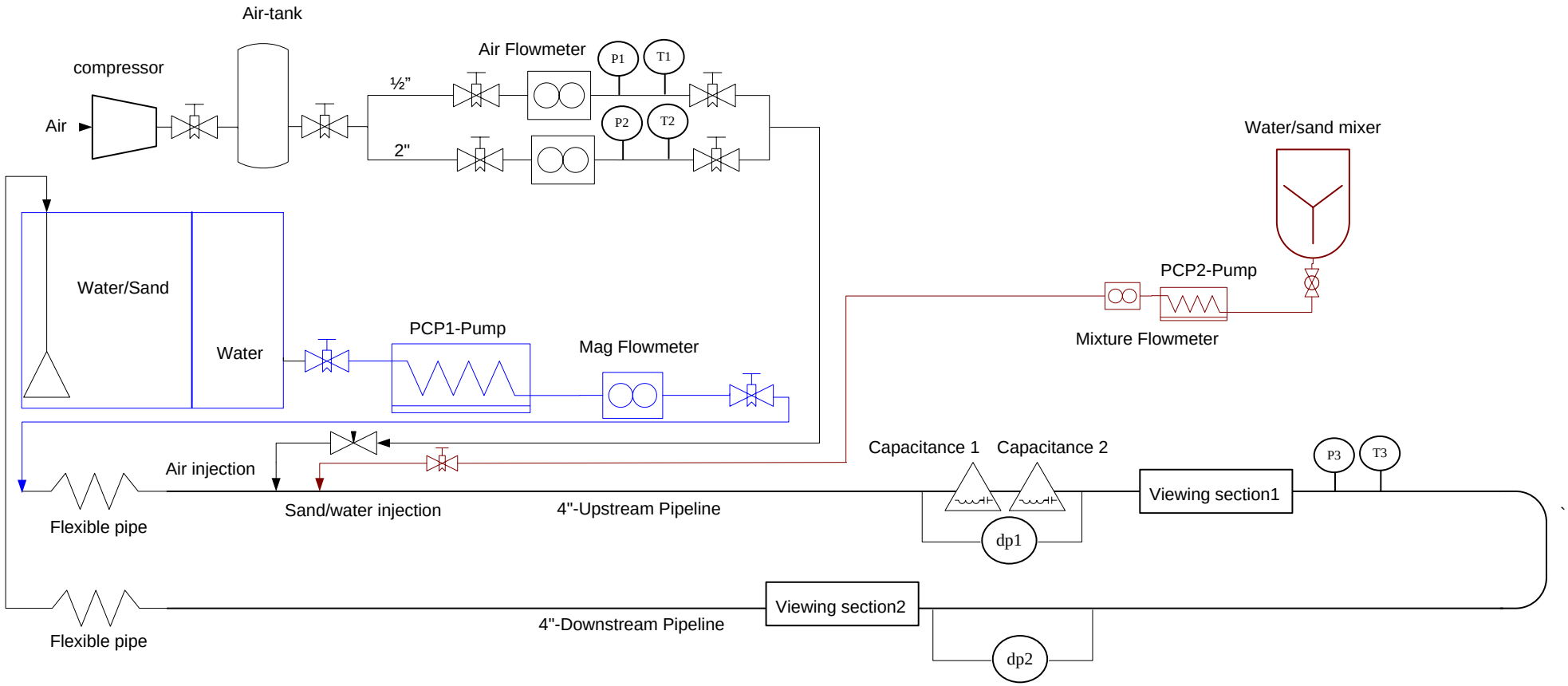

Figure 18: 4 inch sand transportation facility at Cranfield University

a) 5degrees

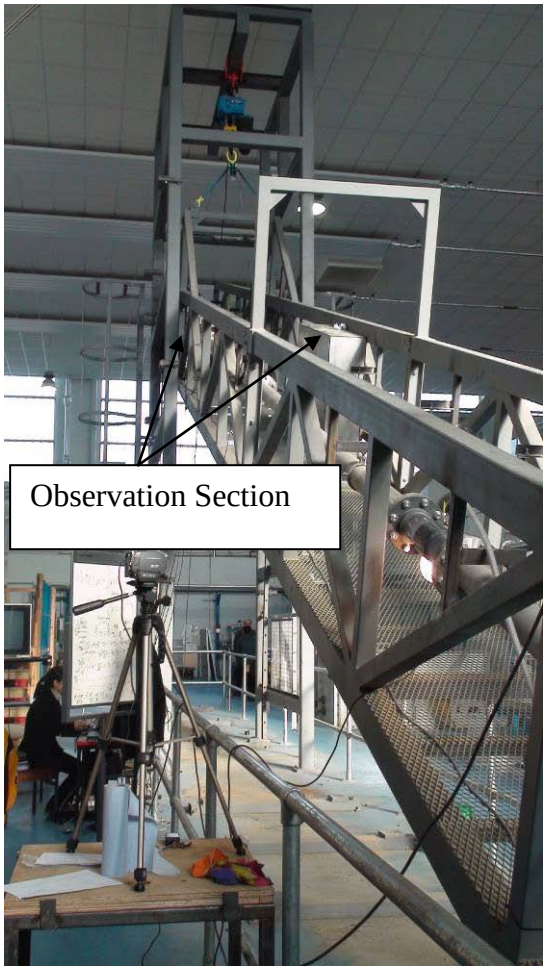

b) 20 degrees

c) vertical section

Figure 19: 4 inch sand transportation rig tilted at 5– 20 degrees with vertical section

After passing through the U-shaped flow loop, the sand is dumped into the water tank. A data acquisition system is installed to monitor water and air volumetric flowrates, line pressure, differential pressure and temperature. The data, which is stored as raw voltage (0 - 10V) using the data acquisition system, NI USB-6210, is converted to engineering units for the corresponding instrument using Labview version 7.

3.4 Instrumental Calibration and Measurement Methodology

In order to obtain the quality data, several instruments were used continuously during the experiments, including capacitance sensor, differential pressure drop sensor and viscometer, etc.

- Differential pressure drop transducer

Two GE Druck differential pressure transducers (Figure 20) are used in the experiment (pressure range is -70 to +70 mbar and accuracy 0.1% over the full scale) to obtain differential pressure under different conditions.

Figure 20: GE Druck differential pressure transducer (side view)

Differential pressure measurements are usually obtained with fluid filled transmission line. In this work, the disadvantage associated with this type of transducer is that sand and air might fall into the transmission lines. In a slurry system, pressure tappings are usually made at 45 degrees deviated from vertical axis from the top on the horizontal pipes to prevent air and sand being trapped in the lines (Brown and Heywood, 1991). However, in this work, water-sand and air-water-sand flows were tested, which air could be easily trapped in transmission line if we placed the pressure tappings at position where slurry system preferred. Therefore, the pressure tappings are located at

45 degrees deviated from vertical axis from the bottom on the horizontal pipes, as shown in Figure 21. The transmission line is constantly checked to assure no entrained gas or sand blockage inside.

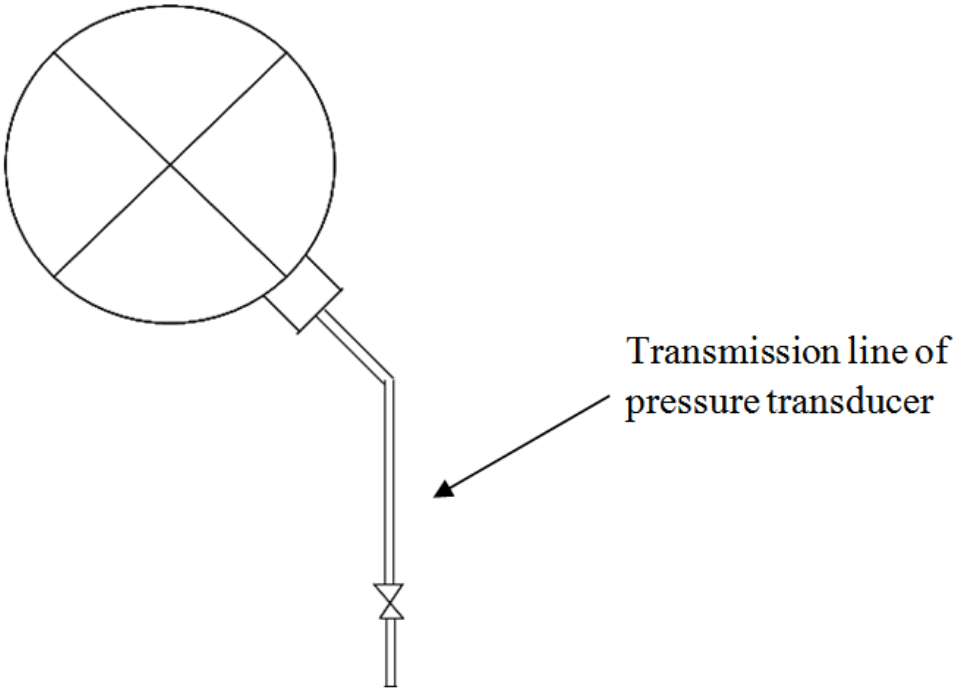

Figure 21: Sketch of the pressure transducer installation in this work (view on cross sectional view)

The calibration of those differential pressure transducers are illustrated in Figure 22 and Figure 23:

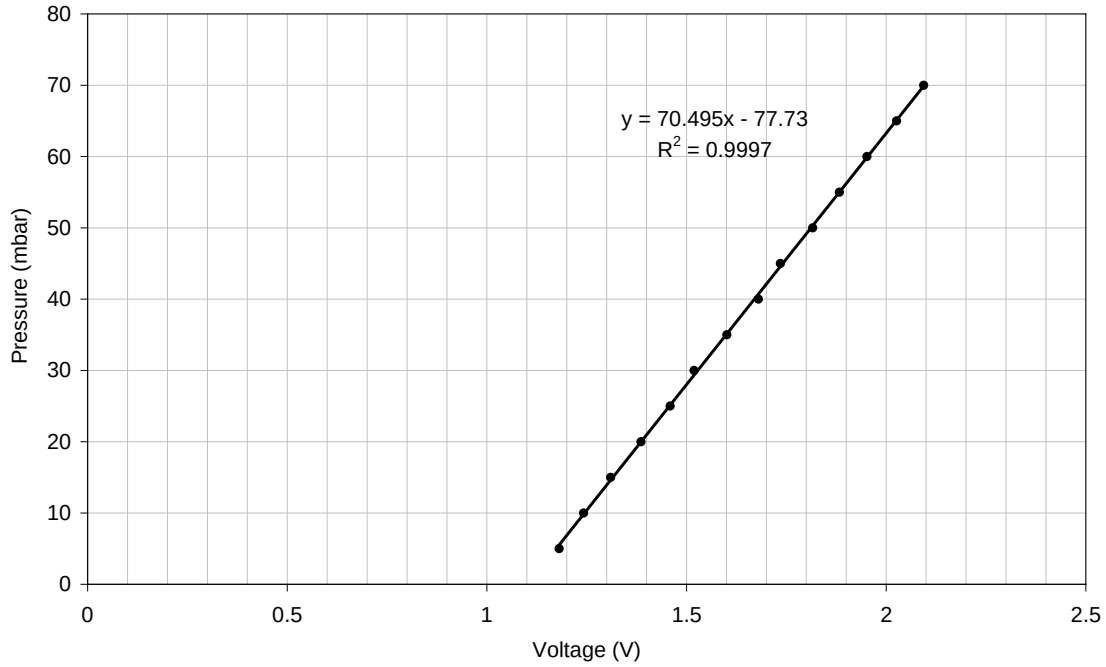

Figure 22: Calibration of differential pressure transducer No.1

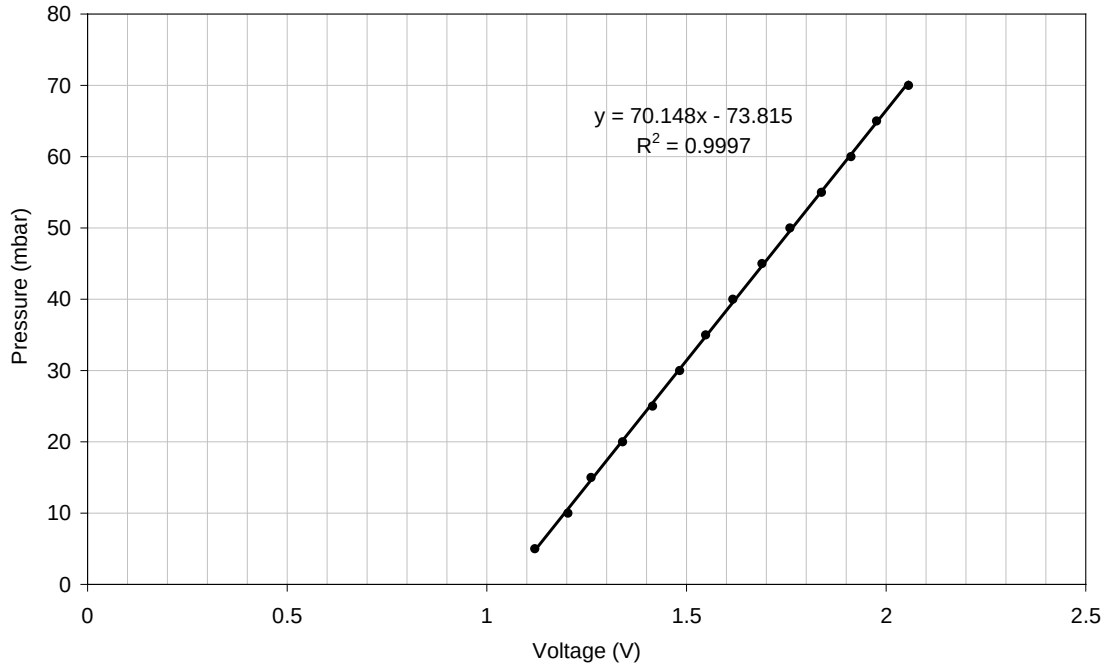

Figure 23: Calibration of differential pressure transducer No.2

The y axis is measured pressure from the pressure calibrator and x axis is measured from a multimeter.

In order to obtain the data on the Labview system, the following equation will normally applied

$$E= a\times (V-V_0) \quad [81]$$

where a is the slop, and V_0 is offset, which both a required as the input of Labview software, and E is the target measurement parameter, differential pressure in this case.

The equation after curve fitting is represented by the following relationship:

$$E= m\times V+c \quad [82]$$

which can be rewrite as:

$$E= m\times[V-(-c/m)] \quad [83]$$

therefore, a=m and V_0= -c/m. The slop and offset for these two transducers used in this work are list in Table 8.

Table 8: Slop and offset setting for these two transducers in Labview system

Transducer No.	Slop	Offset
1	70.495	1.013
2	70.148	1.052

- Viscosity measurement using viscometer

CMC solution (7, 20cP) is used in this work. CMC stands for carboxylmethyl-cellulose. It is a water-soluble polymer used in synthetic detergents, drilling fluids, textiles, cosmetics etc. CMC is sold as a white to bluff-coloured, odourless and free-flowing powder that can be dissolved into water to increase the viscosity of the solution. Prior to any experiments involving CMC solution, the CMC powder is spreaded gradually into the water and well mixed with water by circulating the mixture from bypass line into main tank at highest liquid flowrate. A mixture sample is taken constantly and the viscosity of the sample was measured to check the repeatability. Mixture sample is usually taken from 0.3m depth from the surface of mixture in the water tank at different positions.

The viscosity is metered using a Brookfield Viscometer (LVDV-I Prime) with 0–100 rpm range and viscosity accuracy and repeatability of ± 1% and 0.2% of full scale range in use respectively as shown in Figure 24.

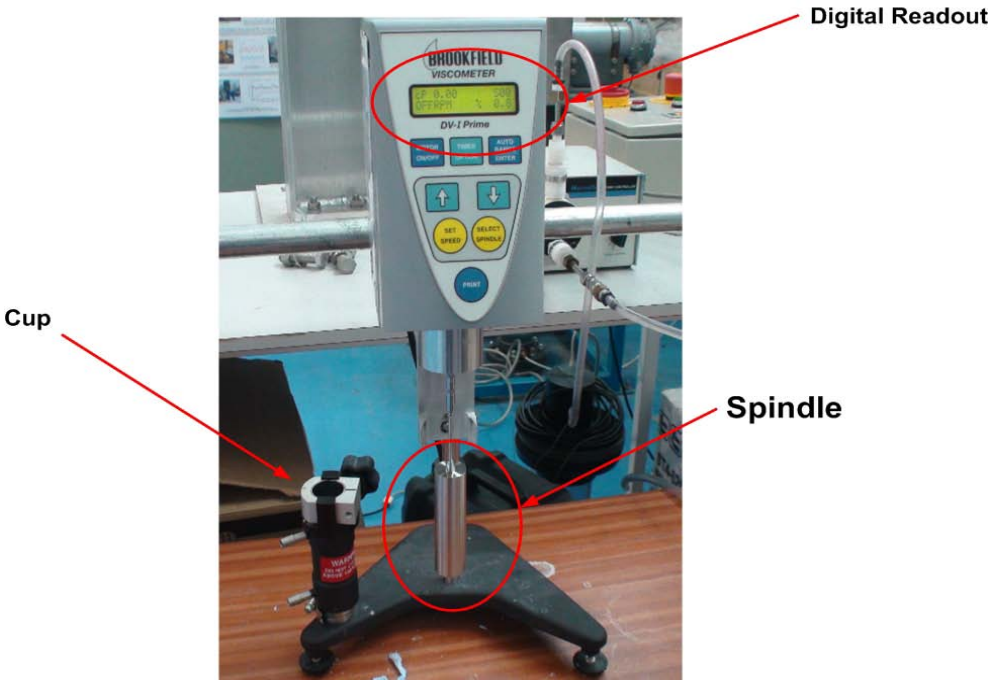

Figure 24: Brookfield Digital Viscometer

The principle of this viscometer is to drive the spindle and measure the couple on this spindle immerged into a liquid contained in the stationary cup. The device measures resistance to flow at a set shear rate. The viscous drag of the liquid against the spindle is measured by the torque (or couple). The speed is normally set at a determined rate while the viscosity is monitored as it varies with the torque. The data can then be analyzed using the shear stress and shear rate relationship.

To treat the data taken from the reading of the viscometer, a power law model is used to determine the behaviour of CMC solutions at different viscosities, especially to know whether the solutions are Newtonian or not. The power law approach can be used to fit to the data:

$$\tau = K \dot{\gamma}^{n} \qquad [84]$$

with:

- $\dot{\gamma}$, the shear rate [s^{-1}]
- τ, the shear stress [Pa s]
- K, the consistency coefficient
- n, the power law exponent [-]

The values taken by the *n* exponent (so called flow index behaviour) are a mean of assessing the degree of deviation from the Newtonian behaviour. Actually, three main thresholds are given by:

- n = 1 : Newtonian, and liquid viscosity μ_l= K
- n > 1 : Dilatant or shear thickening
- n < 1 : Shear thinning

The K and n are obtained for different fluid:

Table 9: Power law constants for water and CMC at different viscosities

Fluid	K	n
Water	0.0013	1.014
7 cP	0.0066	0.9905
20 cP	0.0189	0.9671

Table 9 indicates a drop of *n* exponent from 1.014 to 0.9671 which is an indication that the CMC solution shows a slight trend of behaving as a non-Newtonian fluid, although it is not significant.

In order to test the stability of CMC solutions against the temperature changes, the viscosity of CMC solution was measured at different temperature in static tests, as shown in Figure 25 .

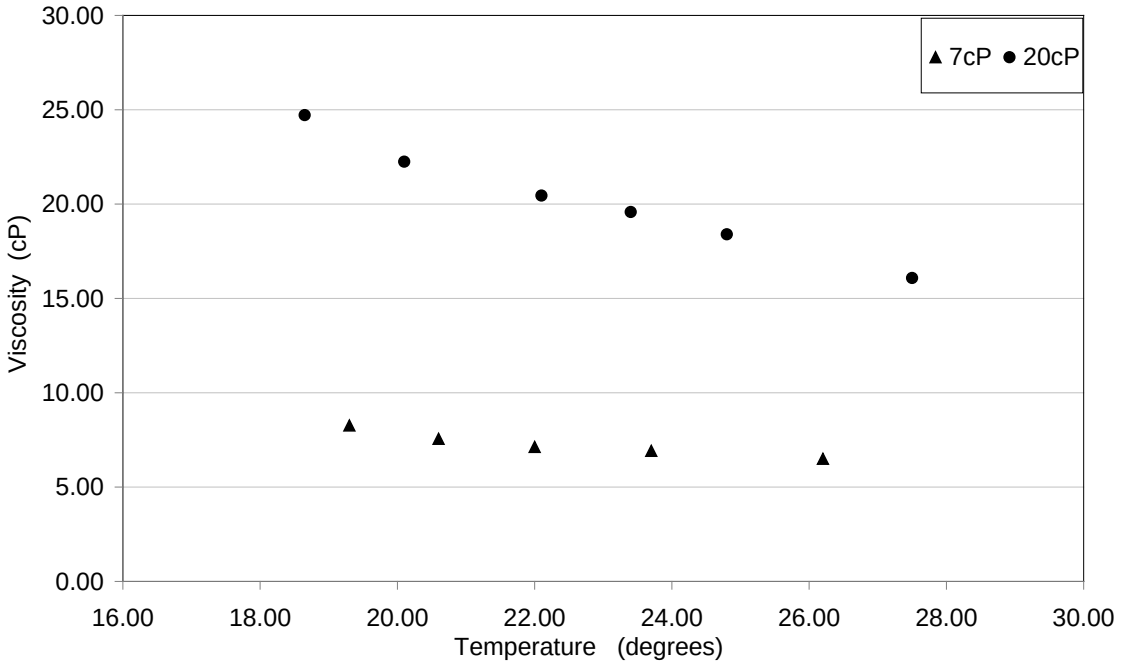

Figure 25: Temperature effect on liquid viscosity of CMC solution

It was found that the viscosity of CMC solution decreased as increasing of the temperature. However, due to all the experiments were conducted under the temperature between 22 to 24 degrees, the viscosity does not have a significant change within this temperature range.

- Slug Translational velocity measurement using capacitance sensors

Conductivity sensors are used to investigate the effect of sand concentration on two-phase flow regime in horizontal pipeline. The conductivity sensors are supplied by Siemens Milltronics Process Instruments B.V. in the Netherlands. Each system comprises a MFT300 flow sensor and a MFT200 detector module as shown in Figure

26. The output signals must be tuned on site for air and water so that 0V (or alternatively 4mA) will correspond to air, and 5V (or alternatively 20mA) will correspond to water.

Figure 26: Conductivity transmitters installed in 4-inch Sand Transportation Rig

Details of the sensors can be found in the instruction manual supplied by Milltronics. For simplicity, the signals are converted through the data acquisition system to show 1 for a pipe full of water and 0 for an empty pipe. As the output signal is not linear, the performance of the sensor must be calibrated to relate the signals to various liquid holdups. The device is capable of following the dynamic changes in the process up to 1000 samples per sec. It responds for both water and oil, although its response for the latter is much lower in signal output.

The aim of the calibration is to characterise the sensors for film height measurement during intermittent flow.

The gas-liquid phase distribution is achieved by introducing known liquid volumes into the test sensor mounted in the horizontal position. Tap water is used and great care is taken to check the inclination of the pipe. This bench calibration involves in blanking both ends of the sensor with graduated transparent flanges and gradually filling the sensors at height intervals of 1 or 2mm and recording the signals from both sensors. Figure 27 (a) and (b) show the calibration curves of the output voltages from conductivity sensors with the height of water in the pipe.

After the 'height' of the water is obtained using the conductivity sensors, the liquid holdup can be deduced from the Equations 85,

$$\varepsilon_L = \frac{1}{\pi}\left(\pi - \cos^{-1}\left(2\left(\frac{H_L}{D}\right)-1\right) + \left(2\left(\frac{H_L}{D}\right)-1\right)\sqrt{1-\left(2\left(\frac{H_L}{D}\right)-1\right)^2}\right) \qquad [85]$$

where H_L is the liquid height.

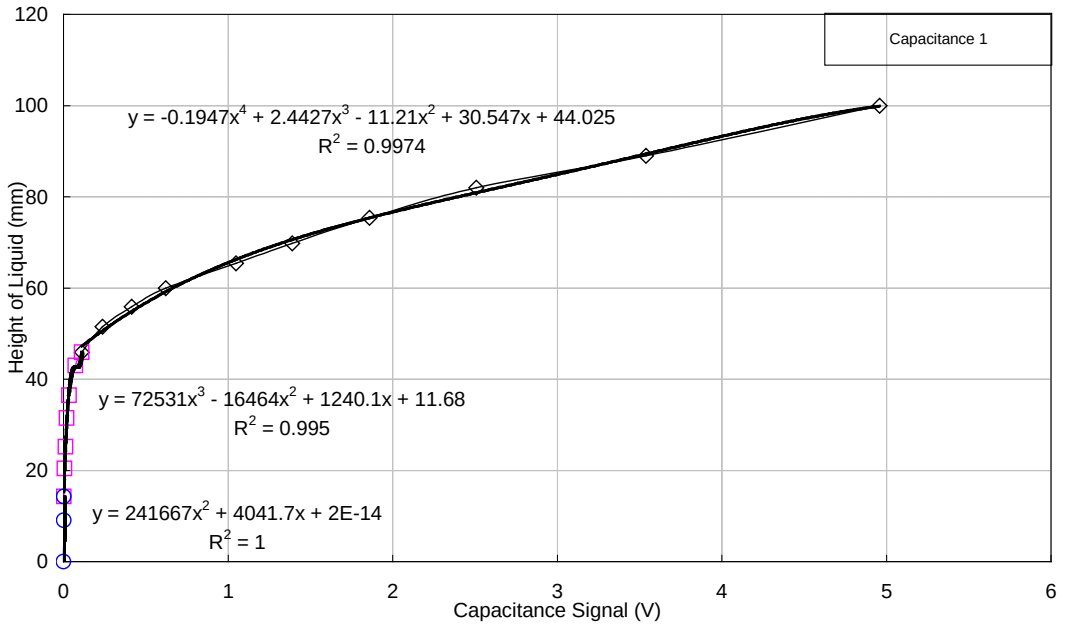

(a) Conductivity 1

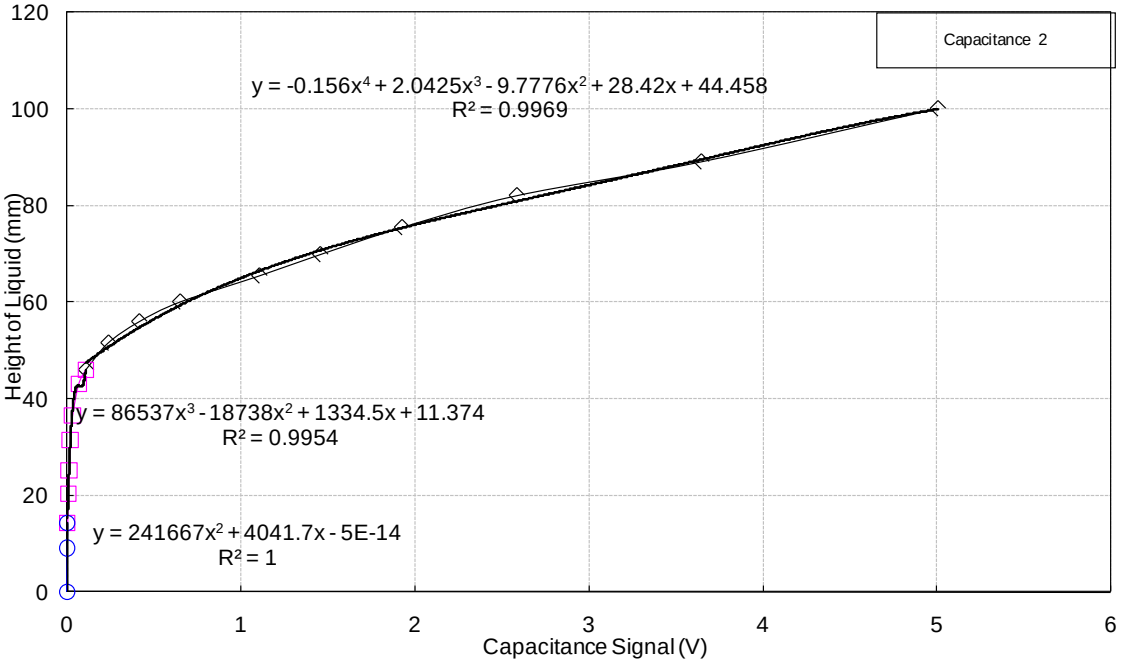

(b) Conductivity 2

Figure 27: Height of water verses conductivity readings

The cross-correlation technique is an attractive approach to determine the slug translational velocity. The slug translational velocity, V_T is obtained by cross correlating the two liquid holdup sensor signals according to the following equation:

$$R_{xy} = \frac{1}{T}\int_0^T x(t-\zeta)y(t)\,dt \qquad [86]$$

where R_{xy} is the value of cross correlation function, T is extraction duration and x(t-ζ) and y(t) are the two liquid holdup values at time (t-ζ) and (t) respectively. The time delay ζ (Figure 28) is when the value of R_{xy} was at maximum.

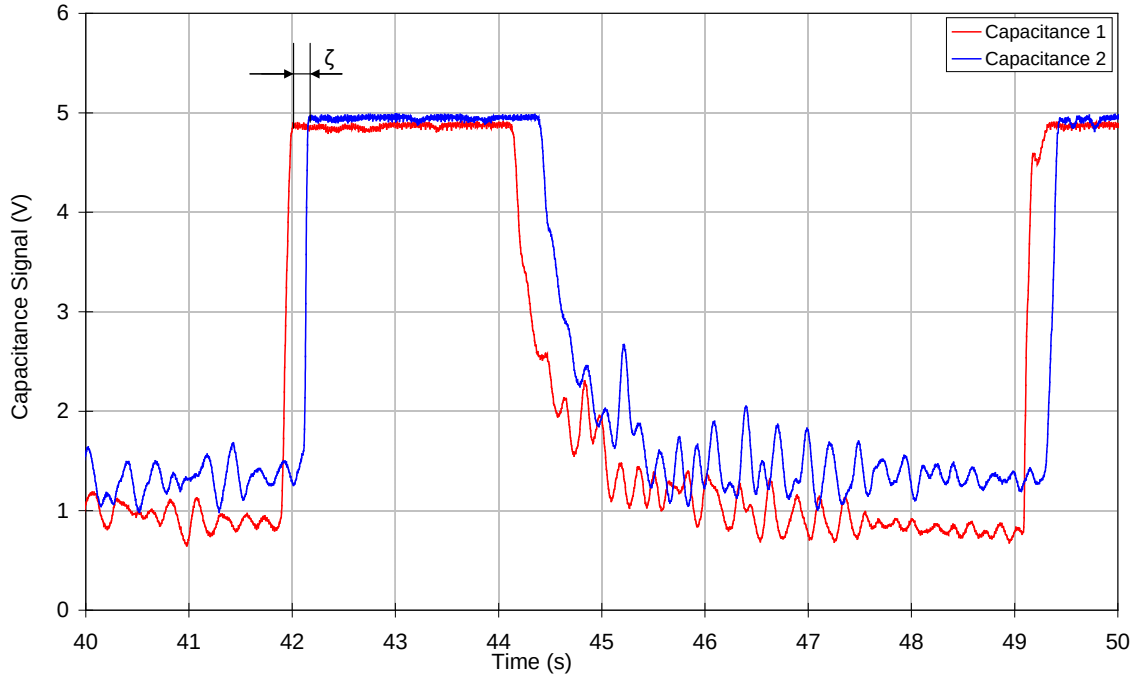

Figure 28: Time delay between the two conductivity transmitters

The slug translational velocity is determined by:

$$V_{T(1-2)} = \frac{L_{(1-2)}}{\zeta_{(1-2)}} \qquad [87]$$

where $V_{T(1-2)}$ is the slug translational velocity determined from the two conductivity sensors $C_{(1)}$ and $C_{(2)}$, $L_{(1-2)}$ is the known separation distance between the two conductivity sensors.

- Azolla oil viscosity measurement using a Coriolis flowmeter

Table 10 and Figure 29 show the viscosity comparison between experimentally measured data and that provided by the manufacturer (Total). However, it is necessary to point out that, most of viscosity data provided by manufacturer is based on calculations from their software (only at 40 degrees is measured).

Table 10: Oil viscosity measurement in this work

Oil Temperature (degrees)	Density ($kg \cdot m^3$)	Dynamic Viscosity (cP)	Kinematic Viscosity (mm^2/s)
35.00	873.34	105.00	120.23
34.82	875.63	108.81	124.26
24.70	880.06	200.45	227.77
24.75	880.28	202.15	229.64
16.40	884.32	343.54	388.48

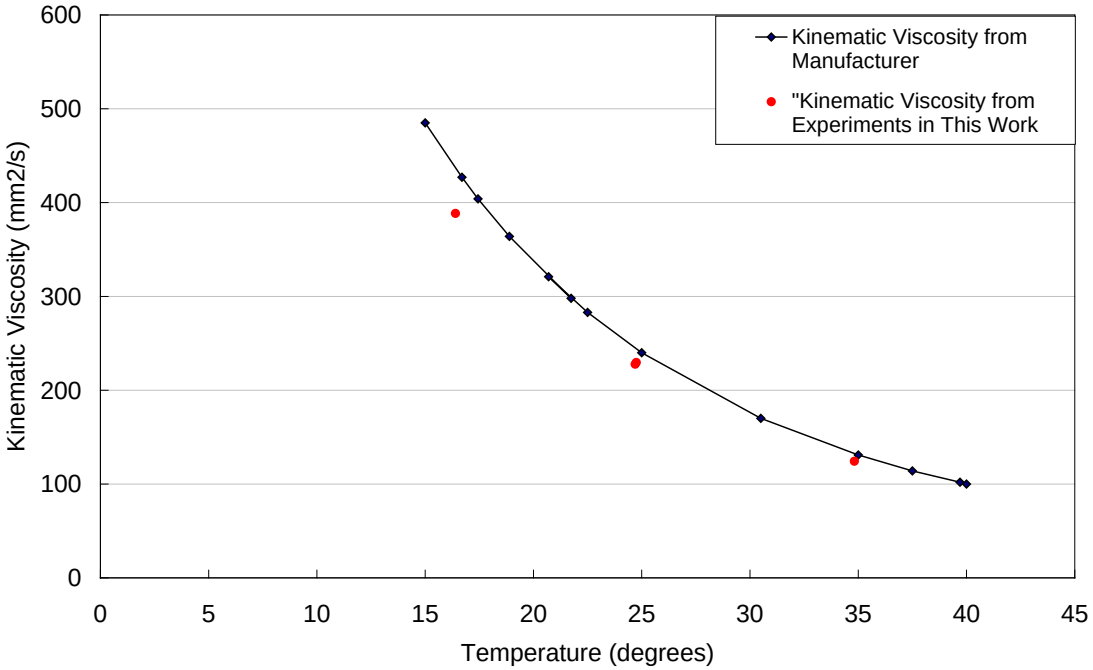

Figure 29: Measured oil kinematic viscosity versus data provided by manufacturer

3.5 Sand Used in Experiments

The sand concentrations used and distribution measured by sand sieves are listed in Table 11 and Figure 30 respectively. The average diameter provided by the manufacturer is approximately 200 microns (HST 50+95, from WBB Mineral) with a mixture density of 2650 $kg \cdot m^{-3}$, while the actual measured d_{50}, which is average or mean particle size representing 50% volume or weight fraction, is approximately 189 microns.

Table 11: Sand concentrations used in tests

Sand concentration (lb/1000bbl)	Volume Fraction (v/v)
5	5.38E-06
15	1.61E-05
50	5.38E-05
200	2.15E-04
500	5.38E-04

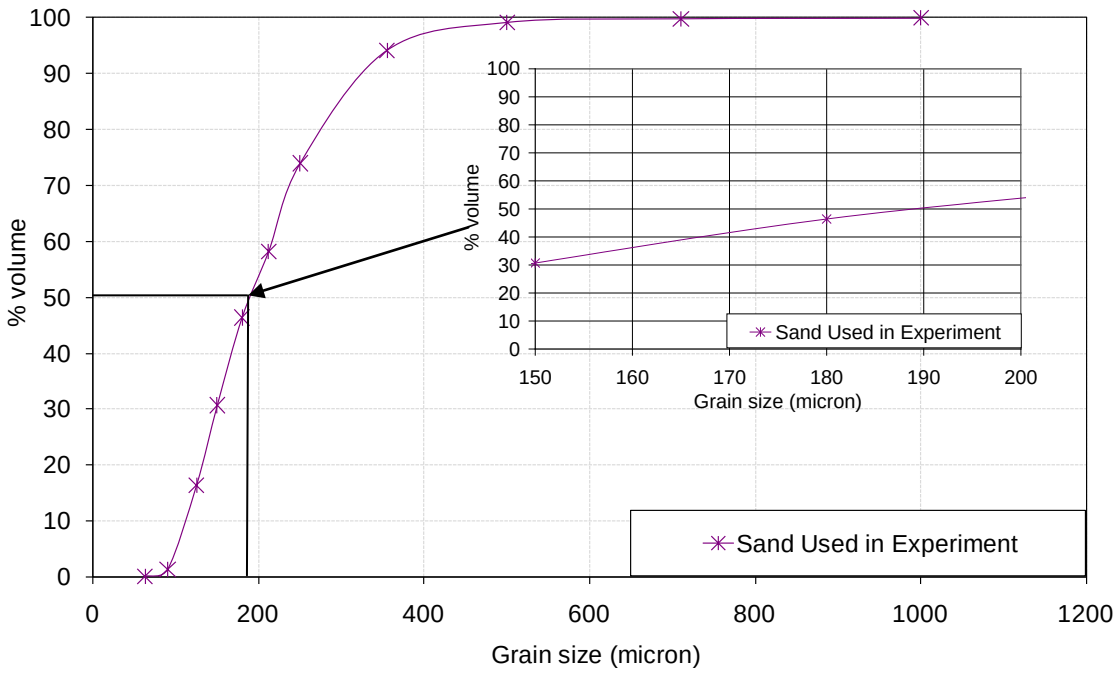

Figure 30: Sand distribution used in the experiments

3.6 Test Methodology

- Test Methodology for Sand-Water Settling Experiment

1) Any sand remaining from previous experiment in the loop is removed by flushing with water.

2) Prepared sand-water mixture of the required concentration in the hopper (sand mixing tank).

3) Start the liquid pump and adjust the controller until the required water velocity (slightly above the expected sand transport velocity) is reached.

4) Inject the sand-water mixture at a constant flowrate to give the required sand concentration

5) Decrease the water velocity until sand begins to settle, and then record the raw data.

- Test Methodology for Sand-Oil Settling Experiment

1) Any sand remaining from previous experiment in the loop is removed by flushing with oil.

2) Prepared sand-oil mixture of the required concentration in the hopper (sand mixing tank).

3) Start the liquid pump and adjust the controller until the required oil velocity (slightly above the expected sand transport velocity) is reached.

4) Inject the sand-oil mixture at a constant flowrate to give the required sand concentration.

5) Decrease the oil velocity until sand begins to settle, and then record the raw data.

- Test Methodology for Sand-Air-Water Settling Experiment

1) Any sand remaining from previous experiment in the loop was removed by flushing with water.

2) Prepared sand-water mixture of the required concentration in the hopper.

3) Start the liquid pump, adjust the controller and the bypass valve until the required water superficial velocity was reached.

4) Inject the sand water mixture at a constant mass flowrate.

5) Open the gas control valve, and increase the gas flowrate until the maximum value was reached (approximately 3 $m \cdot s^{-1}$). The gas flowrate was gradually reduced until the minimum transport condition (MTC) was reached, and record the raw data.

3.7 Sand Concentration Measurement

In pipeline application, the in-situ sand concentration measurement techniques so far includes: weighing the pipe, using Electromagnetic Flow Meters (EFM), Electrical Resistance Tomography (ERT), Electrical Capacitance Tomography (ECT) and Digital Image Processing.

- Weighing the pipe

This method was normally used in slurry system (Gillies et al., 1996, 1999). A section of pipe was designed to be lifted by the electronic load, and flexible couplings were

used to isolate the weighed section from the rest of the loop. By weighing the pipe section and its contents, the in-situ sand concentration can be obtained. This method is more appropriate for solid-liquid system with high sand concentration, and the measurement error will increase when decreasing the sand concentration.

- Electromagnetic Flow Meters (EFM)

Electromagnetic Flow Meters (EFM) have been successfully applied to measure mean velocities of single-phase liquid in industry. Since such meters do not introduce a pressure drop and can provide a fast response to changes in the flow, there are many potential applications for electromagnetic flow meters in solid-liquid flows.

However, due to the complexity of multiphase flow in solid slurry transportation, it is difficult to accurately measure solid concentration and flow rate using a conventional electromagnetic flow meter alone.

- Electrical Resistance Tomography (ERT) and Electrical Capacitance Tomography (ECT)

Electrical Resistance Tomography (ERT) and Electrical Capacitance Tomography (ECT) have been developed for imaging the dynamic processes containing conductive/ dielectric materials. A number of electrodes are mounted externally around a pipe, sensing the changes in conductivity or permittivity between the electrodes due to the change of flow components inside the pipe. Those technique is regarded as the most mature among many different tomography methods, with the advantage of having no radiation, fast response, non-intrusive, robust, can withstand high temperature and high pressure at low cost (Yang, 2010).

However, the limitation of this method is highly dependent on the dimension of electrodes and the algorithm to reconstruct the image. So far, this technique is still having difficulties to accurately measure the very low sand concentration due to the relatively low resolution comparing to small sand particles.

- Digital Image Processing

The digital image processing technique is an established method for multiphase gas-liquid flow visualization and analysis. This non-invasive technique has advantage over existing method of solid phase velocity and hold-up measurement. Also, the fast response of this technique justifies its possible application in multiphase flow. Bello et al. (2005, 2008) attempted to use this technique to study the sand velocity and hold-up distribution in multiphase slug flow. He claimed this technique can provide accurate measurement of sand velocity and holdup spatial distributions under oil-gas-sand multiphase slug flow condition. Although it seems this technique is a promising method to provide valid information of sand transport characteristics, it is still a progressing work without further justifications up to date.

As mentioned in Chapter 1.3, the in-situ sand concentration studied in this work for minimum sand transport condition is very low comparing to the conventional solid-

liquid systems. Therefore, most techniques mentioned above have certain limitation when applying to this work. In addition, the in-situ sand concentration could be not uniform while travelling along a long pipeline. In this case, a new design criterion is required to obtain the required in-situ sand concentrations in the pipeline.

From field data, it was found that the sand minimum transport velocity was around 0.5 ms^{-1} at normal in-situ sand production rate (50lb/1000bbl). Thus, this condition was used as the starting point of pipeline design. The whole design criterion proposed by the author is shown in Figure 31:

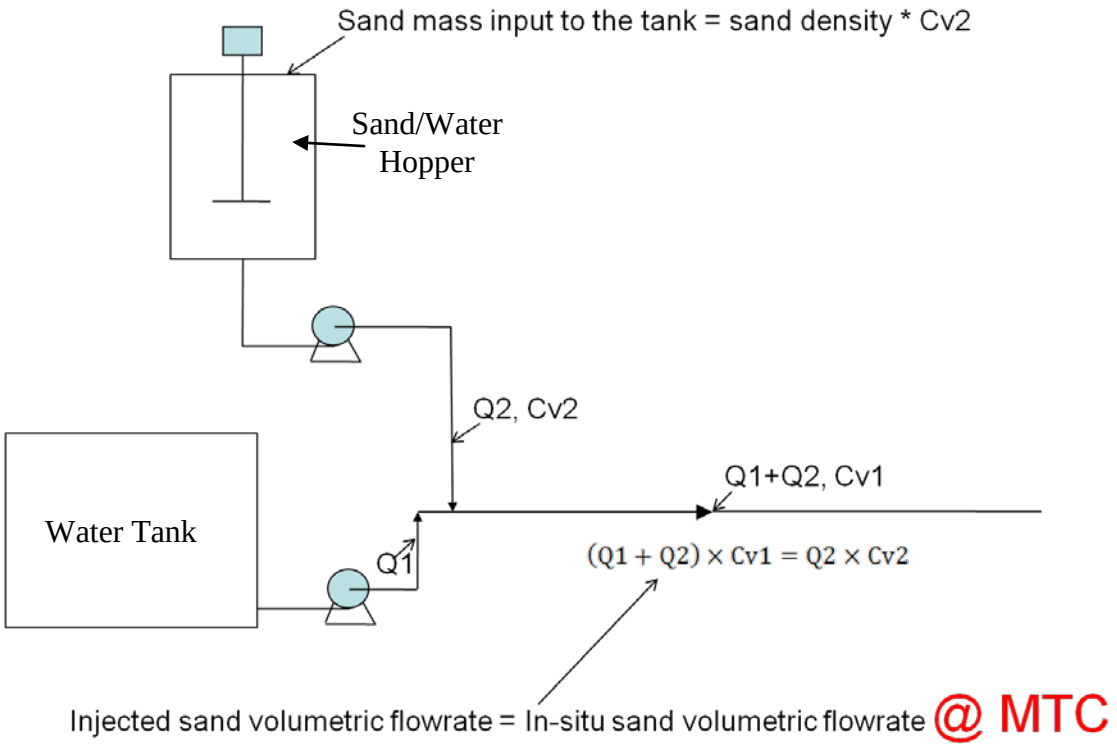

Figure 31: Design criterion to determine the in-situ sand concentration in pipeline

In the above Figure, Q1 indicates the volumetric flowrate from water tank, Q2 represents the volumetric flowrate from sand/water hopper, Cv1 is in-situ sand concentration in the main pipeline and Cv2 is the sand concentration when injecting the sand/water mixture. The total volumetric flowrate is calculated by 0.5 ms^{-1} mixture velocity multiplied the cross sectional area for main pipe. Q2 and Cv1 are known parameters. Therefore, the Cv2 can be obtained based on different required in-situ sand concentrations (Cv1).

Although there is no measurement techniques applied in this work due to their limitations, the design criterion proposed above is able to achieve reasonable accuracy on reflecting the approximate in-situ sand concentration in the field.

4 Results and Discussion for 2 inch Rig

The main aim of the sand transport experiments in the 2 inch rig was to investigate the sand transport characteristics in a small scale pipeline and provide some basic understanding of sand transport mechanism prior to the experiments in the 4 inch rig. The liquid holdup was not measured during the tests with the 2 inch rig. Some information about sand transport characteristics in 2 inch rig with different inclinations were summarized in Appendix A.

4.1 Sand-Water Transport Characteristics in Horizontal Pipeline

To understand the behaviour of the sand in single phase water flow, visual observations were conducted and several video clips were taken under different sand flow regimes. In order to have a good understanding of the sand particles motion in single-phase water flow, pictures were taken from the side of the pipe. Due to the similarity of the sand transport characteristics in water flow for different sand concentration, the sand behaviour at concentration of 50lb/1000bbl is presented below as representative.

The sand settling tests were performed starting from a liquid velocity of 1 $m \cdot s^{-1}$. When the water velocity was reduced to 0.55$m \cdot s^{-1}$, it was observed that the sand particles were moving mostly at the bottom of the pipe (Figure 32), which was close to the sand minimum transport condition (MTC).

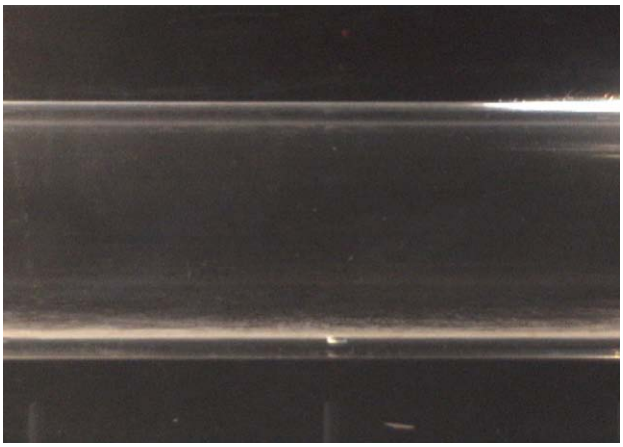

Figure 32: Sand streaks in horizontal sand-water flow
(50lb/1000bbl, V_L=0.55$m \cdot s^{-1}$, view from side, flow direction left to right)

Streaks of active sand particles were observed moving at the bottom of the pipe. Also, sand particles were saltating along or across those streaks. Sand concentration at the streaks which were moving along the centreline of the bottom of the pipe was found to be higher than the others.

When the velocity was decreased down to 0.47 $m \cdot s^{-1}$, as shown in Figure 33, a dense sand streak was formed along the centreline at the bottom of the pipe. At this velocity, every sand particle was still in motion.

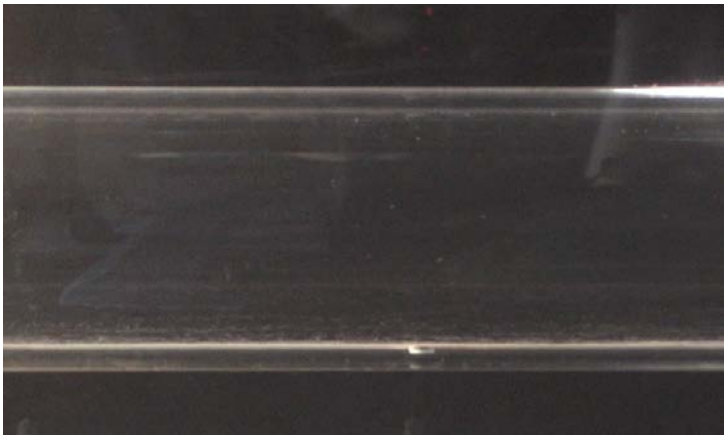

Figure 33: Sand streaks in horizontal sand-water flow
(50lb/1000bbl, V_L=0.47m·s^{-1}, view from side, flow direction left to right)

When the water velocity was further decreased to 0.45 m·s^{-1}, as shown in Figure 34, the dense streak of sand particles were divided into small dunes of sand particles. Several "transient bridges" were formed between two partially formed dunes, which indicated that some sand particles with small grain size were energetic enough to saltate over the sand dune and then finally settled in the transient bridge region.

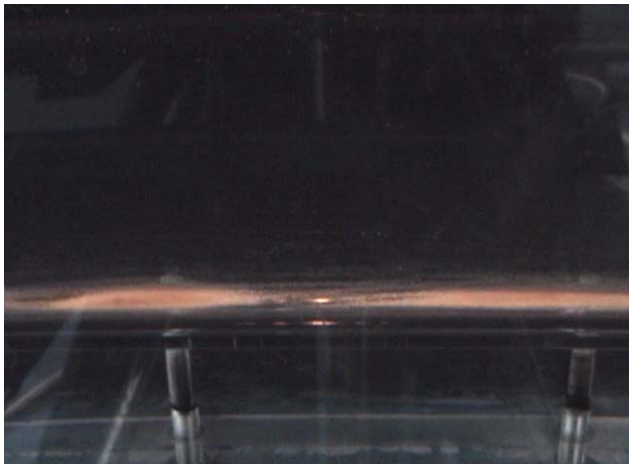

Figure 34: Scouring sand dunes in horizontal sand-water flow
(50lb/1000bbl, V_L=0.45m·s^{-1}, view from side, flow direction left to right)

When liquid velocity was 0.40 m·s^{-1}, the sand dunes were fully developed, as shown in Figure 35. Although there were a few streaks of active sand particles and some sand particles were creeping along the bottom of the pipe, the liquid velocity was far below the minimum transport velocity due to the formation of fully developed sand dunes.

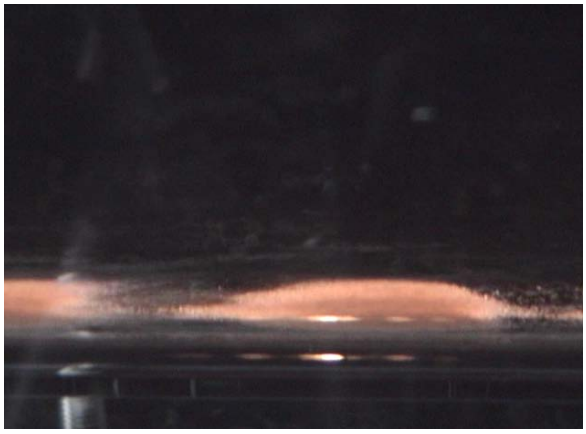

Figure 35: Developed sand dunes in horizontal sand-water flow
(50lb/1000bbl, V_L=0.40m·s^{-1}, view from side, flow direction left to right)

4.2 Sand-Water Transport Characteristics in 5-degree Uphill Pipelines

The sand transport characteristics in 5-degree uphill pipeline were found to be quite similar to that in horizontal pipeline. Dense sand streaks were also observed at water velocity of 0.47m·s^{-1}, as shown in Figure 36:

Figure 36: Sand streaks in 5-degree uphill sand-water flow
(50lb/1000bbl, V_L=0.47m·s^{-1}, view from top, flow direction left to right)

At V_L=0.45 m·s^{-1}, the sand particles were observed becoming less energetic and more compact. Also, the sand dunes were found to begin to form, see Figure 37.

Figure 37: Scouring sand dunes in 5-degree uphill sand-water flow (50lb/1000bbl, V_L=0.45m·s^{-1}, view from top, flow direction left to right)

At V_L= 0.40 m·s^{-1}, the sand dunes were observed to be scouring, as shown in Figure 38. Sand particles were more energetic and were seen to flow round and saltate between the dunes. Streaks of active sand particles were observed on the sides and between two sand dunes. Meanwhile, some of the active sand particles were saltating ahead of the front of the dunes. Interestingly, these active sand particles, mostly of smaller diameters, were scooped backward to the nose of the sand dune. However, streaks of highly energetic sand particles bridged across to the tail of the sand dune ahead. The behaviour of the sand dunes is a complex interaction of the fluid flow fields and particle dynamics.

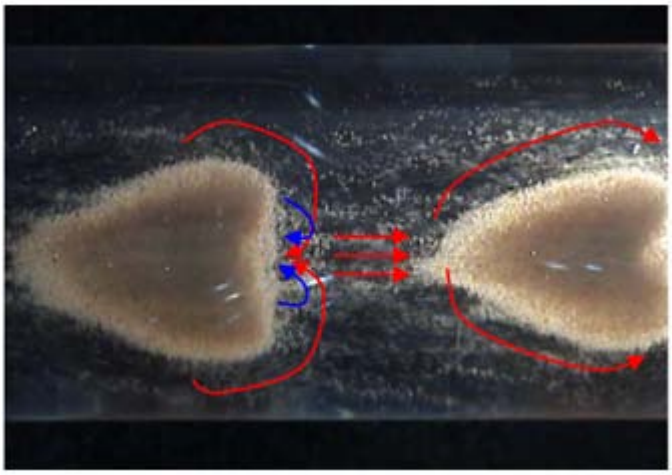

Figure 38: Developed sand dunes in 5-degree uphill sand-water flow (50lb/1000bbl, V_L=0.40m·s^{-1}, view from top, flow direction left to right)

4.3 Sand-Air-Water Transport Characteristics in Horizontal Pipeline

4.3.1 Air-Water Flow Regimes in Horizontal Pipeline

Prior to sand transport experiments, the flow regime characteristic of the test rig was first quantified. Figure 39 shows the observed flow regimes and test points.

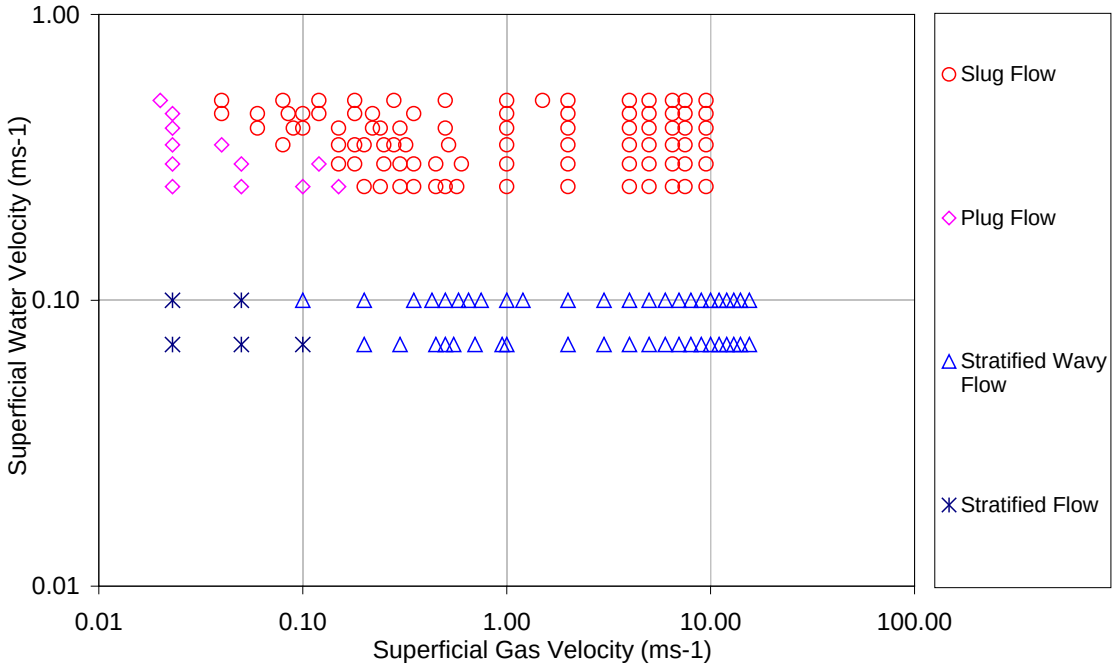

Figure 39: Experimental flow regime map for horizontal 2 inch air-water flow

4.3.2 Sand Transport Characteristics in Segregated Horizontal Flow

Stratified flow regime was observed at water superficial velocity (V_{SL}) of 0.07 $m \cdot s^{-1}$and gas superficial velocity (V_{SG}) below 1 $m \cdot s^{-1}$. In this flow regime no sand particle was observed to be moving.

Increasing the gas superficial velocity to above 1 $m \cdot s^{-1}$, the stratified wavy flow was observed. When sand production rates was 100lb/1000bbl and above, for most of the sand particles, no movement was observed until the gas superficial velocity was increased to 6 $m \cdot s^{-1}$, at which sand dunes were formed in the water layer, as shown in Figure 40.

Figure 41 shows the scouring sand dunes when the V_{SG} was at 8$m \cdot s^{-1}$. With increasing gas superficial velocity, the size of scouring sand dunes was getting bigger. There was a "bridge", streaks of active moving sand particles, between two sand dunes as shown in Figure 42.

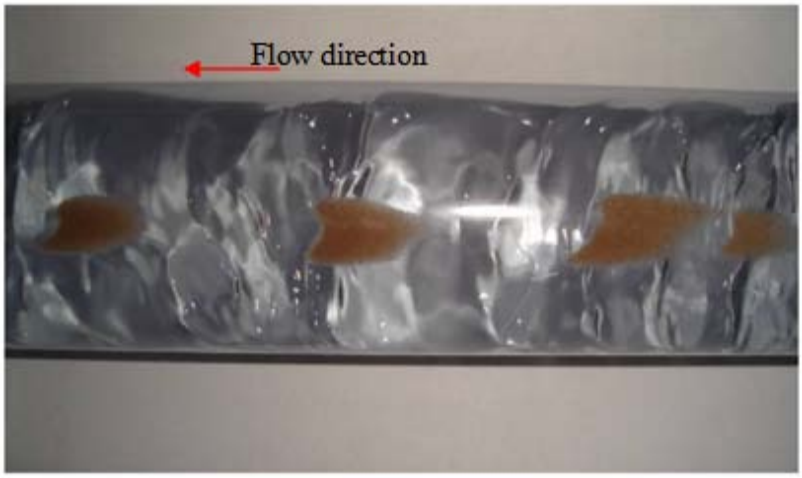

Figure 40: Sand dunes in stratified wavy flow
(V_{SL}= 0.07 m·s^{-1},V_{SG} =6 m·s^{-1}, view from bottom)

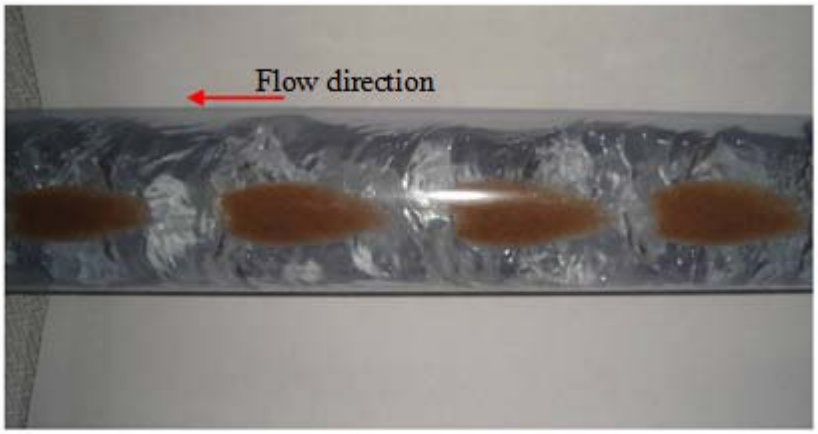

Figure 41: Sand dunes in stratified wavy flow
(V_{SL}= 0.07 m·s^{-1}and V_{SG}=8 m·s^{-1}, view from bottom)

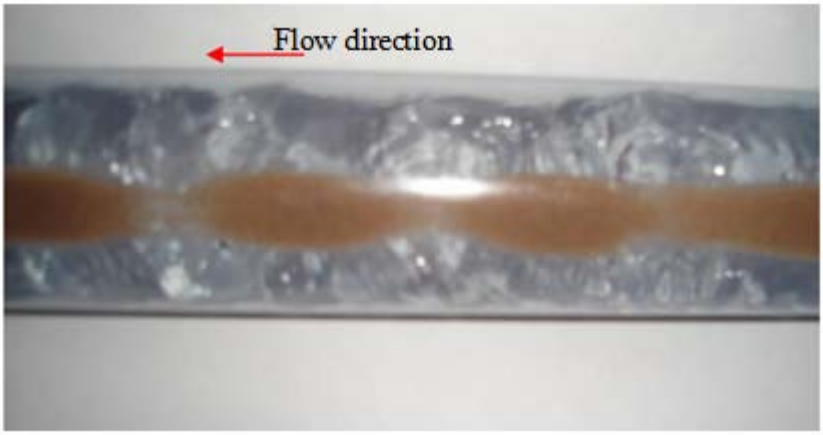

Figure 42: Scouring sand dunes with bridges in stratified wavy flow
(V_{SL}= 0.07 m·s^{-1} and V_{SG} =9 m·s^{-1}, view from bottom)

When the gas superficial velocity was increased beyond 9 m·s^{-1}, scouring dunes no longer exist, as shown in Figure 43. At V_{SG} = 10 m·s^{-1}, sand dunes were observed to link to each other, and, moved as a sliding sand layer. Further increase in gas flow, all

sand particles were observed saltating along the bottom with some particles even suspending in water.

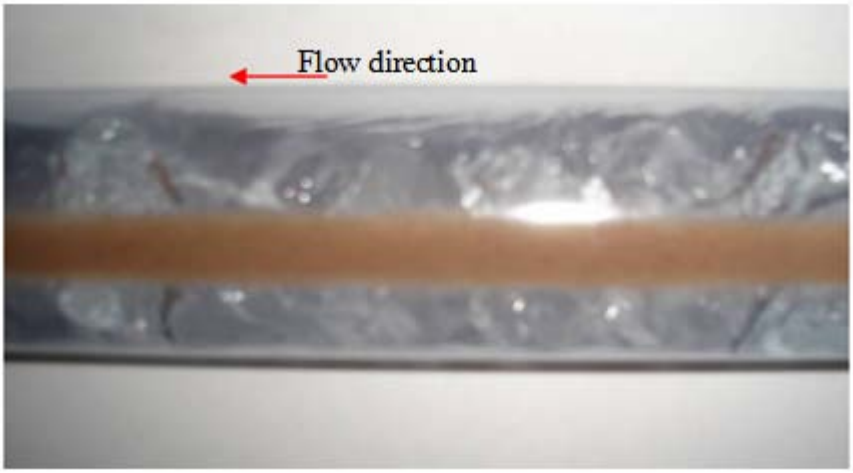

Figure 43: Sliding sand layer in stratified wavy flow (view from bottom)
(V_{SL}= 0.07 m·s^{-1} and V_{SG} =10 m·s^{-1})

With the sand production rates lower than 100lb/1000bbl, no sand dunes were observed as the gas superficial velocity was increased. At gas superficial velocity of up to 2 m·s^{-1}, dense sand streaks could be observed, similar to that observed in single phase water flow. At V_{SG}= 4 m·s^{-1}, all sand particles were observed to move in form of streaks at the bottom of the pipe.

It can be concluded that, in stratified flows, sand particles will deposit at the bottom of the pipe for all sand production rates tested in the experiments. For wavy stratified flows and sand production rates≥ 100lb/1000bbl, minimum sand transport conditions could be reached when the gas superficial velocity was sufficiently high.

4.3.3 Sand Transport Characteristics in Intermittent Horizontal Flow

The observed sand transport characteristics in horizontal air-water intermittent flow were consistent with the findings described by Stevenson et al. (2000).

At V_{SL} = 0.5 m·s^{-1}, slug flow was observed for a range of gas velocities.

Turbulence is generated at the slug front, where the pick-up process occurs. The slowly moving fluid from the liquid film penetrates into the highly turbulent fluid in slug body. The spread of the shear layer (from the film to the slug body) begins at the slug front. Turbulence is diffused along the direction of the penetrating film. When the turbulent eddies reach the sand particles which are settled on the pipe wall they are lifted into the slug body after the slug front has travelled a distance of 0.5~1.5 pipe diameters.

Once the sand particles start to move, they become very energetic due to the kinetic energy imparted to them. Some of the particles are picked up from the pipe bottom into the turbulent core of the slug while others begin to saltate along the bottom of the pipe wall. The behaviour is, probably, depending on the sand size distribution.

At the slug tail, the sand particles begin to shed into the film zone along with the water. As the sand particles enter the film zone, its velocity begins to decelerate partially due to the counter-current flow in the film zone. The active sand particles roll or bounce at the beginning of the film zone. But as energy is continuously consumed, the active sand particles become less energetic and eventually settled at the bottom of the pipe unless they are picked up by another slug body.

It was observed that by increasing the gas superficial velocity, the length of the film zone increased. As a result, more sand would deposit in this zone. The process of sand transport in slug flow is illustrated in Figure 44. Sand is picked up by the slug body and shed in the film. The process repeats for each passing slug.

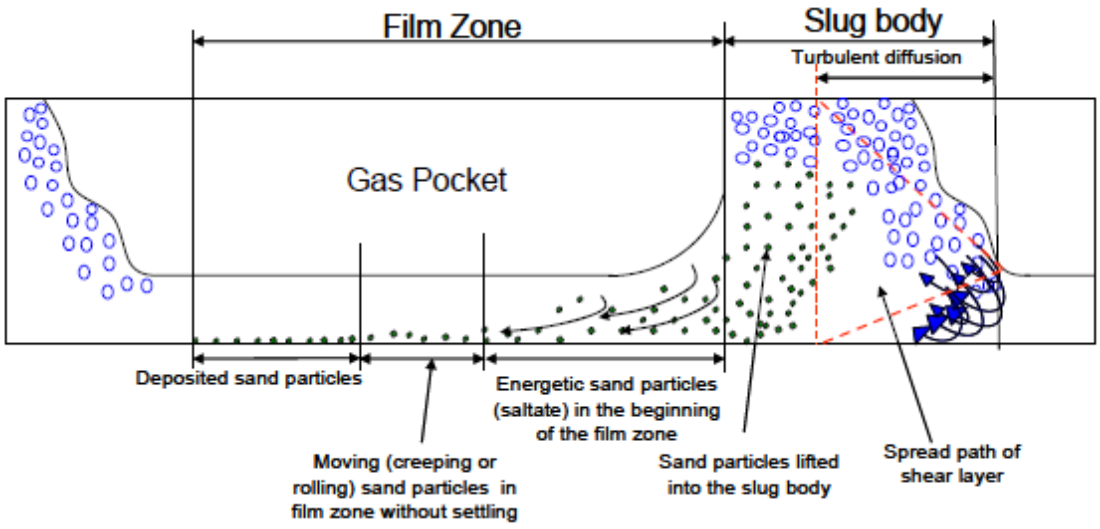

Figure 44: Schematic sand behaviour in slug flow

Increasing the gas superficial velocity at a constant water superficial velocity, V_{SL}= 0.5 $m \cdot s^{-1}$, the enhanced turbulence generated at the slug front increased gradually, increasing the number of gas bubble and chaotic behaviour at the front of the slug body. In the slug body, sand particles were observed to be lifted quicker and higher, which indicates the angle of the spreading shear layer increases with gas superficial velocity.

Thus the transport of sand in slug flow is a rather complex phenomenon. It depends heavily on the characteristics of the slug, like turbulence level, slug body and film length, amongst other factors.

Due to there is lack of definition of sand transport condition in air-liquid multiphase flow from previous work. Based on the experimental investigation, the author proposed the minimum transport condition for the sand particle under slug flow regime：

"the condition at which the sand particles will continue to be energetic enough to keep moving and not deposit in the slug body".

4.4 Sand-Air-Water Transport Characteristics in 5-degree Uphill Pipelines

4.4.1 Air-Water Flow Regimes in 5-degree Uphill Pipeline

The two phase air water flow map for the 5 degree upwardly inclined pipe is shown in Figure 45.

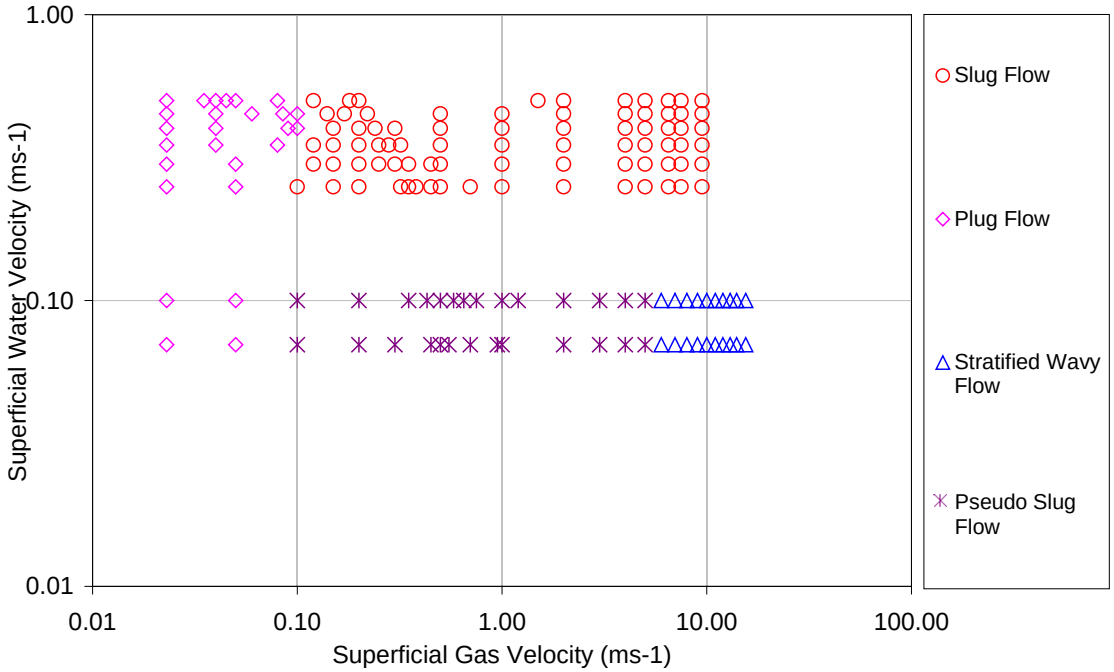

Figure 45: Experimental flow regime map for 5-degree uphill air-water flow

With slightly upward inclined pipe, intermittent (plug and slug) flow dominates. At liquid velocity, V_{SL} below 0.1 $m \cdot s^{-1}$, the flow pattern is mainly wavy stratified. When the gas velocity, V_{SG} was below 6 $m \cdot s^{-1}$, the surface wave occasionally bridged the top of the pipe. This condition is identified as pseudo slug flow to distinguish from hydrodynamic slug flow as the slugs are relatively short and aerated. With higher gas velocity, $V_{SG} > 6$ $m \cdot s^{-1}$, the regime is considered to be stratified wavy.

4.4.2 Sand Transport Characteristics in 5-degree Uphill Segregated Flow

When sand concentration $\leq$ 50lb/1000bbl, stratified wavy flow was observed at V_{SL} = 0.07$m \cdot s^{-1}$ and V_{SG} = 6 $m \cdot s^{-1}$ to 12 $m \cdot s^{-1}$. Sand particles were observed creeping forward or saltating in form of streaks along the bottom of pipe, as shown in Figure 46.

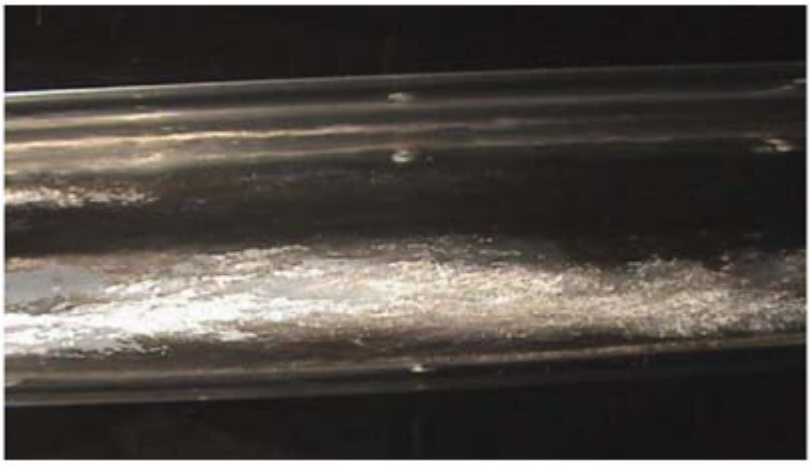

Figure 46: Sand behaviour in the stratified wavy flow
(Sand concentration < 100lb/1000bbl, flow direction left to right)

However, for 100lb/1000bbl and higher, a denser sand sliding layer was observed at the bottom of the pipe. In order to transport the sand sliding bed, the gas velocity has to be increased to V_{SG} = 12 m·s^{-1}. At this velocity, V_{SG} =12 m·s^{-1}, it was also observed some of the sand particles were gently creeping forward and saltating on the top of the sand sliding bed, see Figure 47.

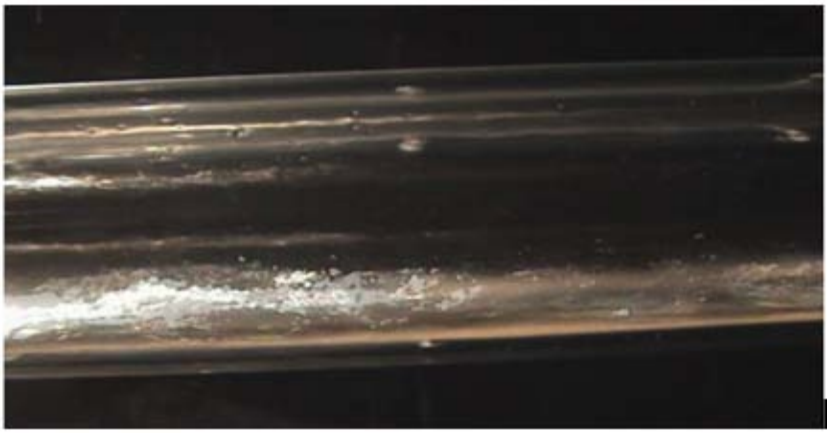

Figure 47: Dense sliding sand bed in the stratified wavy flow
(Sand concentration ≥ 100lb/1000bbl, flow direction left to right)

As the superficial gas velocity was increased, the amplitude as well as the velocity of the surface waves also increased, as shown in Figure 48 and Figure 49. Sprays were created with liquid film on the pipe wall.

Figure 48: Waves generated under stratified wavy flow regime at V_{SG} =10m·s^{-1} (flow direction left to right)

Figure 49:Waves generated under stratified wavy flow regime at V_{SG} =12m·s^{-1} (flow direction left to right)

Sand particles were observed to be saltating under the more vigorous waves and then creeping forward in the less energetic waves when $V_{SG} \geq 12$m·s^{-1}. No reverse flow of sand particles was observed under the stratified wavy flow regime.

4.4.3 Sand Transport Characteristics in 5-degree Uphill Intermittent Flow

At V_{SL} = 0.07m·s^{-1} and 0.5m·s^{-1} slug flow regime was observed when the gas superficial velocity was from V_{SG} = 0.1 m·s^{-1} to 9.5 m·s^{-1}.

For V_{SL} = 0.07 m·s^{-1} and 0.1 m·s^{-1} and V_{SG} = 0.1 m·s^{-1} up to 5 m·s^{-1} the slug body is relatively short and very aerated with long and very active film zone. Sand particles behaviour in slug flow was similar to that observed in the horizontal flow. The lift of sand particles due to turbulent diffusion was also observed as well in the slug body, as shown in Figure 50.

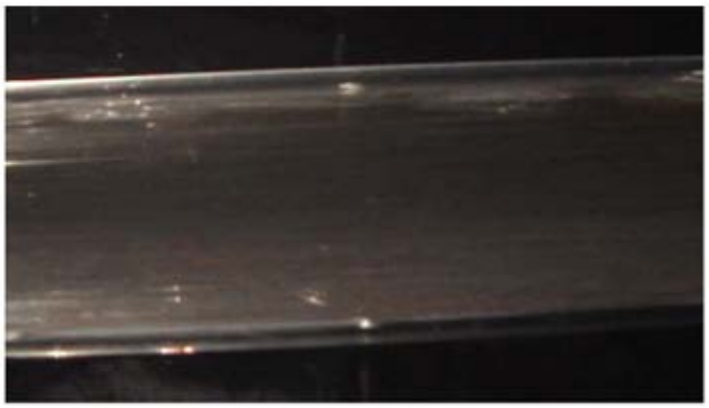

Figure 50: Sand diffusion in the slug body
(V_{SL} =0.5m·s^{-1}, V_{SG} = 2 m·s^{-1}, flow direction left to right)

At water superficial velocity V_{SL} = 0.5 m·s^{-1}, the size of the slug body was much bigger than that at V_{SL} = 0.07m·s^{-1}. Much more sand particles were observed to be entrained in the slug body due to the enhanced turbulent energy generated at the front of slug body. Therefore, the sand transport was more efficient when the water superficial velocity was V_{SL} = 0.5m·s^{-1}. The sand particles behaviour in slug flow unit in pipeline inclined 5 degrees upward is schematically shown in Figure 51 and Figure 52.

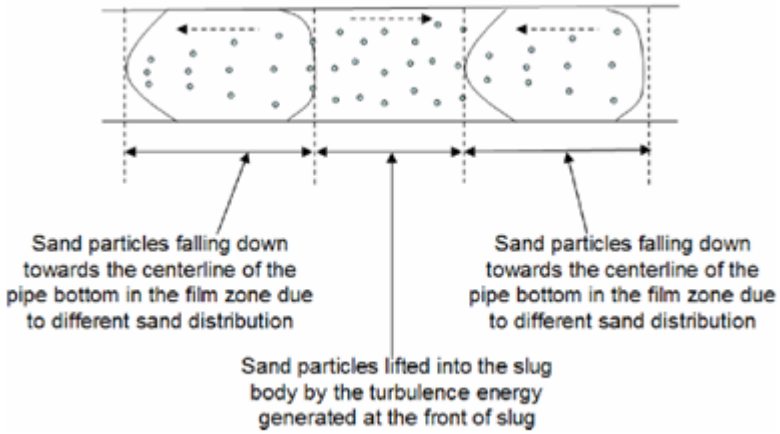

Figure 51: Schematic drawing of the sand particles behaviour in slug flow (top view)

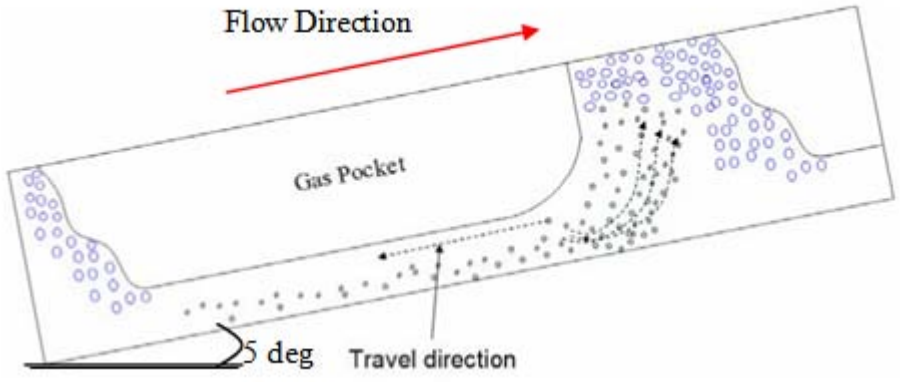

Figure 52: Schematic drawing of the sand particles behaviour in slug flow (side view)

Once the sand particles entered the film zone of the slug unit, they immediately stopped moving forward due to the shedding process and the effect of gravity caused by the inclination. Therefore, the sand particles tended to move backward with the backflow rather than settled. Meanwhile, due to the difference of the sand size distribution, some of the sand particles began to fall down towards the centreline of the bottom of the pipe while travelling with the water film until they were picked up by the next slug body, see Figure 53.

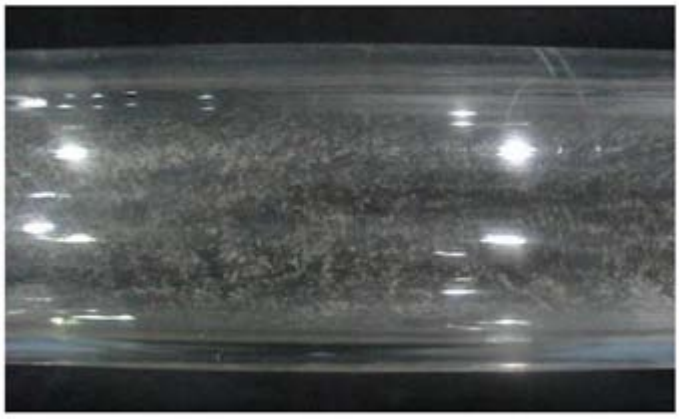

Figure 53: Sand particles behaviour once entered into the film zone
(View from top, V_{SL} =0.07m·s^{-1} and V_{SG} = 0.5 m·s^{-1}, flow direction left to right)

5 Results and Discussion for 4 inch Rig

This section described the typical behaviours for different sand concentration in 4 inch water, air-water and air-CMC flows. All the sand transport characteristics in 4 inch rig with different inclinations were summarized in Appendix A.

5.1 Sand-Water Transport Characteristics in Horizontal Pipeline

From visual observations at different water velocities, it was found that the sand minimum transport condition for 15lb/1000bbl ranges from V_L= 0.50 — 0.60 m·s^{-1} as illustrated in Figure 54.

V_L =0.60 m·s^{-1} V_L =0.50 m·s^{-1}

Figure 54: Sand streaks observed in horizontal water flow when V_L> 0.50 m·s^{-1} (15lb/1000bbl, view from bottom, flow direction left to right)

From Figure 55, at water velocity ≤ 0.35 m·s^{-1}, hardly any sand particles were observed at the bottom of the Perspex pipe section. There were two reasons which caused this phenomenon. One of them was the difference in the pipe material roughness between the Perspex and steel pipes. However, in this work, the smooth steel pipe was used with the roughness 0.0001m. The other one was the roughness increase due to the sand particles settling. When the water velocity was below the MTC, bigger sand particles started settling at the bottom of the pipe first due to sand size distribution, which influenced the movement of other particles. Therefore, the friction was increased by the increasing amount of settled particles. As a result, early settlement of the sand particles might occur at the bottom of the steel pipe section at these low water velocities. Also, at 15lb/100bbl sand concentration and low water velocities ≤ 0.35 m·s^{-1}, no sand dunes were observed.

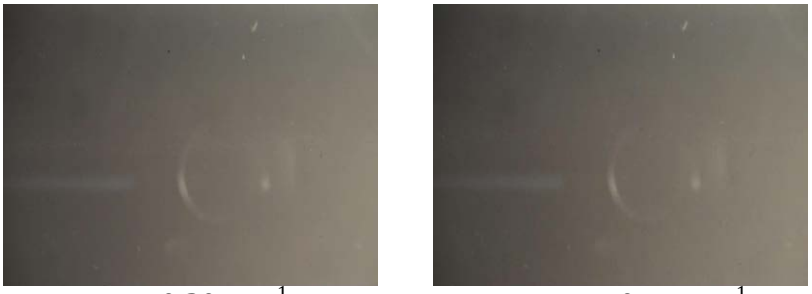

V_L =0.30 m·s^{-1} V_L =0.15 m·s^{-1}

Figure 55: Sand transport characteristics in horizontal water flow when V_L < 0.35 m·s^{-1} (15lb/1000bbl, view from bottom, flow direction left to right)

In order to confirm the observed MTC was the actual MTC happened in the steel pipeline, the additional water flushing procedure was performed:

1) Any sand remaining from previous experiment in the loop is removed by flushing with water.

2) Prepare sand-water mixture of the required concentration in the hopper (sand mixing tank).

3) Start the liquid pump and adjust the controller until the observed MTC in previous test, then maintain this flowrate for 5 minutes.

4) Increase the flowrate rapidly and observe whether there was sudden increase of sand concentration in the Perspex viewing section.

5) Repeat 1), 2), then adjust the controller until the velocity was slightly lower than observed MTC in previous test, then maintain this flowrate for 5 minutes.

6) Repeat 4) until clearly observing sudden increase of sand concentration in the Perspex viewing section. The velocity at this stage was below the lower limit of MTC velocity.

By applying this approach, the low limit for MTC in steel pipeline was confirmed each time after identifying the MTC initially for all the sand concentrations.

For 200lb/1000bbl sand concentration, the observed sand minimum transport velocity was V_L= 0.65 – 0.75 m·s^{-1}, see Figure 56. Sand dunes were observed at this concentration when V_L= 0.45 m·s^{-1} or even lower, as illustrated in Figure 57.

V_L =0.75 m·s^{-1} V_L =0.65 m·s^{-1}

Figure 56: Sand streaks observed in horizontal water flow when V_L> 0.65 m·s^{-1} (200lb/1000bbl, view from bottom, flow direction left to right)

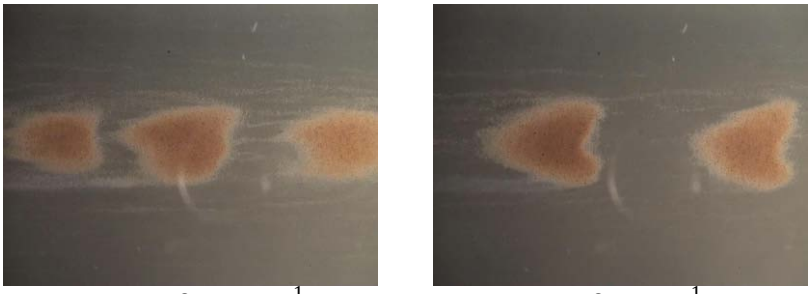

V_L =0.45 m·s^{-1} V_L =0.4 m·s^{-1}

Figure 57: Sand dunes observed in horizontal water flow (200lb/1000bbl, view from bottom, flow direction left to right)

The sand minimum transport conditions were much higher for 500lb/1000bbl due to the increased sand concentration. For 500lb/1000bbl, when approaching the sand minimum transport condition, sand particles were observed moving in form of several streaks, spreading along the bottom of the pipe. The dense streaks could be observed but broken up by the flow from time to time. However, when further reducing the water velocity from the sand minimum transport condition, the sand streaks tends to fall towards the centerline of the bottom of the pipe, and a dense streak can be always observed during the test. From visual observation as presented in Figure 58, the sand minimum transport condition was between 0.75 and 0.85 m·s^{-1} for 500lb/1000bbl. Sand dunes were observed at this concentration for water velocities range from 0.45 m·s^{-1} to 0.3 m·s^{-1} as illustrated in Figure 59.

V_L =0.85 m·s^{-1} V_L =0.75 m·s^{-1}

Figure 58: Sand streaks observed in horizontal water flow when V_L> 0.75 m·s^{-1} (500lb/1000bbl, view from bottom, flow direction left to right)

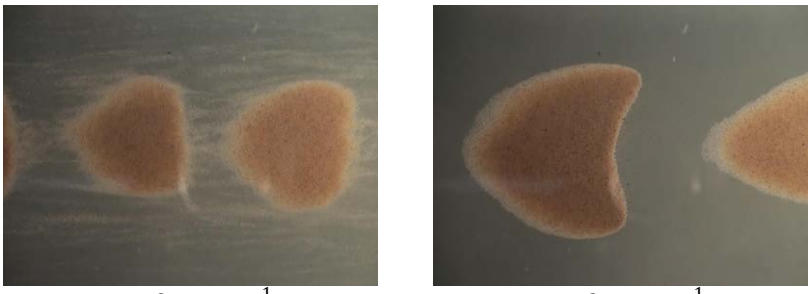

V_L =0.45m·s^{-1} V_L =0.15m·s^{-1}

Figure 59: Sand dunes observed in horizontal water flow
(500lb/1000bbl, view from bottom, flow direction left to right)

5.2 Sand-Water Transport Characteristics in Uphill Inclined Pipelines (5, 10, 20 degrees)

The sand transport characteristics in 5, 10 and 20 degrees uphill inclined pipe were found to be similar to that in horizontal pipe flow. The appearance of dense streaks of the sand particles at the bottom of the pipe centreline indicated that the sand minimum transport condition was approached. Also, the sand minimum transport conditions for different concentrations were found to be similar to that in horizontal water flow.

The sand transport characteristics in 5-degree uphill pipeline are described below as an example for the other two inclinations. For 15lb/1000bbl, from these visual observations and at different water velocities, it was found that the sand minimum transport condition for 15lb/1000bbl ranges from V_L= 0.5 – 0.6 m·s^{-1} as illustrated in Figure 60, and sand dunes were not observed at low water velocities ≤ 0.35 m·s^{-1}.

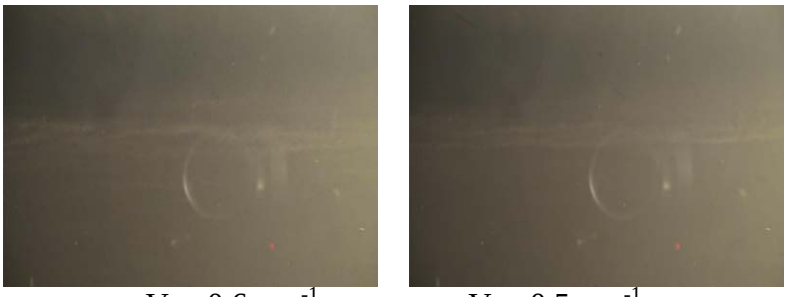

V_L =0.6 m·s^{-1} V_L =0.5 m·s^{-1}

Figure 60: Sand streaks observed in 5-degree uphill water flow
(15lb/1000bbl, view from bottom, flow direction left to right)

For 200lb/1000bbl sand concentration, the observed sand minimum transport velocity was V_L= 0.65 – 0.75 m·s^{-1} (Figure 61). Sand dunes were observed at this concentration for water velocities ≤ 0.45 m·s^{-1}(Figure 62).

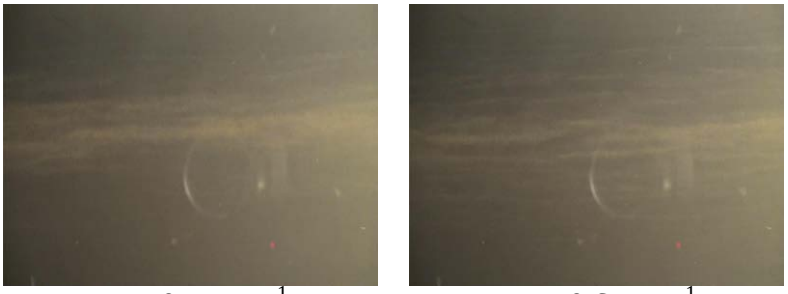

V_L =0.75 m·s^{-1} V_L =0.65 m·s^{-1}

Figure 61: Sand streaks observed in 5-degree uphill water flow (200lb/1000bbl, view from bottom, flow direction left to right)

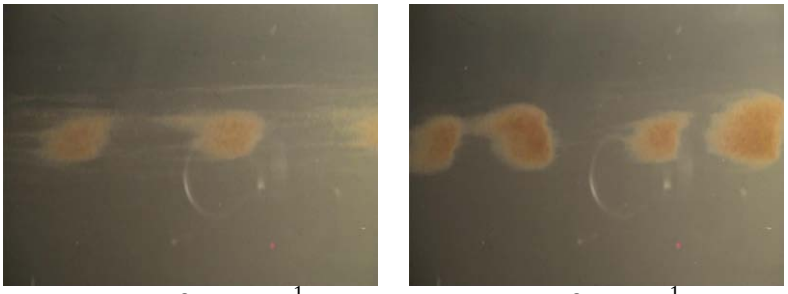

V_L =0.45 m·s^{-1} V_L =0.4 m·s^{-1}

Figure 62: Sand dunes observed in 5-degree uphill water flow (200lb/1000bbl, view from bottom, flow direction left to right)

For 500lb/1000bbl, the sand minimum transport condition ranges from 0.75 m·s^{-1} to 0.85 m·s^{-1} as depicts in Figure 63. Sand dunes were observed at this concentration for water velocities ≤ 0.45 m·s^{-1}(Figure 64).

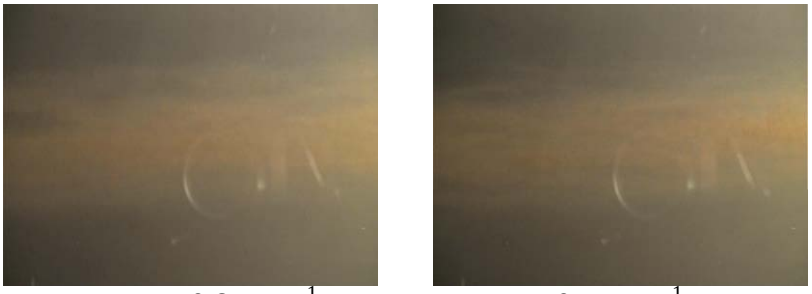

V_L =0.85 m·s^{-1} V_L =0.75 m·s^{-1}

Figure 63: Sand streaks observed in 5-degree uphill water flow (500lb/1000bbl, view from bottom, flow direction left to right)

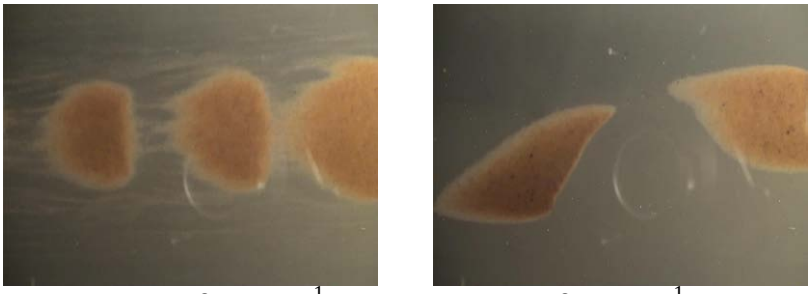

V_L =0.45 m·s^{-1} V_L =0.15 m·s^{-1}

Figure 64: Sand dunes observed in 5-degree uphill water flow (500lb/1000bbl, view from bottom, flow direction left to right)

5.3 Sand-Air-Water Transport Characteristics in Horizontal Pipeline

5.3.1 Air-Water Flow Regimes in Horizontal Pipeline

In order to understand the sand transport characteristics under different air-water flow conditions, the flow regime characteristic of the 4 inch test rig was identified prior to the sand experiments. Figure 65 shows the observed two-phase air-water flow regimes and test points for the horizontal 4 inch steel pipelines.

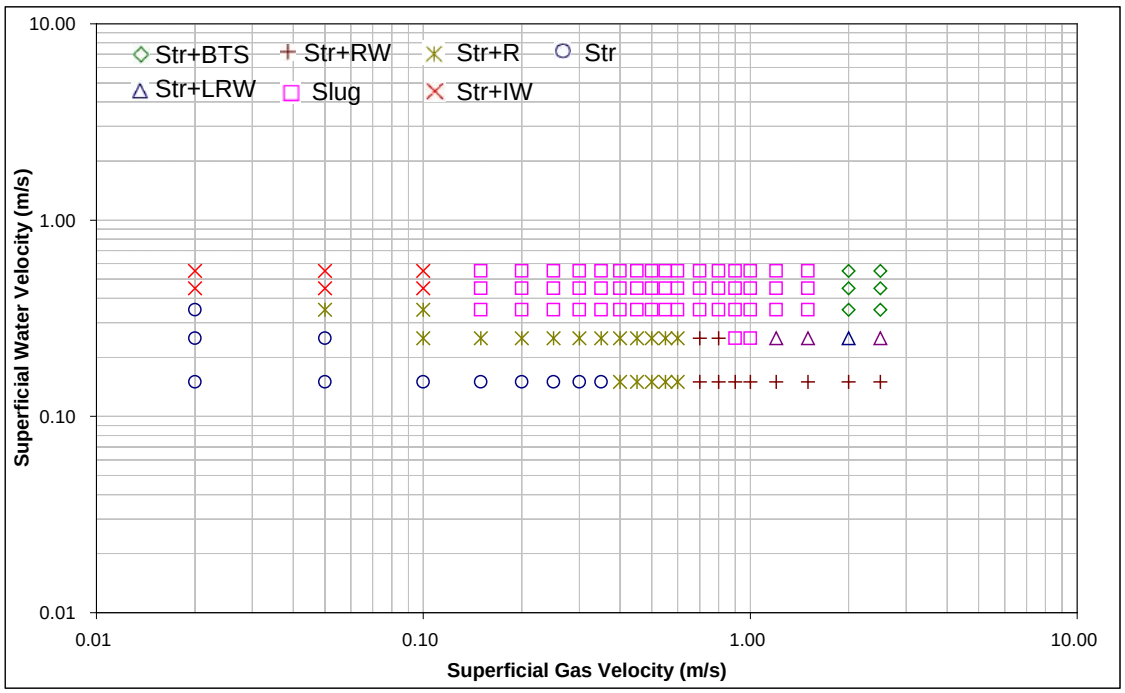

Figure 65: 4 inch horizontal experimental flow regimes

* Str+BTS : Stratified + Blow through slug, pseudo slug without bridging the top of the pipe
Str+IW: Plug flow, the liquid almost fully bridge the top of the pipe
Str+RW: Stratified + Roll wave, stratified wavy flow with high amplitude waves
Str+R: Stratified + Ripple, stratified flow with stable waves
Str: Stratified flow
Str+LRW: Stratified + Large roll wave, stratified wavy flow with highest amplitude waves

The observed flow regime in the 4 inch test facility was classified according to Spedding and Spence (1993), as shown in Figure 66. The test points are also listed in Table 12.

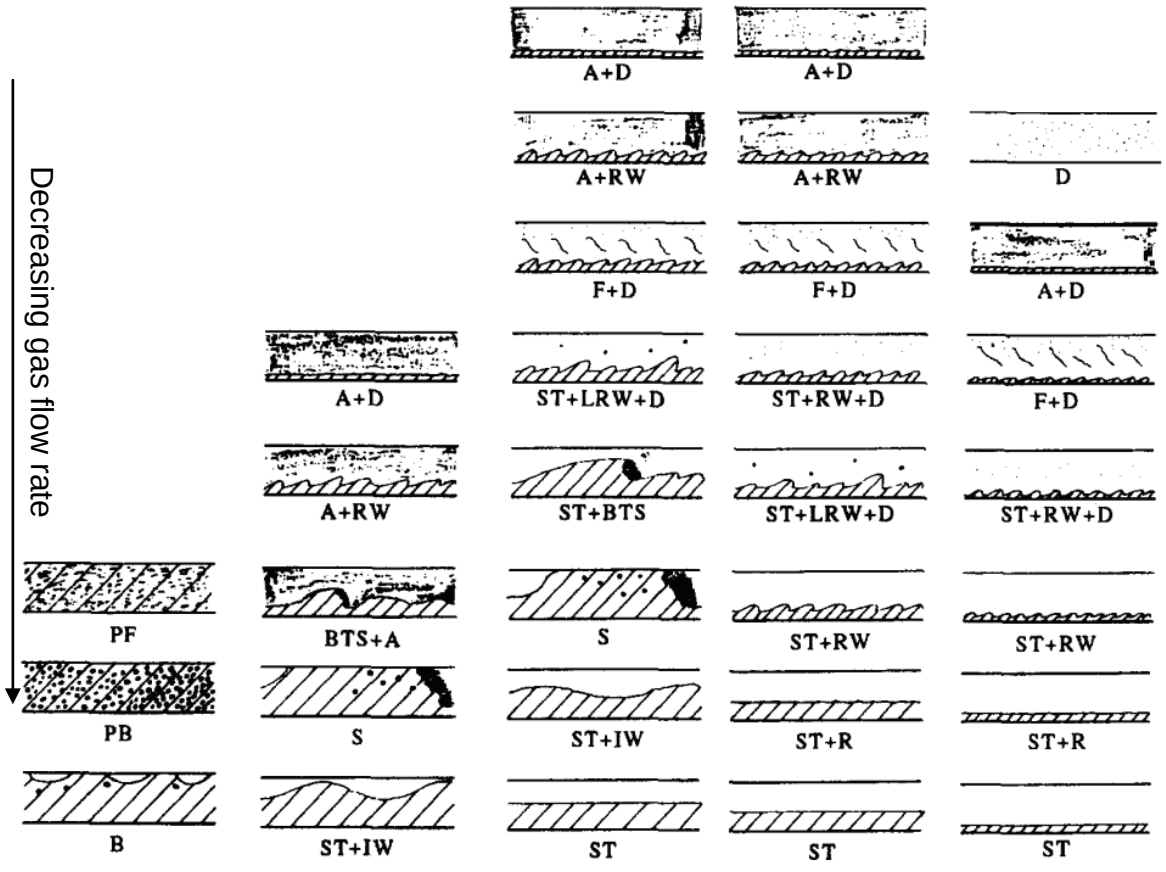

Figure 66: 4 inch horizontal air/water flow regimes according to Spedding and Spence (1993) ,ID=0.0935m

Table 12: Test matrix and observed flow regime

V_{SG} ($m \cdot s^{-1}$)	V_{SL} ($m \cdot s^{-1}$)				
	0.55	**0.45**	**0.35**	**0.25**	**0.15**
2.5	Str+BTS	Str+BTS	Str+BTS	Str+LRW	Str+RW
2	Str+BTS	Str+BTS	Str+BTS	Str+LRW	Str+RW
1.5	Slug	Slug	Slug	Str+LRW	Str+RW
1.2	Slug	Slug	Slug	Str+LRW	Str+RW
1	Slug	Slug	Slug	Slug	Str+RW
0.9	Slug	Slug	Slug	Slug	Str+RW
0.8	Slug	Slug	Slug	Str+RW	Str+RW
0.7	Slug	Slug	Slug	Str+RW	Str+RW
0.6	Slug	Slug	Slug	Str+R	Str+R
0.55	Slug	Slug	Slug	Str+R	Str+R
0.5	Slug	Slug	Slug	Str+R	Str+R
0.45	Slug	Slug	Slug	Str+R	Str+R
0.4	Slug	Slug	Slug	Str+R	Str+R
0.35	Slug	Slug	Slug	Str+R	Str
0.3	Slug	Slug	Slug	Str+R	Str
0.25	Slug	Slug	Slug	Str+R	Str
0.2	Slug	Slug	Slug	Str+R	Str
0.15	Slug	Slug	Slug	Str+R	Str
0.1	Str+IW	Str+IW	Str+R	Str	Str
0.05	Str+IW	Str+IW	Str+R	Str	Str
0.02	Str+IW	Str+IW	Str	Str	Str

5.3.2 Sand Transport Characteristics in Intermittent Horizontal Flow

From Table 12, the intermittent stratified+inertial wave (plug) flow and slug flow regimes occurred at a range of water and gas superficial velocities. As illustrations, the sand particles behaviour under slug and plug flows at constant water superficial velocity, V_{SL} = 0.45 $m \cdot s^{-1}$ and gas superficial velocities between 0.02 $m \cdot s^{-1}$ to 2.5 $m \cdot s^{-1}$ are described.

At V_{SL} = 0.45 $m \cdot s^{-1}$

- When $V_{SG} \leq 0.1$ $m \cdot s^{-1}$, ***stratified+ inertial wave (Plug) flow*** was observed. The liquid plug was in the form of a big wave without bridging the top of the pipe.

At 15lb/1000bbl, sand particles were observed to saltate as streaks during the passing of the liquid plug body. The majority of sand particles settled immediately within the film region after the plug is passed. However, a few sand particles were observed sliding away the centerline of the bottom of the pipe, see Figure 67.

a) sand saltating in plug body b)sand sliding in plug film region

Figure 67: Sand characteristic in plug flow
(V_{SL}=0.45m·s^{-1}, V_{SG}=0.1m·s^{-1},15lb/1000bbl)
(view from bottom, flow direction left to right)

For 200lb/1000bbl and 500lb/1000bbl, a dense sliding bed was observed in plug flow regime, as shown in Figure 68 and Figure 69, respectively. The concentration of the sand in the middle of the pipe bottom increases with sand concentration.

a) sand bed in plug body b)sand bed in film region

Figure 68: Sand characteristic in plug flow
(V_{SL}=0.45m·s^{-1}, V_{SG}=0.1m·s^{-1}, 200lb/1000bbl)
(view from bottom, flow direction left to right)

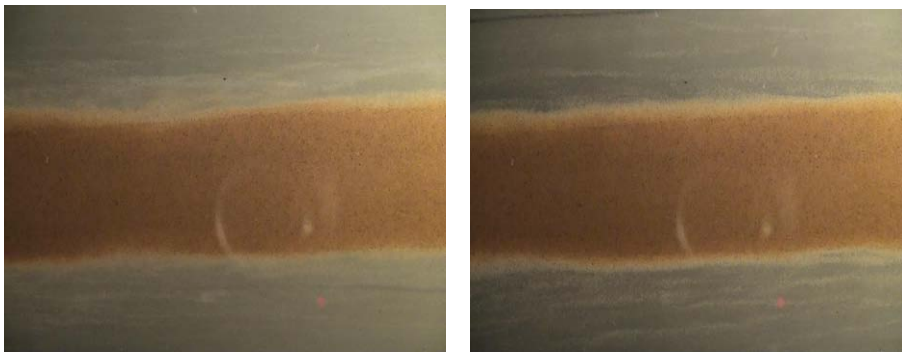

a) sand bed in plug body b)sand bed in film region

Figure 69: Sand characteristic in plug flow (V_{SL}=0.45m·s^{-1}, V_{SG}=0.1m·s^{-1} 500lb/1000bbl)
(view from bottom, flow direction left to right)

- When $V_{SG} \geq 0.1$ m·s^{-1}, ***slug flow*** was observed.

The sand behaviour in slug flow was found to be similar to that in the 2 inch tests. Turbulence is generated at the front of the slug, where the pick-up process occurs. Turbulence is enhanced with the slowly moving fluid in the film region penetrating into the slug body. The spread of the shear layer (from the film to the slug body) begins at the slug front and is diffused along the direction of the penetrating film. As the turbulent energy reaches the sand particles that are settled on the pipe wall, they will be picked up and lifted into the slug body.

At the slug tail, the sand particles begin to shed into the film zone. As the sand particles enter the film zone, its velocity begins to decelerate partly due to the counter-current flow in the film zone. The process repeats for each passing slug (Figure 70 and Figure 71).

Figure 70: Sand behaviour in slug body
(200lb/1000bbl, view from side, flow direction left to right)

Figure 71: Sand behaviour in slug film zone
(200lb/1000bbl, view from side, flow direction left to right)

Figure 72, Figure 73 and Figure 74, illustrated respectively the sand particles behaviour in slug body and film zone for 15, 200 and 500lb/1000bbl at V_{SL}= 0.45 m·s^{-1} and V_{SG}= 0.35 m·s^{-1}.

At V_{SL}= 0.45 m·s^{-1}, V_{SG}= 0.35 m·s^{-1} and 15lb/1000bbl, it was observed that sand particles were lifted by turbulence at the front of the slug and transported in both the slug body and the liquid film. The sand minimum transport velocity for this concentration was observed to occur at V_{SG} = 0.1m·s^{-1} and V_{SL}= 0.45 m·s^{-1}.

For 200 lb/1000bbl, V_{SL}= 0.45 m·s^{-1} and V_{SG}= 0.35 m·s^{-1}, a few sand particles were observed gently rolling at the front of the film zone (slug tail shedding region) and eventually settled at the end of the film zone. Below this flow condition, the slug body was not energetic (not aerated) enough; and, as a result, sand particles also settled in the slug body. For this concentration of 200lb/1000bbl, the MTC was observed to occur at V_{SL} = 0.45m·s^{-1} and V_{SG}= 0.30 m·s^{-1}. Considering that sand could accumulate upstream in the steel pipe, similar water flushing procedure, as stated in Section 7.1, was performed for each concentration to assure the correct transport condition was recorded.

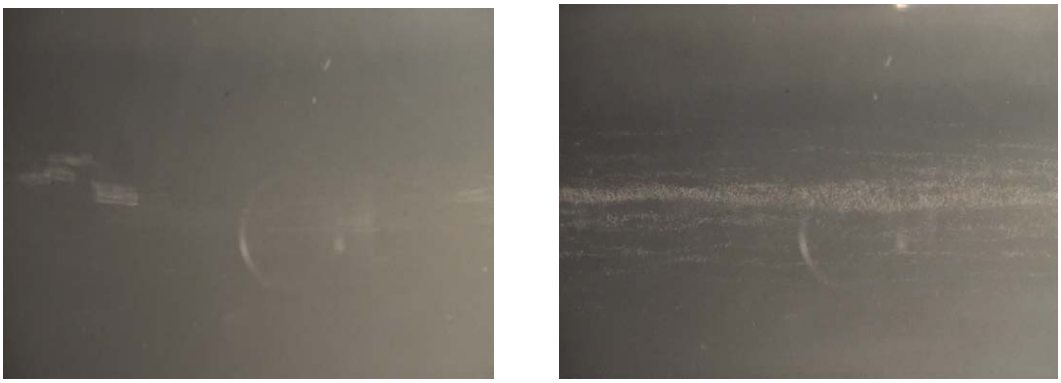

a) slug body b) film zone

Figure 72: Sand characteristic in slug flow
(V_{SL}= 0.45 m·s^{-1} and V_{SG}= 0.35 m·s^{-1} 15lb/1000bbl)
(view from bottom, flow direction left to right)

a) slug body b) film zone

Figure 73: Sand characteristic in slug flow
(V_{SL}= 0.45 m·s^{-1} and V_{SG}= 0.35 m·s^{-1} 200lb/1000bbl)
(view from bottom, flow direction left to right)

For 500 lb/1000bbl, and at V_{SL}= 0.45 m·s^{-1} and V_{SG}= 0.35 m·s^{-1}, sand particles were settled in both film zone and slug body. And the MTC for 500 lb/1000bbl was observed at V_{SG} = 0.60 m·s^{-1} and V_{SL}= 0.45 m·s^{-1}.

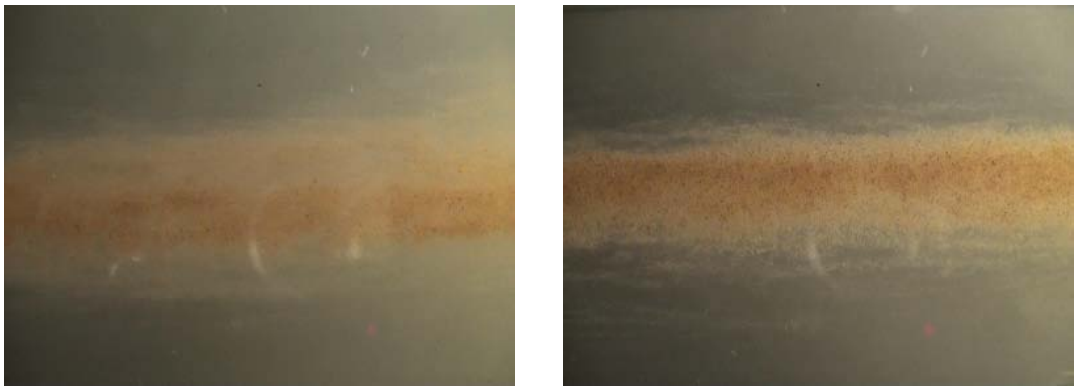

a) slug body b) film zone

Figure 74: Sand characteristic in slug flow
(V_{SL}= 0.45 m·s^{-1} and V_{SG}= 0.35 m·s^{-1} 500lb/1000bbl)
(view from bottom, flow direction left to right)

5.3.3 Sand Transport Characteristics in Segregated Horizontal Flow

The sand particles behaviour in segregated flows (stratified+ ripple flow and stratified wavy flow) was demonstrated below, at constant water superficial velocity, V_{SL} = 0.15 m·s^{-1} when V_{SG} = 0.02 —2.5 m·s^{-1}.

- When $V_{SG} \leq$ 0.7 m·s^{-1}, stratified **+ *ripple flow*** was observed. In stratified flow regime, the sand particles were observed to have no obvious movements in the liquid film for all the concentration tested.

At 15lb/1000bbl, a few sand particles were observed in the film region, as shown in Figure 75.

Figure 75: Sand characteristic in stratified flow
(V_{SL}=0.15m·s^{-1}, V_{SG}=0.4m·s^{-1} 15lb/1000bbl)
(view from bottom, flow direction left to right)

However, at 200lb/1000bbl and 500lb/1000bbl, sand dunes were observed in the liquid film region, as shown in Figure 76.

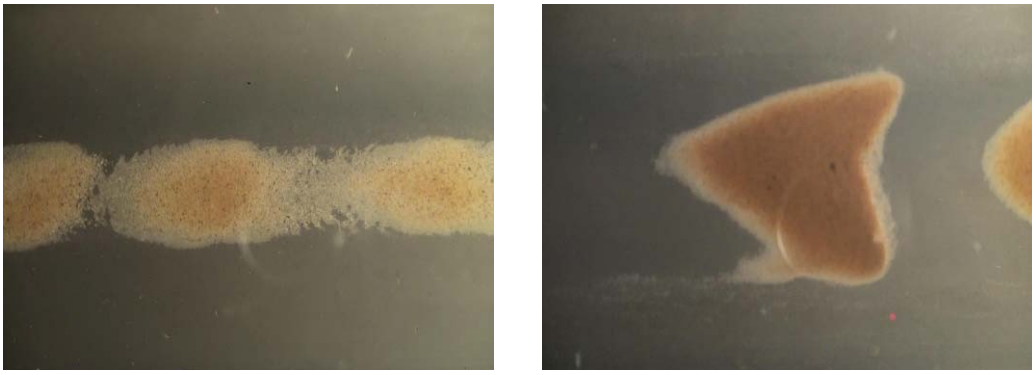

a) 200lb/1000bbl b) 500lb/1000bbl

Figure 76: Sand characteristic in stratified flow
(V_{SL}=0.15m·s^{-1}, V_{SG}=0.4m·s^{-1})
(view from bottom, flow direction, left to right)

The height and size of dunes for 500lb/1000bbl is much bigger than the dunes formed for 200lb/1000bbl. Only a few particles were observed sliding along the top and aside the sand dunes.

- When $V_{SG} \geq 0.7$ m·s^{-1}and V_{SL} =0.15 m·s^{-1} , ***stratified + roll wavy flow*** was observed.

The transition from smooth stratified to stratified wavy occurred when the gas superficial velocity was increased beyond 0.7 m·s^{-1}. This transition resulted in the formation of waves as shown in Figure 77. The waves formed were observed to have different amplitudes. The wave was caused by the gas flow as a result of energy transfer between the gas and liquid phase. In other words, the gas flow trigger the transition from laminar to turbulent flow within the mean thickness of the liquid layer, thus the wave body is a very active medium and energetic enough to induce the transportation the sand particle. Several researchers, e.g. Taitel and Dukler (1976), Barnea et al. (1980) and Lioumbas et al (2004) investigated the level of energy in the wave. The investigation was based on velocity and consequently the corresponding critical Reynolds number for three regions, i) before the wave, ii) wave body and iii) after the wave. As a result, they concluded that the Reynolds number showed its highest value for the wave body (ii).

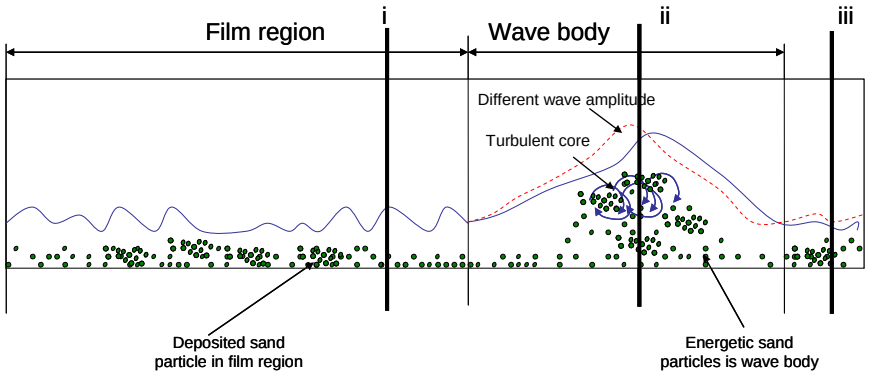

Figure 77: Schematic drawing for sand behaviour in stratified wavy flow

For 15lb/1000bbl and at high superficial gas velocities of 2.5 and 1.5 $m \cdot s^{-1}$, see Figure 78 and Figure 79 respectively, the sand particles were observed saltating energetically along the bottom of the pipe. However, the activity and energy of sand particles were more enhanced in the wave body

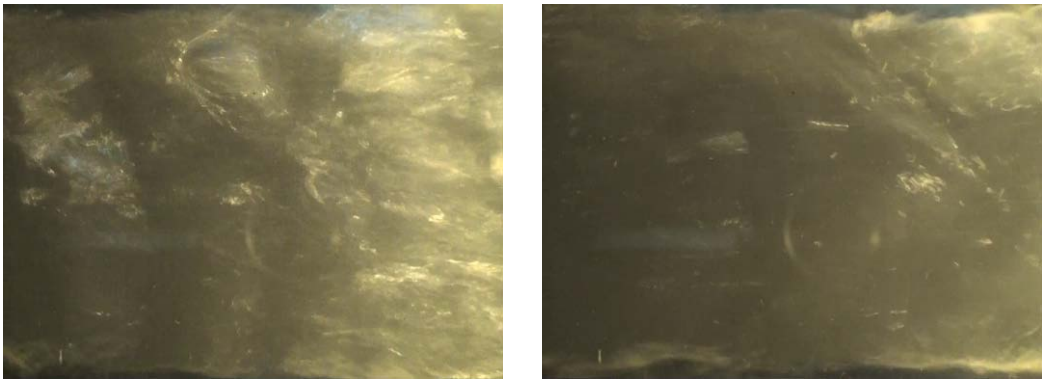

a) sand in wave body b)sand in film region

Figure 78: Sand characteristic in stratified wavy flow
(V_{SL}=0.15$m \cdot s^{-1}$, V_{SG}=1.2 $m \cdot s^{-1}$ 15lb/1000bbl)
(view from bottom, flow direction left to right)

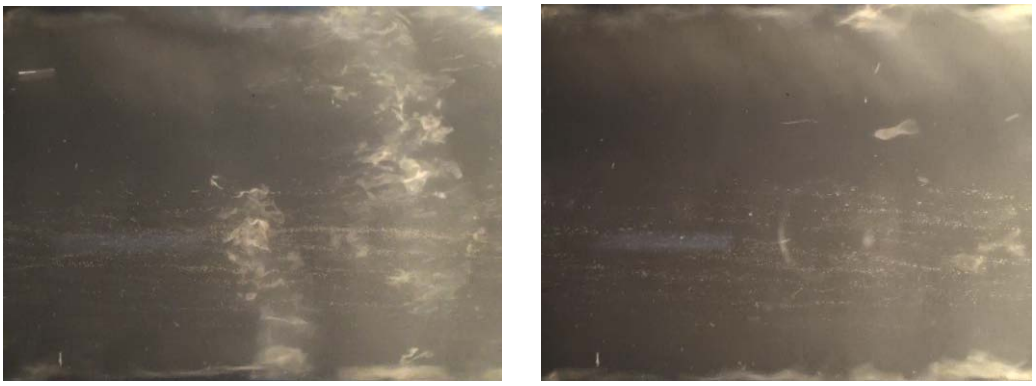

a) sand in wave body b)sand in film region

Figure 79: Sand characteristic in stratified wavy flow
(V_{SL}=0.15$m \cdot s^{-1}$, V_{SG}=1.5$m \cdot s^{-1}$ 15lb/1000bbl)
(view from bottom, flow direction left to right)

By reducing the V_{SG}, fewer sand particles can be observed in the viewing section, as shown in Figure 80. However, no high amplitude waves were observed during the test for 15lb/1000bbl.

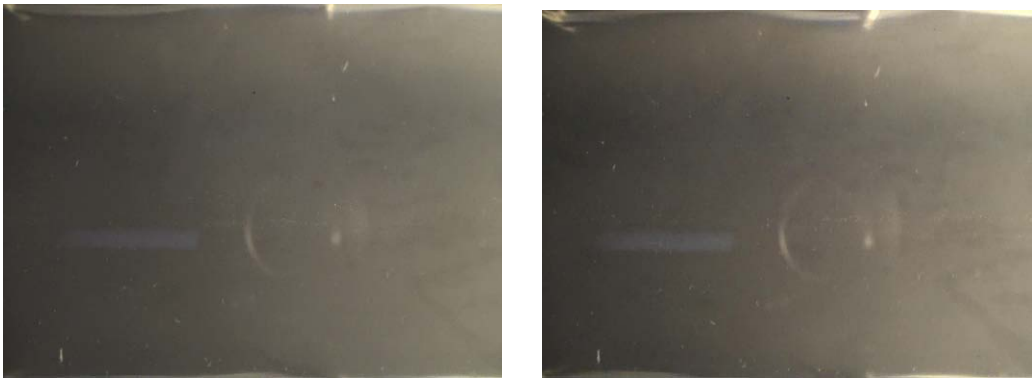

a) sand in wave body b)sand in film region

Figure 80: Sand characteristic in stratified wavy flow
(V_{SL}=0.15m·s^{-1}, V_{SG}=0.8m·s^{-1} 15lb/1000bbl)
(view from bottom, flow direction left to right)

However, for 200lb/1000bbl and 500lb/1000bbl, high amplitude waves were observed and they were energetic enough for transporting sand particles efficiently. Sliding and settled sand particles were observed in the liquid film region for 200lb/1000bbl (Figure 81). A highly concentrated sand bed was observed at the bottom of the pipe for 500lb/1000bbl, as shown in Figure 82.

a) sand in big waves b)sand in film region

Figure 81: Sand characteristic in stratified wavy flow
(V_{SL}=0.15m·s^{-1}, V_{SG}=1.0m·s^{-1} 200lb/1000bbl)
(view from bottom, flow direction left to right)

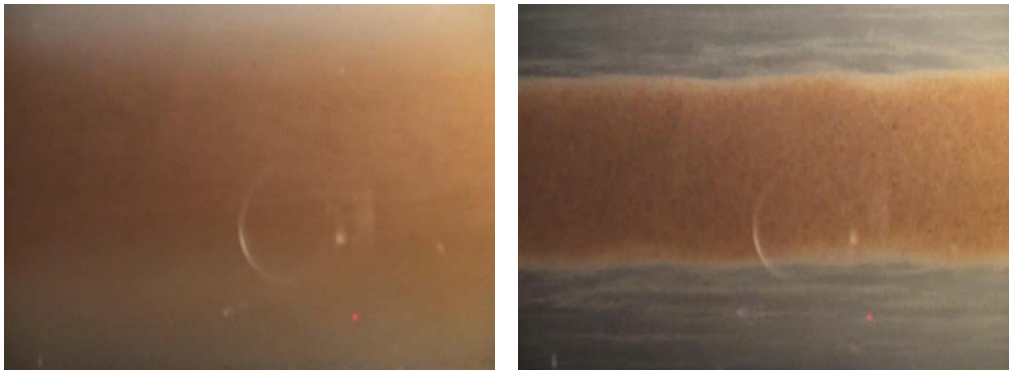

a) sand in big waves b)sand in film region

Figure 82: Sand characteristic in stratified wavy flow
(V_{SL}=0.15m·s^{-1}, V_{SG}=1.0m·s^{-1} 500lb/1000bbl)
(view from bottom, flow direction, left to right)

By further reducing the superficial gas velocity down to V_{SG}=0.8 m·s^{-1}, the sand particles were observed settled in the high amplitude wave in the form of sand bed for 200lb/1000bbl, whereas sand dunes were formed in the film region as illustrated in Figure 83.

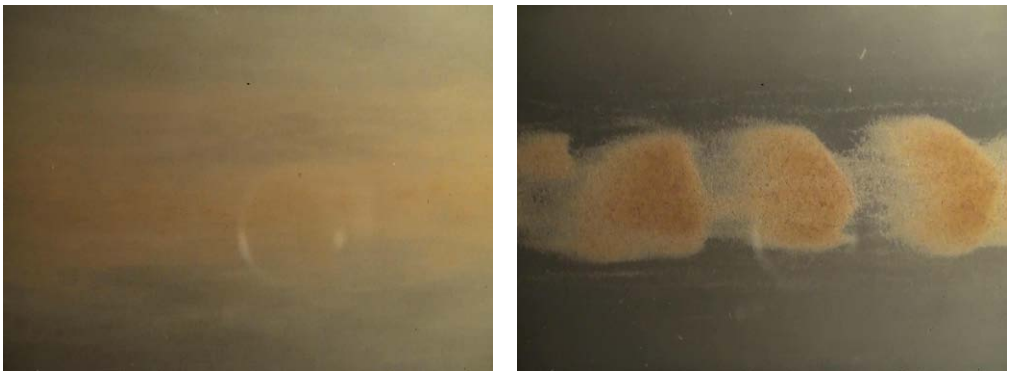

a) sand in wave body b)sand in film region

Figure 83: Sand characteristic in stratified wavy flow
(V_{SL}=0.15m·s^{-1}, V_{SG}=0.8m·s^{-1} 200lb/1000bbl)
(view from bottom, flow direction left to right)

For 500lb/1000bbl, V_{SL}=0.15m·s^{-1} and V_{SG}=0.8m·s^{-1}, the intensity of the sand bed in the wave body was more pronounced for this concentration (Figure 84). In the film region, the sand dunes were observed to be thicker and connected with each other by thick streaks of very low energetic sand particles. It was observed that streaks of sand particles were formed as a result of sand dune shedding process.

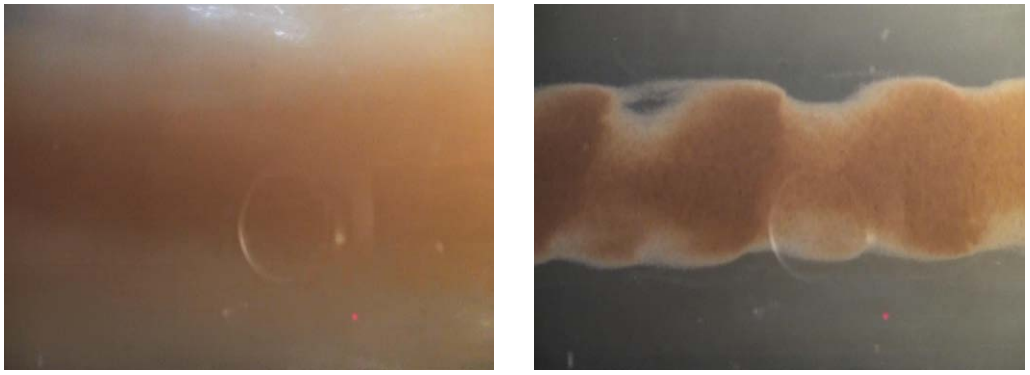

a) sand in wave body b)sand in film region

Figure 84: Sand characteristic in stratified wavy flow (V_{SL}=0.15m·s^{-1}, V_{SG}=0.8m·s^{-1} 500lb/1000bbl) (view from bottom, flow direction left to right)

5.4 Sand-Air-Water Transport Characteristics in Uphill Inclined Pipelines (5, 10, 20 degrees)

5.4.1 Air-Water Flow Regimes in Uphill Pipeline

To investigate the inclination effect on the sand transport characteristics in two-phase air-water inclined pipelines, the two-phase air-water flow regimes were identified for different flow conditions for 5, 10 and 20 degrees uphill inclined pipeline. The intermittent flow (plug and slug) was found to be dominant in 5, 10 and 20-degree uphill pipeline as illustrated in Figure 85. Unlike hydrodynamic slug generated in horizontal pipeline, the formation of plug and slug flow in inclined pipeline is also due to the gravity of water, which could be easily merged with following liquid and block the pipe. Hence, plug and slug flows were found to be the dominant flow regimes in inclined pipe.

It was also found that, at fixed pipeline inclination, the superficial gas velocity required for the transition of plug to slug flow regime increased with the increase of the superficial liquid velocity. For fixed superficial liquid velocity, the superficial gas velocity required for plug to slug transition increased with the increase of the degree of the pipeline inclination.

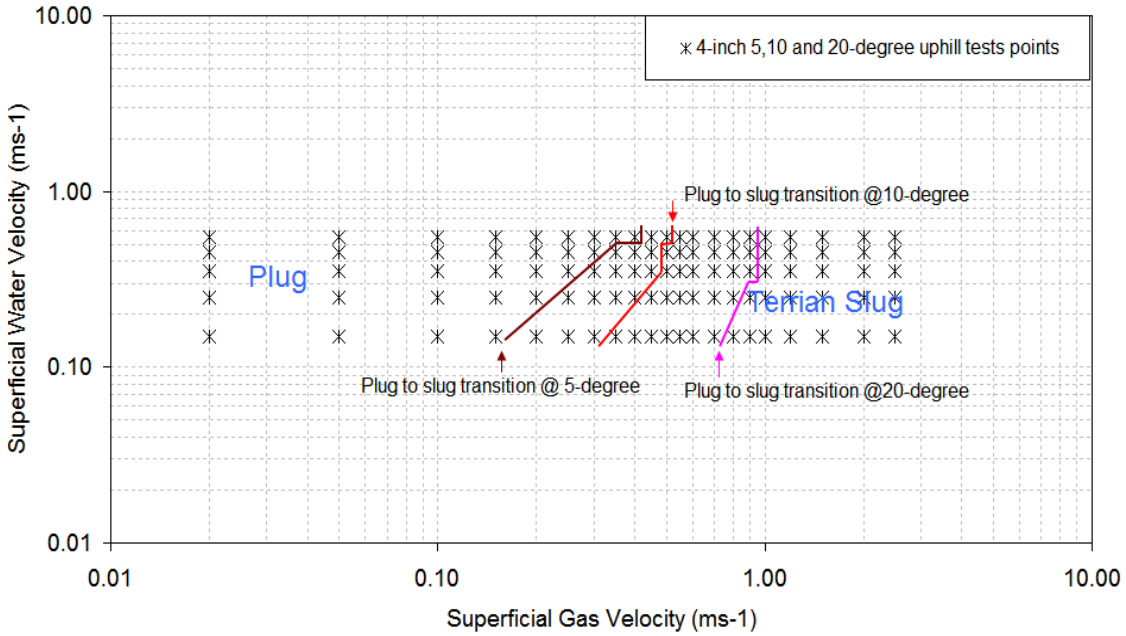

Figure 85: 4 inch uphill flow regimes

In addition, it was found that the slug and plug frequency increased with the increase of the pipeline inclination, as shown in Figure 86. This is also due to the effect of water gravity affecting the formation of slugs in uphill inclined pipe. More inclined the pipe is, more significant influence of water gravity can be found.

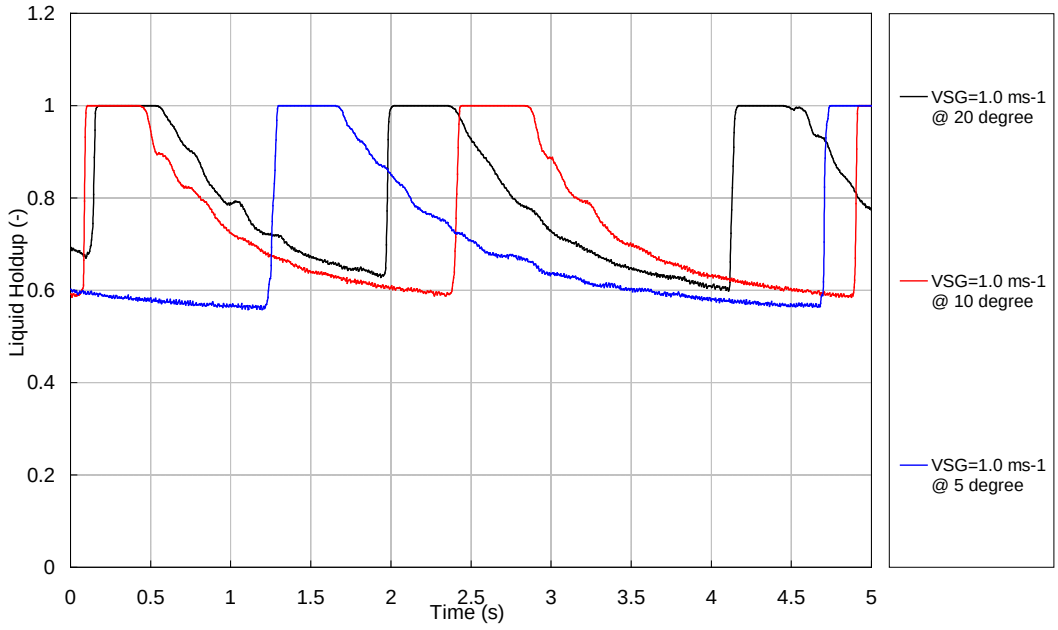

Figure 86: Slugs for 5, 10 and 20 pipeline inclination flow (V_{SL} = 0.45 m·s^{-1})

Because of the similarity of the observed two-phase air-water flow regimes for 5, 10 and 20 degrees uphill flows, only the sand particles behaviour in 5-degree inclined pipeline was reported below.

Also, as the sand transport characteristic for different V_{SL} at fixed inclination are similar, only the behaviours of sand particles at V_{SL} = 0.35m·s^{-1} was presented as they are representative of the characteristics for all the V_{SL} investigated.

5.4.2 Sand Transport Characteristics in Slug Flow

When reducing the V_{SG} from 2.5 m·s^{-1} down to 0.7m·s^{-1}, the sand particles were observed transported in the liquid slug body. However, as the sand particles shed from the liquid slug tail into the film region, they suddenly stopped and distributed uniformly at the bottom of the pipe, as shown in Figure 87.

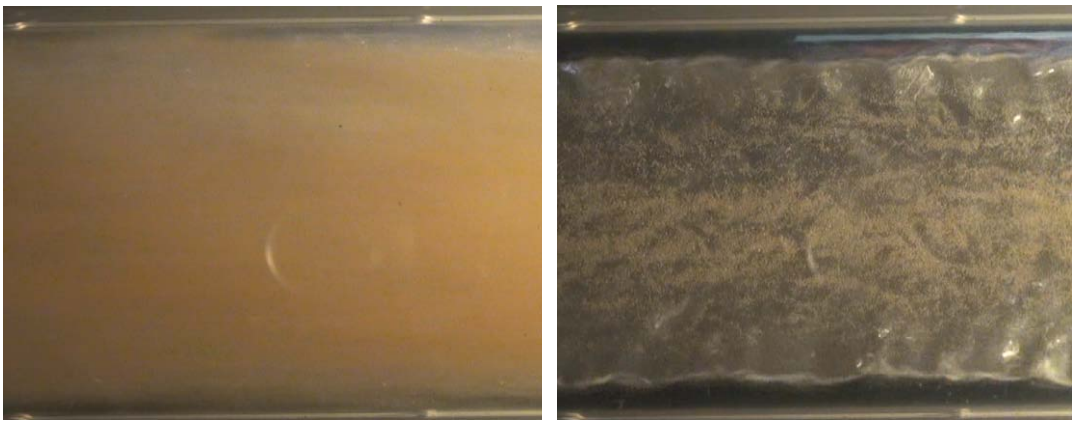

(a) slug body (b) film region

Figure 87: Sand characteristics in 5-degree uphill pipeline
(V_{SL} = 0.35m·s^{-1}, V_{SG} = 2.0m·s^{-1})
(500lb/1000bbl, view from bottom, flow direction left to right)

After the sand particles were uniformly distributed in the film region, then they moved backward with the water stream due to the gravity force. The sand particles settled for few seconds before they moved backward and gathered towards the centre of the bottom of the pipe forming a thick sand layer as shown in Figure 88.

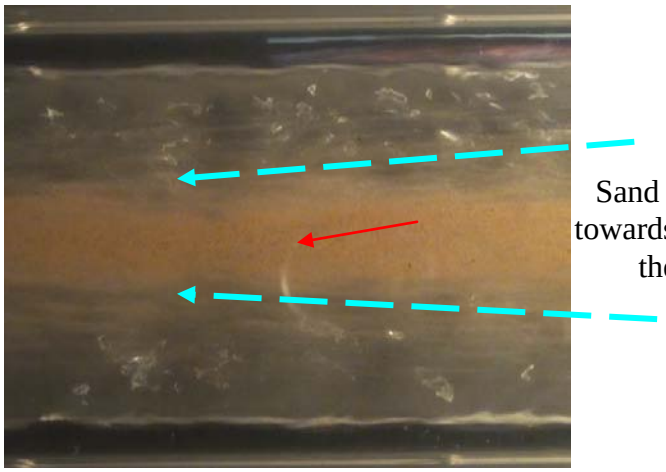

(a) Sand falling back in film region

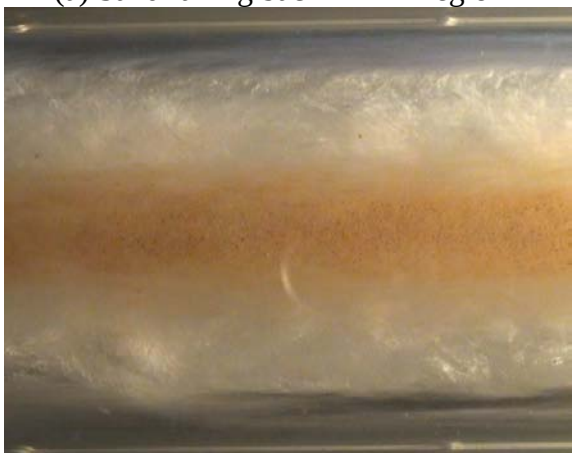

(b) Sand stirred up by the following slug

Figure 88: Sand characteristics in 5-degree uphill pipeline
(V_{SL} = 0.35m·s^{-1}, V_{SG} = 2.5m·s^{-1})
(500lb/1000bbl, view from bottom, flow direction left to right)

By decreasing the superficial gas velocity form 0.6 m·s^{-1} down to 0.3m·s^{-1}, sand particles were observed to continue to transport in slug body. Slug frequency increased with the increase of the superficial gas velocity. As a result, the water falling backward was not observed at these conditions, as shown in Figure 89.

(a) Sand transport in slug body

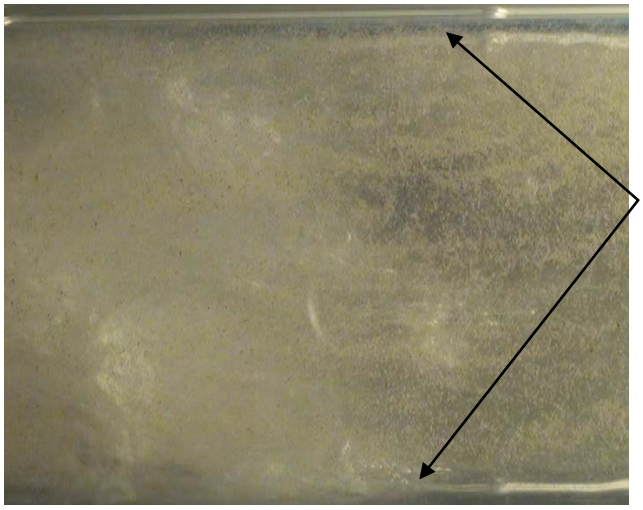

(b) Sand particles still uniformly distributed before the arrival of the following slug

Figure 89: Sand characteristics in 5-degree uphill pipelines
(V_{SL} = 0.35m·s^{-1}, V_{SG} = 0.6m·s^{-1})
(500lb/1000bbl, view from bottom, flow direction left to right)

5.4.3 Sand Transport Characteristics in Plug-Slug Transition

When the superficial gas velocity was further reduced from 0.25 $m \cdot s^{-1}$ down to 0.15 $m \cdot s^{-1}$, sand dunes were observed in the liquid film region, as shown in Figure 90.

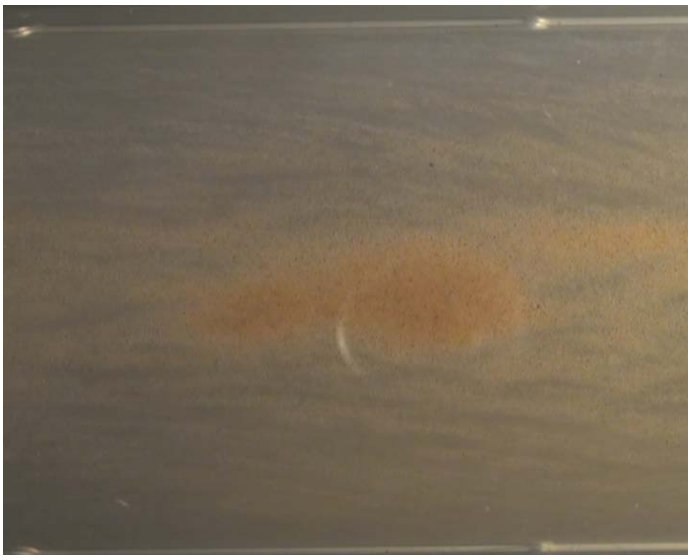

Figure 90: Sand in liquid film in 5-degree uphill pipeline
(V_{SL} = 0.35$m \cdot s^{-1}$, V_{SG} = 0.25$m \cdot s^{-1}$, 500lb/1000bbl, view from bottom)
(flow direction left to right)

At this inclined flow condition, sand dune experienced the impact of the impingement of backward slow-moving plug of fluid into the upward moving fluid plug. As a result, turbulent energy was generated in form of turbulent vortices; see Figure 91 (a). The surface vortices penetrated through the sand dune and distributed its particles in form of streaks as illustrated in Figure 91 (b).

(a) Initiation of turbulent vortices

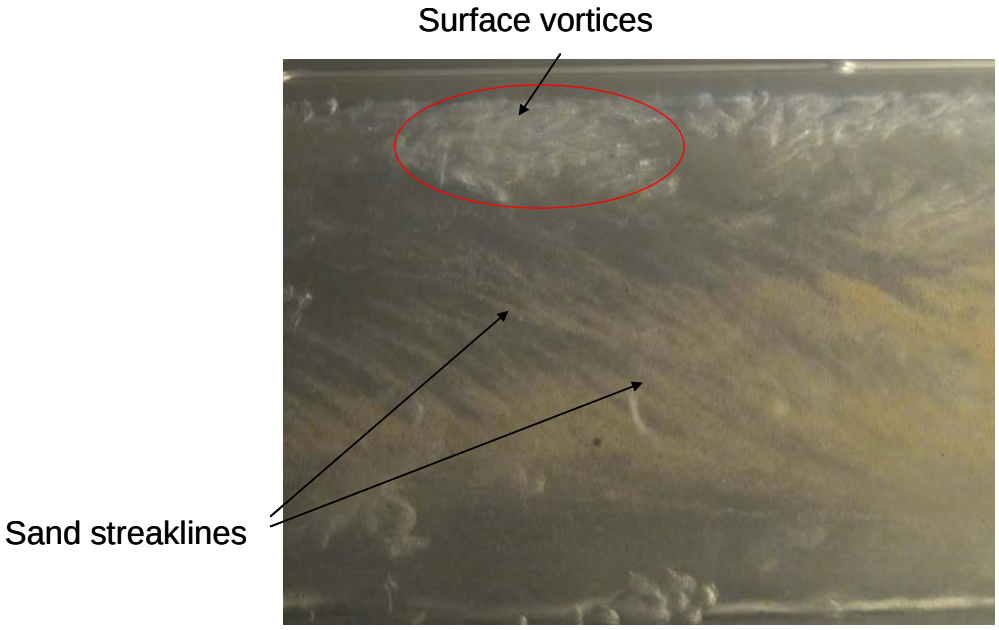

(b) Sand dune breaks into form of sand streaklines

Figure 91: Break of sand dune in 5-degree uphill pipeline
(V_{SL} = 0.35m·s^{-1}, V_{SG} = 0.25m·s^{-1}, 500lb/1000bbl)
(view from bottom, flow direction left to right)

At V_{SL} = 0.35 m·s^{-1} and V_{SG} = 0.15 m·s^{-1}, sand particles were considered to settle and not transported. Sand dunes were stationary formed at the bottom of the pipe.

5.4.4 Sand Transport Characteristics in Plug Flow

The plug flow regime was observed when the superficial gas velocity is below 0.1 $m \cdot s^{-1}$. Under this flow condition, the majority of the sand particles were not energetic, thus they settled as sand dunes at the bottom of the pipe as shown in Figure 92.

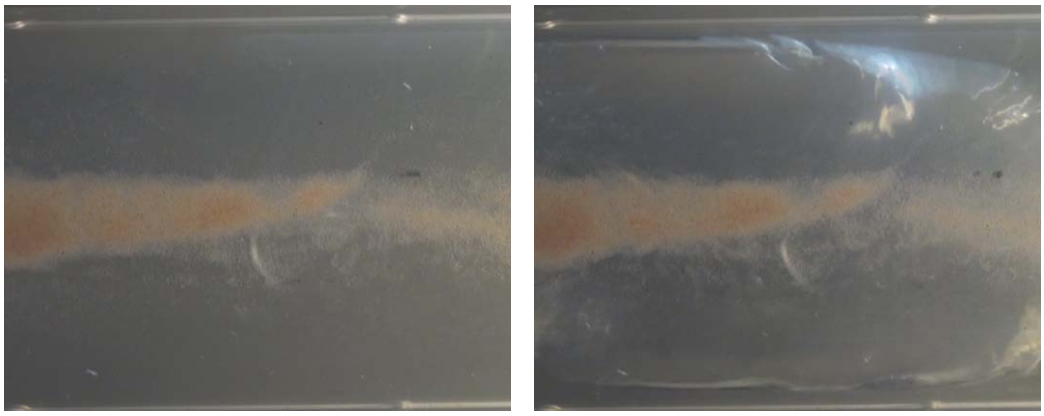

a) Plug body b) liquid film region

Figure 92: Still sand dunes in 5-degree uphill pipeline
(V_{SL} = 0.35$m \cdot s^{-1}$, V_{SG} = 0.05$m \cdot s^{-1}$, 500lb/1000bbl, view from bottom)
(Flow direction, from left to right)

The vortices observed in plug-slug transition were no longer observed in plug flow. Only a few sand particles were observed to move slightly in the plug body, but then stopped once entering the liquid film. However, at low V_{SG} such as at 0.05 $m \cdot s^{-1}$, no sand accumulation or falling back was found at the inlet Perspex pipe of sand injection point, as shown in Figure 93.

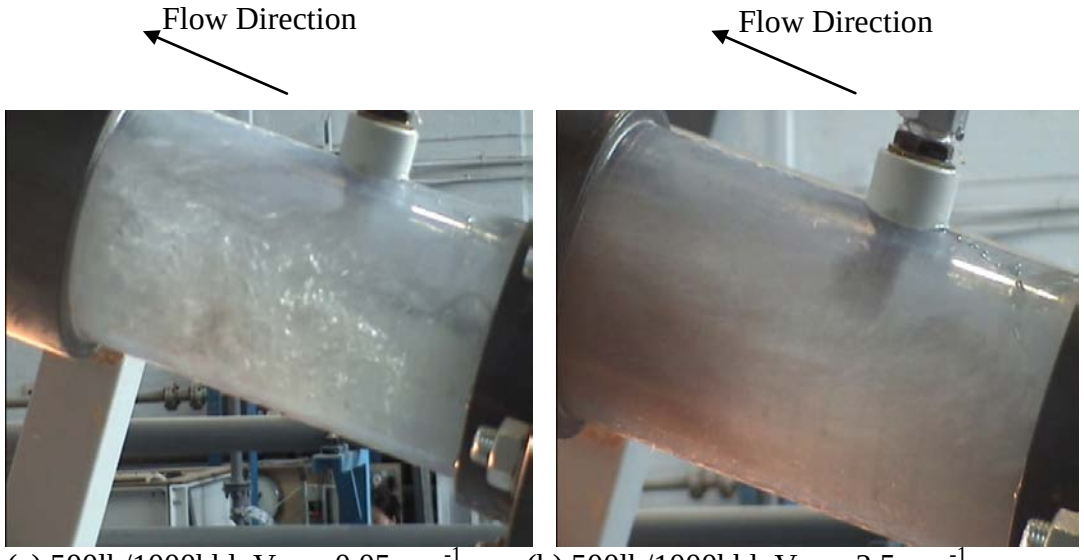

(a) 500lb/1000bbl, V_{SG} = 0.05 $m \cdot s^{-1}$ (b) 500lb/1000bbl, V_{SG} = 2.5 $m \cdot s^{-1}$

Figure 93: Sand at injection point (V_{SL} = 0.15$m \cdot s^{-1}$, view from side)

5.5 Sand-CMC (7cP, 20cP) Transport Characteristics in Horizontal and 5-degree Uphill Pipelines

The sand transport characteristics in single phase CMC solution (7cP and 20cP) were found to be similar to those in water flow, as illustrated in Figure 94.

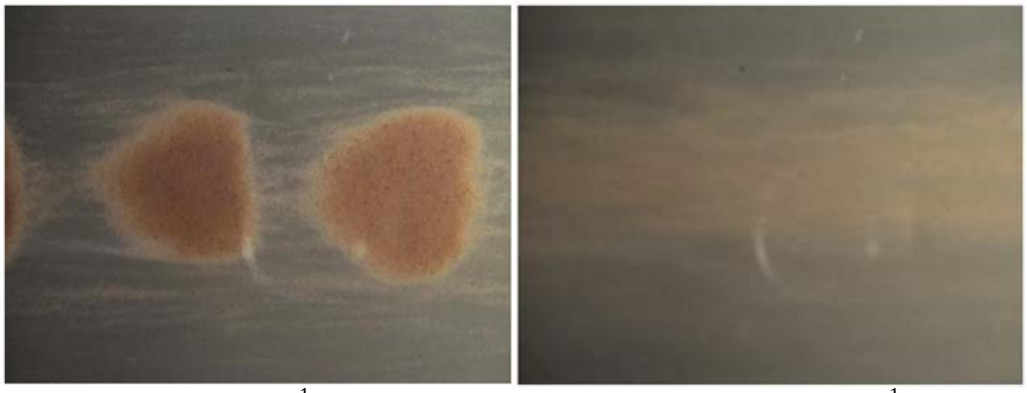

V_L=0.6m·s^{-1} V_L=0.75m·s^{-1}

a) Water (1cP)

V_L=0.7m·s^{-1} V_L=0.85m·s^{-1}

b) CMC solution (7cP)

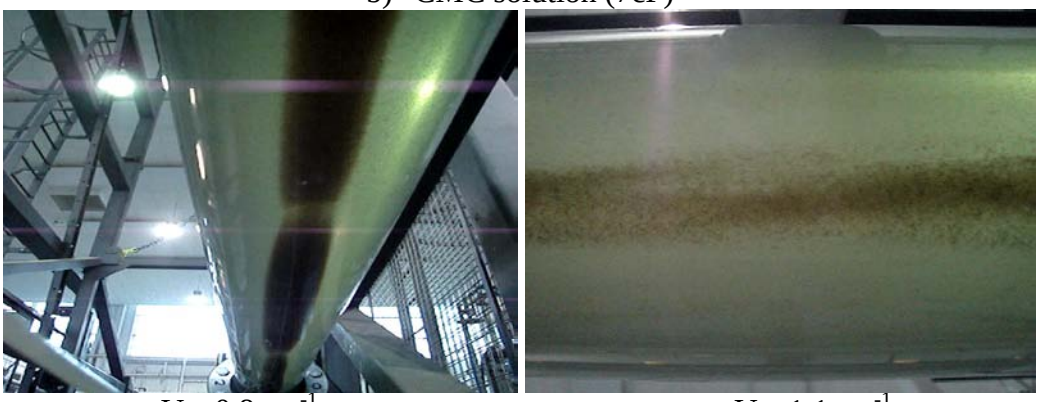

V_L=0.8m·s^{-1} V_L=1.1m·s^{-1}

c) CMC solution (20cP)

Figure 94: Sand transport characteristics comparison - 4 inch single phase liquid of different fluid viscosity flows

(500lb/1000bbl, view from bottom, flow direction left to right)

It was observed that, at transport condition, sand behaviour in different viscosity fluid was similar. Sand particles were observed moving in form of streaks; however the width of the band of streaks was found to decrease with increasing fluid viscosity. When the liquid velocity was below the minimum transport velocity, the sand dunes were observed for all liquid viscosities. However, the size of the sand dunes increased with liquid viscosity. At 20cP, the sand dunes were observed to be almost connected with each other to form an intensive sand bed.

Similar to the observation in single phase water flow, little orientation effect was observed when the 4 inch pipeline was tilted up to 5 degrees.

5.6 Sand- Air-CMC (7cP, 20cP) Transport Characteristics in Horizontal and 5-degree Uphill Pipelines

The sand transport characteristics in air- CMC solution two phase slug flows were also found to be similar with those in air-water flow, as illustrated in Figure 95.

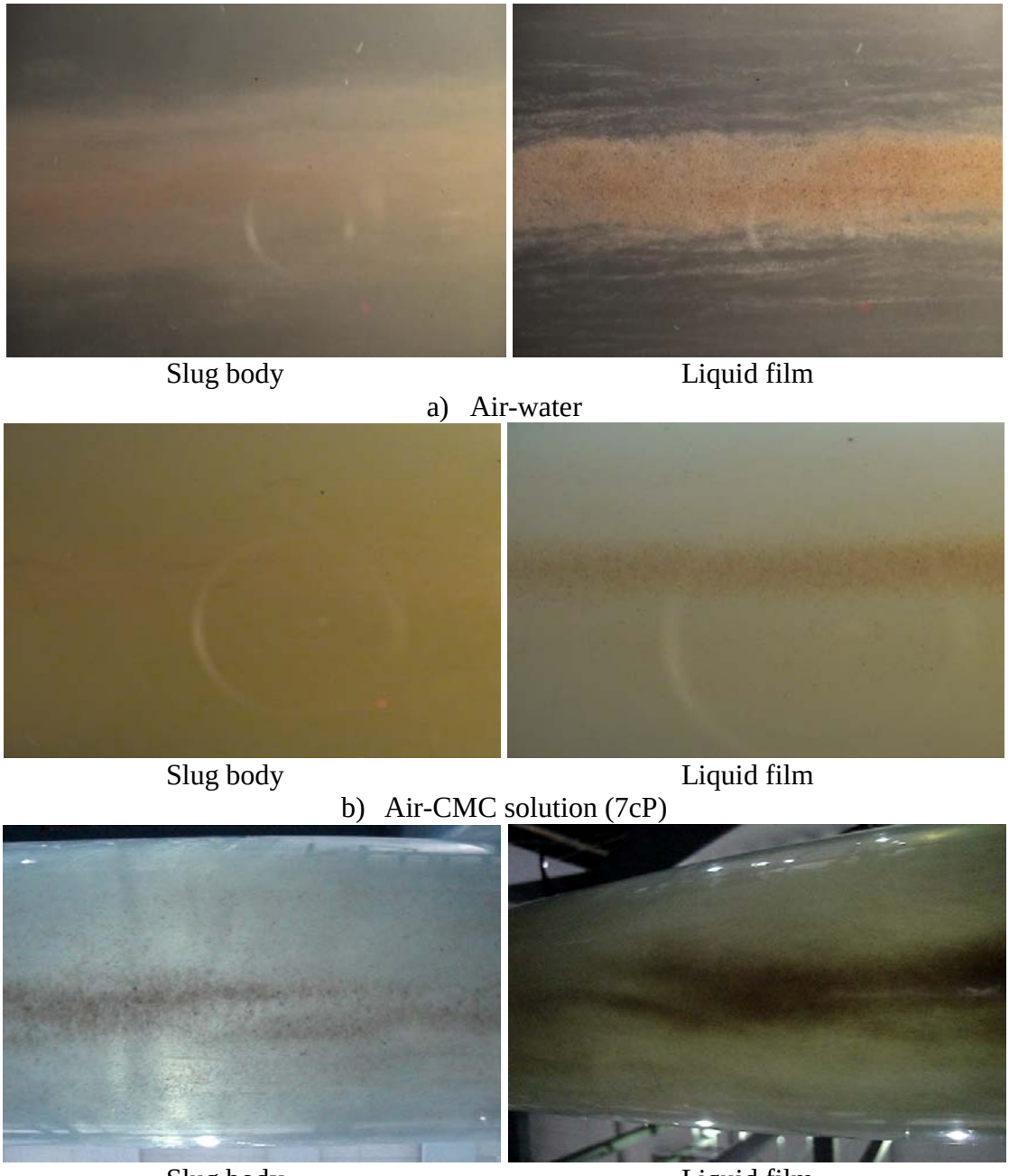

Slug body Liquid film

a) Air-water

Slug body Liquid film

b) Air-CMC solution (7cP)

Slug body Liquid film

c) Air-CMC solution (20cP)

Figure 95: Sand transport characteristics comparison - 4 inch air-liquid (of different viscosity) flows
(500lb/1000bbl, view from bottom, flow direction left to right)

It was observed that the sand particles were transported in the slug body and then settled in the liquid film region.

When the pipe was tilted up to 5 degrees, it was observed the slugs were also more prevailing in uphill air-CMC solution flows. As a result, sand transportation was found to be easier in 5-degree uphill pipeline than horizontal pipeline.

6 Results and Discussion for 3 inch Rig

This section described the typical behaviours for different sand concentration in 3inch oil flow. All the sand transport characteristics in this section were also summarized in Appendix A.

Sand particles movement and behaviours were observed for oil with 340cP at 16^{O}C, 200cP at 24.7^{O}C and 105cP at 34.7 ^{O}C. The oil viscosity, density and mass flowrate were measured using a Coriolis flowmeter. Figure 96 shows the viscosity traces of the Azolla oil measured using the Coriolis flowmeter. The viscosity reading from Coriolis flowmeter was found fluctuating when oil temperatures at 24.7^{O}C and 34.7 ^{O}C. This might indicate that the heating of oil would have certain effect on stability of the response from Coriolis flowmeter.

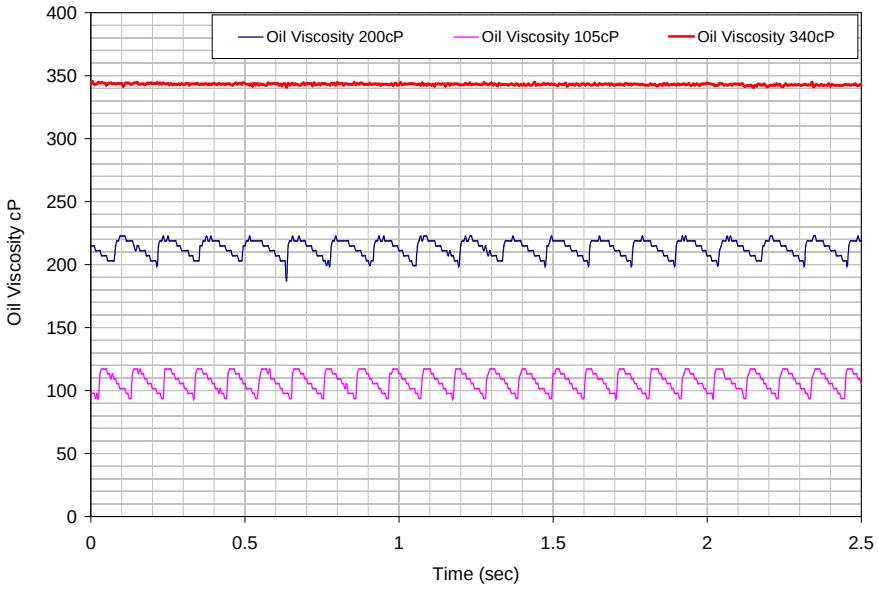

Figure 96: Oil viscosities used in the oil-sand experiments

The sand particles behaviour in the 3 inch pipe with oil when approaching the minimum sand transport velocity for concentrations of 50lb/1000bbl and 200lb/1000bbl are illustrated in Figure 97 and Figure 98. It was found that the sand particles were rolling, sliding and floating towards downstream, when the oil velocity was higher than the minimum transport velocity. The sand particles appeared to settle at the bottom of pipe and became more compact at oil velocity below sand transport condition. Unlike in water flow, no sand dunes were observed for all oil velocities. At oil viscosity of 340cP, the bulk flow at sand minimum transport condition was laminar.

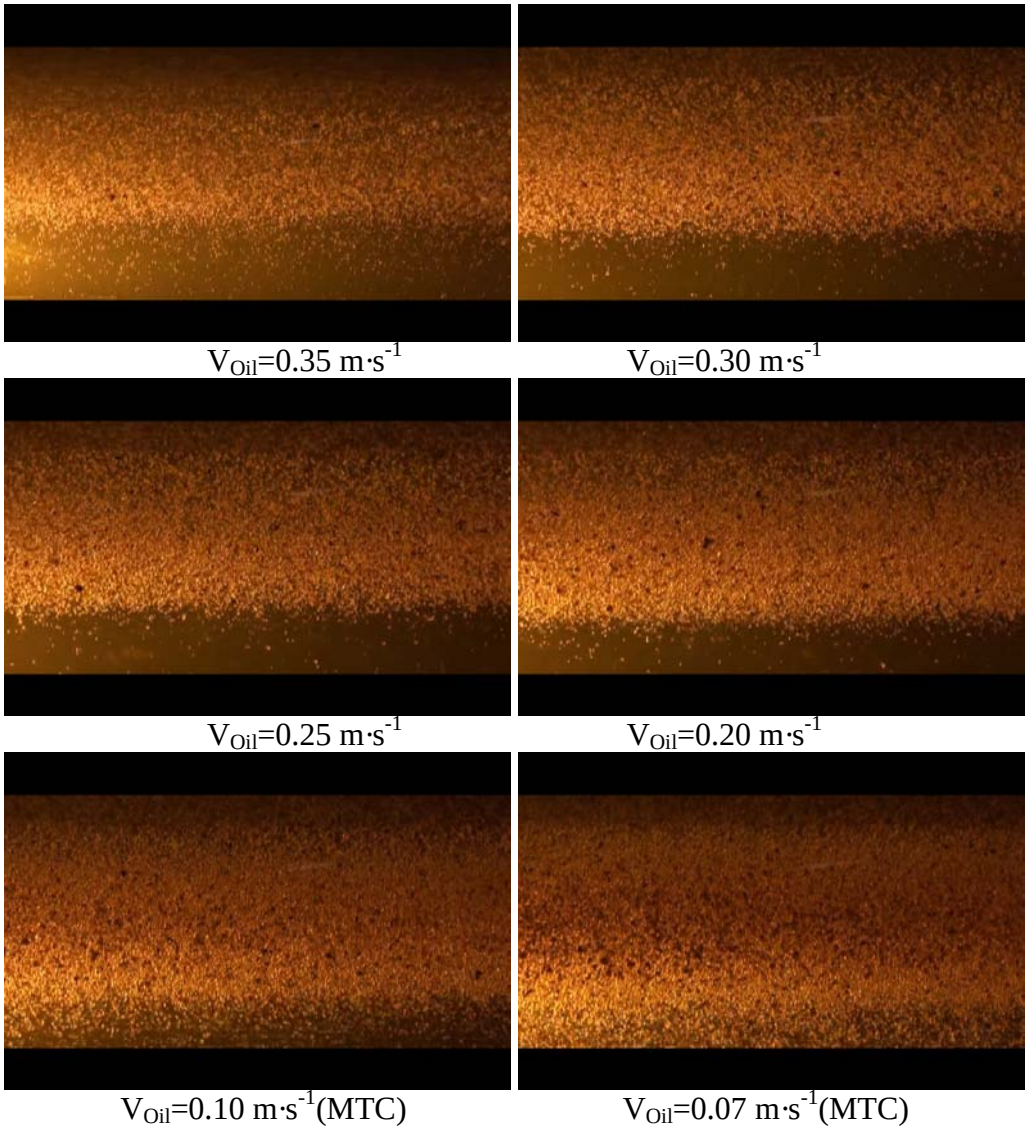

Figure 97: Sand transport characteristics in oil flow
(340cP at 16^{O}C, 50lb/1000bbl, view from bottom, flow direction left to right)

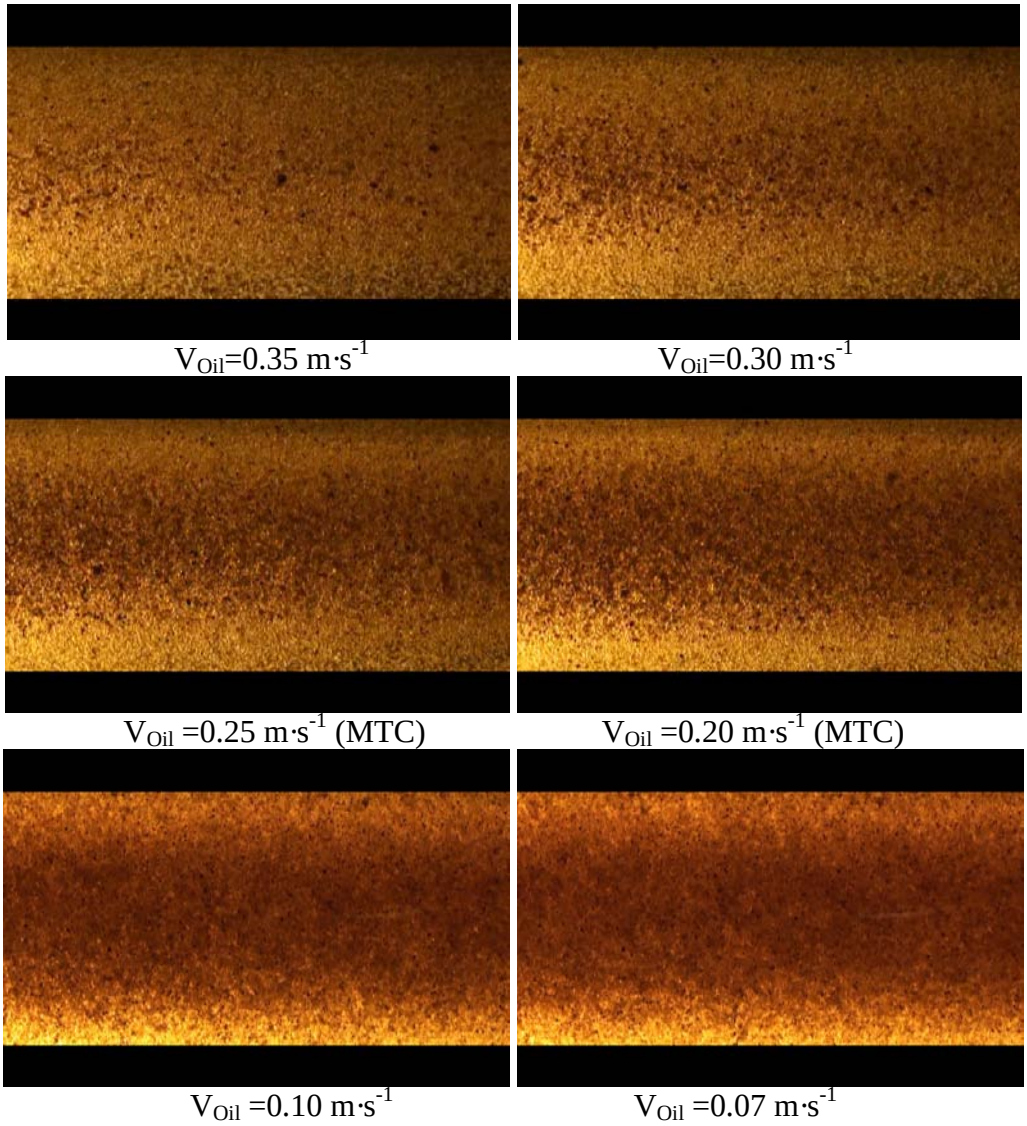

Figure 98: Sand transport characteristics in oil flow
(340cP at 16^{O}C, 200lb/1000bbl, view from bottom, flow direction left to right)

To obtain viscosities 200cP and 105cP, the Azolla 100 was heated to approximately 24.7^{O}C and 34.7^{O}C respectively in the oil tank. Similar sand transport characteristics were observed as that for 340cP. At 200cP and 105cP, sand beds were observed when oil velocity was lower than minimum sand transport velocity which was enlarged when the velocity was reduced, as shown in Figure 99 and Figure 100. Again, no sand dunes were observed.

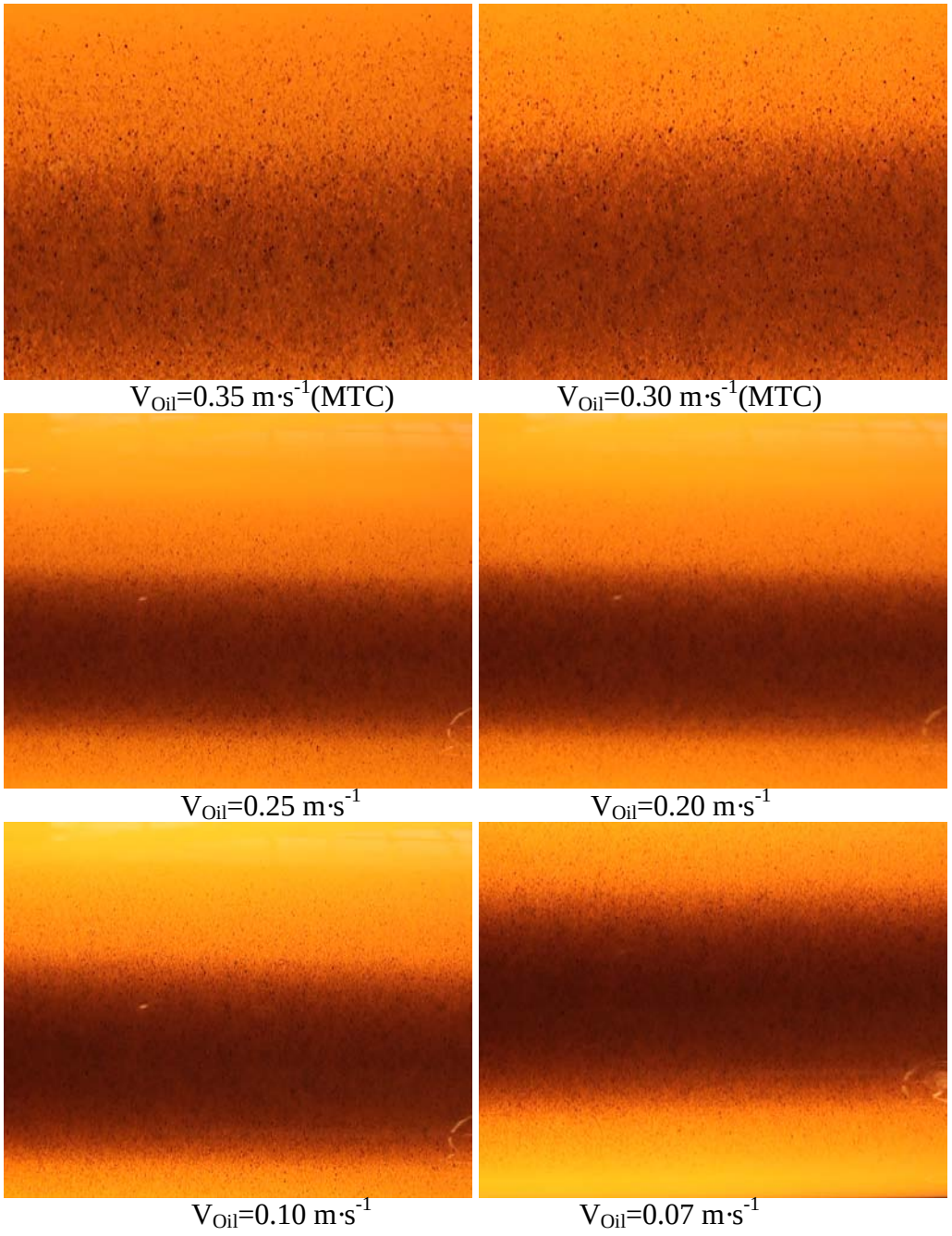

Figure 99: Sand transport characteristics in oil flow
(200cP at 24.7^{O}C, 200lb/1000bbl, view from bottom, flow direction left to right)

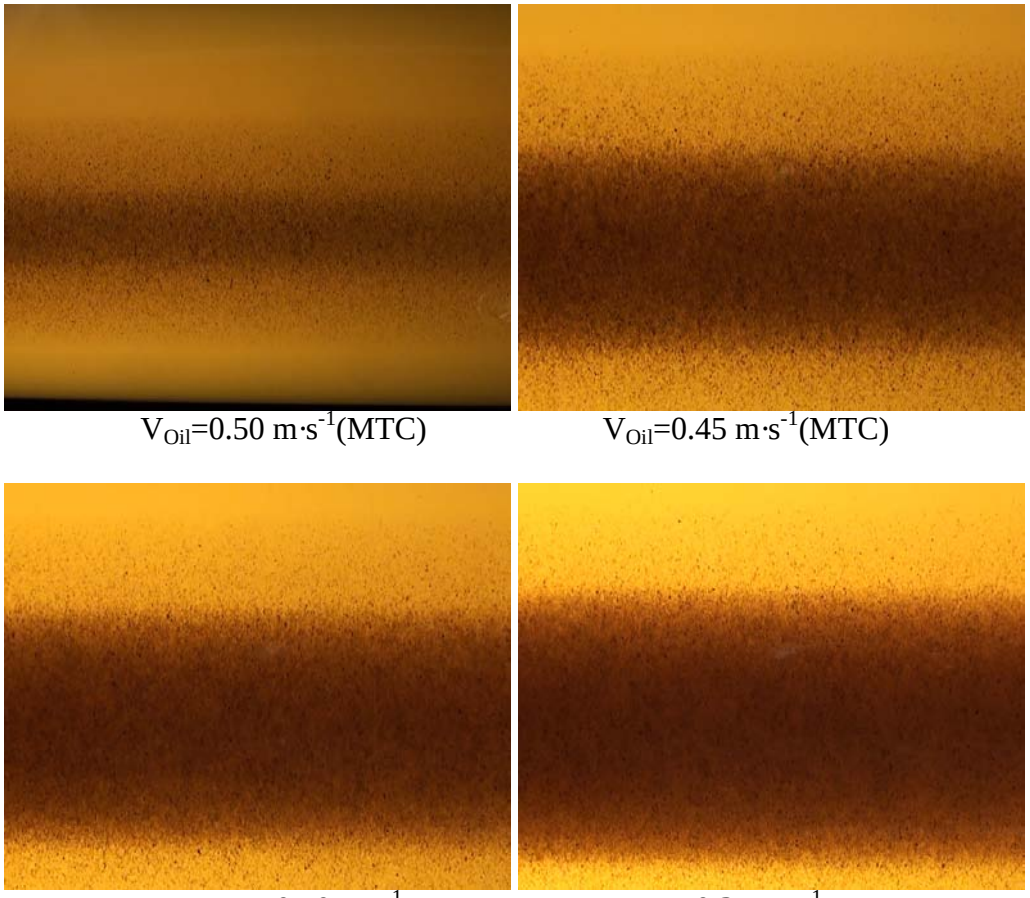

V_{Oil}=0.50 m·s^{-1}(MTC) V_{Oil}=0.45 m·s^{-1}(MTC)

V_{Oil}=0.40 m·s^{-1} V_{Oil}=0.35 m·s^{-1}

Figure 100: Sand transport characteristics in oil flow
(105cP at 34.7^{O}C, 200lb/1000bbl, view from bottom, flow direction left to right)

7 Factors Affecting the Sand Minimum Transport Condition (MTC)

7.1 Sand Concentration Effect

In slurry flow systems, particle transport velocities were found to increase with sand concentration. However, beyond a certain concentration, the transport velocity was hardly affected by solid concentration. Figure 101 shows the general trend of particle transport velocity with solid v/v (C_v) by previous researchers. The particle diameters of these studies were similar to the present work at around 200 microns.

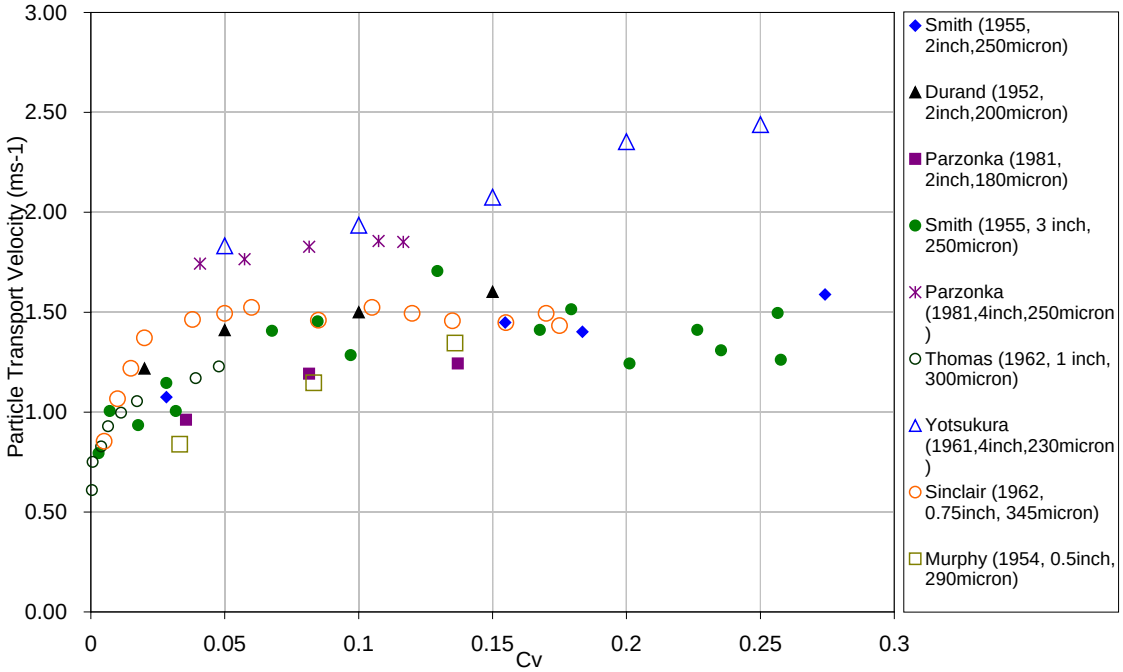

Figure 101: Particle transport velocities data by previous researchers

As mentioned before, the sand concentration involved in slurry studies (C_v > 0.01v/v) is usually much higher than the present study, which based on typical sand concentration experienced in oil pipelines, (0.000005 to 0.00005 v/v, 5lb/1000bbl—50lb/1000bbl). Sometimes, the maximum sand concentration can reach 200lb/1000bl (i.e. 0.0002 v/v) and even 500 lb/1000bbl (i.e. 0.0005 v/v) due to shut down or maintenance. Although, these are still extremely low compared with those found in slurry pipelines.

Table 13 shows a comparison between sand minimum transport velocity in horizontal 2 inch and 4 inch pipelines. It was found that the minimum transport velocity increased with sand concentration. More energy was required to keep sand particles moving with higher concentration.

Table 13: MTC comparison between horizontal 2 inch and 4 inch pipeline

Sand Concentration (lb/1000bbl)	C_v	V_{MTC} ($m \cdot s^{-1}$) (horizontal, 2 inch pipeline)	V_{MTC} ($m \cdot s^{-1}$) (horizontal, 4 inch pipeline)
500	5.38E-04	0.65-0.75	0.75-0.85
200	2.15E-04	0.60-0.70	0.65-0.75
100	1.08E-04	0.55-0.65	0.60-0.70
50	5.38E-05	0.50-0.55	0.50-0.60
15	1.61E-05	0.45-0.50	0.50-0.60
5	5.38E-06	0.40-0.45	0.45-0.50

Figure 102 and Figure 103 show the comparison between experimental MTC for 2 inch and 4 inch pipeline respectively from this work and those calculated by other published correlations.

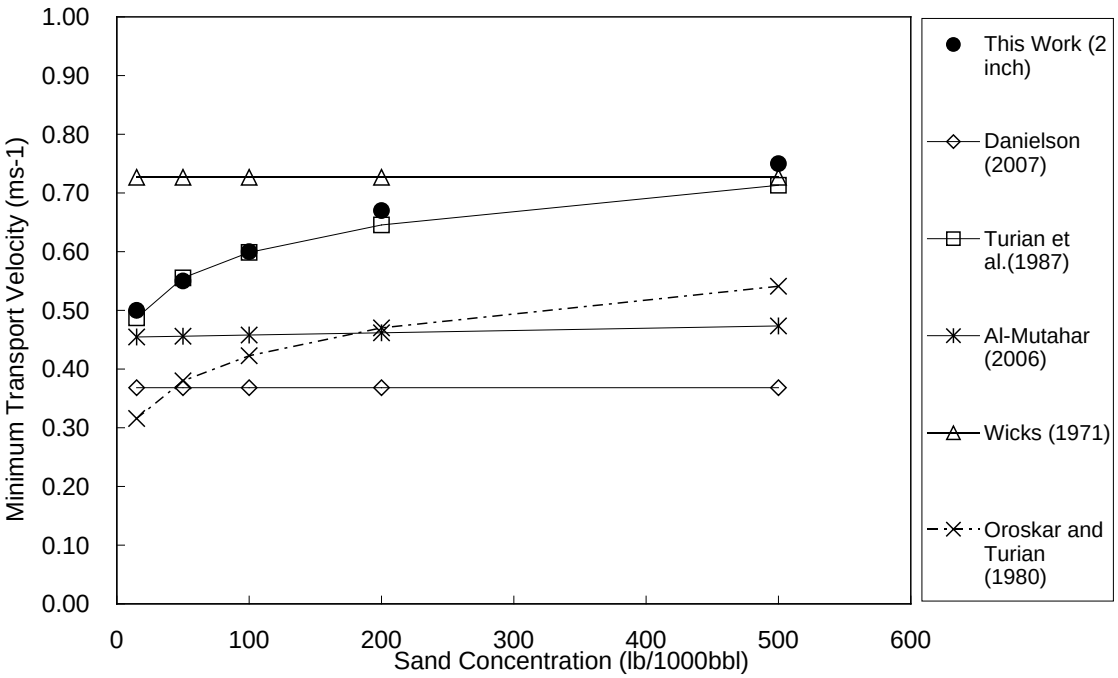

Figure 102: MTC comparison with other correlations for 2 inch pipeline

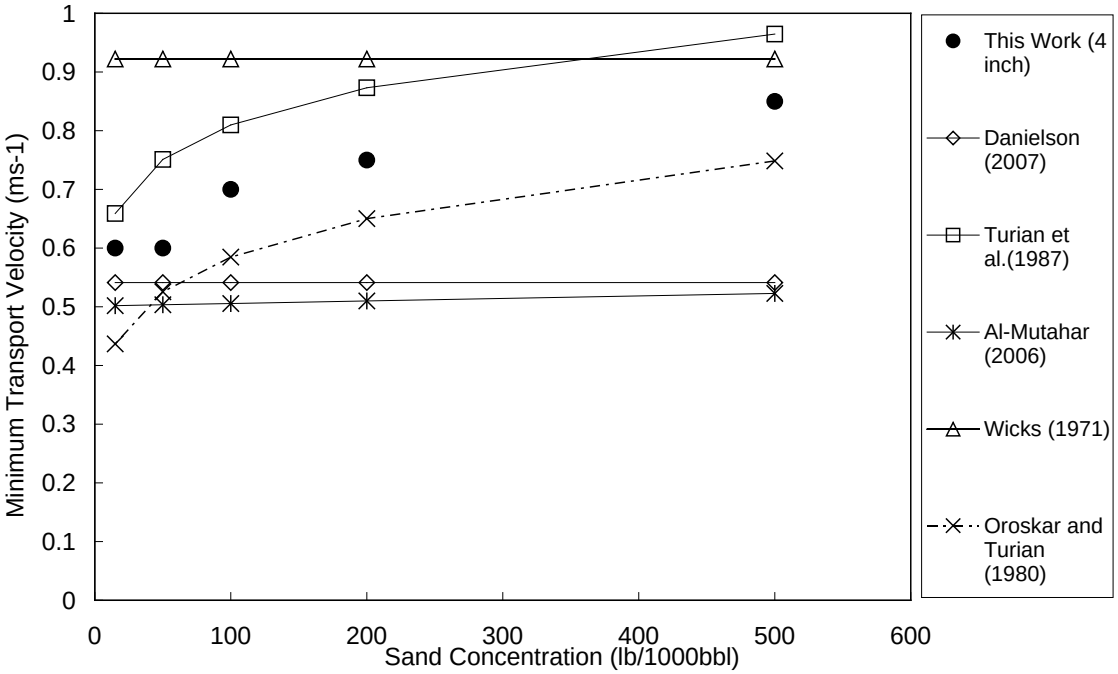

Figure 103: MTC comparison with other correlations for 4 inch pipeline

It is necessary to point out that the published correlations were developed based on the experimental data for high sand concentration in conventional slurry systems. As mentioned previously, very few experimental data for critical velocity existed within low sand concentration range tested in this work (Figure 101). Therefore, some discrepancies are expected when applying those published correlations into low concentration tested in this work.

From Figure 102 and Figure 103, it was found that correlation Turian et al. (1987) predicted the sand transport velocities at different sand concentration fairly well in 2 inch pipeline. However, for 4 inch pipeline, it over-predicted the transport velocities. Wicks' (1971) model only agrees with the experimental MTC at 500lb/1000bbl for both 2 and 4 inch pipeline. This might due to that Wicks' correlation was developed for sand removal from a stationary bed.

For air-water flows in the 2 inch and 4 inch pipeline, it was also found that higher flow velocities were required to transport the sand as increasing the sand concentration, as shown in Figure 104 and Figure 105.

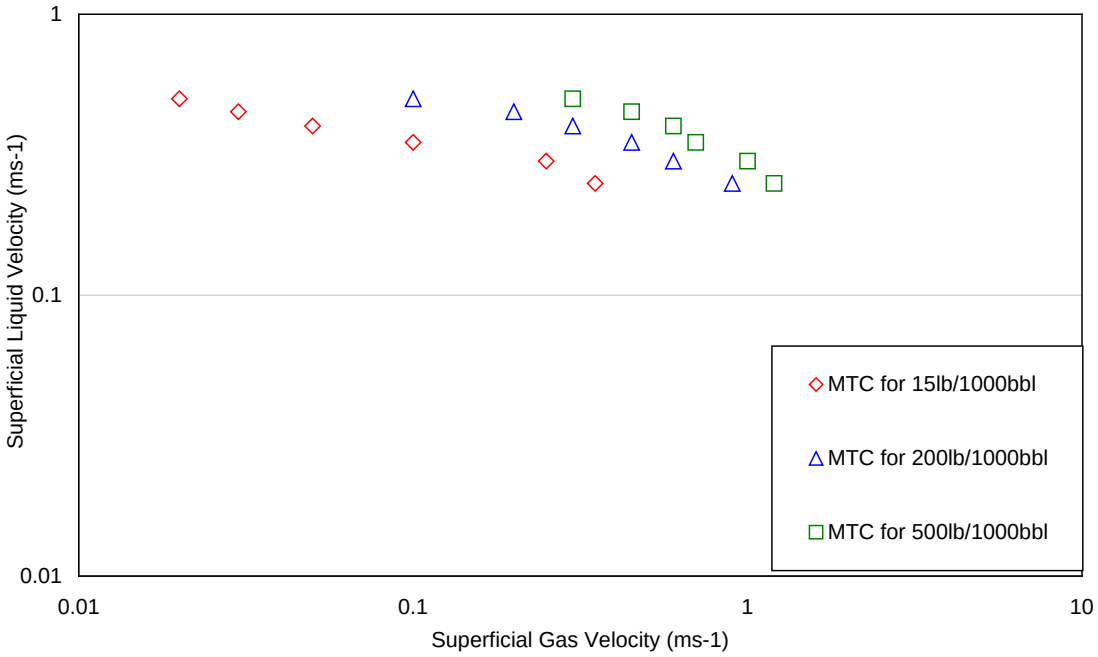

Figure 104: Sand MTC in 2 inch horizontal air-water flows

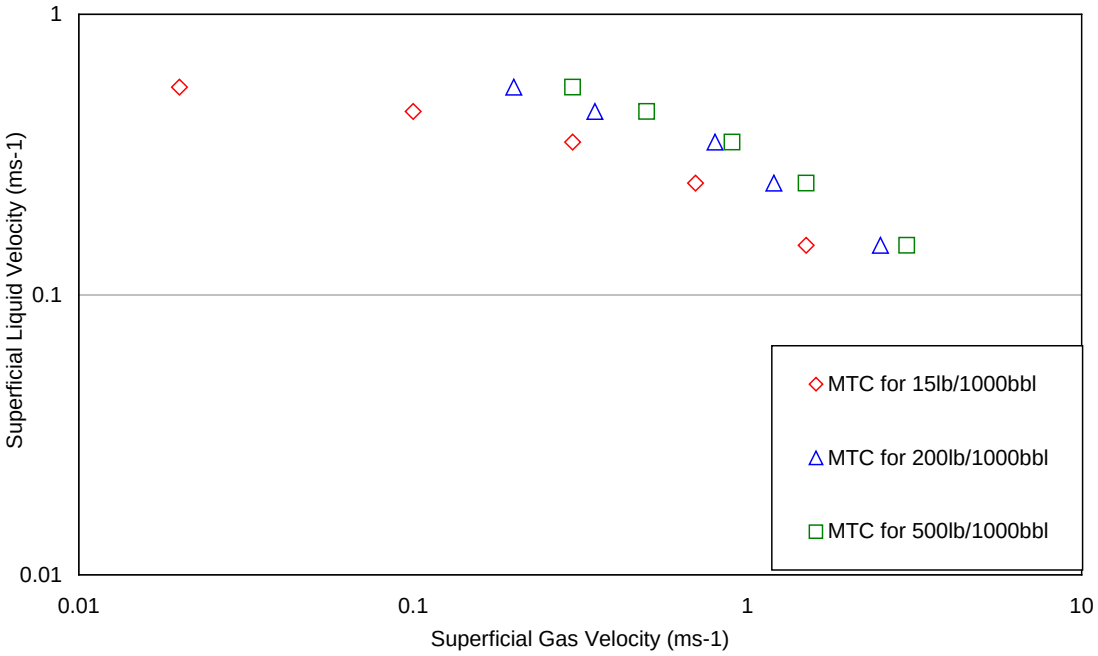

Figure 105: Sand MTC in 4 inch horizontal air-water flows

7.2 Pipe Diameter Effect

Generally, it was reported that the critical velocity increased with the increase of pipe diameter in slurry. Wicks (1971) compared several well-known correlations developed for slurry transport including Durand and Condolios (1953), Spells (1955), Sinclair (1962), Hughmark (1961) and Condolios and Chapus (1963). Figure 106 presents a comparison the critical velocity for 0.25mm sand at v/v of 0.01 in water flowing calculated by these five methods for various size pipes.

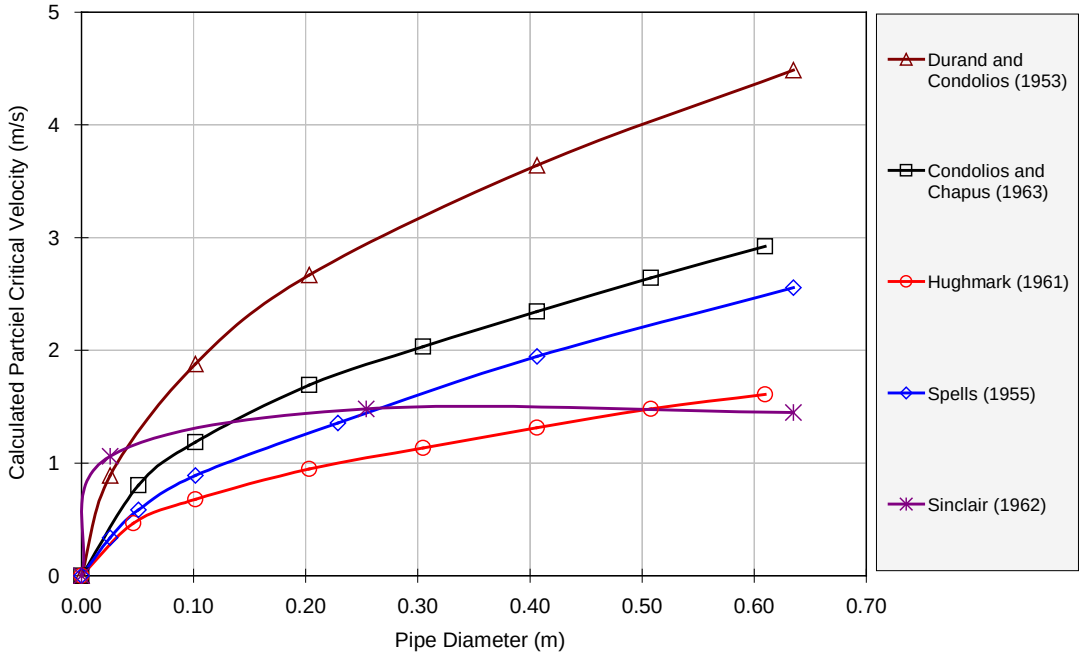

Figure 106: Pipe diameter effect on critical velocity (Wicks, 1971)

The wide deviations in their transport-velocity predictions could be indicative of the variation of interpretation for critical sand transport conditions.

From Table 13, it can be seen that the flow velocity at MTC in the 4 inch pipeline is slightly higher than that for the 2 inch pipeline. The laminar sublayer in 4 inch pipeline is thicker than that in 2 inch pipeline for the same averaged velocity, and the velocity gradient in the vicinity of pipe bottom in the 4 inch pipeline is lower than that in 2 inch pipeline, as shown in Table 14:

Table 14: Laminar sublayer thickness comparison in different diameter pipes

Pipe Diameter (inch)	Sand Concentration (lb/1000bbl)	V_{MTC} ($m \cdot s^{-1}$)	Laminar Sublayer Thickness (microns)
2	5	0.45	522
4	5	0.45	570

As a result, the shear induced drag and lift force acting on the sand particles are less for larger pipe at the same liquid velocity.

Figure 107 shows the MTC comparison with 15lb/1000bbl and 500lb/1000bbl for horizontal air-water flow in 2 inch and 4 inch pipelines.

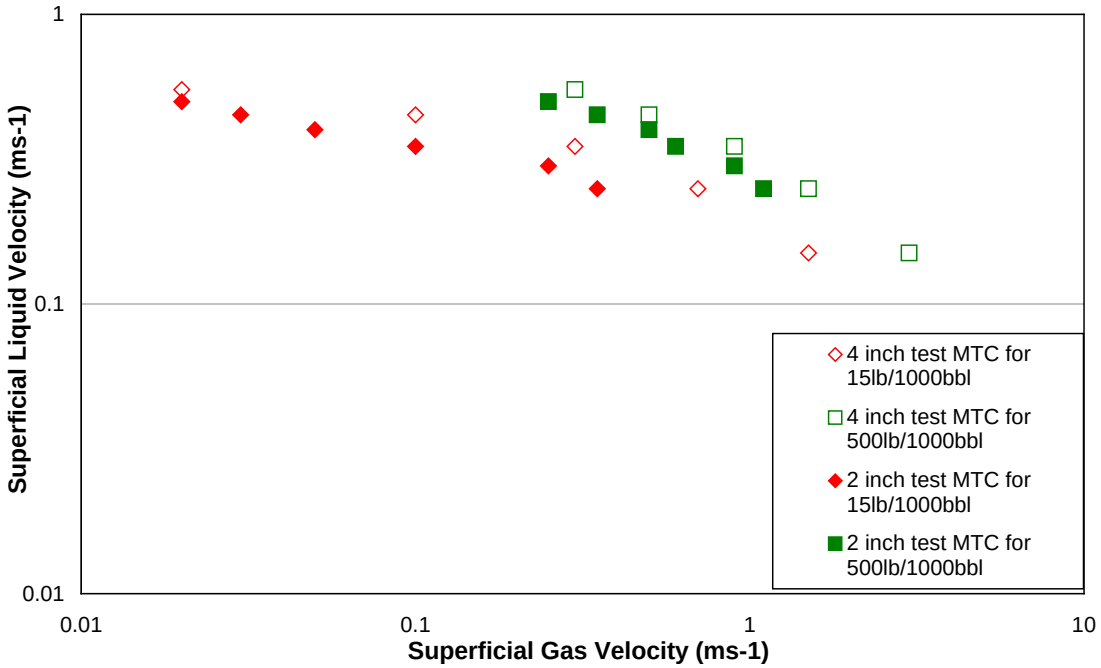

Figure 107: MTC in 2 inch and 4 inch horizontal air-water flow

The MTC in 4 inch pipeline was slightly higher than that in 2 inch pipeline, which is consistent with the findings in water flow.

King et al. (2000) presented some sand (diameter 255 microns) MTC data for the 2inch and 4inch rigs from bHRg. Figure 108 shows the comparison of sand MTC data between bHRg and the present Cranfield tests.

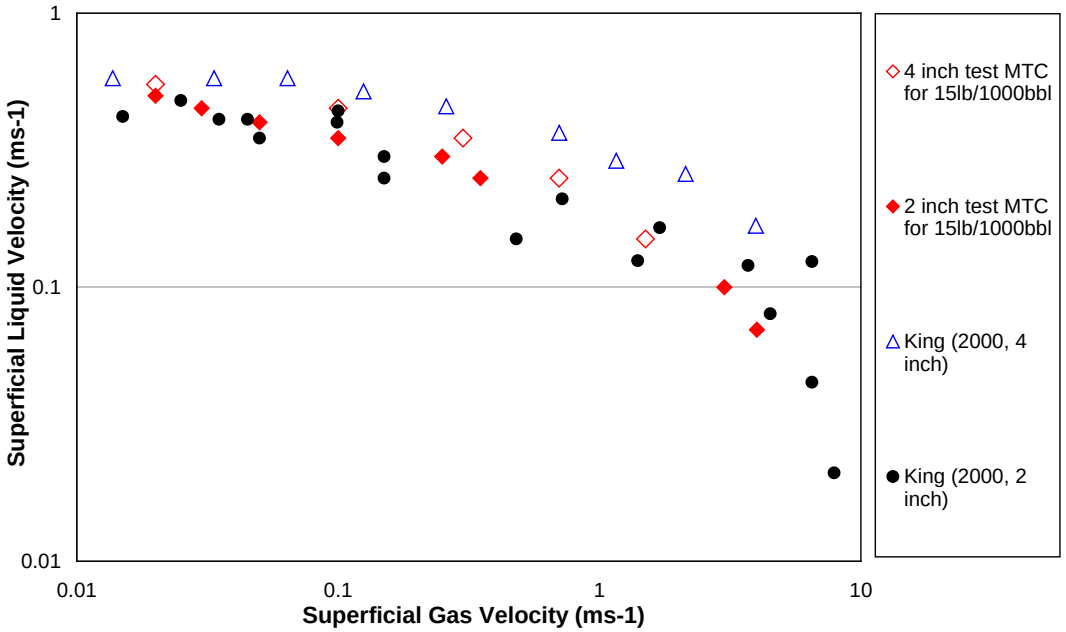

Figure 108: MTC comparison between King et al (2000) and the present Cranfield tests

Both sets of data show that the MTC velocity is higher for the larger diameter pipe. The sand MTC velocities obtained from 2 inch experiments at Cranfield were found to be similar with those at bHRg. However, the sand MTC for the 4 inch experiments show larger discrepancies. Two main reasons could cause the differences:

1. Different experimental conditions. In King et al. (2000), the sand concentration was not clearly stated. However, as the work was focused on common sand concentrations existing in oil pipelines, which should vary between 15 to 50lb/1000bbl. In addition, sand used in this work has a diameter around 200 microns, while 255 microns sand was applied in King's work.

2. Different definition used for MTC condition in air-water flow. Table 15 shows the flow pattern comparison between this work and King et al. (2000) at MTC conditions. All the flow conditions at MTC are mapped on Cranfield flow regime map for 4 inch facility, due to there is no experimental flow regime information was reported by King et al. (2000).

Table 15: Flow pattern comparison between this work and King et al. (2000) at MTC

Cranfield test (15lb/1000bbl)			Experimental data from King et al. (2000)		
V_{SL} ($m \cdot s^{-1}$)	V_{SG} ($m \cdot s^{-1}$)	Flow patterns based on Cranfield flow regime map	V_{SL} ($m \cdot s^{-1}$)	V_{SG} ($m \cdot s^{-1}$)	Flow patterns based on Taitel and Duckler (1976) flow regime map
0.55	0.02	Str+IW (Plug)	0.52	0.12	Slug
0.45	0.10	Str+IW (Plug)	0.46	0.20	Slug
0.35	0.30	Slug	0.37	0.70	Slug
0.25	0.70	Str+RW	0.26	2.12	Str+LRW
0.15	1.5	Str+RW	0.17	3.96	/

When $V_{SL} \geq 0.35$ $m \cdot s^{-1}$, the sand particles were observed to be transported in either STR+IW (plug flow) or slug flow regime for the Cranfield tests, whereas most of transport conditions from King's work (2000) occurs in slug flow. Moreover, the superficial gas velocity, V_{SG}, required at MTC condition (similar V_{SL}) for this work was found lower than that in the work from King et al. (2000). The MTC condition defined in this work was "no sand deposit in liquid (slug or plug) body", which means the MTC can be observed at any flow regimes where sand is transported. Also, if in slug flow, slug frequency could be very low as long as the sand was transport once the liquid body passing. No clear definition based on observation was raised for MTC condition in air-water flow from King et al. (2000).

When $V_{SL} < 0.35$ $m \cdot s^{-1}$,the STR+RW flow regime was observed at MTC condition, which in the transition region between slug and stratified wavy flows (i.e. stratified+rolling wavy with higher speed but relatively small amplitude). Although the frequency of the roll wave body was really low, the sand particles were observed still being transported within the rolling waves once generated. However, the experimental MTC conditions from King et al. (2000) are most likely observed in stratified wavy flow regime, especially at $0.17 m \cdot s^{-1}$ superficial liquid velocity. Again, the superficial gas velocity, V_{SG}, required at MTC condition for this work was found lower than that in the work from King et al. (2000).

Based on the analysis above, it seems that King et al. (2000) investigated sand MTC condition mainly in slug or stratified wavy flow regimes. From their experimental results, although the no definition for MTC is given, it appears they did not treat low frequency slug or (roll wave) condition as their transport condition. Therefore, there is a large discrepancy on experimental sand MTC between this work and King's work for the 4 inch rig. The discrepancy of MTC data in 2 inch rig is not significant comparing to 4 inch rig, which might due to the transition regions between different flow regimes is bigger in a larger diameter pipeline.

7.3 Pipeline Inclination Effect

The observed sand minimum transport velocities in water flow at different inclinations in 4 inch pipeline are shown in Table 16. For the sand concentrations tested in this study, no significant differences in sand transport velocities were detected when the pipe was tilted up between +5 to +20 degrees.

Table 16: Pipeline inclination effect on MTC

Pipeline Orientation (degree)	V_{MTC} ($m \cdot s^{-1}$)		
	15lb/1000bbl	200lb/1000bbl	500lb/1000bbl
0	0.50 ~ 0.60	0.65 ~ 0.75	0.75 ~ 0.85
+5	0.50 ~ 0.60	0.65 ~ 0.75	0.75 ~ 0.85
+10	0.50 ~ 0.60	0.65 ~ 0.75	0.75 ~ 0.85
+20	0.50 ~ 0.60	0.65 ~ 0.75	0.75 ~ 0.85

Shook and Roco (1991) commented that "the critical velocity increased slightly (of the order of 10%) for uphill flows at +15 degrees in slurry system" based on Roco (1977) and other researchers' experiments. In addition, Angelsen et al. (1989) also stated that inclination angle up to +15 degrees had less than 10% change in sand critical velocity. Rix and Wilkinson (1991), along with Danielson (2007) also gave similar comments based on their experimental results. The sand concentration tested in present work was very low compared to the previous work of slurry systems. In addition, the slight difference for water velocity at MTC in different pipeline inclination might be not able to be distinguished by visual observation. As a result, no significant differences between the MTC could be observed in water flow.

In air-water flow, limited data was found for the inclination effect on sand transport. Angelsen et al. (1989) investigated inclination effects (1 degree) on the velocity of sand removal from a bed only in stratified wavy flows (ID=0.1m). He found that the effect of pipe inclination on the transport condition in inclined stratified flow was very pronounced. Stevenson et al. (2001b, 2002) investigated the behaviour of isolated sand grains (particle diameter 0.0011m) in intermittent flow in slightly inclined pipeline and stratified flow in slightly declined pipeline (ID=0.04 and 0.07m). He noticed backwards movement of the particles in the film section. However, he claimed that, with the inclinations (up to 3 degrees) he tested, the sand transport was not strongly dependent on the pipe inclination. The contribution of the backwards movement in the slug film was negligible compared to the net transport by the slug flow. Danielson (2007) also noticed that sand bed formation could be strongly correlated to the pipe angle due to the liquid velocity is a strong function of pipe angle without any further information. However, previous investigations were mostly focused on one specific flow regime, and the relationship between the sand transport conditions and flow regime were not available in these papers.

The present work showed that sand transport was strongly flow regime dependent. In 4 inch air-water flows, pipeline inclination appeared to have positive effects on MTC see Figure 109. For 5 degrees incline, the gas and liquid velocities required to transport sand were less than the horizontal pipe. This is due to intermittent flows (slugs) are more prevailing when the pipe is inclined, which provide more kinetic energy to transport sand particles. Similar behaviour was observed in the 2 inch tests, as illustrated in Figure 110:

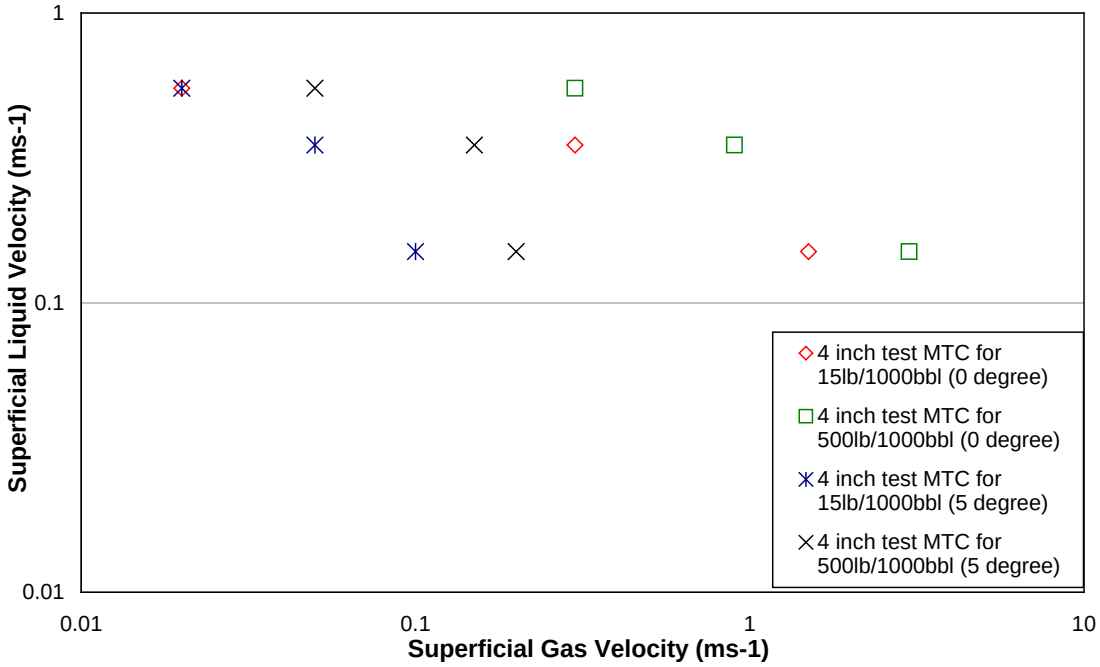

Figure 109: MTC for 4 inch horizontal and 5 degree uphill air-water flows

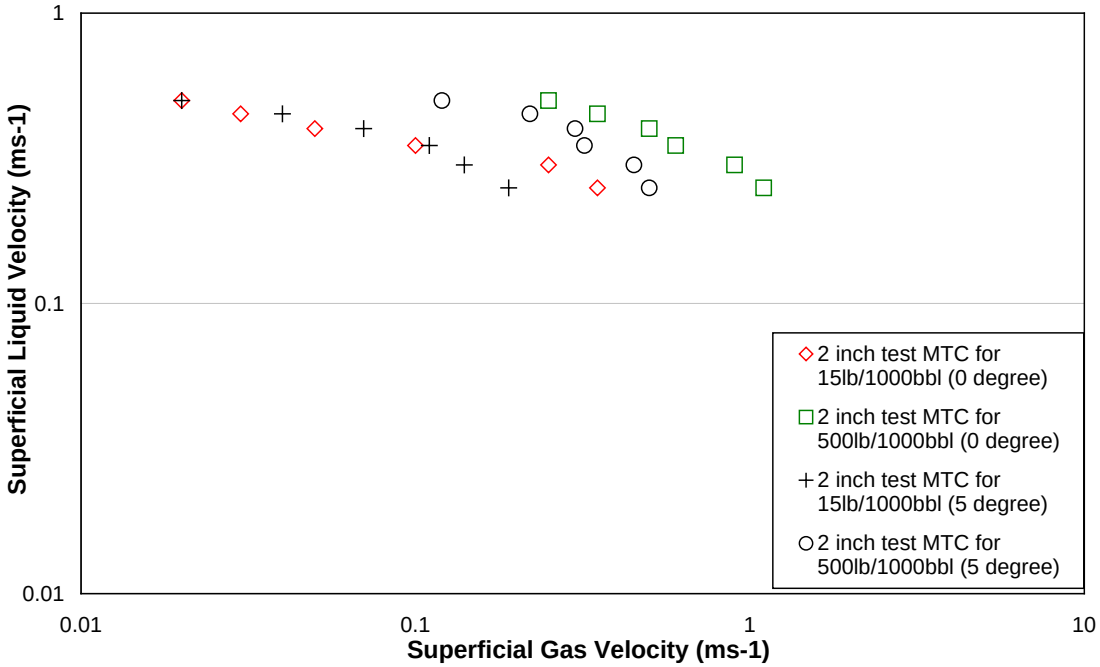

Figure 110: MTC in 2 inch horizontal and 5 degree uphill air-water flow

From Figure 110, it can be seen that, for 15lb/1000bbl, when the superficial liquid velocity was higher than 0.25m·s^{-1}, the gas velocities at sand MTC were found to be similar in both horizontal and 5 degree uphill pipes. However, when superficial liquid velocity was equal or lower than 0.25m·s^{-1}, the gas velocity at sand MTC was lower in 5 degree uphill than those in horizontal flow. For 500lb/1000bbl, all the sand MTC observed in 5 degree uphill air-water flow were lower than those in horizontal flow.

7.4 Liquid Viscosity Effect

Table 17 and Table 18 show the comparisons between sand transport velocity and the bulk flow regimes for sand concentrations of 50 and 200lb/1000bbl.

Table 17: Comparisons of MTC for different tested liquids for 50lb/1000bbl

Fluids	Liquid Viscosity (cP)	Liquid velocity at MTC (m·s^{-1})	Pipe Diameter (m)	Re	Type of Flow	Laminar Sublayer Thickness (microns)
Water	1	0.5	0.1	50000.00	Turbulent	520
CMC solution (7cP)	7	0.7	0.1	10000.00	Turbulent	2852
CMC solution (20cP)	20	0.75	0.1	3750.00	Transition	7147
Oil 105cP	105	0.35	0.0776	226.33	Laminar	/
Oil 200cP	200	0.25	0.0776	85.36	Laminar	/
Oil 340cP	340	0.07	0.0776	14.11	Laminar	/

Table 18: Comparisons of MTC for different tested liquids for 200lb/1000bbl

Fluids	Liquid Viscosity(cP)	Liquid velocity at MTC (m·s^{-1})	Pipe Diameter (m)	Re	Type of Flow
Water	1	0.7	0.1	70000.00	Turbulent
CMC solution (7cP)	7	0.75	0.1	10714.29	Turbulent
CMC solution (20cP)	20	0.8	0.1	4000.00	Transition
Oil 105cP	105	0.45	0.0776	291.00	Laminar
Oil 200cP	200	0.3	0.0776	102.43	Laminar
Oil 340cP	340	0.2	0.0776	40.31	Laminar

From Table 17, it was found that the sand minimum transport velocity increased slightly as the fluid viscosity increased when bulk flow is turbulent. However, as increasing the

fluid viscosity, the tendency of increase in V_{MTC} is becoming less. When the flow became laminar, the sand minimum transport velocity decreased as the fluid viscosity increased. This is due to the increasing shear force acting on the sand particles from the liquid and the decreasing settling velocity of sand particles due to the high viscous fluid. This finding was also consistent to similar work done by Gillies et al. (1997) which using water (1cP) and oil (78cP). The sand transport velocity was found lower in oil flow (78cP) than that in water flow at the same sand concentration. In an earlier study, Gillies et al. (1994) found that sand was transported for high viscous fluids (up to 7500 cP) regardless of the velocity used.

From Table 17 and Table 18, it was also found, at the same liquid viscosity, the sand minimum transport velocity were observed always increased with the increase of sand concentration.

Table 19 and Table 20 shows the comparison between the experimental MTC and other correlations regarding to the viscosity effect at different sand concentration in single phase liquid flow in 4 inch pipeline.

Table 19: Comparison between the experimental MTC and other correlations regarding to the viscosity effect at 50lb/1000bbl

Liquid viscosity (cP)	Experimental V_{MTC} ($m \cdot s^{-1}$)	Oroskar and Turian (1980, $m \cdot s^{-1}$)	Salama (2000, $m \cdot s^{-1}$)	Turian et al. (1987, $m \cdot s^{-1}$)	Kokpinar et al. (2001, $m \cdot s^{-1}$)	Al-Mutahar (2006, $m \cdot s^{-1}$)	Wicks (1970, $m \cdot s^{-1}$)	Danielson (2007, $m \cdot s^{-1}$)
1.00	0.5	0.52	0.36	0.75	0.30	0.50	0.92	0.54
7.00	0.7	0.44	0.31	0.75	0.09	0.38	0.90	0.44
20.00	0.75	0.40	0.28	0.75	0.05	0.33	0.88	0.39
105.00	0.35	0.34	0.24	0.74	0.01	0.28	0.87	0.31
200.00	0.25	0.32	0.22	0.74	0.01	0.25	0.86	0.29
340.00	0.07	0.30	0.21	0.73	0.01	0.23	0.85	0.27

Table 20: Comparison between the experimental MTC and other correlations regarding to the viscosity effect at 200lb/1000bbl

Liquid viscosity (cP)	Experimental V_{MTC} ($m \cdot s^{-1}$)	Oroskar and Turian (1980, $m \cdot s^{-1}$)	Salama (2000, $m \cdot s^{-1}$)	Turian et al. (1987, $m \cdot s^{-1}$)	Kokpinar et al. (2001, $m \cdot s^{-1}$)	Al-Mutahar (2006, $m \cdot s^{-1}$)	Wicks (1970, $m \cdot s^{-1}$)	Danielson (2007, $m \cdot s^{-1}$)
1.00	0.7	0.65	0.36	0.87	0.43	0.51	0.92	0.54
7.00	0.75	0.54	0.31	0.87	0.13	0.39	0.90	0.44
20.00	0.8	0.49	0.28	0.87	0.07	0.33	0.88	0.39
105.00	0.45	0.42	0.24	0.86	0.02	0.28	0.87	0.31
200.00	0.3	0.39	0.22	0.86	0.01	0.25	0.86	0.29
340.00	0.2	0.37	0.21	0.85	0.01	0.23	0.85	0.27

From Table 19 and Table 20, it was found that none of the previous correlations could predict the MTC well with the whole range viscosities tested. It is due to all the correlations, apart from Danielson (2007), were developed based on hydraulic transport without considering viscosity effect. However, for 50lb/1000bbl, correlations from Oroskar and Turian (1980) and Danielson (2007) could predict MTC fairly well when the fluid was water with 1cP viscosity and oil with the viscosities of 105 and 200 cP, whereas Turian et al's correlation (1987) predicted well when liquid was CMC solution with viscosity of 7 and 20cP. More importantly, the experiments indicate that the MTC velocity initially increase with viscosity but reduces rapidly when the flow condition became laminar. All the correlations examined show a monotonic decrease of transport velocity with the increase of viscosity and also an increase as increasing sand concentration.

In horizontal air-CMC flows, it was also found the sand MTC increased slightly as the fluid viscosity increased, as shown in Figure 111:

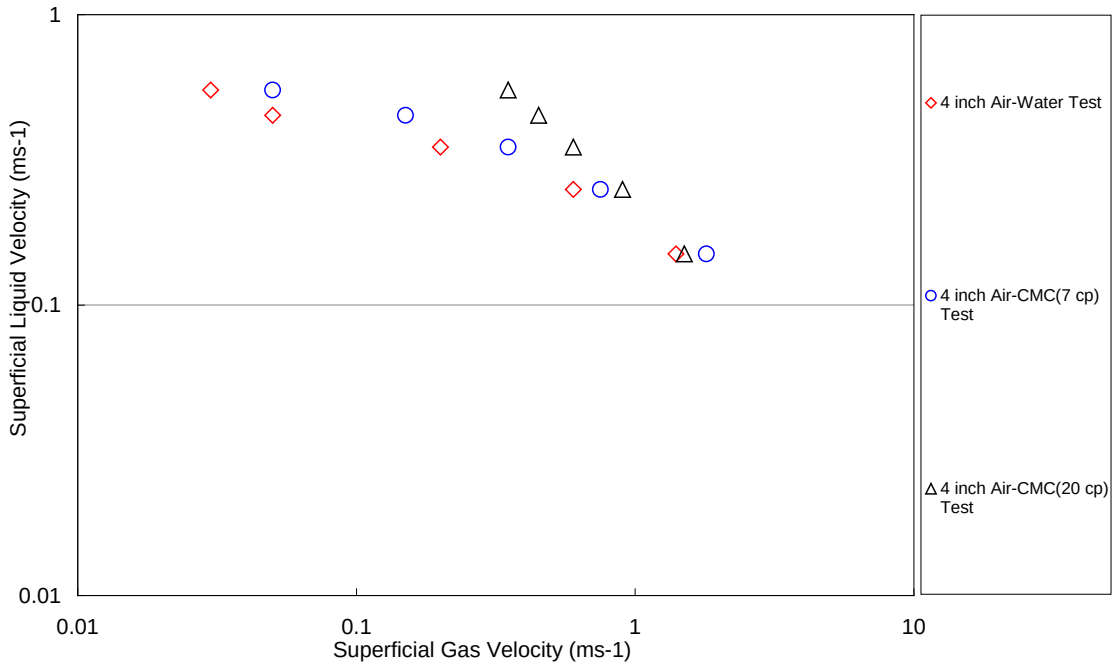

a) 15lb/1000bbl

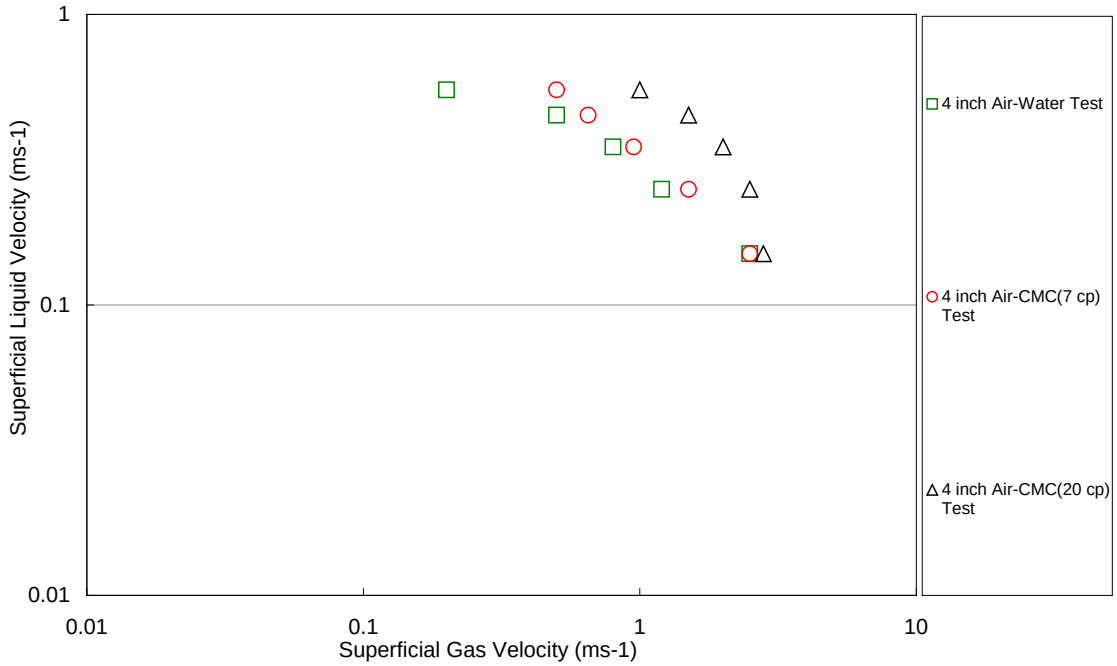

b) 500lb/1000bbl

Figure 111: Viscosity effect on sand MTC in air-CMC solution flows

King et al. (2000) reported an similar trend over a wider range of fluid viscosity (3cP, 150cP and 300cP), saying that the threshold velocity for solids transport in air- viscous liquid flow is significantly higher than for a light liquid. Unlike the other studies, they used certain amount of fluid to place in the dip pipeline, and a sand layer was placed 5 m downstream of the dip. The net forward transport condition was visually obtained as increasing the superficial gas velocity. Although the more viscous fluid (beyond 20 cP) was not tested in air-liquid flow in this work, the result by King et al. (2000) might be not representative and can not be compared with other studies due to their methodology applied.

7.5 Preliminary Study on Particle Size and Vertical Pipe Orientation Effect

The aim of these preliminary studies was to understand how the particle size would affect the sand transport characteristics and what was the difference in sand behaviour and MTC in vertical and horizontal pipelines. The sand transport characteristics and MTC were obtained only in single phase water flow as a starting point. Details for these preliminary studies were given in Appendix B.

Generally, the observed MTC in vertical sand-water flow is much lower than that required in horizontal pipeline. It is due to the mechanism for sand transport in vertical flow is different from that in horizontal and near horizontal flows. In horizontal flow, sand compaction and friction between sand and pipe wall are major resistances to prevent the transportation. However, in upward vertical flow, the effect of above two

factors are minimised. Therefore, the transport velocity in vertical flow is much lower than that in horizontal flow.

The particle size effect on MTC in water flow was preliminarily studied using two types of sand particles with average size of 200 microns and 750 microns respectively. It was found that, for 5lb/1000bbl, less water velocity was required to transport bigger sand particles. Fewer particles were observed for 750 microns sand than 200 microns sand at this concentration, which resulted in less interaction of sand particles observed for 750 microns sand particles. For 50lb/1000bbl, the water velocity at MTC for 750 microns sand was found to be close to that for 200 microns. The sand streaks were also observed at MTC for 750 microns sand, which indicating the sand interactions were enhanced due to the increased number of sand particles at higher concentration. Therefore, it can be concluded that the particle interaction has a significant effect on MTC. However, more work need to be done to examine the particle size effect on MTC in air-water flow.

8 Pressure Gradients and Liquid Velocities Analysis at MTC in Water and Air-Water Flow

Pressure gradient (indicating energy loss) and liquid velocity are two of many principle factors in pipeline design. In this work, the analysis on the pressure gradient and liquid velocity is of utmost importance due to that those two factors are reflecting the energy required to assure the sand transportation in some way.

8.1 Pressure Gradient Analysis at MTC for Water and Air-Water Flow

King et al. (2000) proposed an equivalent pressure gradient method in order to predict the MTC in air-water flow. By assuming that, at MTC, the pressure gradient for air-water flow should be equal or slightly higher than the pressure gradient when sand particles were transported in single phase water flow, he proposed to use Thomas model (1962) to calculate the pressure gradients at MTC in sand-water flow, and then equalise it with pressure gradients in air-water flow using Beggs and Brill correlation (1976) to identify the V_{SL} and V_{SG}, which is the MTC in air-water flow:

$$\left|\frac{\Delta P}{\Delta x}\right|_{\text{Beggs and Brill for air-water flow}} \approx \left|\frac{\Delta P}{\Delta x}\right|_{\text{MTC}} \quad [88]$$

However, there were no justifications reported in their paper for using measured pressure gradients. In order to validate this concept, the pressure gradients were also measured in this work under different flow conditions (sand-water and air-water flows) and at different sand concentration.

Table 21 and Table 22 are listed the MTC for different sand concentrations (15lb/1000bbl and 200lb/1000bbl respectively) observed during the 4 inch sand-air-water experiments, and also compare the pressure gradients measured at those conditions in air-water flow with that measured at MTC for sand-water flow at the same sand concentration. The pressure gradients were also measured during 2 inch test. However, the fact that sand falling into the impulse line affected the pressure gradient reading due to that the differential pressure transducer was placed at the bottom of the pipe, whereas they were placed 45 degree deviated from the bottom in the 4 inch pipeline. Therefore, only the measure pressure gradients for the 4 inch tests were considered in this section.

Table 21: Measured pressure gradients comparison at MTC in 4 inch sand-water flow and air-water flow (15lb/1000bbl)

V_{SL} ($m \cdot s^{-1}$)	V_{SG} ($m \cdot s^{-1}$)	Measured Pressure Gradients at MTC in Water flow ($Pa \cdot m^{-1}$)	Measure Pressure Gradients in Air-Water flow ($Pa \cdot m^{-1}$)	Percentage Difference (%)
0.55	0.02	34.37	38.08	10.24
0.45	0.1	34.37	31.80	7.77
0.35	0.3	34.37	39.36	13.54
0.25	0.7	34.37	35.77	3.99
0.15	1.5	34.37	38.02	10.08

Table 22: Measured pressure gradients comparison at MTC in 4 inch sand-water flow and air-water flow (200lb/1000bbl)

V_{SL} ($m \cdot s^{-1}$)	V_{SG} ($m \cdot s^{-1}$)	Measured Pressure Gradients at MTC in Water flow ($Pa \cdot m^{-1}$)	Measure Pressure Gradients in Air-Water flow ($Pa \cdot m^{-1}$)	Percentage Difference (%)
0.55	0.2	54.80	46.97	15.39
0.35	0.8	54.80	57.24	4.36
0.15	2.5	54.80	53.94	1.58

From experimental results, it was found the percentage difference between the pressure gradients measured in air-water flow when the sand MTC occurred and those measured at MTC in sand-water flow for the corresponding sand concentration were reasonably small. As a result, for the purpose of design, the equivalent pressure gradient concept proposed by King et al. (2000) to predict the sand MTC in two phase air-water flow was valid. However, the accuracy of this approach still depends on the performances of Thomas model (1962) and Beggs and Brill correlation (1976) on predicting the pressure gradient for sand-water flow at MTC condition and for air-water flow respectively.

Table 23 shows the pressure gradient comparisons between measured and predicted by several empirical pressure gradient correlations with percentage error, PE, (Beggs and Brill, 1976; Friedel, 1979; Lockhart and Martinelli, 1949; Müller and Heck, 1986; Gronnerud, 1979) in air-water flow at (V_{SL}, V_{SG}) when MTC occurred.

Table 23: Pressure gradients comparison between measured and predicted by several empirical pressure gradients in 4 inch air-water flow

V_{SL} ($m \cdot s^{-1}$)	V_{SG} ($m \cdot s^{-1}$)	Measured Pressure Gradients	Beggs and Brill (1976) ($Pa \cdot m^{-1}$)	PE against Measured (%)	Friedel (1979) ($Pa \cdot m^{-1}$)	PE against Measured (%)	Lockhart and Martinelli (1949) ($Pa \cdot m^{-1}$)	PE against Measured (%)	Müller and Heck (1986) ($Pa \cdot m^{-1}$)	PE against Measured (%)	Gronnerud (1979) ($Pa \cdot m^{-1}$)	PE against Measured (%)
0.55	0.02	38.08	39.28	3.05	47.02	19.01	34.17	11.44	31.25	21.86	33.48	13.74
0.45	0.1	31.80	41.55	23.47	82.83	61.61	33.46	4.96	21.98	44.68	27.65	15.01
0.35	0.3	39.36	37.56	4.79	189.85	79.27	45.27	13.06	14.13	178.56	23.46	67.77
0.25	0.7	35.77	38.02	5.92	436.08	91.80	85.27	58.05	7.80	358.59	17.60	103.24
0.15	1.5	38.02	38.53	1.32	973.36	96.09	221.05	82.80	3.12	1118.59	9.64	294.40
0.55	0.2	46.97	66.73	29.61	168.02	72.04	58.10	19.16	31.21	50.50	53.76	12.63
0.35	0.8	57.24	63.19	9.42	564.80	89.87	119.86	52.24	14.1	305.96	41.86	36.74
0.15	2.5	53.94	61.62	12.46	1830.79	97.05	514.87	89.52	3.06	1662.75	14.76	265.45

From Table 23, it can be concluded that Beggs and Brill correlation (1976) did give the best prediction for the pressure gradient in air-water flow among these correlations tested. Also, it was found that, apart from Beggs and Brill correlation (1976), the percentage error for other correlations increased with the decrease of V_{SL}, where in the transition region from slug flow regime to stratified wavy flow regime.

8.2 Liquid Velocities Analysis at MTC in Water and Air-Water Flow

As discussed in previous section, the sand transportation always occurs within the liquid phase. In water flow, sand will transport along with the water at the bottom of the pipe. In air-water flow, sand transportation usually enhanced within the liquid slug body. In this section, the sand minimum transport velocities in water flow were compared with the slug translational velocities sand MTC in air-water flow, attempting to find some insights on the relationships for local liquid velocities at MTC in water flow and in air-water flow.

Table 24 to Table 26 list the mixture velocities, slug translational velocities at MTC and the MTC in single phase water flow for different sand concentrations.

Table 24: Comparison of mixture velocities, slug translational velocities at MTC and the MTC in single phase water flow for 15lb/1000bbl

V_{SL} ($m \cdot s^{-1}$)	V_{SG} ($m \cdot s^{-1}$)	V_{mix} ($m \cdot s^{-1}$)	V_T ($m \cdot s^{-1}$)	MTC in water tests ($m \cdot s^{-1}$)	Flow regime
0.55	0.02	0.57	1.30	0.5~0.6	Str+IW (Plug)
0.45	0.1	0.55	1.31		Str+IW (Plug)
0.35	0.3	0.65	1.28		Slug
0.25	0.7	0.95	1.48		Str+RW
0.15	1.5	1.65	2.09		Str+RW

Table 25: Comparison of mixture velocities, slug translational velocities at MTC and the MTC in single phase water flow for 200lb/1000bbl

V_{SL} ($m \cdot s^{-1}$)	V_{SG} ($m \cdot s^{-1}$)	V_{mix} ($m \cdot s^{-1}$)	V_T ($m \cdot s^{-1}$)	MTC in water tests ($m \cdot s^{-1}$)	Flow regime
0.55	0.2	0.75	1.99	0.65~0.75	Slug
0.45	0.3	0.75	1.93		Slug
0.35	0.8	1.15	2.01		Slug
0.25	1.2	1.45	2.25		Str+LRW
0.15	2.5	2.65	3.37		Str+RW

Table 26: Comparison of mixture velocities, slug translational velocities at MTC and the MTC in single phase water flow for 500lb/1000bbl

V_{SL} ($m \cdot s^{-1}$)	V_{SG} ($m \cdot s^{-1}$)	V_{mix} ($m \cdot s^{-1}$)	V_T ($m \cdot s^{-1}$)	MTC in water tests ($m \cdot s^{-1}$)	Flow regime
0.55	0.30	0.85	2.18	0.75~0.85	Slug
0.45	0.40	0.85	2.15		Slug
0.35	0.90	1.25	2.18		Slug
0.25	1.5	1.75	3.28		Str+LRW
0.15	3.0	3.15	3.98		Str+RW

From Table 24 to Table 26, it was found that, when V_{SL}= 0.55 and 0.45 $m \cdot s^{-1}$, the mixture velocities at MTC in air-water tests were found similar to the MTC in single phase water tests for those sand concentrations tested, whereas when V_{SL}= 0.15 - 0.35 $m \cdot s^{-1}$, the mixture velocities at MTC in air-water tests were found higher than the MTC in single phase water tests. When decreasing the superficial liquid velocity, the transition from slug flow to stratified + roll waves occurs. As described in previous section, the sand behaviour in roll wave was similar to that in slug flow. However, the liquid body of roll waves are smaller than slugs, where less sand particles could be transported. And due to less liquid content, the frequency of roll waves is lower than slugs, which causes more sand particles compact when the flow is stratified. As a result, more energy was required to transport the sand particles at low superficial liquid velocity.

However, it was found that the slug translational velocities at MTC were higher than both the MTC in single phase water tests and the mixture velocities in air-water tests for all the sand concentrations tested.

9 New Minimum Sand Transport Velocity Correlation

9.1 Validation of Thomas Lower Model against Experimental MTC

King et al. (2000) recommended Thomas's lower model (1962) to calculate friction velocity u_0^* (Equation 55, 56) at the minimum transport condition for liquid turbulent flow. The associated frictional pressure gradient (Equation 57) at MTC was then calculated.

From Equation13 to 15, it can be seen that, the Thomas lower model did not considered the pipeline orientation. It was also noticed that, unlike the Thomas upper model (1962, Equation 56), the Thomas lower model (1962, Equation 55) did not have a concentration correction term. In an earlier paper (Thomas, 1961), he claimed that for particles smaller than the laminar sublayer, the wall shear velocity remained constant at C_v from 0.01 to 0.06 v/v. Therefore, he used the friction velocity at C_v = 0.01 v/v as the friction velocity at infinite dilution ($C_v \approx 0$, i.e. very few particles). However, this method was dubious due to the absence of data for friction velocity when C_v ranging from 0.01v/v down to infinite dilution.

King et al. (2000) stated that the thickness of laminar sublayer could be calculated by:

$$\delta = 62D\left(DV_{SL}\rho_l/\mu_l\right)^{-7/8} \qquad [89]$$

In the work of this thesis, sand with 200 microns mean particle diameter was used, which settling according to intermediate law. The particle diameter will not exceed the thickness until V_{SL} = 1.35 $m \cdot s^{-1}$ for water flow. Therefore, in this work, the sand particles were found smaller than the thickness of laminar sublayer, and only Thomas lower model would be applied.

Table 27 shows the comparison between some 4 inch experimental MTC data with those predicted by the Thomas lower model.

Table 27: Comparison between 4 inch experimental MTC and those predicted by the Thomas lower model

	Experimental V_{MTC} ($m \cdot s^{-1}$)		
Liquid viscosity (cP)	50lb/1000bbl	200lb/1000bbl	Thomas Lower Model (1962)
Water	0.50 ~ 0.60	0.65 ~ 0.75	0.48
7	0.70 ~ 0.80	0.80 ~ 0.90	1.06
20	0.75 ~ 0.85	0.90 ~ 1.00	1.89
105	0.35	0.45	6.78
200	0.25	0.3	9.52
340	0.07	0.2	12.60

As estimated from experimental observations, the MTC velocity for different sand concentration is different in both water and air-water flow. Therefore, it will result in inaccuracies if applying the Thomas lower model to predict MTC with absence of consideration for sand concentration.

From Table 27, it was found that the Thomas lower model (1962) over-predicted the sand MTC when as the fluid viscosity increased. In laminar flows (liquid viscosity higher than 105cP, combining Table 17 and Table 18), the prediction showed an opposite trend comparing to the experimental observations. This is due to that the Thomas lower model was generated based on MTC data for solid-water flow. The bulk flow regime was turbulent rather than laminar. Therefore, the Thomas lower model cannot be applied to predict the liquid viscosity effects when the flow is laminar.

9.2 Development of Correlation for MTC for Sand-Liquid Flows and Sand-Gas-Liquid Flows

One of the main objectives of the present work was to extend the Thomas lower model and develop a new correlation for MTC in the form of friction velocity, which covers the very low sand concentrations (up to 500lb/1000bbl) encountered in oil and gas transport lines.

To develop new sand transport velocity under MTC definition, sand-water experiments were performed in the 2 inch pipeline. The sand concentration (v/v) tested ranged from 5.38E-06 (5lb/1000bbl) up to 5.38E-02 (50000lb/1000bbl). The observed sand velocities at minimum transport condition for the 2 inch water experiments are listed in Table 28.

Table 28: 2 inch experiment results

Sand Concentration lb/1000bbl	C_v (v/v)	V_{MTC}	Sand Concentration lb/1000bbl	C_v (v/v)	V_{MTC}
5	5.38E-06	0.40~0.45	2000	2.15E-03	0.90~1.00
15	1.61E-05	0.45~0.50	5000	5.38E-03	1.00~1.10
50	5.38E-05	0.50~0.55	10000	1.08E-02	1.10~1.20
100	1.08E-04	0.55~0.65	15000	1.61E-02	1.20~1.30
200	2.15E-04	0.65~0.75	20000	2.15E-02	1.20~1.30
500	5.38E-04	0.70~0.80	30000	3.23E-02	1.30~1.40
1000	1.08E-03	0.80~0.90	50000	5.38E-02	1.30~1.40

These data are plotted on the same graph of as some 2 inch up to 4 inch slurry test data for particles of around 250microns, as shown in Figure 112.

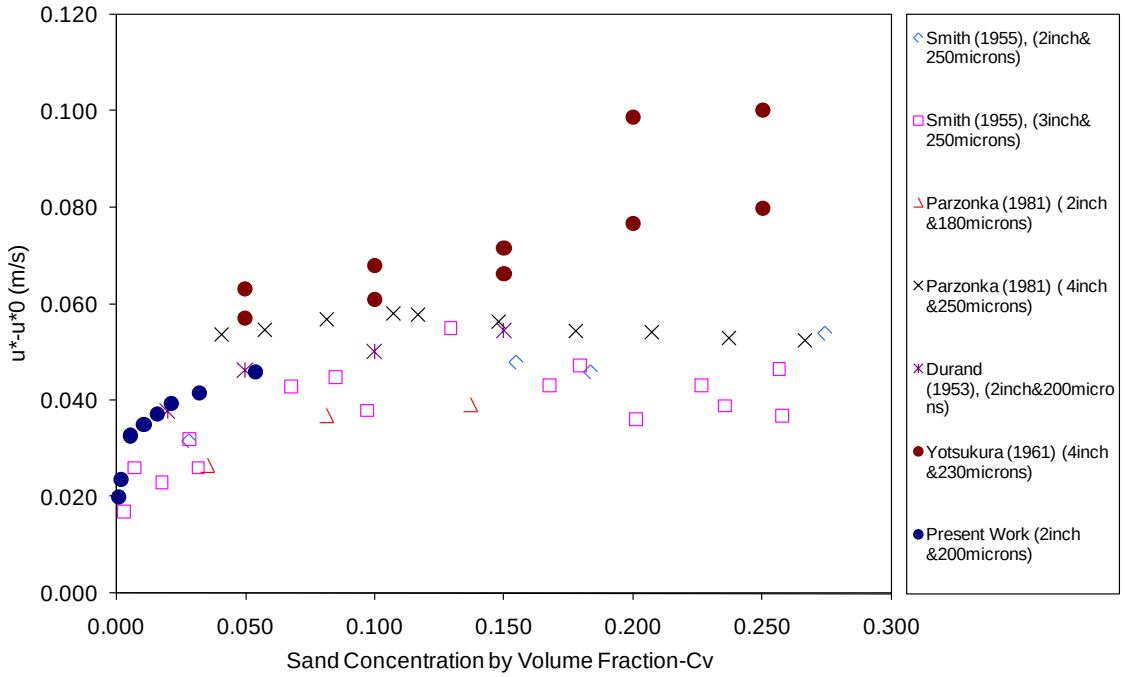

Figure 112: Friction velocity data at MTC from different researchers

As mentioned in previous sections, there are significant scatters in the published data. The reasons though not clear but could be attributed to the different transport velocity definitions. Assuming sand were distributing uniformly at the bottom of the pipe, it was found that when C_v is below 0.0005 (500lb/1000bbl), sand particles, if moved continuously with the liquid, can hardly form a continuous line along the bottom of the pipe. Therefore, it is suggested that the sand concentration of 500lb/1000bbl could be used as a dividing boundary for correlation development to account for the ultra low and 'high' sand concentration.

Dual range sand transport correlation:

Range 1: Friction velocity at MTC when sand concentration C_v <0.0005

Range 2: Friction velocity at MTC when sand concentration C_v >0.0005

Range 1

Due to the lack of data in this range, only the present 2 inch test data was applied to develop the friction velocity at MTC. The form of correlation, $u_c^* - u_0^* = KC_v^{\alpha}$, between the friction velocity or "wall shear velocity" and particle concentration by volume fraction was used (K in the unit of $m \cdot s^{-1}$). This form was recommended by several researchers including Thomas (1962) and Zandi and Hayden (1971). The diagram of correlation development for the ultra low particle concentration is schematically presented in Figure 113. Here, the frictional velocity at 5lb/1000bbl were used for infinite dilution condition, which is the lowest concentration experienced in oil pipeline.

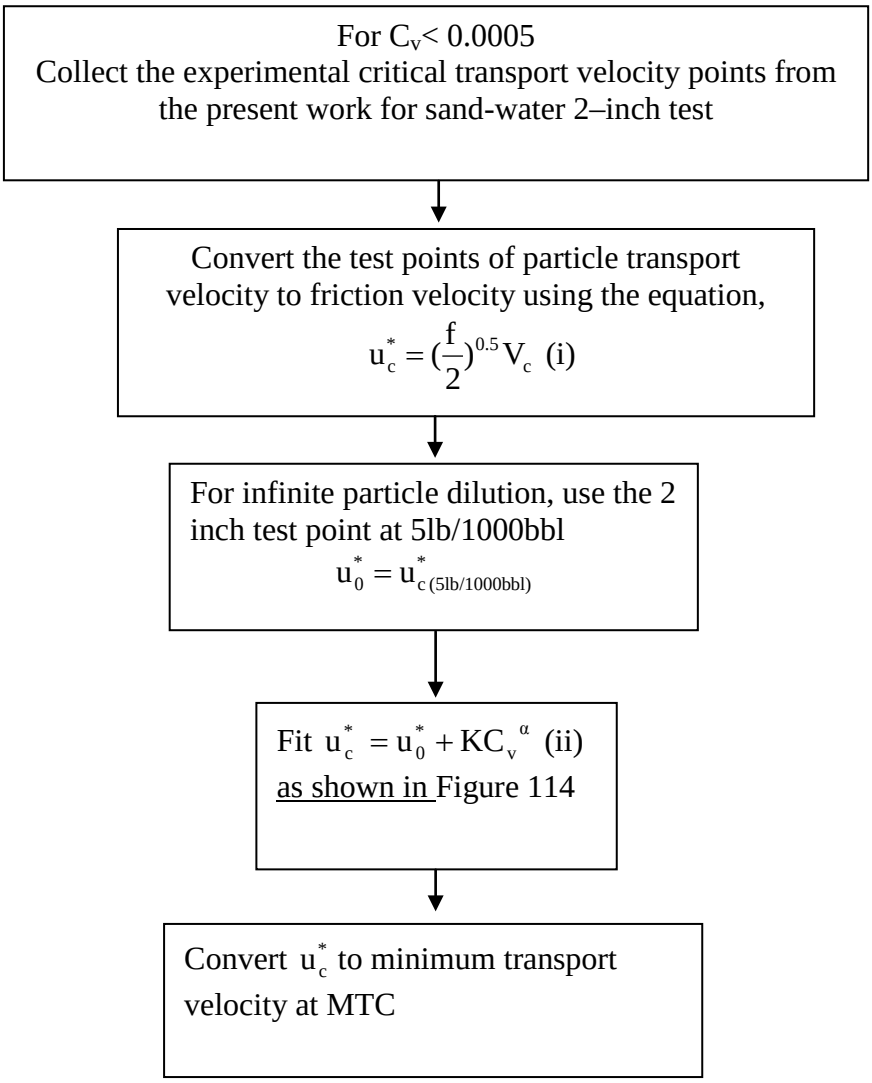

Figure 113: Calculation of concentration correction term for friction velocity

Figure 114 shows the fitting of data points for C_v < 0.0005

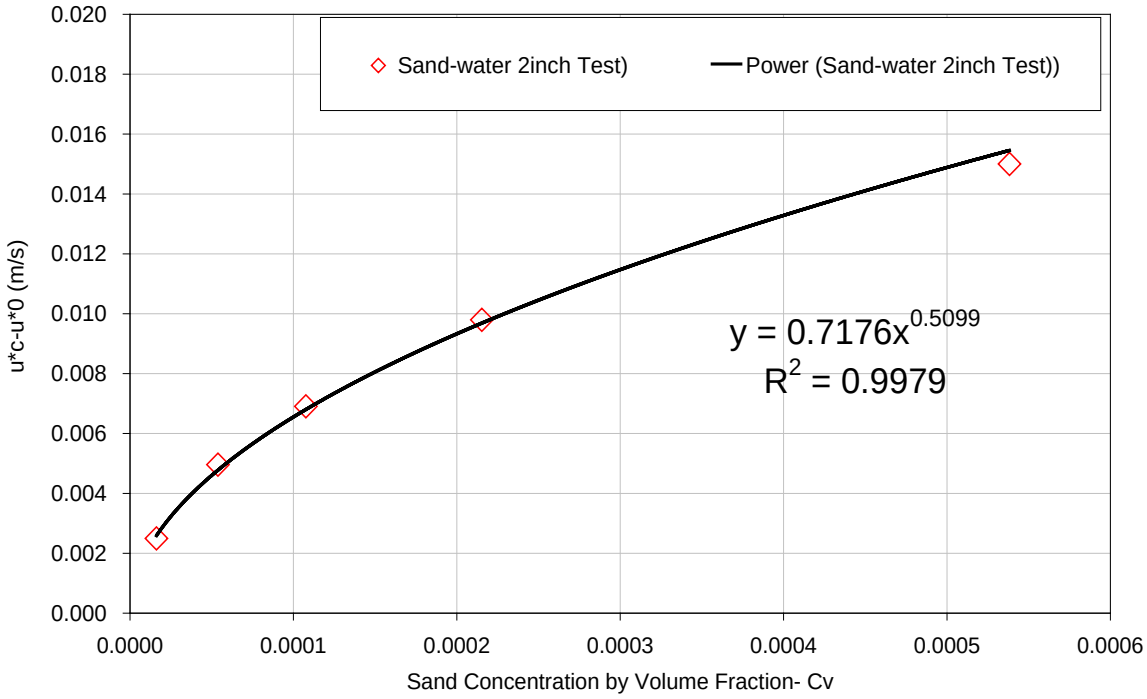

Figure 114: Data fitting for C_v<0.0005

The final form for range 1 (C_v < 0.0005v/v (500lb/1000bbl)) is given as:

$$u_c^* = u_0^* + 0.7176 C_v^{0.5099} \quad [90]$$

Range 2

Based on the data from selected previous works and the present 2 inch data, another correlation was developed to account for sand concentration C_v >0.0005 v/v. The diagram of model development for range 2 is shown in Figure 115

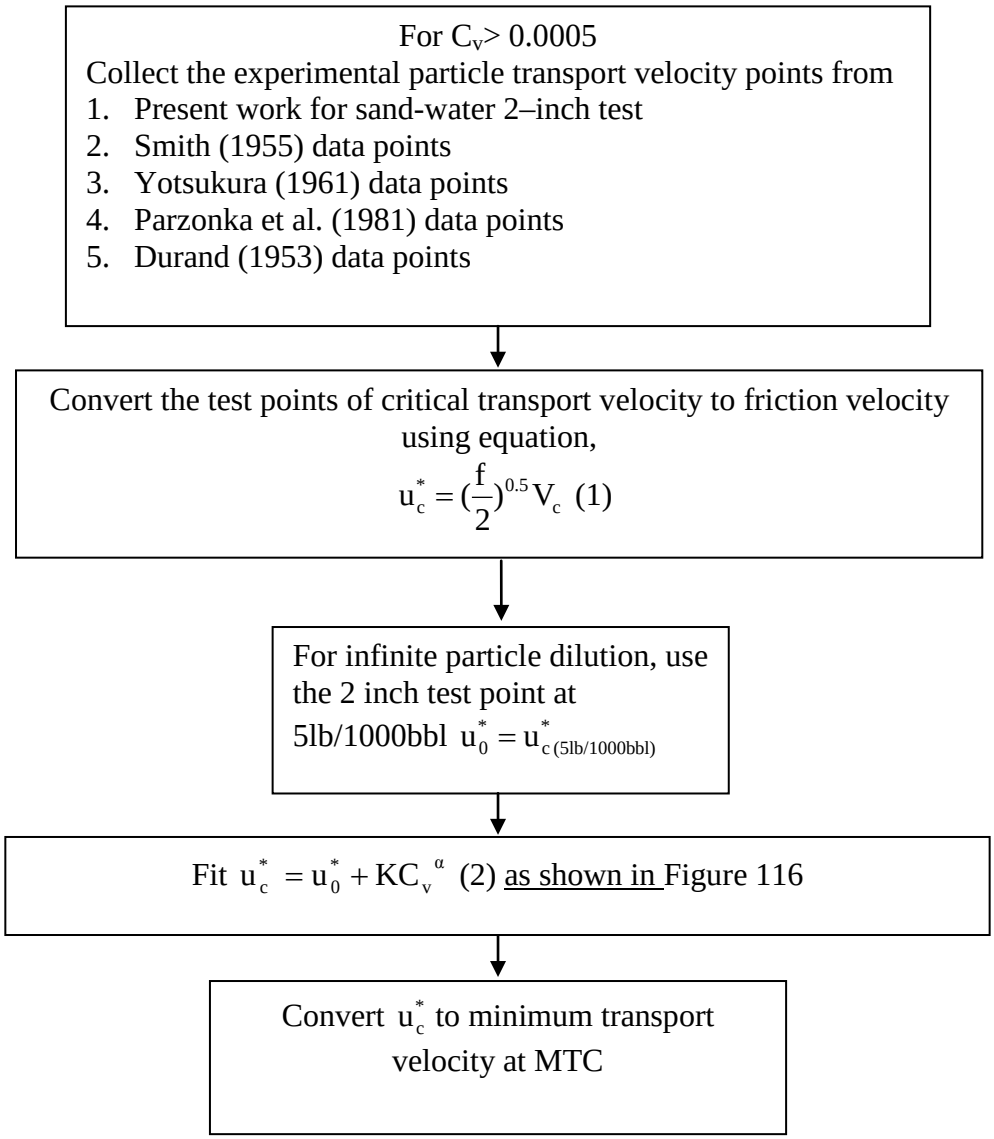

Figure 115: Calculation of the friction velocity concentration correction term

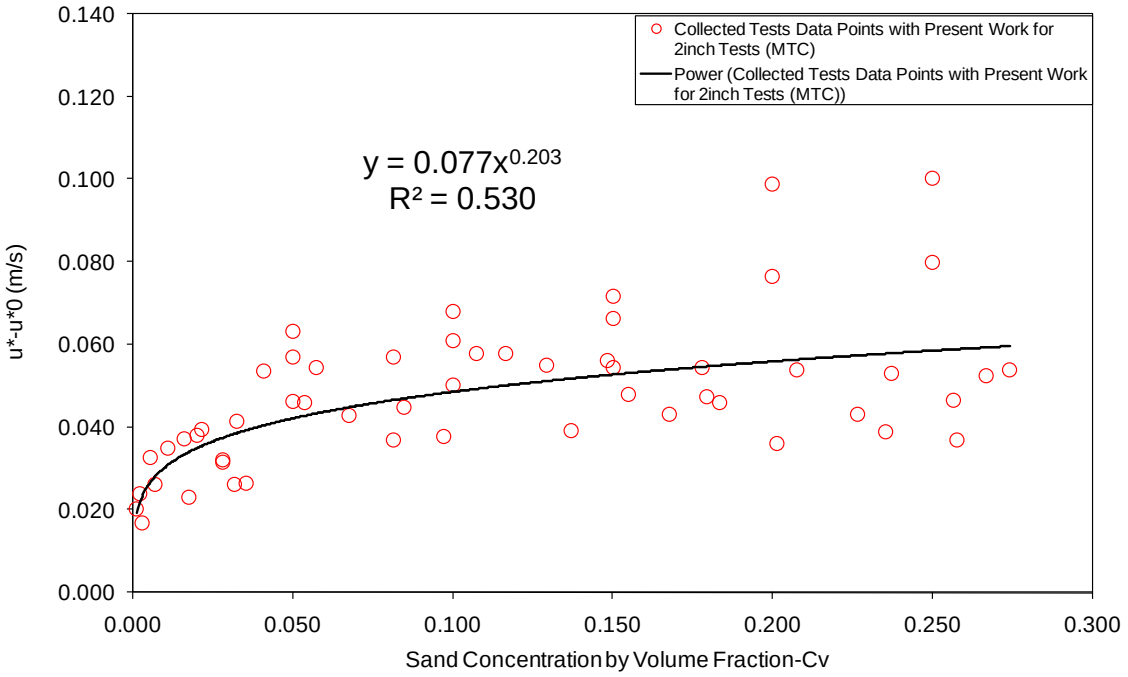

Figure 116: Data fitting for C_v> 0.0005

Figure 116 shows the fitting of data points for C_v > 0.0005.

Meanwhile, it was found that the u_0* in 2 inch and 4 inch experiments were close to that predicted by Thomas (1962), as shown in Table 29.

Table 29: u_0* from experiment and Thomas prediction

u_0* (Thomas, 1962) ($m \cdot s^{-1}$)	u_0* (2 inch test) ($m \cdot s^{-1}$)	u_0* (4 inch test) ($m \cdot s^{-1}$)
0.0266	0.023	0.0255

Therefore, it is suggested that Thomas prediction can be applied in the final form of the proposed model for calculating the friction velocity at infinite dilution.

The final form of new proposed correlations (Dual ranges) for sand minimum transport condition is:

$$u_0^* = \left[100 u_t \left(\frac{\nu}{d_p}\right)^{2.71}\right]^{0.269} \qquad [18]$$

$$u_c^* = u_0^* + 0.7176 C_v^{0.5099} \qquad C_v < 0.0005 \text{ (500lb/1000bbl) (correlation 1)} \qquad [91]$$

$$u_c^* = u_0^* + 0.0776 C_v^{0.2032} \qquad C_v \geq 0.0005 \text{ (correlation 2)} \qquad [92]$$

while particle diameters ranges from 180 microns up to 250 microns and pipe diameter ranges from 2 inch up to 4 inch.

Another attempt was made to generate a general form of friction velocity to account for the sand concentration ranging from ultra low sand concentration (C_v = 5.38E-06 (15lb/1000bbl)) up to high sand concentration (C_v = 0.3). Using all the data points collected from the present 2 inch water-sand experiment and from previous works (Figure 117),

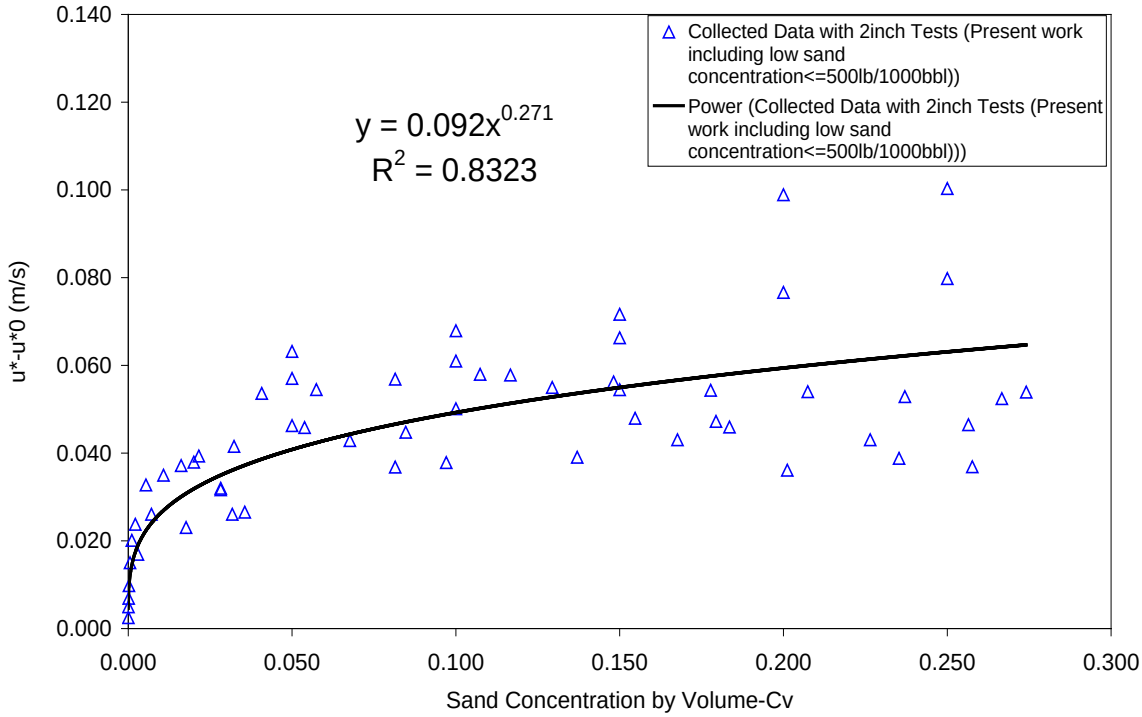

Figure 117: Data fitting for 5.38E-06 ≤ C_v < 0.3v/v

The final form of new proposed correlations (Single range) for sand minimum transport condition is:

$$u_0^* = \left[100 u_t \left(\frac{\nu_l}{d_p}\right)^{2.71}\right]^{0.269} \qquad [18]$$

$$u_c^* = u_0^* + 0.092 C_v^{0.271} \qquad 5.38\text{E-}06 \le C_v < 0.3\text{v/v (correlation 3)} \qquad [93]$$

The actual velocity then will be calculated based on the equation $u_c^* = (f/2)^{0.5} \times V_{MTC}$ for single phase flow, using the Fanning friction factor correlation proposed by Chen (1979):

$$\frac{1}{\sqrt{f}} = -4.0\log\left[0.2698\left(\frac{\varepsilon}{D}\right) - \frac{5.0452}{Re}\log\left(0.3539\left(\frac{\varepsilon}{D}\right)^{1.1098} + \frac{5.8506}{Re^{0.8981}}\right)\right] \qquad [94]$$

9.3 Validation of New Proposed Sand Transport Correlation with Experimental MTC

Table 30 and Table 31 illustrate the performance on predicting MTC of proposed dual ranges and single range model for different sand concentrations tested in single phase water flow.

Table 30: V_{MTC} comparison between the proposed dual ranges model and observation

Sand Concentration (lb/1000bbl)	V_{MTC}(Proposed dual ranges model, 2 inch)	V_{MTC} (this work, 2 inch)	V_{MTC}(Proposed dual ranges model, 4 inch)	V_{MTC} (this work, 4 inch)
500	0.79	0.65~0.75	0.87	0.75~0.85
200	0.67	0.60~0.70	0.74	0.65~0.75
100	0.61	0.55~0.65	0.67	0.60~0.70
50	0.57	0.50~0.55	0.63	0.50~0.60
15	0.52	0.45~0.50	0.58	0.50~0.60

Table 31: V_{MTC} comparison between the proposed single ranges model and observation

Sand Concentration (lb/1000bbl)	V_{MTC}(Proposed single range model, 2 inch)	V_{MTC} (this work, 2 inch)	V_{MTC}(Proposed single range model, 4 inch)	V_{MTC} (this work, 4 inch)
500	0.72	0.65~0.75	0.79	0.75~0.85
200	0.66	0.60~0.70	0.73	0.65~0.75
100	0.63	0.55~0.65	0.69	0.60~0.70
50	0.60	0.50~0.55	0.66	0.50~0.60
15	0.56	0.45~0.50	0.62	0.50~0.60

It can be seen that the dual ranges correlation had better performance than the single range correlation when the sand concentration ranges from 15lb/1000bbl to 50lb/1000bbl. When sand concentration was equal or higher than 100lb/1000bbl, the two correlations both could predict the MTC fairly well.

10 Conclusions and Future Work

10.1 Conclusions

The sand transport characteristics and the sand MTC in multiphase flows have been experimentally observed from viewing sections in 2 inch (PVC), 3 inch (PVC) and 4 inch (stainless steel) multiphase facilities. The investigations were conducted with horizontal and inclined pipelines with sand particles of an average diameter of 200 microns. The sand concentration tested in this work ranged from 5lb/1000bbl (0.000005v/v) up to 500lb/1000bbl (0.0005v/v).

- Similar sand behaviours were observed in sand-water flow for different sand concentration in the 2 inch and 4 inch horizontal pipelines. It was found that the water velocities at MTC increased with the increase of sand concentrations. Moreover, the water velocities at MTC in 4 inch pipeline were found slightly higher than those in 2 inch pipeline at same sand concentration, which is due to the laminar sublayer in 4 inch pipeline is thicker than that in 2 inch pipeline at the same averaged velocity.

- In sand-air-water flow, the sand transport characteristics and MTC were strongly dependent on the air-water flow regime. The slug flow regime was found to be more efficient for sand transportation in both 2 inch and 4 inch pipelines. In the 2 inch pipeline, the sand transport characteristics in stratified and stratified wavy flow regime were found to be similar to those in sand-water flow. However, in the 4 inch pipeline, the sand particles were observed transported in stratified + roll wavy flow.

- The pipeline orientation effect (+5~+20 degrees) was studied in this work. In sand-water flow, there was little inclination effect observed on sand behaviours and MTC in both 2 inch and 4 inch pipeline. In sand-air-water flow, the sand transport characteristics in slug body were similar to those in horizontal pipeline. However, the sand particles were observed moving backward with the liquid film until swept up by another slug. As in a horizontal pipeline, the sand MTC in sand-air-water flows in inclined pipelines were also flow regime dependent. In both 2 inch and 4 inch inclined pipelines, the slugs were found more prevailing. As a result, the superficial gas and liquid velocities required to transport sand were lower than those in the horizontal pipeline.

- The liquid viscosity effect was investigated on sand transport characteristics and MTC in single phase liquid flow. The CMC solution (7cP and 20cP) and Azolla oil (340cP at 16^{O}C, 200cP at 24.7^{O}C and 105cP at 34.7 ^{O}C) were used instead of water in 4 inch pipeline and 3 inch pipeline, respectively. It was found that the sand MTC increased slightly as the fluid viscosity increased (from 1 to 20cP). However, when the flow become laminar (viscosity higher than 105cP), the MTC decreased as the fluid viscosity increased.

- Pressure gradients and liquid velocities at MTC were compared in water and air-water flow in order to provide some insights for relating the MTC in water flow and those in air-water, thus provide the guideline for pipeline design. King's equivalent pressure gradients concept (2000) was validated by measured pressure gradients at MTC in water and air-water flow for different sand concentration. It was found this concept is valid. However, the accuracy of this approach in pipeline design is depending on the accuracy of pressure gradient prediction at both MTC in sand-water flow and in the air-water flows. The measured air-water pressure gradients, when MTC would occur, were also compared with several empirical pressure gradient correlations (Beggs and Brill, 1976; Friedel, 1979; Lockhart and Martinelli, 1949; Müller and Heck, 1986; Gronnerud, 1979) and with modelling software OLGA 2000. Beggs and Brill's correlation (1976) was found to have the best prediction for pressure gradients in air-water flow.

- Thomas lower model was found to give good prediction at normal sand concentration (5 to 50 lb/1000bbl). However, there were no sand concentration and pipeline orientation effects accounted in the model. In addition, it over-predicts the MTC as fluid viscosity increases and showed an opposite trend on predicted MTC when the liquid flow became laminar. The Thomas lower model was extended to account for sand concentration. Two sets of correlations (dual range and single range correlations) were proposed to cover the concentration range in this work (0.0005 up to 0.3v/v). In dual range correlations, correlation for range 1 accounted for v/v ranged from 0.000005 to 0.0005 (5-500lb/1000bbl), while correlation for range 2 could be applied when v/v ranged from 0.0005 to 0.3. However, the correlation for single range covered the v/v from 0.000005 up to 0.3. The proposed concentration correction correlations were incorporated into Thomas lower model to predict the frictional velocity at MTC in water flow. It was found that dual range correlations predicted MTC better than the single range correlation when sand concentration was lower than 200lb/1000bbl. When the sand concentration was equal to or higher than 200lb/1000bbl, dual and single range correlations showed the similar performance.

10.2 Future Work Recommendation

- In this work, the Thomas lower model was extended to account for sand concentration. However, the Thomas lower model was found to over-predict the sand MTC as the fluid viscosity increases, which could result from that Thomas correlation was for water flow. Moreover, experimental observations showed an opposite trend comparing to the prediction when in laminar flows (liquid viscosity higher than 105cP). Therefore, a "viscosity correction" on Thomas lower model, or even a new correlation is needed to take account into high viscosity crude.

- The amount of sand MTC data is limited for uphill pipelines for inclinations between +20 and +90 degrees, and more investigations need to be done in this pipe orientations range. In this work it was found that the MTC in +20 degrees water flow was higher than that in vertical water flow. Therefore, a maximum MTC might exist when the pipe orientation was between +20 and +90 degrees. For air-water flows within this pipe orientation range, a higher MTC might also be required than that in horizontal pipe due to the change of flow regime. A preliminary study on sand transport characteristics in vertical pipeline was illustrated in Appendix B.

- More work is also required to generalise the Thomas lower model to account for particle size effect. The Thomas lower model was based on experimental data for small particle diameter (56~78microns), which assumed particle size is smaller than the laminar sub-layer. Experimental investigation also showed the lower model appeared accurate when d_p ranged from 200~255 microns at normal concentration (15~50lb/1000bbl) in pipeline. Therefore, more MTC data in multiphase flow is required for larger particles (bigger than laminar sublayer) and extreme fine particles (smaller than 50 microns) to validate the Thomas model. A preliminary study on sand transport characteristics in a vertical pipeline was detailed in Appendix B.

- Currently, little is known for sand transportation in stratified wavy and annular flow regimes, especially at low water cut. In stratified wavy flow with low water cut (wet gas pipeline), the liquid can be transported as a thin film at the bottom of the pipe, where wet sand bed could be formed. In annular flow, sand may be transported in liquid film and in gas core. Moreover, the erosion rate need to be considered while investigating the sand transport condition since the velocities are high in annular flow.

- Limited data is available regarding sand transportation in air-water-oil flows. The flow regimes of air-water-oil flow are the function of the flowrates, experimental setup and, crucially, the physical properties of the fluids, which mean that for any particular set of in-situ volume flowrates, the fluid in contact with the sand is not likely to be easily predictable. Phase inversion will also in turn have an effect on the solids transport (water-wetted and oil-wetted sand). All these factors are very difficult to quantify and very little research has been done in this area until very recently.

- The sand transportation in dip configuration of the pipeline is another increasing concern. In oil field, “sand accumulated at the bottom of the export riser leading to a partial blockage and a reduced production capacity” (King et al., 2000). As a result, it is worthy studying sand behaviour (accumulation and washed-out) in dip pipeline at different dip angles to provide valuable data for pipeline design.

References

1. Al-Mutahar, Faisal, (2006), "*Modeling of Critical Deposition Velocity of Sand in Horizontal and Inclined Pipes*", MSc Thesis, Department of Mechanical Engineering, The University of Tulsa, Tulsa.

2. API, 1981, ''*API RP 14E Recommended Practice for Design and Installation of Offshore Production Platform Piping Systems*'' 3rd Edition, American Petroleum Institute, Washington, DC, p. 22

3. API, 1981, ''*API RP 14E Recommended Practice for Design and Installation of Offshore Production Platform Piping Systems*'' 5th Edition, American Petroleum Institute, Washington, DC, p. 23

4. Ambrose, H.H., (1953), "The Transportation of Sand in Pipes", *Proceedings of the fifth Hydraulics Conference Engineering Bulletin*, No. 34, p77-78.

5. Angelsen, S., Kvernvold, O., Lingelem,M., Olsen, S., (1989), "Long-Distance Transport of Unprocess HC Sand Settling in Multiphase Pipelines", *Proceedings of The Fourth International Conference on Multiphase Flow*, Nice, France, June, pp.19-21.

6. Beggs, H. D. and Brill, J. P., (1973), "A Study of Two-Phase Flow in Inclined Pipes", *J. Pet. Tech.*, pp. 607-617

7. Blatch, N.S., (1906), "Discussion of 'Works for the purification of the water Supply Washington D.C.'", *Trans Amer. Soc. Civil Engrs*., Vol.57, pp. 400-409.

8. Cairns, R. C., Lawther, K. R. and Turner, K. S., (1960), "Flow Characteristics of Dilute Small Particle Suspensions", *Brit. Chem. Eng.*, Vol. 5, pp. 849-856.

9. Charles, M. E., (1970), "Transport of Solids by Pipelines", *Hydrotransport 1*, pp. A3-A25.

10. Chen, N.H., (1979), "An Explicit Equation for Friction Factor in Pipe", *Ind. Eng. Chem. Fund.*, 18, 296.

11. Chien, S.F., (1993), "Critical Velocity of Sand-Fluid Mixtures in Horizontal Pipe Flow", *FED*, Vol. 189, 231-247.

12. Condolios, E. and Chapus, E. E., (1963), "Transporting Solid Materials in Pipelines", *Chem. Eng.*, Vol. 24, pp. 93-98.

13. Coulson, J.M.; Richardson, J.F.; Backhurst, J.R.; Harker, J.H., *Coulson and Richardson's Chemical Engineering Volume 1 - Fluid Flow, Heat Transfer and Mass Transfer (6th Edition)*, Elsevier, 1999

14. Cowe, T. C., (2005),"*Multiphase Flow Handbook*".*1st edition*.CRS Press, USA.

15. Craven, J. P., (1953), "The Transportation of Sand in Part-full Pipe Flows", *Proc. of the Fifth Hydraulics Conference Bulletin 34*, State University of Iowa Studies in Engineering, Iowa State University, Iowa.

16. Davies, J.T., (1987), "Calculation of Critical Velocities to Maintain Solids in Suspension in Horizontal Pipes", *Chem. Engg. Sci,* Vol. 42, 7, pp. 1667-1670.

17. Durand, R., (1953), "Basic Relationships of the Transportation of Solids in Pipes Experimental Research", *Proceedings Minnesota International Hydraulics Convention*, pp. 89-103.

18. Durand, R and Condolios, E., (1952), "The Hydraulic Transportation of Coal and Solid Material in Pipes", *Processing of Colloquium on Hransport of Coal*, National Coal Board, November 5, London, UK.

19. Fairhurst, C. P. & Baker, P. J., (1983), "*Multiphase Sand Transport in Oil Production Flowlines*", Draft report on BHRA Project RP D00935, bHRA, Cranfield, Bedfordshire, UK.

20. Friedel L., (1979), "Improved Friction Drop Correlations for Horizontal and Vertical Two-Phase Pipe Fow", *European Two-Phase Flow Group Meeting*, paper E2, Ispra, Italy.

21. Garde, R. J., (1956), "*Sediment Transport through Pipes*", MSc Thesis, Colorado A&M University at Fort Collins, Colo.

22. Gillies, R. G., Shook, C., Kristoff, B. & Parker, P., (1994), "Sand Transport in Horizontal Wells", *11th Annual Calgary University Heavy Oils and Oil Sands Technology Symposium*, March 2nd.

23. Gillies, R.G., McKibben, M.J. and Shook, C.A. (1997), "Pipeline Flow of Gas, Liquid and Sand Mixtures at Low Velocities", *J.Can.Pet.Tech,* Vol. 36, pp. 36-42.

24. Graf, W. H., (1971), "*Hydraulics of Sediment Transport*", McGraw-Hill Book Co., Inc., New York.

25. Grönnerud, R., (1979), "Investigation of Liquid Hold-up, Flow-resistance and Heat Transfer in Circulation Type of Evaporators, Part iv: Two-phase Flow Resistance in Boiling Refrigerants", *Annexe 1972-1*, *Bull*. de l'Inst. Froid.

26. Howard, G. W., (1939), "Transportation of Sand and Gravel in Four Inch Pipe", *Transaction, ASCE*, Vol. 104, Paper No.2039, pp.1334-1348.

27. Howard, C. D. D., (1962b), "*Effect on Fines on Pipeline Flow of Sand Water Mixtures*", MSc Thesis, University of Alberta.

28. Hughmark, G. A. (1961), "Aqueous Transport of Settling Slurry", *Industrial and Engrg. Chem*, Vol. 55, pp. 389-390.

29. Kay, J.M., Nedderman, R.M., *Fluid Mechanics and Transfer Process*, Cambridge University Press, 1985, pp 206~210.

30. King, M.J.S., Farhurst, C.P. and Hill, T.J., (2000), "Solids Transport in Multiphase Flows Application to High Viscosity Systems", *Energy Sources Tech Conf, New Orleans*, pp. 14-17.

31. Kokpinar, M.A., and Gogus, M., (2001), "Critical Flow Velocity in Slurry Transporting Horizontal Pipelines", *Journal of Hydraulic engineering*, Vol. 127, pp. 763-771.

32. Kvernvold, O., and Sandberg, R., (1998), ''*ERBEND 2—Erosion in Pipe Bends*'', Det Norske Veritas (DNV), Norway.

33. Lockhart R.W., Martinelli R.C., (1949), "Proposed Correlation of Data for Isothermal Two-phase Two-component in Pipes", *Chem. Eng. Process*, Vol. 45, pp. 39–48.

34. Lockett, T. J., Beech, P. M., Birchenough, P. M., McCarthy, P., Dawson, S. G. B., and Worraker, W. J., (1997), ''*Erosion/Corrosion in Sweet Multiphase Systems*,'AEAT Report No. 1174, AEA Technology plc., UK

35. Meyer-Peter, E. and Müller, R., (1948), "Formulas for Bed-load Transport", *Proceedings of the 2nd Meeting of the International Association for Hydraulic Structures Research*, pp. 39-64

36. Müller-Steinhagen H., Heck, K., (1986), "A Simple Friction Pressure Correlation for Two-phase Fow in Pipes", *Chem. Eng. Process*, Vol. 20, pp. 297–308.

37. Nakayama, Y.; Boucher, R.F., *"Introduction to Fluid Mechanics"*, Elsevier, 2000

38. Newitt, D. M., Richardson, J. F., Abbott, M. and Turtle, R. B., (1955), "Hydraulic Conveying of Solids in Horizontal Pipes", *Trans. Inst. Chem. Eng.*, Vol. 33, 2, pp. 93-113.

39. Oroskar, A. R., and Turian, R. M., (1980), "The Critical Velocity in Pipeline Flow of Slurries", *AIChE Journal*, Vol. 26, pp. 550-558.

40. Oudeman, P., (1993), "Sand Transport and Deposition in Horizontal Multiphase Trunklines of Subsea Satellite Developments", *SPE Production & Facilities*, pp.237-241.

41. Parzonka, W., Kenchington, J.M. and Charles, M.E., (1981), "Hydrotransport of Solids in Horizontal Pipes: Effects of Solids Concentration and Particle Size on the Deposit Velocity", *Canadian Journal of Chemical Engineering* Vol. 59, pp. 291–296.

42. Rix, S.J. and Wilkinson, S.J., (1991), "*The Conveying of Sand by Two-phase Flows in Horizontal and Inclined Pipes",* Research Project Report, University of Cambridge, Cambridge UK.

43. Salama, M.M., (2000), "Sand Production Management" , *Journal of Energy Resources Technology*, Vol. 122, pp. 29-33.

44. Salama, M. M., and Venkatesh, E. S., (1983), ''Evaluation of API RP 14E Erosional Velocity Limitations for Offshore Gas Wells,'' *Proc., 15th Offshore Technology Conference*, Paper OTC 4485

45. Shirazi, S. A., McLaury, B. S., Shadley, J. R., and Rybicki, E. F., (1995) ''Generalization of the API RP 14E Guidelines for Erosive Services,'' *J. Pet. Technol.*, 47, No. 8, pp. 693–698

46. Shook, C.A. and Roco, M.C., (1991), "*Slurry Flow – Principles and Practice"*, Butterworth-Heinemann series in chemical engineering, pp. 116-118

47. Shook, C. A., Schriek, W., Smith, L. G., and Husband, W. H. W, (1973), "*Experimental Studies of the Transport of Sands in Liquids of Varying Properties in 2- and 4-inch Pipelines*". Report E73-20, Saskatchewan Research Council, Saskatoon, Sask., Canada, November.

48. Spedding, P. L., Spence, D. R., (1993), "Flow Regimes in Two-phase Gas-liquid Flow", *Int. J. Multiphase Flow*, Vol. 19, 2, pp. 245-280.

49. Spells, K. E., (1955), "Correlations for Use in Transport of Aqueous Suspensions of Fine Solids through Pipes," Trans. Instn. Chem. Engrs., Vol. 33, pp. 79-84.

50. Sinclair, C.G., (1962), "The Limit Deposit-Velocity of Heterogeneous Suspension", *Proceeding of the Symposium on Interaction between Fluids and Particles*, European Federation of Chemical Engineers, London, England, June, pp.26-29.

51. Smith, L. G., Haas, D. B., Schriek, W., and Husband, W. H., (1973), "*Experimental Studies on the Hydraulic Transport of Potash*". Report E73-16, Saskatchewan Research Council, Saskatoon, Sask., Canada, October.

52. Smith, R. A., (1955), "Experiments on the Flow of Sand-water Slurries in Horizontal Pipes", *Trans. Inst. Chem. Engrs.*, Vol. 33, pp. 85-92

53. Stevenson, P. and Preston, A.P., (1996), "*Sand Transport in Pipes in Inclined Slug Flow - Pt. II Project Report",* Dept. Chem. Eng., University of Cambridge.

54. Stevenson, P., Thorpe, R.B., Kennedy, J.E. and McDermott C., (2001), "The Similarity of Sand Transport by Slug Flow and Hydraulic Conveying", *Proc. 10 th Int. Conf. On Multiphase Flow*, B.H.R. Group, Cannes, France, pp. 13-15

55. Stevenson, P., (2001), "*Particle Transport in Pipes by Two-phase Flows"*, Ph.D. Thesis, University of Cambridge, Cambridge UK.

56. Stevenson, P., Thorpe, R.B., Kennedy, J.E. and McDermott, C., (2001a), "The Similarity of Sand Transport by Slug Flow and Hydraulic Conveying", *Proceedings of 10th Int. Conf. on Multiphase Flow*, bHRA, France, pp. 249-260.

57. Stevenson, P., Thorpe, R.B., Kennedy, J.E. and McDermott, C., (2001b), "The Transport of Particles at Low Loading in Near-horizontal Pipes by Intermittent Flow", *Chem. Eng. Sci.*, Vol. 56, pp. 2149-59.

58. Stevenson, P., Thorpe, R.B., (2002), "Velocity of Isolated Particles along a Pipe in Smooth Stratified Gas Liquid Flow", *AIChE J.*, Vol. 48, 5, pp. 963-969.

59. Stevenson, P., Thorpe, R.B., (2003), "Energy Dissipation at the Slug Nose and the Modeling of Solids Transport in Intermittent Flow", *J. Can. Chem. Eng,* Vol. 81, pp. 271-278.

60. Taitel, Y. and Dukler, A.E., (1976), "A Model for Predicting Flow Regime Transitions in Horizontal and Near Horizontal Gas–Liquid Flow", *AIChE J.*, Vol. 22, pp. 47–55.

61. Thomas, D.G. (1961), "Transport Characteristics of suspensions Part Ⅱ. Minimum Transport Velocity of Flocculated Suspensions in Horizontal Pipes", *AIChE J.*, Vol. 7, 3, 423-430.

62. Thomas, D.G. (1962), "Transport Characteristics of suspensions Part VI. Minimum Transport Velocity of Large Particle Size Suspensions in Round Horizontal Pipes", *AIChE J.*, Vol. 8, 3, 373-377.

63. Thomas, D.G. (1964), "Transport Characteristics of suspensions Part IX. The representation of Periodic Phenomena on a Flow Regime Diagram for Dilute Suspension Transport", *AIChE J.*, Vol. 10, 3, pp 303-308.

64. Thomas J. Danielson, (2007), "Sand Transport Modeling in Multiphase Pipelines", *Offshore Technology Conference*, OTC paper 18691.

65. Wani, G. A., Sarkar, M. K. and Mani, B. P., (1982), "Critical Velocity in Multisize Particle Transportation through Horizontal Pipes", *Journal of Pipelines,* Vol. 2, 1, pp. 57-62.

66. Wasp, E.J., Aude,T.C., Kenny, J.P., Seiter, R.H., Jacques, R.B., (1970) ,"Deposition Velocities, Transition Velocities and Spatial Distribution of Solids in Slurry Pipelines", *Proceedings of Hydrotransport 1*, bHRA Fluid Engineering, Cranfield, Bedford, England, Paper H4.

67. Weisman, J., (1963), "Minimum Power Requirements for Slurry Transport," *American Institute of Chemical Engineers Journal*, January.

68. Whitfield Jennifer, (2009), "*Sand Transport in Multiphase Flow*", BP Internal Communication.

69. Wicks, M., (1971), "Transport of Solids at Low Concentrations in Horizontal Pipes", In Zandi, I (Ed.), *Advances in Solid-Liquid Flow in Pipes and its Applications*, Pergamon Press, pp.101-123.

70. W.Yan, S.Al-lababidi, H. Yeung, "*Sand Transportation in Multiphase Pipelines"*, BP Project Report (submitted to EPTG, BP Exploration, Sunbury, UK), Report Number 09/HY/540, 2009

71. Yotsukura, N., (1961), "*Sediment Transport in a Pipe*", PhD Thesis, Colorado State University at Fort Collins, Colo.

72. Yufin, A. P., (1949), "Izvest. Akad. Nauk. Uzbekh. S.S.R.", *Ser. Tekh. Nauk*. No. 8, pp. 1146 .

73. Zandi, I., Haydon, J. A., (1971), "A Pneumo Slurry System of Collecting and Removing Solids Waste", In Zandi, I (Ed.), *Advances in Solid-Liquid Flow in Pipes and its Applications*, Pergamon Press.

74. Zandi, I., and Govatos, G., (1967), "Heterogeneous Flow of Solids in Pipelines," Journal of the Hydrualics Division, ASCE, Vol.93, No.HY3, Proc.Paper 5244, May, pp.145-159

Appendix A: Sand Transport Behaviour in 2-inch, 3-inch and 4-inch Rig

Table 32: Sand behaviour in water flow in 2 inch horizontal pipeline

V_L	Sand Behaviour (Observations)		
$m \cdot s^{-1}$	15lb/1000bbl	200lb/1000bbl	500lb/1000bbl
1	Sand transported in form of streaks	Sand transported in form of streaks	Sand transported in form of streaks
0.95	Sand transported in form of streaks	Sand transported in form of streaks	Sand transported in form of streaks
0.9	Sand transported in form of streaks	Sand transported in form of streaks	Sand transported in form of streaks
0.85	Sand transported in form of streaks	Sand transported in form of streaks	Sand transported in form of streaks
0.8	Sand transported in form of streaks	Sand transported in form of streaks	Sand transported in form of streaks
0.75	Sand transported in form of streaks	Sand transported in form of streaks	**Sand transported in form of streaks (MTC)**
0.7	Sand transported in form of streaks	**Sand transported in form of streaks (MTC)**	
0.65	Sand transported in form of streaks		
0.6	Sand transported in form of streaks		Sliding sand layer
0.55	Sand transported in form of streaks	Scouring sand dunes	Scouring sand dunes
0.5	**Sand transported in form of streaks (MTC)**	Scouring sand dunes	Scouring sand dunes
0.45		Scouring sand dunes	Scouring sand dunes
0.4	Scouring sand dunes	Scouring sand dunes	Scouring sand dunes
0.35	Scouring sand dunes	Scouring sand dunes	Scouring sand dunes
0.3	Scouring sand dunes with less particles moving	Scouring sand dunes with less particles moving	Scouring sand dunes with less particles moving
0.25	Less particles moving	Less particles moving	Less particles moving
0.2	Less particles moving	Less particles moving	Less particles moving
0.15	Few particles moving	Few particles moving	Few particles moving

Table 33: Sand behaviour in water flow in 2 inch +5 degree pipeline

V_L	Sand Behaviour (Observations)		
$m \cdot s^{-1}$	15lb/1000bbl	200lb/1000bbl	500lb/1000bbl
1	Sand transported in form of streaks	Sand transported in form of streaks	Sand transported in form of streaks
0.95	Sand transported in form of streaks	Sand transported in form of streaks	Sand transported in form of streaks
0.9	Sand transported in form of streaks	Sand transported in form of streaks	Sand transported in form of streaks
0.85	Sand transported in form of streaks	Sand transported in form of streaks	Sand transported in form of streaks
0.8	Sand transported in form of streaks	Sand transported in form of streaks	Sand transported in form of streaks
0.75	Sand transported in form of streaks	Sand transported in form of streaks	**Sand transported in form of streaks (MTC)**
0.7	Sand transported in form of streaks	**Sand transported in form of streaks (MTC)**	
0.65	Sand transported in form of streaks		
0.6	Sand transported in form of streaks		Sliding sand layer
0.55	Sand transported in form of streaks	Scouring sand dunes	Scouring sand dunes
0.5	**Sand transported in form of streaks (MTC)**	Scouring sand dunes	Scouring sand dunes
0.45		Scouring sand dunes	Scouring sand dunes
0.4	Scouring sand dunes	Scouring sand dunes	Scouring sand dunes
0.35	Scouring sand dunes	Scouring sand dunes	Scouring sand dunes
0.3	Scouring sand dunes with less particles moving	Scouring sand dunes with less particles moving	Scouring sand dunes with less particles moving
0.25	Less particles moving	Less particles moving	Less particles moving
0.2	Less particles moving	Less particles moving	Less particles moving
0.15	Few particles moving	Few particles moving	Few particles moving
0.1	Few particles moving	Few particles moving	Few particles moving

Table 34: Sand behaviour in water flow in 4 inch horizontal pipeline

V_L	Sand Behaviour (Observations)		
$m \cdot s^{-1}$	15lb/1000bbl	200lb/1000bbl	500lb/1000bbl
1	Sand transported in form of streaks	Sand transported in form of streaks	Sand transported in form of streaks
0.95	Sand transported in form of streaks	Sand transported in form of streaks	Sand transported in form of streaks
0.9	Sand transported in form of streaks	Sand transported in form of streaks	Sand transported in form of streaks
0.85	Sand transported in form of streaks	Sand transported in form of streaks	**Sand transported in form of streaks (MTC)**
0.8	Sand transported in form of streaks	Sand transported in form of streaks	Sand transported in form of streaks
0.75	Sand transported in form of streaks	**Sand transported in form of streaks (MTC)**	**Sand transported in form of streaks (MTC)**
0.7	Sand transported in form of streaks	Sand transported in form of streaks	Sand amount observed decreased due to accumulation upstream
0.65	Sand transported in form of streaks	**Sand transported in form of streaks (MTC)**	Sand amount observed decreased due to accumulation upstream
0.6	**Sand transported in form of streaks (MTC)**	Sand amount observed decreased due to accumulation upstream	Sand amount observed decreased due to accumulation upstream
0.55	Sand transported in form of streaks	Sand amount observed decreased due to accumulation upstream	sliding sand layer observed
0.5	**Sand transported in form of streaks (MTC)**	Sand amount observed decreased due to accumulation upstream	Scouring dunes observed
0.45	Sand amount observed decreased due to accumulation upstream	Scouring dunes observed	Scouring dunes observed
0.4	Sand amount observed decreased due to accumulation upstream	Scouring dunes observed	Scouring dunes observed
0.35	Sand amount observed decreased due to accumulation upstream	Scouring dunes observed	Scouring dunes observed

0.3	Sand amount observed decreased due to accumulation upstream	Stationary sand dunes	Stationary sand dunes
0.25	Few sand particles observed	Stationary sand dunes	Stationary sand dunes
0.2	Few sand particles observed	Stationary sand dunes	Stationary sand dunes
0.15	Few sand particles observed	Stationary sand dunes	Stationary sand dunes
0.1	Few sand particles observed	Stationary sand dunes	Stationary sand dunes

Table 35: Sand behaviour in water flow in 4 inch +5degrees pipeline

V_L	Sand Behaviour (Observations)		
$m \cdot s^{-1}$	15lb/1000bbl	200lb/1000bbl	500lb/1000bbl
1	Sand transported in form of streaks	Sand transported in form of streaks	Sand transported in form of streaks
0.95	Sand transported in form of streaks	Sand transported in form of streaks	Sand transported in form of streaks
0.9	Sand transported in form of streaks	Sand transported in form of streaks	Sand transported in form of streaks
0.85	Sand transported in form of streaks	Sand transported in form of streaks	**Sand transported in form of streaks (MTC)**
0.8	Sand transported in form of streaks	Sand transported in form of streaks	Sand transported in form of streaks
0.75	Sand transported in form of streaks	**Sand transported in form of streaks (MTC)**	**Sand transported in form of streaks (MTC)**
0.7	Sand transported in form of streaks	Sand transported in form of streaks	Sand amount observed decreased due to accumulation upstream
0.65	Sand transported in form of streaks	**Sand transported in form of streaks (MTC)**	Sand amount observed decreased due to accumulation upstream
0.6	**Sand transported in form of streaks (MTC)**	Sand amount observed decreased due to accumulation upstream	Sand amount observed decreased due to accumulation upstream
0.55	Sand transported in form of streaks	Sand amount observed decreased due to accumulation upstream	sliding sand layer observed
0.5	**Sand transported in form of streaks (MTC)**	Sand amount observed decreased due to accumulation upstream	Scouring dunes observed
0.45	Sand amount observed decreased due to accumulation upstream	Scouring dunes observed	Scouring dunes observed
0.4	Sand amount observed decreased due to accumulation upstream	Scouring dunes observed	Scouring dunes observed
0.35	Sand amount observed decreased due to accumulation upstream	Scouring dunes observed	Scouring dunes observed

0.3	Sand amount observed decreased due to accumulation upstream	Stationary sand dunes	Stationary sand dunes
0.25	Few sand particles observed	Stationary sand dunes	Stationary sand dunes
0.2	Few sand particles observed	Stationary sand dunes	Stationary sand dunes
0.15	Few sand particles observed	Stationary sand dunes	Stationary sand dunes
0.1	Few sand particles observed	Stationary sand dunes	Stationary sand dunes

Table 36: Sand behaviour in CMC solution (7cP) in 4 inch horizontal pipeline

V_L	Sand Behaviour (Observations)	
$m \cdot s^{-1}$	50lb/1000bbl	200lb/1000bbl
1	Sand transported in form of streaks	Sand transported in form of streaks
0.95	Sand transported in form of streaks	Sand transported in form of streaks
0.9	Sand transported in form of streaks	Sand transported in form of streaks
0.85	Sand transported in form of streaks	Sand transported in form of streaks, sand were found more concentrated on the pipe bottom
0.8	Sand transported in form of streaks, sand were found more concentrated on the pipe bottom	Sand transported in form of streaks, sand were found more concentrated on the pipe bottom
0.75	Sand transported in form of streaks, sand were found more concentrated on the pipe bottom	**Sand transported in form of streaks, sand were found more concentrated on the pipe bottom (MTC)**
0.7	**Sand transported in form of streaks, sand were found more concentrated on the pipe bottom (MTC)**	Scouring sand dunes were observed
0.65	Sand amount observed were decreased, few sand streaks were observed	Scouring sand dunes were observed, moving very slowly
0.6	Sand dunes were observed, moving very slowly	Scouring sand dunes were observed, moving very slowly
0.55	Sand amount observed were decreased, few sand streaks were observed	Scouring sand dunes were observed, moving very slowly
0.5	Sand dunes were observed, moving very slowly	Scouring sand dunes were observed, moving very slowly
0.45	Sand dunes were observed, moving very slowly	Scouring sand dunes were observed, moving very slowly
0.4	Sand dunes were observed, moving very slowly	Scouring sand dunes were observed, moving very slowly
0.35	Sand dunes were observed, moving very slowly	Scouring sand dunes were observed, moving very slowly

0.3	Stationary sand dunes observed, with few particles moving	Stationary sand dunes observed, with few particles moving
0.25	Stationary sand dunes observed, with few particles moving	Stationary sand dunes observed, with few particles moving
0.2	Stationary sand dunes observed	Stationary sand dunes observed
0.15	Stationary sand dunes observed	Stationary sand dunes observed
0.1	Stationary sand dunes observed	Stationary sand dunes observed

Table 37: Sand behaviour in CMC solution (20cP) in 4 inch horizontal pipeline

V_L	Sand Behaviour (Observations)	
$m \cdot s^{-1}$	50lb/1000bbl	200lb/1000bbl
1	Sand transported in form of streaks	Sand transported in form of streaks
0.95	Sand transported in form of streaks	Sand transported in form of streaks
0.9	Sand transported in form of streaks	Sand transported in form of streaks, sand were found more concentrated on the pipe bottom
0.85	Sand transported in form of streaks, sand were found more concentrated on the pipe bottom	Sand transported in form of streaks, sand were found more concentrated on the pipe bottom
0.8	Sand transported in form of streaks, sand were found more concentrated on the pipe bottom	**Sand transported in form of streaks, sand were found more concentrated on the pipe bottom (MTC)**
0.75	**Sand transported in form of streaks, sand were found more concentrated on the pipe bottom (MTC)**	Big sand dunes observed, dunes were observed connected with each other with sand particles
0.7	Big sand dunes observed, dunes were observed connected with each other with sand particles	Big sand dunes observed, dunes were observed connected with each other with sand particles
0.65	Big sand dunes observed, dunes were observed connected with each other with sand particles	Big sand dunes observed, dunes were observed connected with each other with sand particles
0.6	Big sand dunes observed, dunes were observed connected with each other with sand particles	Big sand dunes observed, dunes were observed connected with each other with sand particles
0.55	Big sand dunes observed, dunes were observed connected with each other with sand particles	Stationary sand dunes observed, with few particles moving
0.5	Big sand dunes observed, dunes were observed connected with each other with sand particles	Stationary sand dunes observed, with few particles moving
0.45	Stationary sand dunes observed, with few particles moving	Stationary sand dunes observed, with few particles moving

0.4	Stationary sand dunes observed, with few particles moving	Stationary sand dunes observed, with few particles moving
0.35	Stationary sand dunes observed, with few particles moving	Stationary sand dunes observed
0.3	Stationary sand dunes observed, with few particles moving	Stationary sand dunes observed
0.25	Stationary sand dunes observed	Stationary sand dunes observed
0.2	Stationary sand dunes observed	Stationary sand dunes observed
0.15	Stationary sand dunes observed	Stationary sand dunes observed
0.1	Stationary sand dunes observed	Stationary sand dunes observed

Table 38: Sand behaviour in oil flow (340cP@ 16 degrees) in 3 inch horizontal pipeline

V_L	Sand Behaviour (Observations)	
$m \cdot s^{-1}$	50lb/1000bbl	200lb/1000bbl
0.35	Sand rolling, sliding and floating towards the downstream	Sand rolling, sliding and floating towards the downstream
0.3	Sand rolling, sliding and floating towards the downstream	Sand rolling, sliding and floating towards the downstream
0.25	Sand rolling, sliding and floating towards the downstream	**Sand rolling, sliding and floating towards the downstream (MTC)**
0.2	Sand rolling, sliding and floating towards the downstream	**Sand rolling, sliding and floating towards the downstream (MTC)**
0.15	Sand rolling, sliding and floating towards the downstream	sand settled on the pipe bottom, stationary bed observed
0.1	**Sand rolling, sliding and floating towards the downstream (MTC)**	sand settled on the pipe bottom, stationary bed observed
0.07	**Sand rolling, sliding and floating towards the downstream (MTC)**	sand settled on the pipe bottom, stationary bed observed

Table 39: Sand behaviour in oil flow (200cP@ 24.7 degrees) in 3 inch horizontal pipeline

V_L	Sand Behaviour (Observations)	
$m \cdot s^{-1}$	50lb/1000bbl	200lb/1000bbl
0.45	Sand rolling, sliding and floating towards the downstream	Sand rolling, sliding and floating towards the downstream
0.4	Sand rolling, sliding and floating towards the downstream	Sand rolling, sliding and floating towards the downstream
0.35	Sand rolling, sliding and floating towards the downstream	**Sand rolling, sliding and floating towards the downstream (MTC)**
0.3	**Sand rolling, sliding and floating towards the downstream (MTC)**	**Sand rolling, sliding and floating towards the downstream (MTC)**
0.25	**Sand rolling, sliding and floating towards the downstream (MTC)**	sand settled on the pipe bottom, stationary bed observed
0.2	sand settled on the pipe bottom, stationary bed observed	sand settled on the pipe bottom, stationary bed observed
0.15	sand settled on the pipe bottom, stationary bed observed	sand settled on the pipe bottom, stationary bed observed
0.1	sand settled on the pipe bottom, stationary bed observed	sand settled on the pipe bottom, stationary bed observed

Table 40: Sand behaviour in oil flow (105cP @ 34.7 degrees) in 3 inch horizontal pipeline

V_L	Sand Behaviour (Observations)	
$m \cdot s^{-1}$	50lb/1000bbl	200lb/1000bbl
0.50	Sand rolling, sliding and floating towards the downstream	Sand rolling, sliding and floating towards the downstream (MTC)
0.45	Sand rolling, sliding and floating towards the downstream	Sand rolling, sliding and floating towards the downstream (MTC)
0.4	Sand rolling, sliding and floating towards the downstream (MTC)	sand settled on the pipe bottom, stationary bed observed
0.35	Sand rolling, sliding and floating towards the downstream (MTC)	sand settled on the pipe bottom, stationary bed observed
0.3	sand settled on the pipe bottom, stationary bed observed	sand settled on the pipe bottom, stationary bed observed
0.25	sand settled on the pipe bottom, stationary bed observed	sand settled on the pipe bottom, stationary bed observed
0.2	sand settled on the pipe bottom, stationary bed observed	sand settled on the pipe bottom, stationary bed observed
0.15	sand settled on the pipe bottom, stationary bed observed	sand settled on the pipe bottom, stationary bed observed
0.1	sand settled on the pipe bottom, stationary bed observed	sand settled on the pipe bottom, stationary bed observed

Table 41: Sand behaviour in stratified and stratified wavy air-water flow in 2 inch rig

Stratified Flow and Stratified Wavy				
V_{SL}	V_{SG}	Flow Regime	Low Sand Concentration	High Sand Concentration
$m \cdot s^{-1}$	$m \cdot s^{-1}$	(Observations)	<100lb/1000bbl	≥100lb/1000bbl
0.07	0	Stratified	Stationary condition	Stationary condition
0.07	1	Stratified	Small sand particles observed creeping or gently rolling	Sand particles were gently creeping or rolling
0.07	2	Stratified	Small sand particles observed creeping or gently rolling	Sand particles were gently creeping or rolling
0.07	3	St Wavy	Streaklines of active sand particles formed, and were moving very slowly	Sand particles were gently creeping or rolling
0.07	4	St Wavy	Sand particles observed to be saltating (MTC)*	Sand particles were gently creeping or rolling
0.07	5	St Wavy	Transport Condition	Sand particles were gently creeping or rolling
0.07	6	St Wavy	Transport Condition	Sand dunes formed
0.07	7	St Wavy	Transport Condition	Sand dunes formed
0.07	8	St Wavy	Transport Condition	Sand dunes formed
0.07	9	St Wavy	Transport Condition	Sliding sand bed (MTC)**
0.07	10	St Wavy	Transport Condition	Active sand particles saltate along the sliding sand bed
0.07	11	St Wavy	Transport Condition	Active sand particles saltate along the sliding sand bed
0.07	12	St Wavy	Transport Condition	Active sand particles saltate along the sliding sand bed
0.07	13	St Wavy	Transport Condition	Active sand particles saltate along the sliding sand bed

(MTC)*: at low sand concentrations, sand particles are *saltating or bouncing* within the liquid film layer
(MTC)**: at high sand concentrations, sand particles moves in form of *sliding sand bed* within the liquid film layer

Table 42: Sand behaviour in slug flow in 2 inch rig

Intermittent Flow				
V_{SL}	**V_{SG}**	**Flow Regime**	**15,50,100,200 and 500lb/1000bbl**	**15,50,100,200 and 500lb/1000bbl**
$m \cdot s^{-1}$	$m \cdot s^{-1}$	**(Observations)**	**Film Zone**	**Slug Body**
0.5	0.5	Slug	Few sand particles move "creep" or "rolling" in the film zone	Sand particles lifted in long turbulent diffusion region
0.5	1	Slug	Sand particles become more energetic and start to transport (MTC)+	Sand particles lifted in long turbulent diffusion region
0.5	1.5	Slug	Sands transport in film zone (active film zone)	Sand particles lifted in long turbulent diffusion region
0.5	2	Slug	Sands transport in film zone (active film zone)	Sand particles lifted in short turbulent diffusion region
0.5	2.5	Slug	Sands transport in film zone (active film zone)	Sand particles lifted in short turbulent diffusion region
0.5	3	Slug	Sands transport in film zone (active film zone)	Sand particles lifted in short turbulent diffusion region
0.5	3.5	Slug	Sands transport in film zone (active film zone)	Sand particles lifted in short turbulent diffusion region
0.5	4	Slug	Sands transport in film zone (active film zone)	Sand particles lifted in shorter turbulent diffusion region
0.5	4.5	Slug	Sands transport in film zone (active film zone)	Sand particles lifted in shorter turbulent diffusion region

(MTC)+: MTC at (V_{SL}=0.5$m \cdot s^{-1}$ and V_{SL}=1 $m \cdot s^{-1}$) is observed for the highest sand concentration of 500lb/1000bbl.

Table 43: Sand behaviour in air-water flow in 4 inch horizontal pipeline (V_{SL}=0.55m·s^{-1})

V_{SL} m·s^{-1}	V_{SG} m·s^{-1}	Flow Regime	Sand Behaviour (Observations)		
			15lb/1000bbl	200lb/1000bbl	500lb/1000bbl
0.55	3	Str+BTS	Sand was energetic to move in both slug body and film region	Sand was energetic to move in both slug body and film region	Sand was energetic to move in both slug body and film region
0.55	2.5	Str+BTS	Sand was energetic to move in both slug body and film region	Sand was energetic to move in both slug body and film region	Sand was energetic to move in both slug body and film region
0.55	2	Str+BTS	Sand was energetic to move in both slug body and film region	Sand was energetic to move in both slug body and film region	Sand was energetic to move in both slug body and film region
0.55	1.5	Slug	Sand was energetic to move in both slug body and film region	Sand was energetic to move in both slug body and film region	Sand was energetic to move in both slug body and film region
0.55	1.2	Slug	Sand was energetic to move in both slug body and film region	Sand was energetic to move in both slug body and film region	Sand was energetic to move in both slug body and film region
0.55	1	Slug	Sand was energetic to move in both slug body and film region	Sand was energetic to move in both slug body and film region	Sand was energetic to move in both slug body and film region
0.55	0.9	Slug	Sand was energetic to move in both slug body and film region	Sand was energetic to move in both slug body and film region	Sand was energetic to move in both slug body and film region
0.55	0.8	Slug	Sand was energetic to move in both slug body and film region	Sand was energetic to move in both slug body and film region	Sand was energetic to move in both slug body and film region
0.55	0.7	Slug	Sand was energetic to move in both slug body and film region	Sand was energetic to move in both slug body and film region	Sand was energetic to move in the slug body
0.55	0.6	Slug	Sand was energetic to move in both slug body and film region	Sand was energetic to move in both slug body and film region	Sand was energetic to move in the slug body
0.55	0.55	Slug	Sand was energetic to move in both slug body and film region	Sand was energetic to move in both slug body and film region	Sand was energetic to move in the slug body
0.55	0.5	Slug	Sand was energetic to move in	Sand was energetic to move in	Sand was energetic to move in the slug

			both slug body and film region	both slug body and film region	body
0.55	0.45	Slug	Sand was energetic to move in both slug body and film region	Sand was energetic to move in both slug body and film region	Sand was energetic to move in the slug body
0.55	0.4	Slug	Sand was energetic to move in both slug body and film region	Sand was energetic to move in both slug body and film region	**Sand was energetic to move in the slug body (MTC,Video)**
0.55	0.35	Slug	Sand was energetic to move in both slug body and film region	Sand was energetic to move in both slug body and film region	Sand amount observed decreased, indicating accumulation started upstream
0.55	0.3	Slug	Sand was energetic to move in both slug body and film region	Sand was energetic to move in both slug body and film region	Sand amount observed decreased, indicating accumulation started upstream
0.55	0.25	Slug	Sand was energetic to move in both slug body and film region	Sand was energetic to move in both slug body and film region	Sand amount observed decreased, indicating accumulation started upstream
0.55	0.2	Slug	Sand was energetic to move in both slug body and film region	**Sand was energetic to move in both slug body and film region (MTC)**	Sand amount observed decreased, indicating accumulation started upstream
0.55	0.15	Slug	Sand was energetic to move in both slug body and film region	Sand amount observed decreased, indicating accumulation started upstream	Sand amount observed decreased, indicating accumulation started upstream
0.55	0.1	Str+IW	Sand was energetic to move in the body of inertial wave	Sand amount observed decreased, indicating accumulation started upstream	Sand amount observed decreased, indicating accumulation started upstream
0.55	0.05	Str+IW	Sand was energetic to move in the body of inertial wave	Sand amount observed decreased, indicating accumulation started upstream	Sand amount observed decreased, indicating accumulation started upstream
0.55	0.02	Str+IW	**Sand was energetic to move in the body of inertial wave (MTC)**	Sand amount observed decreased, indicating accumulation started upstream	Sand amount observed decreased, indicating accumulation started upstream

Table 44: Sand behaviour in air-water flow in 4 inch horizontal pipeline (V_{SL}=0.45m·s^{-1})

0.45	3	Str+BTS	Sand was energetic to move in both slug body and film region	Sand was energetic to move in both slug body and film region	Sand was energetic to move in both slug body and film region
0.45	2.5	Str+BTS	Sand was energetic to move in both slug body and film region	Sand was energetic to move in both slug body and film region	Sand was energetic to move in both slug body and film region
0.45	2	Str+BTS	Sand was energetic to move in both slug body and film region	Sand was energetic to move in both slug body and film region	Sand was energetic to move in both slug body and film region
0.45	1.5	Slug	Sand was energetic to move in both slug body and film region	Sand was energetic to move in both slug body and film region	Sand was energetic to move in both slug body and film region
0.45	1.2	Slug	Sand was energetic to move in both slug body and film region	Sand was energetic to move in both slug body and film region	Sand was energetic to move in both slug body and film region
0.45	1	Slug	Sand was energetic to move in both slug body and film region	Sand was energetic to move in both slug body and film region	Sand was energetic to move in both slug body and film region
0.45	0.9	Slug	Sand was energetic to move in both slug body and film region	Sand was energetic to move in both slug body and film region	Sand was energetic to move in both slug body and film region
0.45	0.8	Slug	Sand was energetic to move in both slug body and film region	Sand was energetic to move in both slug body and film region	Sand was energetic to move in the slug body
0.45	0.7	Slug	Sand was energetic to move in both slug body and film region	Sand was energetic to move in both slug body and film region	Sand was energetic to move in the slug body
0.45	0.6	Slug	Sand was energetic to move in both slug body and film region	Sand was energetic to move in both slug body and film region	Sand was energetic to move in the slug body
0.45	0.55	Slug	Sand was energetic to move in both slug body and film region	Sand was energetic to move in both slug body and film region	Sand was energetic to move in the slug body
0.45	0.5	Slug	Sand was energetic to move in both slug body and film region	Sand was energetic to move in both slug body and film region	**Sand was energetic to move in the slug body (MTC)**
0.45	0.45	Slug	Sand was energetic to move in both slug body and film region	Sand was energetic to move in both slug body and film region	Sand was observed forming a sliding layer

0.45	0.4	Slug	Sand was energetic to move in both slug body and film region	Sand was energetic to move in the slug body	Sand was observed forming a sliding layer
0.45	0.35	Slug	Sand was energetic to move in both slug body and film region	**Sand was energetic to move in the slug body (MTC)**	Sand was observed forming a sliding layer
0.45	0.3	Slug	Sand was energetic to move in both slug body and film region	Sand amount observed decreased, indicating accumulation started upstream	Sand was observed forming a sliding layer
0.45	0.25	Slug	Sand was energetic to move in both slug body and film region	Sand amount observed decreased, indicating accumulation started upstream	Sand was observed forming a sliding layer
0.45	0.2	Slug	Sand was energetic to move in both slug body and film region	Sand amount observed decreased, indicating accumulation started upstream	Sand was observed forming a sliding layer
0.45	0.15	Slug	Sand was energetic to move in both slug body and film region	Sand amount observed decreased, indicating accumulation started upstream	a stationary sand layer observed
0.45	0.1	Str+IW	**Sand was energetic to move in the body of inertial wave (MTC)**	Sand amount observed decreased, indicating accumulation started upstream	a stationary sand layer observed
0.45	0.05	Str+IW	Sand amount observed decreased, indicating accumulation started upstream	Sand amount observed decreased, indicating accumulation started upstream	a stationary sand layer observed
0.45	0.02	Str+IW	Sand amount observed decreased, indicating accumulation started upstream	Sand amount observed decreased, indicating accumulation started upstream	a stationary sand layer observed

Table 45: Sand behaviour in air-water flow in 4 inch horizontal pipeline (V_{SL}=0.35m·s^{-1})

V_{SL} m·s^{-1}	V_{SG} m·s^{-1}	Flow Regime	Sand Behaviour (Observations)		
			15lb/1000bbl	200lb/1000bbl	500lb/1000bbl
0.35	3	Str+BTS	Sand was energetic to move in both slug body and film region	Sand was energetic to move in both slug body and film region	Sand was energetic to move in both slug body and film region
0.35	2.5	Str+BTS	Sand was energetic to move in both slug body and film region	Sand was energetic to move in both slug body and film region	Sand was energetic to move in both slug body and film region
0.35	2	Str+BTS	Sand was energetic to move in both slug body and film region	Sand was energetic to move in both slug body and film region	Sand was energetic to move in both slug body and film region
0.35	1.5	Slug	Sand was energetic to move in both slug body and film region	Sand was energetic to move in both slug body and film region	Sand was energetic to move in the slug body
0.35	1.2	Slug	Sand was energetic to move in both slug body and film region	Sand was energetic to move in both slug body and film region	Sand was energetic to move in the slug body
0.35	1	Slug	Sand was energetic to move in both slug body and film region	Sand was energetic to move in both slug body and film region	Sand was energetic to move in the slug body
0.35	0.9	Slug	Sand was energetic to move in both slug body and film region	Sand was energetic to move in the slug body	**Sand was energetic to move in the slug body (MTC)**
0.35	0.8	Slug	Sand was energetic to move in both slug body and film region	**Sand was energetic to move in the slug body (MTC)**	Sand amount observed decreased, indicating accumulation started upstream
0.35	0.7	Slug	Sand was energetic to move in both slug body and film region	Sand amount observed decreased, indicating accumulation started upstream	Sand amount observed decreased, indicating accumulation started upstream
0.35	0.6	Slug	Sand was energetic to move in both slug body and film region	Sand amount observed decreased, indicating accumulation started upstream	Sand amount observed decreased, indicating accumulation started upstream
0.35	0.55	Slug	Sand was energetic to move in both slug body and film region	Sand amount observed decreased, indicating	Sand amount observed decreased, indicating accumulation started

				accumulation started upstream	upstream
0.35	0.5	Slug	Sand was energetic to move in both slug body and film region	Sand amount observed decreased, indicating accumulation started upstream	Sand amount observed decreased, indicating accumulation started upstream
0.35	0.45	Slug	Sand was energetic to move in both slug body and film region	Sand amount observed decreased, indicating accumulation started upstream	Sand amount observed decreased, indicating accumulation started upstream
0.35	0.4	Slug	Sand was energetic to move in both slug body and film region	Sand amount observed decreased, indicating accumulation started upstream	Sand amount observed decreased, indicating accumulation started upstream
0.35	0.35	Slug	Sand was energetic to move in both slug body and film region	Sand amount observed decreased, indicating accumulation started upstream	Sand amount observed decreased, indicating accumulation started upstream
0.35	0.3	Slug	**Sand was energetic to move in both slug body and film region (MTC)**	Sand amount observed decreased, indicating accumulation started upstream	Sand amount observed decreased, indicating accumulation started upstream
0.35	0.25	Slug	Sand amount observed decreased with low slug frequency	Sand amount observed decreased, indicating accumulation started upstream	Sand amount observed decreased, indicating accumulation started upstream
0.35	0.2	Slug	Sand amount observed decreased with low slug frequency	Sand amount observed decreased, indicating accumulation started upstream	Sand amount observed decreased, indicating accumulation started upstream
0.35	0.15	Slug	Sand amount observed decreased with low slug frequency	Sand amount observed decreased, indicating accumulation started upstream	Sand amount observed decreased, indicating accumulation started upstream
0.35	0.1	Str+R	Sand amount observed decreased, indicating accumulation started upstream	Sand amount observed decreased, indicating accumulation started upstream	Sand amount observed decreased, indicating accumulation started upstream
0.35	0.05	Str+R	Sand amount observed decreased, indicating	Sand amount observed decreased, indicating	Sand amount observed decreased, indicating accumulation started

			accumulation started upstream	accumulation started upstream	upstream
0.35	0.02	Str+R	Sand amount observed decreased, indicating accumulation started upstream	Sand amount observed decreased, indicating accumulation started upstream	Sand amount observed decreased, indicating accumulation started upstream

Table 46: Sand behaviour in air-water flow in 4 inch horizontal pipeline (V_{SL}=0.25m·s^{-1})

V_{SL} m·s^{-1}	V_{SG} m·s^{-1}	Flow Regime	Sand Behaviour (Observations)		
			15lb/1000bbl	200lb/1000bbl	500lb/1000bbl
0.25	3	Str+LRW	Sand was energetic to move in the body and film region of large roll wave	Sand was energetic to move in both slug body and film region	Sand was energetic to move in the body of large roll wave
0.25	2.5	Str+LRW	Sand was energetic to move in the body and film region of large roll wave	Sand was energetic to move in both slug body and film region	Sand was energetic to move in the body of large roll wave
0.25	2	Str+LRW	Sand was energetic to move in the body and film region of large roll wave	Sand was energetic to move in both slug body and film region	Sand was energetic to move in the body of large roll wave
0.25	1.5	Str+LRW	Sand was energetic to move in both slug body and film region	Sand was energetic to move in both slug body and film region	**Sand was energetic to move in the body of slug (MTC)**
0.25	1.2	Str+LRW	Sand was energetic to move in both slug body and film region	**Sand was energetic to move in the slug body (MTC)**	Sand amount observed decreased, indicating accumulation started upstream
0.25	1	Slug	Sand was energetic to move in the body and film region of roll wave	Sand amount observed decreased, indicating accumulation started upstream	Sand amount observed decreased, indicating accumulation started upstream
0.25	0.9	Slug	Sand was energetic to move in the body and film region of roll wave	Sand amount observed decreased, indicating accumulation started upstream	Sand amount observed decreased, indicating accumulation started upstream
0.25	0.8	Str+RW	Sand was energetic to move in the body of roll wave	Sand amount observed decreased, indicating accumulation started upstream	Sand amount observed decreased, indicating accumulation started upstream
0.25	0.7	Str+RW	**Sand was energetic to move in the body of roll wave**	Sand amount observed decreased, indicating	Sand amount observed decreased, indicating accumulation started

			(MTC)	accumulation started upstream	upstream
0.25	0.6	Str+R	Sand amount observed decreased, indicating accumulation started upstream	Sand amount observed decreased, indicating accumulation started upstream	Sand amount observed decreased, indicating accumulation started upstream
0.25	0.55	Str+R	Sand amount observed decreased, indicating accumulation started upstream	Sand amount observed decreased, indicating accumulation started upstream	Sand amount observed decreased, indicating accumulation started upstream
0.25	0.5	Str+R	Sand amount observed decreased, indicating accumulation started upstream	Sand amount observed decreased, indicating accumulation started upstream	Sand amount observed decreased, indicating accumulation started upstream
0.25	0.45	Str+R	Sand amount observed decreased, indicating accumulation started upstream	Sand amount observed decreased, indicating accumulation started upstream	Sand amount observed decreased, indicating accumulation started upstream
0.25	0.4	Str+R	Sand amount observed decreased, indicating accumulation started upstream	Sand amount observed decreased, indicating accumulation started upstream	Sand amount observed decreased, indicating accumulation started upstream
0.25	0.35	Str+R	Sand amount observed decreased, indicating accumulation started upstream	Sand amount observed decreased, indicating accumulation started upstream	Sand amount observed decreased, indicating accumulation started upstream
0.25	0.3	Str+R	Sand amount observed decreased, indicating accumulation started upstream	Sand amount observed decreased, indicating accumulation started upstream	Sand amount observed decreased, indicating accumulation started upstream
0.25	0.25	Str+R	Sand amount observed decreased, indicating accumulation started upstream	Sand amount observed decreased, indicating accumulation started upstream	Sand amount observed decreased, indicating accumulation started upstream
0.25	0.2	Str+R	Sand amount observed decreased, indicating accumulation started upstream	Sand amount observed decreased, indicating accumulation started upstream	Sand amount observed decreased, indicating accumulation started upstream
0.25	0.15	Str+R	Sand amount observed	Sand amount observed	Sand amount observed decreased,

			decreased, indicating accumulation started upstream	decreased, indicating accumulation started upstream	indicating accumulation started upstream
0.25	0.1	Str	Sand amount observed decreased, indicating accumulation started upstream	Sand amount observed decreased, indicating accumulation started upstream	Sand amount observed decreased, indicating accumulation started upstream
0.25	0.05	Str	Sand amount observed decreased, indicating accumulation started upstream	Sand amount observed decreased, indicating accumulation started upstream	Sand amount observed decreased, indicating accumulation started upstream
0.25	0.02	Str	Sand amount observed decreased, indicating accumulation started upstream	Sand amount observed decreased, indicating accumulation started upstream	Sand amount observed decreased, indicating accumulation started upstream

Table 47: Sand behaviour in air-water flow in 4 inch horizontal pipeline (V_{SL}=0.15m·s^{-1})

V_{SL} m·s^{-1}	V_{SG} m·s^{-1}	Flow Regime	Sand Behaviour (Observations)		
			15lb/1000bbl	200lb/1000bbl	500lb/1000bbl
0.15	3	Str+RW	Sand was energetic to move in the body and film region of roll wave	Sand was energetic to move in the body and film region of roll wave	**Sand was energetic to move in the body of roll wave (MTC)**
0.15	2.5	Str+RW	Sand was energetic to move in the body and film region of roll wave	**Sand was energetic to move in the body of roll wave (MTC)**	Sand was observed forming a sliding layer
0.15	2	Str+RW	Sand was energetic to move in the body of roll wave	Sand amount observed decreased, indicating accumulation started upstream	Sand was observed forming a sliding layer
0.15	1.5	Str+RW	**Sand was energetic to move in the body of roll wave (MTC)**	Sand was observed forming a sliding layer	Sand was observed forming a sliding layer
0.15	1.2	Str+RW	Sand amount observed decreased, indicating accumulation started upstream	Sand was observed forming a sliding layer	Sand was observed forming a sliding layer
0.15	1	Str+RW	Sand amount observed decreased, indicating accumulation started upstream	Sand was observed forming a sliding layer	Sand was observed forming a sliding layer
0.15	0.9	Str+RW	Sand amount observed decreased, indicating accumulation started upstream	Sand was observed forming a sliding layer	Sand was observed forming a sliding layer
0.15	0.8	Str+RW	Sand amount observed decreased, indicating accumulation started upstream	Sand was observed forming a sliding layer	Sand was observed forming a sliding layer

0.15	0.7	Str+RW	Sand amount observed decreased, indicating accumulation started upstream	Sand was observed forming a sliding layer	Big sand dunes observed
0.15	0.6	Str+R	Sand amount observed decreased, indicating accumulation started upstream	Sand was observed forming a sliding layer	Big sand dunes observed
0.15	0.55	Str+R	Sand amount observed decreased, indicating accumulation started upstream	Sand was observed forming a sliding layer	Big sand dunes observed
0.15	0.5	Str+R	Sand amount observed decreased, indicating accumulation started upstream	Sand amount observed decreased, indicating accumulation started upstream	Stantionary dunes observed
0.15	0.45	Str+R	Sand amount observed decreased, indicating accumulation started upstream	Sand amount observed decreased, indicating accumulation started upstream	Stantionary dunes observed
0.15	0.4	Str+R	Sand amount observed decreased, indicating accumulation started upstream	Sand amount observed decreased, indicating accumulation started upstream	Stantionary dunes observed
0.15	0.35	Str	Sand amount observed decreased, indicating accumulation started upstream	a stationary sand layer observed	Stantionary dunes observed
0.15	0.3	Str	Sand amount observed decreased, indicating accumulation started upstream	a stationary sand layer observed	Stantionary dunes observed
0.15	0.25	Str	Sand amount observed decreased, indicating accumulation started upstream	a stationary sand layer observed	Stantionary dunes observed
0.15	0.2	Str	Sand amount observed decreased, indicating accumulation started upstream	a stationary sand layer observed	Stantionary dunes observed

0.15	0.15	Str	Sand amount observed decreased, indicating accumulation started upstream	a stationary sand layer observed	Stantionary dunes observed
0.15	0.1	Str	Sand amount observed decreased, indicating accumulation started upstream	a stationary sand layer observed	Stantionary dunes observed
0.15	0.05	Str	Sand amount observed decreased, indicating accumulation started upstream	a stationary sand layer observed	Stantionary dunes observed
0.15	0.02	Str	Sand amount observed decreased, indicating accumulation started upstream	a stationary sand layer observed	Stantionary dunes observed

Table 48: Sand behaviour in air-water flow in 4 inch +5degrees pipeline (V_{SL}=0.55m·s^{-1})

V_{SL}	V_{SG}	Flow Regime	Sand Behaviour (Observations)	
m·s^{-1}	m·s^{-1}		15lb/1000bbl	500lb/1000bbl
0.55	3	Slug	Sand transported in slug body	
0.55	2.5	Slug	Sand transported in slug body	
0.55	2	Slug	Sand transported in slug body, and falling backwards in the film region	Sand transported in slug body, and falling backwards in the film region
0.55	1.5	Slug	Sand transported in slug body, and falling backwards in the film region	Sand transported in slug body, and falling backwards in the film region
0.55	1.2	Slug	Sand transported in slug body, and falling backwards in the film region	Sand transported in slug body, and falling backwards in the film region
0.55	1	Slug	Sand transported in slug body, and falling backwards in the film region	Sand transported in slug body, and falling backwards in the film region
0.55	0.9	Slug	Sand transported in slug body, and falling backwards in the film region	Sand transported in slug body, and falling backwards in the film region
0.55	0.8	Slug	Sand transported in slug body, and falling backwards in the film region	Sand transported in slug body, and falling backwards in the film region
0.55	0.7	Slug	Sand transported in slug body	Sand transported in slug body, and falling backwards in the film region
0.55	0.6	Slug	Sand transported in slug body, and falling backwards in the film region	Sand transported in slug body, and falling backwards in the film region
0.55	0.55	Slug	Sand transported in slug body, and falling backwards in the film region	Sand transported in slug body, and falling backwards in the film region
0.55	0.5	Slug	Sand transported in slug body, and falling backwards in the film region	Sand transported in slug body, and falling backwards in the film region
0.55	0.45	Slug	Sand transported in slug body, and falling backwards in the film region	Sand transported in slug body, and falling backwards in the film region

0.55	0.4	Plug	Sand transported in plug body	Sand transported in slug body, and falling backwards in the film region
0.55	0.35	Plug	Sand transported in plug body	Sand transported in slug body, and falling backwards in the film region
0.55	0.3	Plug	Sand transported in plug body	Sand transported in slug body, and falling backwards in the film region
0.55	0.25	Plug	Sand transported in plug body	Sand transported in slug body, and falling backwards in the film region
0.55	0.2	Plug	Sand transported in plug body	Sand transported in plug body
0.55	0.15	Plug	Sand transported in plug body	Sand transported in plug body
0.55	0.1	Plug	Sand transported in plug body	Sand transported in plug body
0.55	0.05	Plug	Sand transported in plug body	**Sand transported in plug body (MTC)**
0.55	0.02	Plug	**Sand transported in plug body (MTC)**	Sand amount observed decreased, indicating accumulation started upstream

Table 49: Sand behaviour in air-water flow in 4 inch +5degrees pipeline (V_{SL}=0.35m·s^{-1})

V_{SL}	V_{SG}	Flow Regime	Sand Behaviour (Observations)	
m·s^{-1}	m·s^{-1}		15lb/1000bbl	500lb/1000bbl
0.35	3	Slug	Sand transported in slug body	Sand transported in slug body
0.35	2.5	Slug	Sand transported in slug body	Sand transported in slug body
0.35	2	Slug	Sand transported in slug body, and falling backwards in the film region	Sand transported in slug body, and falling backwards in the film region
0.35	1.5	Slug	Sand transported in slug body, and falling backwards in the film region	Sand transported in slug body, and falling backwards in the film region
0.35	1.2	Slug	Sand transported in slug body, and falling backwards in the film region	Sand transported in slug body, and falling backwards in the film region
0.35	1	Slug	Sand transported in slug body, and falling backwards in the film region	Sand transported in slug body, and falling backwards in the film region
0.35	0.9	Slug	Sand transported in slug body, and falling backwards in the film region	Sand transported in slug body, and falling backwards in the film region
0.35	0.8	Slug	Sand transported in slug body	Sand transported in slug body, and falling backwards in the film region
0.35	0.7	Slug	Sand transported in slug body	Sand transported in slug body
0.35	0.6	Slug	Sand transported in slug body, and falling backwards in the film region	Sand transported in slug body, and falling backwards in the film region
0.35	0.55	Slug	Sand transported in slug body, and falling backwards in the film region	Sand transported in slug body, and falling backwards in the film region
0.35	0.5	Slug	Sand transported in slug body, and falling backwards in the film region	Sand transported in slug body, and falling backwards in the film region
0.35	0.45	Slug	Sand transported in slug body, and falling backwards in the film region	Sand transported in slug body, and falling backwards in the film region

0.35	0.4	Slug	Sand transported in slug body, and falling backwards in the film region	Sand transported in slug body, and falling backwards in the film region
0.35	0.35	Slug	Sand transported in slug body, and falling backwards in the film region	Sand transported in slug body, and falling backwards in the film region
0.35	0.3	Slug	Sand transported in slug body, and falling backwards in the film region	Sand transported in slug body, and falling backwards in the film region
0.35	0.25	Plug	Sand transported in plug body	Sand transported in plug body
0.35	0.2	Plug	Sand transported in plug body	Sand transported in plug body
0.35	0.15	Plug	Sand transported in plug body	**Sand transported in plug body (MTC)**
0.35	0.1	Plug	Sand transported in plug body	Sand settled at the bottom of the pipe
0.35	0.05	Plug	**Sand transported in plug body (MTC)**	Sand settled at the bottom of the pipe
0.35	0.02	Plug	Sand settled at the bottom of the pipe	Sand settled at the bottom of the pipe

Table 50: Sand behaviour in air-water flow in 4 inch +5degrees pipeline (V_{SL}=0.15m·s^{-1})

V_{SL}	V_{SG}	Flow Regime	Sand Behaviour (Observations)	
m·s^{-1}	m·s^{-1}		15lb/1000bbl	500lb/1000bbl
0.15	3	Slug	Sand transported in slug body	Sand transported in slug body
0.15	2.5	Slug	Sand transported in slug body	Sand transported in slug body
0.15	2	Slug	Sand transported in slug body	Sand transported in slug body
0.15	1.5	Slug	Sand transported in slug body, and falling backwards in the film region	Sand transported in slug body, and falling backwards in the film region
0.15	1.2	Slug	Sand transported in slug body, and falling backwards in the film region	Sand transported in slug body, and falling backwards in the film region
0.15	1	Slug	Sand transported in slug body, and falling backwards in the film region	Sand transported in slug body, and falling backwards in the film region
0.15	0.9	Slug	Sand transported in slug body, and falling backwards in the film region	Sand transported in slug body, and falling backwards in the film region
0.15	0.8	Slug	Sand transported in slug body, and falling backwards in the film region	Sand transported in slug body, and falling backwards in the film region
0.15	0.7	Slug	Sand transported in slug body, and falling backwards in the film region	Sand transported in slug body, and falling backwards in the film region
0.15	0.6	Slug	Sand transported in slug body, and falling backwards in the film region	Sand transported in slug body, and falling backwards in the film region
0.15	0.55	Slug	Sand transported in slug body, and falling backwards in the film region	Sand transported in slug body, and falling backwards in the film region
0.15	0.5	Slug	Sand transported in slug body, and falling backwards in the film region	Sand transported in slug body, and falling backwards in the film region
0.15	0.45	Slug	Sand transported in slug body, and falling backwards in the film region	Sand transported in slug body, and falling backwards in the film region

0.15	0.4	Slug	Sand transported in slug body, and falling backwards in the film region	**Sand transported in slug body, and falling backwards in the film region (MTC)**
0.15	0.35	Slug	Sand transported in slug body, and falling backwards in the film region	Sand settled at the bottom of the pipe
0.15	0.3	Slug	Sand transported in slug body, and falling backwards in the film region	Sand settled at the bottom of the pipe
0.15	0.25	Slug	Sand transported in slug body, and falling backwards in the film region	Sand settled at the bottom of the pipe
0.15	0.2	Slug	Sand transported in slug body, and falling backwards in the film region	Sand settled at the bottom of the pipe
0.15	0.15	Plug	Sand transported in plug body	Sand settled at the bottom of the pipe
0.15	0.1	Plug	**Sand transported in plug body (MTC)**	Sand settled at the bottom of the pipe
0.15	0.05	Plug	Sand were found not energetic enough to transport	Sand settled at the bottom of the pipe
0.15	0.02	Plug	Sand were found not energetic enough to transport	Sand settled at the bottom of the pipe

Appendix B: Preliminary Study on Particle Size Effect and Vertical Pipe Orientation Effect

The aim of these preliminary studies was to understand how the particle size would affect the sand transport characteristics and what was the difference in sand behaviour and MTC in vertical and horizontal pipelines. The sand transport characteristics and MTC were obtained only in single phase water flow as a starting point.

- Particle Size Effect on MTC in 4 inch Horizontal Sand-Water Flow

Two types of sieved sand particles were used to investigate the particle size effect: average size 200 microns (180-212 microns) and average size 750 microns (710-800micorns). Figure 118 shows particle size effect on MTC at different sand concentrations.

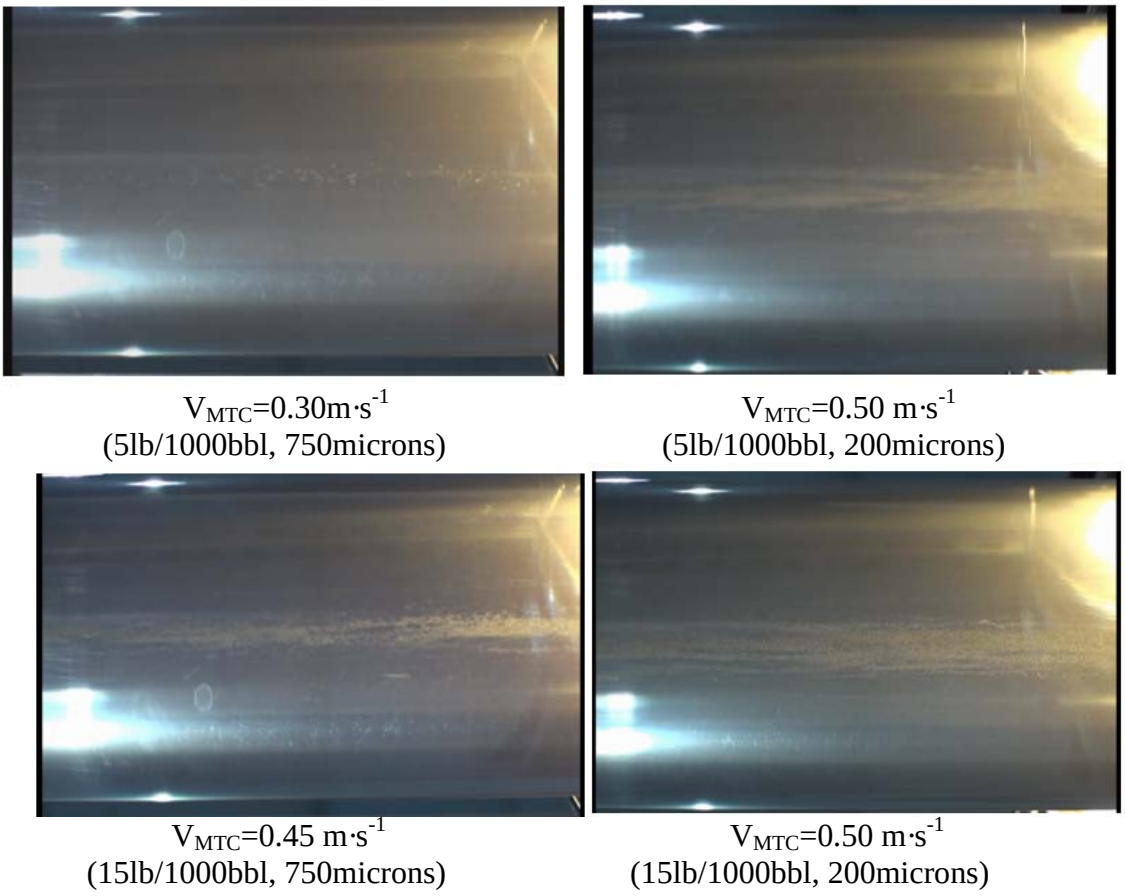

V_{MTC}=0.30m·s^{-1} (5lb/1000bbl, 750microns)

V_{MTC}=0.50 m·s^{-1} (5lb/1000bbl, 200microns)

V_{MTC}=0.45 m·s^{-1} (15lb/1000bbl, 750microns)

V_{MTC}=0.50 m·s^{-1} (15lb/1000bbl, 200microns)

Figure 118: Sand transport characteristics at MTC for sand particles of different size distribution (view from bottom, flow direction left to right)

Table 51: Particle size effect on MTC

Sand Concentration	Particle size (microns)	V_{MTC} ($m \cdot s^{-1}$)
Single Particle	200	0.13-0.16
5lb/1000bbl	200	0.45-0.50
15lb/1000bbl	200	0.45-0.50
Single Particle	750	0.21-0.23
5lb/1000bbl	750	0.25-0.30
15lb/1000bbl	750	0.40-0.45

From Figure 118, it was observed that, for 5lb/1000bbl, lower water velocity was required to transport the bigger sand particles. Only few particles were observed for 750microns sand at MTC, whereas some sand streaks were observed for smaller sand particles. At the same sand concentration, the number of sand particles for 750microns is less than that for 200microns, therefore the particle interactions is less for bigger sand particles. On the other hand, bigger sand particles are likely to stick out the laminar sublayer. As a result, the drag and lift forces induced by vortices in transition or turbulent layer are able to aid the sand transportation.

For 50lb/1000bbl sand concentration, the water velocity at sand MTC for 750microns were found to be close to that for 200microns (Table 51). The sand streaks were observed for both 750microns and 200microns sand, which indicating the sand interactions for 750microns were enhanced due to the increased number of sand particles.

Although higher sand concentrations have not been tested in this work, based on the data from general slurry system practice, it was found that the transport velocity increased as the increase of sand particle size (Section 4.3.5, Figure 13). As a result, it can be concluded that the particle interaction has a significant effect on MTC. However, more work need to done to examine the particle size effect on MTC in air-water flow.

- Sand Transport Characteristics and Particle Size Effect in 4 inch Vertical Sand-Water Flow

The sand transport characteristics were also observed in 4 inch vertical pipeline, as shown in Figure 119.

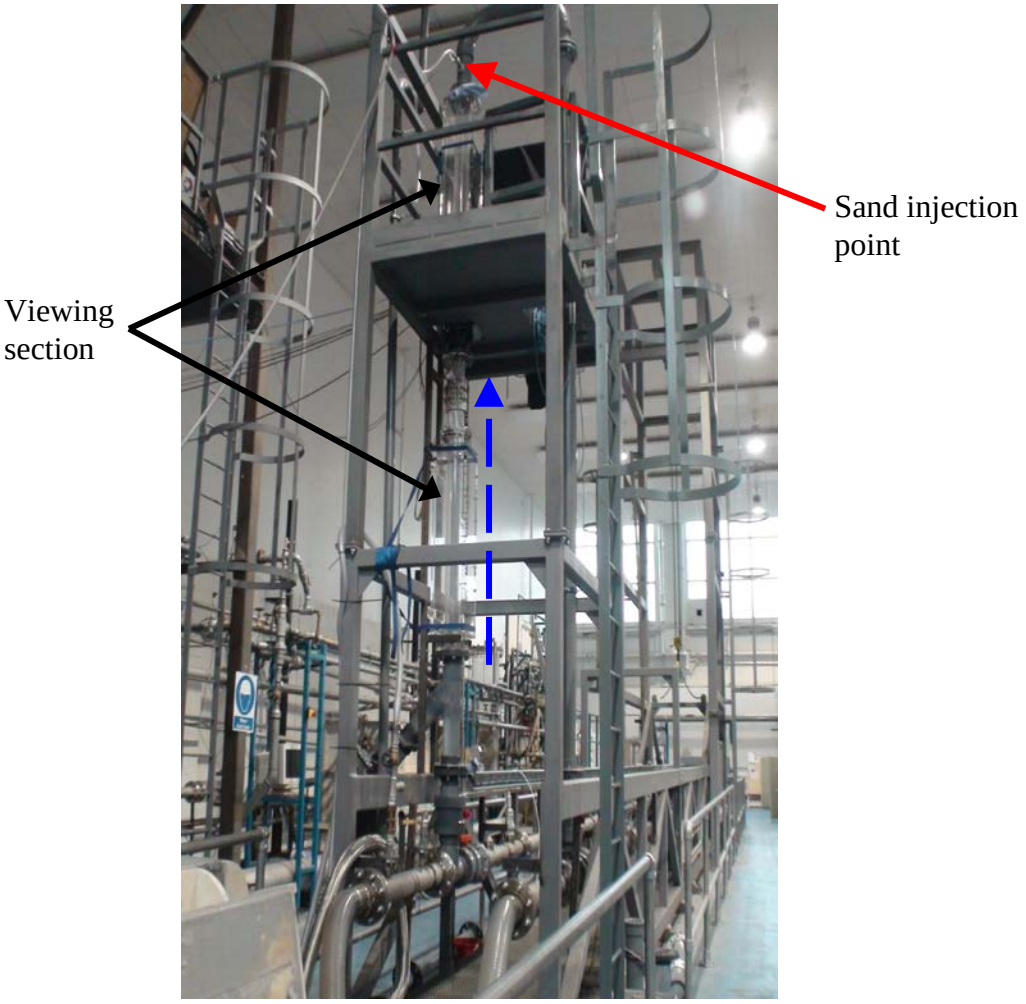

Figure 119: 4 inch sand transportation rig (vertical section)

The sand-water mixture was injected at the top of the vertical section, whereas the main water flow was pumped upwards to lift the sand particles (dashed line with arrow indicating the flow direction). By gently adjusting the water velocity, the sand particles behaviour was observed in two Perspex viewing sections.

The sand-water transport characteristics in a vertical pipeline were found to be different from those in horizontal or inclined pipeline, as shown in Figure 120.

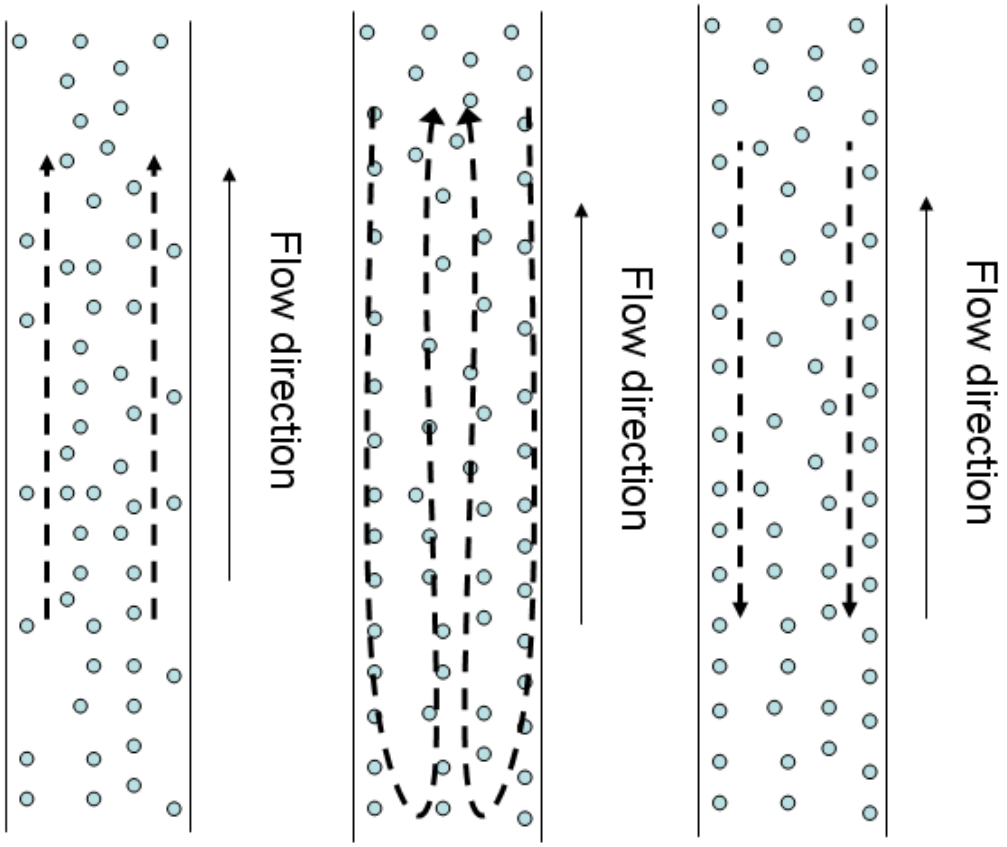

(a) $V_L > V_{MTC}$ (b) $V_L \approx V_{MTC}$ c) $V_L < V_{MTC}$

Figure 120: Sand transport characteristics in vertical water flow (schematic drawing)

In Figure 120, the trajectories of sand particles were indicated by the bold dashed lines with arrows. It was observed that, when $V_L > V_{MTC}$, the majority of sand particles were transported within the core of water flow, few particles were found moving upward slowly close to the pipe wall (Figure 120(a)); When $V_L \approx V_{MTC}$, a "circulation phenomena" was observed (Figure 120(b)). More sand particles were found to be at the vicinity of the pipe wall, falling down instead of moving upward. However, most of the falling sand particles were observed to be lifted by the vortices generated by the turbulence and transported again in the centre of the pipe which is due to the liquid velocity profile near the pipe wall. As reducing the V_L, the "circulation" of the sand particles was also decreased, less sand particles were observed lifted again, and eventually all the sand particles were falling down in the pipe (Figure 120(c)).

For 15lb/1000bbl, the observed MTC in vertical pipe ranged V_{MTC}=0.09 - 0.10 $m \cdot s^{-1}$. Compared to that in horizontal or inclined pipe (V_{MTC}=0.5 - 0.6 $m \cdot s^{-1}$), the sand transportation was found easier in vertical water flow. Although the V_{MTC} was not obtained for higher sand concentration in this work, it can be estimated that V_{MTC} increases with the increase of sand concentration, and the vertical pipe orientation had a positive effect for sand transportation due to this "circulation" phenomena.

Govier and Aziz (1972) commented that the critical transport velocity should be at least two times higher than the terminal settling velocity. Figure 121 shows the comparison

between V_{MTC} and settling velocity in vertical pipeline when using 200 microns and 750 microns sand at 15lb/1000bbl.

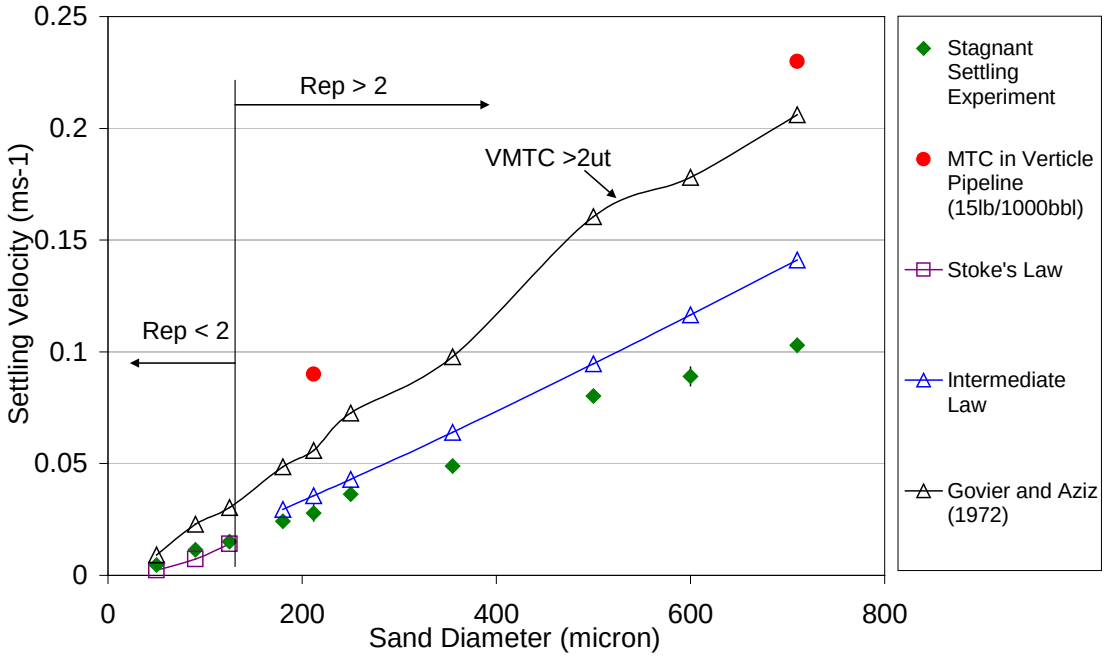

Figure 121: Comparison between V_{MTC} and settling velocity in vertical pipeline

By droping a single particle into the middle of a vertical pipe (ID=0.1m), the settling distance and settling time was measured for different size sand particles in the stagnant settling test, then the terminal settling velocities (u_t) was calculated.

It was found that the settling laws predicted the terminal settling velocity well when d_p was smaller than 350 microns. However, the settling laws were used to predict the well-rounded solid particles, while the shape of bigger sand used in this test was irregular. Therefore, the discrepancy between the predicted and calculated terminal settling velocity was found increased for bigger sand particle (d_p > 350 microns).

Also, the V_{MTC} observed for 200 microns and 750 microns sand was found higher than $2u_t$, which was consistent with the findings from Govier and Aziz (1972). However, comparing to transport velocity in horizontal flows, the V_{MTC} in vertical flows is much lower. In horizontal flow, sand compaction and friction between sand and pipe wall are major resistances to prevent the transportation. However, in upwated vertical flow, the effect of above two factors are minimised. Thus, the transport velocity in upward vertical flow is much lower than that in horizontal flow. From design point of view, the pipeline should be designed based on transport velocity in horizontal flow to prevent any sand deposition.

However, sand transport characteristics and MTC could be different in vertical air-water flow due to that they are highly flow regime dependent. Further work is required in this area.